MARTIN MARIETTA ENERGY SYSTEMS LIBRARIES

3 4456 0377739 4

ornl

ORNL/TM-12403

OAK RIDGE
NATIONAL
LABORATORY

MARTIN MARIETTA

Multicomponent Liquid Ion Exchange with Chabazite Zeolites

S. M. Robinson
W. D. Arnold, Jr.
C. W. Byers

OAK RIDGE NATIONAL LABORATORY
CENTRAL RESEARCH LIBRARY
CIRCULATION SECTION
4500N ROOM 175
LIBRARY LOAN COPY
DO NOT TRANSFER TO ANOTHER PERSON
If you wish someone else to see this report, send in name with report and the library will arrange a loan.
UCN-7969 (3 9-77)

MANAGED BY
MARTIN MARIETTA ENERGY SYSTEMS, INC.
FOR THE UNITED STATES
DEPARTMENT OF ENERGY

This report has been reproduced directly from the best available copy.

Available to DOE and DOE contractors from the Office of Scientific and Technical Information, P.O. Box 62, Oak Ridge, TN 37831; prices available from (615) 576-8401, FTS 626-8401.

Available to the public from the National Technical Information Service, U.S. Department of Commerce, 5285 Port Royal Rd., Springfield, VA 22161.

This report was prepared as an account of work sponsored by an agency of the United States Government. Neither the United States Government nor any agency thereof, nor any of their employees, makes any warranty, express or implied, or assumes any legal liability or responsibility for the accuracy, completeness, or usefulness of any information, apparatus, product, or process disclosed, or represents that its use would not infringe privately owned rights. Reference herein to any specific commercial product, process, or service by trade name, trademark, manufacturer, or otherwise, does not necessarily constitute or imply its endorsement, recommendation, or favoring by the United States Government or any agency thereof. The views and opinions of authors expressed herein do not necessarily state or reflect those of the United States Government or any agency thereof.

ORNL/TM-12403

401

4

MULTICOMPONENT LIQUID ION EXCHANGE WITH CHABAZITE ZEOLITES

S. M. Robinson
W. D. Arnold, Jr.
C. W. Byers

Engineering Development Section
Chemical Technology Division
Oak Ridge National Laboratory*
Oak Ridge, TN 37831

Date Published: October 1993

Managed by Martin Marietta Energy Systems, Inc., for the U.S. Department of Energy under contract DE-AC05-84OR21400.

MARTIN MARIETTA ENERGY SYSTEMS LIBRARIES

3 4456 0377739 4

CONTENTS

1. INTRODUCTION 1

2. LITERATURE REVIEW 6

2.1 Equilibrium Behavior 9

2.2 Mass-transfer Mechanisms 14

2.3 Methods of Solution 20

3. EXPERIMENTAL 22

3.1 Materials 22

3.2 Analytical Methods 26

3.3 Experimental Equipment 27

4. ION-EXCHANGE CAPACITY STUDIES 31

5. EQUILIBRIUM STUDIES 34

5.1 Impact of Experimental Conditions 34

5.2 Binary and Multicomponent Isotherms 42

5.3 Isotherm Equations 48

6. BATCH REACTOR KINETIC STUDIES 59

6.1 Experimental Results 59

6.2 Data Evaluation 63

7. MODEL DEVELOPMENT 69

7.1 Homogenous Diffusion Model 70

7.2 Heterogenous Diffusion Models 73

7.2.1 Parallel Macropore and Micropore Diffusion 73

7.2.2 Series Macropore and Micropore Diffusion 75

7.2.3 Macropore Diffusivity Equations 79

8. MODELING RESULTS 80

9. VALIDATION WITH COLUMN DATA 92

9.1 Experimental Results 92

9.2 Data Evaluation 97

10. SUMMARY 103

BIBLIOGRAPHY 106

APPENDIXES 113

Appendix A. EQUILIBRIUM DATA 114

Appendix B. BATCH KINETIC DATA 136

Appendix C. COLUMN KINETIC DATA 142

Appendix D. ORTHOGONAL COLLOCATIONAL NUMERICAL METHODS 157

Appendix E. MODELS FOR ION EXCHANGE IN BATCH REACTORS 161

E.1 Homogenous Diffusion Model with Constant Diffusivities . 162

E.2 Homogenous Diffusion Model with Variable Diffusivities . 164

E.3 Heterogenous Parallel Diffusion Model with Constant Diffusivities 166

E.4. Heterogenous Parallel Diffusion Model with Variable Micropore Diffusivity 169

E.5. Heterogenous Series Diffusion Model with Constant Diffusivities 170

E.6 Heterogenous Series Diffusion Model with Parabolic Concentration Profile in Zeolite Crystals 172

E.7. Heterogenous Series Diffusion Model with Variable Diffusivities 173

Appendix F. FIXED-BED ION-EXCHANGE COLUMN MODEL 178

Appendix G. COMPUTER PROGRAMS 186

LIST OF TABLES

1. Radiochemical composition of ORNL process wastewater 3

2. Chemical composition of ORNL process wastewater 3

3. Average composition of Ionsiv IE-96 zeolite 25

4. Physical properties of Ionsiv IE-90 and IE-96 zeolite 25

5. Cation-exchange capacity of Ionsiv IE-90 and IE-96 zeolite 32

6. Experimental conditions for equilibrium method tests using Ionsiv IE-96 .. 36

7. Initial solution phase concentration for isotherm tests 43

8. Summary of equilibrium data using standard equilibrium method 44

9. Model parameters for binary isotherms 50

10. Parameters for modified Dubinin-Polyani isotherm equation 55

11. Error variances for multicomponent equilibrium models 58

12. Summary of batch reactor kinetic experiments 60

13. Film mass-transfer coefficients for the batch reactor 66

14. Micropore diffusivities for Ionsiv IE-90 81

15. Effective micropore diffusivities for Ionsiv IE-96 81

16. Macropore diffusivities for Ionsiv IE-96 82

17. Summary of column ion-exchange experiments 93

18. Film mass-transfer coefficients for the short-bed column 101

A.1. Equilibrium data for run SR-1 115

A.2. Equilibrium data for run SR-2 116

A.3. Equilibrium data for run SR-3 119

A.4. Equilibrium data for run SR-4 122

A.5. Equilibrium data for run SR-5 123

A.6. Equilibrium data for run SR-6 127

A.7. Equilibrium data for run SR-17 128

A.8. Equilibrium data for run SR-18 129

A.9. Equilibrium data for run SR-23 130

A.10. Equilibrium data for run SR-25 131

A.11. Equilibrium data for run SR-26 132

A.12. Equilibrium data for run SR-27 133

A.13. Equilibrium data for run SR-34 134

A.14. Equilibrium data for run SR-35 135

B.1. Batch reactor operating conditions 137

B.2. Single component batch reactor data for Ionsiv IE-90 138

B.3. Multicomponent component batch reactor data for Ionsiv IE-90 139

B.4. Single component batch reactor data for Ionsiv IE-96 140

B.5. Multicomponent component batch reactor data for Ionsiv IE-96 141

C.1. Column operating conditions 144

C.2. Single component short bed column kinetic tests 145

C.3. Single component short bed column calcium kinetic tests 146

C.4. Multicomponent short bed column kinetic tests 147

C.5. Single component long bed column kinetic tests 150

C.6. Multicomponent long bed column kinetic tests 152

LIST OF FIGURES

1. Performance of an ion-exchange column: (a) the exhausted, the exchanging, and the unconverted zones in the column; (b) the axial concentration profile inside the column and (c) the resulting breakthrough curve. 7

2. Schematic diagram of a composite pellet showing the three principle resistances to mass transfer 15

3. Schematic representation showing the framework structures of chabazite zeolite. To translate the schematic diagram into the actual structure, a Si or Al is placed at each vertex and an 0 at or near the center of each line 23

4. Schematic of experimental system for column isotherm tests 28

5. Schematic of batch reactor for mass-transfer experiments 29

6. Experimental data from column isotherm test using Ionsiv IE-96: (a) Sr-Na and (b) Cs-Na 37

7. The effect of experimental method on binary exchange with Ionsiv IE-96: (a) Sr-Na isotherm and (b) Cs-Na isotherm. 38

8. The effect of experimental method on ternary Sr-Cs-Na ion exchange with Ionsiv IE-96: (a) Sr isotherm and (b) Cs isotherm. 39

9. Strontium isotherms for binary and ternary systems using Ionsiv IE-96 40

10. Effect of initial solution concentration on Sr-Cs-Ca-Mg-Na ion exchange with Ionsiv IE-96: (a) Sr isotherm; (b) Cs isotherm; (c) Ca isotherm and (d) Mg isotherm. 41

11. Isotherms for binary exchange with Ionsiv IE-96: (a) Sr-Na; (b) Cs-Na; (c) Ca-Na and (d) Mg-Na 46

12. Isotherms for Sr-Cs-Ca-Mg-Na ion exchange 47

13. Example models for binary Sr-Na ion-exchange isotherm with Ionsiv IE-96 . . . 51

14. Langmuir models for the binary data with Ionsiv IE-96: (a) strontium isotherm; (b) cesium isotherm; (c) calcium isotherm and (d) magnesium isotherm 52

15. Example models for Sr isotherm for Sr-Cs-Ca-Mg-Na ion exchange with Ionsiv IE-96 54

16. Modified Dubinin-Polyani models for the multicomponent data with Ionsiv IE-96: (a) strontium isotherm; (b) cesium isotherm; (c) calcium isotherm and (d) magnesium isotherm 56

17. Effect of particle size on uptake rate for a batch reactor using $CaCl_2$ feed and Ionsiv IE-96: (a) solution phase and (b) solids phase 61

18. Uptake rates for batch reactor tests: (a) IE-90 binary systems; (b) IE-90 multicomponent system; (c) IE-96 binary systems and (d) IE-96 multicomponent system 62

19. Models of Sr-Na uptake curves: (a) Ionsiv IE-90 using $D_{c,eff}$ or $D_{c,o}$ and (b) Ionsiv IE-96 using $D_{c,eff}$ from Ionsiv IE-90 data 83

20. Models of Sr uptake curve for Sr-Cs-CA-Mg-Na ion exchange using effective diffusivities obtained from single- and multicomponent data 84

21. Models of Cs-Na uptake curves for Ionsiv IE-96: (a) effect of film mass transfer and (b) effect of heterogenous model assumptions 85

22. Effect of particle size on models for Ca-Na uptake curves using Ionsiv IE-96 86

23. Models of Sr-Cs-Ca-Mg-Na ion exchange using Ionsiv IE-96: (a) strontium and (b) magnesium 87

24. Effect of experimental conditions on breakthrough curves for short-bed column with $CaCl_2$ feed and Ionsiv IE-96: (a) flow rate and (b) particle size . 94

25. Breakthrough curves for short-bed adsorber: (a) single-component system and (b) multicomponent system 95

26. Breakthrough curves for long-bed ion-exchange column with multicomponent feed 96

F.1. Schematic representation of fixed-bed adsorption column models with the film, macropore, and micropore diffusion 181

F.2. Location of orthogonal collocation points in the axial and radial directions for two internal points 184

LIST OF SYMBOLS

a	geometry constant; 1 for planar, 2 for cylindrical, 3 for spherical
a_i	isotherm constant for cation i
a_{0i}	constant in Equation 69
a_{2i}	constant in Equation 69
A_{ji}	collocation constant to replace gradient
A_s	equivalent fraction of cation A in solution phase
A_z	equivalent fraction of cation A in solid phase
b_i	isotherm constant for cation i
B_{ji}	collocation constant to replace Laplacian operator
B_s	equivalent fraction of cation B in solution phase
B_z	equivalent fraction of cation B in solid phase
c_i	concentration of cation i in liquid, meq/mL
C_i	dimensionless concentration of cation i in liquid, c_i/c_{0i}
c_{di}	concentration of cation i in bulk liquid, meq/mL
c_{pi}	concentration of cation i in liquid in macropores, meq/mL
c_{si}	solubility of cation i in Equations 7, 10 and 11, meq/mL; concentration of cation i in liquid at the particle surface, meq/mL
c_{0i}	initial concentration of cation i in liquid, meq/mL
D_{ci}	micropore diffusivity for cation i, cm^2/s
D_{gi}	$3\rho(1-\epsilon)q_{0i}/\epsilon c_{0i}$
d_i	impeller diameter, cm
D_{li}	liquid diffusivity for cation i, cm^2/s
D_{pi}	macropore diffusivity for cation i, cm^2/s
D_{si}	surface diffusivity for cation i, cm^2/s

D_{s0i} corrected surface diffusivity for cation i, cm^2/s

d_t tank diameter, cm

D_{zi} axial dispersion coefficient for cation i, cm/s

D_{0i} corrected diffusivity for cation i, cm^2/s

E_s equivalent fraction of cation E in solution phase

E_z equivalent fraction of cation E in solid phase

F_i root of collocation polynomial

g_i charge of cation i

G acceleration due to gravity in Equation 19, cm/s^2; trail function for orthogonal collation in Equations 88-92

k_{ci} micropore mass-transfer coefficient for cation i, cm/s

k_{fi} film mass-transfer coefficient for cation i, cm/s

k_i isotherm constant for cation i

k_{gi} $3k_{fi}(1-\epsilon)/\epsilon R_p$ or $3k_{fi}(1-\epsilon)/\epsilon r_c$

k_{pi} macropore mass-transfer coefficient for cation i, cm/s

L column length, cm

m number of solutes

n_i isotherm constant for cation i

P specific power input, cm^2/s^3

P_i Jacobi polynomials

Pe vL/D_z

q_i concentration of cation i in solid phase, meq/g

Q_i concentration of cation i in solid phase, q_i/q_{0i}

$\bar{q}_i$ average concentration of cation i in zeolite crystal, meq/g

$\bar{\bar{q}}_i$	average concentration of cation i in solid phase, meq/g
qsi	saturation concentration of cation i in solid phase, meq/g
q_{0i}	concentration of cation in equilibrium with c_{0i}, meq/g
r	radial coordinate for microparticle, cm
$\bar{r}$	dimensionless radial coordinate for zeolite crystal, r/r_c
r_c	microparticle radius, cm
R	gas constant in Equations 10 and 11, cal/gmole°K; radial coordinate for macroparticle, cm
$\bar{R}$	dimensionless radial coordinate for zeolite particle, R/R_p
R_p	macroparticle radius, cm
Re	$2\rho_l R_p v\epsilon/\mu$
Re_p	$(2R_p)^{4/3}(pg_c/V_l)^{1/3}\rho_l^{2/3}/\mu$, p is power in Nm/s.
Sc	$\mu/\rho_l D_l$
Sh	$2R_p k_f/D_l$
St	$k_f L(1-\epsilon)/R_p v\epsilon$
t	time, s
t_c	L/v, s
$\bar{t}$	dimensionless time, tv/L
T	temperature, K
U	trial function for orthogonal collocation
v	fluid velocity, cm/s
V_l	liquid volume, cm^3
$\bar{V}_i$	partial molar volume of component i, cm^3/meq
V_m	molar volume of sorbate, cm^3/meq
W	volume of liquid in micropores, cm^3/g
W_i	collocation constant for integration
W_o	volume of liquid in micropores at saturation, cm^3/g
X_i	mole fraction of cation in solid phase

X_i	mole fraction of cation in solid phase
z	axial position in column, cm
Z	dimensionless axial position in column, z/L
α	collocation trail function constant
$\alpha_{A,B}$	separation factor
β	collocation trail function constant
ϵ	voidage in bed
ϵ_p	fraction of binder in particle
η	variable in orthogonal collocation trail function
λ	variable in orthogonal collocation trial function
μ	viscosity, g/cm•s
ξ_i	$c_{0i}\epsilon_p/(1-\epsilon_p)q_{0i}\rho$
ρ	density of particles, g/cm^3
ρ_l	density of liquid, g/cm^3
τ	tortuosity factor
ϕ	isotherm constant

ABSTRACT

In spite of the increasing commercial use of zeolites for binary and multicomponent sorption, the understanding of the basic mass-transfer processes associated with multicomponent zeolite ion-exchange systems is quite limited. This study was undertaken to evaluate Na-Ca-Mg-Cs-Sr ion exchange from an aqueous solution using a chabazite zeolite.

Mass-transfer coefficients and equilibrium equations were determined from experimental batch-reactor data for single and multicomponent systems. The Langmuir isotherm was used to represent the equilibrium relationship for binary systems, and a modified Dubinin-Polyani model was used for the multicomponent systems. The experimental data indicate that diffusion through the microporous zeolite crystals is the primary diffusional resistance. Macropore diffusion also significantly contributes to the mass-transfer resistance.

Various mass-transfer models were compared to the experimental data to determine mass-transfer coefficients. Effective diffusivities were obtained which accurately predicted experimental data using a variety of models. Only the model which accounts for micropore and macropore diffusion occurring in series accurately predicted multicomponent data using single-component diffusivities. Liquid and surface diffusion both contribute to macropore diffusion. Surface and micropore diffusivities were determined to be concentration dependent.

1. INTRODUCTION

Fixed-bed ion exchange in which resins serve as the granular medium has been established for many years as an important technique for water purification and the recovery of ionic components from mixtures. Inorganic media, such as porous, crystalline, aluminosilicate zeolites, have had limited application as ion exchangers in the past. However, zeolite molecular sieves have several characteristics that are unique compared to ion-exchange resins. They are porous crystalline aluminosilicates with rigid frameworks and open crystal lattice containing pores of precisely uniform dimensions. Therefore, zeolites exhibit both molecular-sieve and ion-exchange properties. They also tend to be cheaper than many organic resins and are resistant to thermal and radiation degradation. These properties are causing the use of zeolite for ion-exchange applications to increase (Sherman, 1978).

Some of these considerations have led Oak Ridge National Laboratory (ORNL) to use chabazite zeolites for decontamination of process wastewater containing parts-per-billion levels of ^{90}Sr and ^{137}Cs. A typical characterization of the ORNL process waste stream is shown in Tables 1 and 2. Treatability studies (Robinson and Parrott, 1988; Robinson, 1991) indicated that chabazite zeolites are highly selective for cesium and strontium over calcium and magnesium. They have distribution coefficients of 20 to 40 times greater than organic resins and are thus suited to the removal of trace amounts of ^{137}Cs and ^{90}Sr from wastewaters. The zeolite process will reduce the secondary waste generation by > 50 %, and the zeolite will be in a form that is more amenable to disposal as solid waste. These studies also indicated that the efficiency of the zeolite system depends strongly on the column design and operating conditions and, through optimization of the design of full-scale columns, one could halve the generation rate of loaded zeolite requiring disposal. The design of zeolite systems

Table 1. Radiochemical composition of ORNL process wastewater

Radionuclide	Concentration (Bq/L)	Concentration (*N*)
Gross alpha	5	-
Gross beta	6000	-
^{60}Co	25	2.0E-14
^{90}Sr	4000	1.7E-11
^{137}Cs	400	9.1E-13
^{106}Ru	10	2.3E-15

Table 2. Chemical composition of ORNL process wastewater

Cation	Concentration (mg/L)	Concentration (*N*)	Cation	Concentration (mg/L)	Concentration (*N*)
Ca^{2+}	40	2.0E-03	HCO_3^-	93	1.5E-03
Mg^{2+}	8	6.6E-04	SO_4^{2-}	23	4.8E-04
Na^+	5	2.2E-04	Cl^-	10	2.8E-04
K^+	2	5.1E-05	NO_3^-	11	1.8E-04
Si^{3+}	2	2.1E-04	CO_3^{2-}	7	2.3E-04
Sr^{2+}	0.1	2.3E-06	F^-	1	5.3E-05
Al^{3+}	0.1	1.1E-05			
Fe^{2+}	0.1	3.6E-06			
Zn^{2+}	0.1	3.1E-06			

for minimization of secondary waste is a key to economic operation of the zeolite ion-exchange plant for treatment of radioactive waste.

Several mathematical models have been developed to predict ion-exchange column operation, but equilibrium and mass-transfer data needed for these models are often not available. Experimental studies with zeolite systems have been particularly limited (Palekar and Rjadhyaksha, 1986). Many industrial multicomponent ion-exchange columns are still designed using rather crude scale-up techniques based on laboratory- and pilot-scale data (Wankat, 1986). A semi-empirical model developed by Thomas is frequently used in the industry to scale-up experimental data (Tan, 1984). Previous zeolite tests at ORNL (Robinson and Parrott, 1988; Robinson, 1991) indicated that the Thomas equation is not adequate for design of zeolite columns for multicomponent ion exchange.

This dissertation summarizes the results of an investigation directed at modeling multicomponent ion exchange in chabazite zeolites for application in treating slightly contaminated ground water. The prime objective of this study is to identify diffusion mechanisms and determine their relative importance for multicomponent diffusion in chabazite. The impact of multicomponent solute interactions will be investigated. This will result in rate parameters for ion-exchange models that can be used to predict the performance of a multicomponent fixed-bed zeolite system.

This study consists of three phases: (1) equilibrium studies, (2) mass transfer studies, and (3) mathematical modeling. The first phase included determination of the equilibrium isotherms for single and multicomponent cations in an aqueous solution. In the second phase, kinetic data were obtained using a batch reactor system for single and multicomponent systems. Various mathematical models containing mass-transfer coefficients as variables were

developed in the third phase of the study. The modeling results were superimposed on experimental data to determine effective diffusivities for a given system.

2. LITERATURE REVIEW

Although fixed-bed ion exchange has been an important unit operation for purification and component recovery for many years, the analysis of its application to this process is complex. Ion exchange in a fixed-bed column is characterized by a breakthrough curve that is the effluent concentration profile as a function of the volume of liquid processed. A typical breakthrough curve is shown in Figure 1. The rate of appearance and the shape of breakthrough profiles depend on several factors, including the physical and chemical properties of the sorbate and sorbent, the equilibrium relationship between the solution and solid phases, the rate limiting mass-transfer mechanisms (film diffusion, particle diffusion, pore diffusion, axial dispersion, or reaction kinetics), the bed depth, and the fluid velocity. The objective of fixed-bed column design is to predict the characteristics of the breakthrough curve for a particular column operating under a given set of conditions.

Models of multicomponent liquid ion-exchange systems were virtually nonexistent before the 1980s. Considerable effort was made during the 1980s in this area, and several models have now been developed to predict breakthrough curves for a variety of adsorption and ion-exchange systems (Wankat, 1986; Weber and Smith, 1987; Gierke, 1990). However, the ability to predict the behavior of multicomponent systems is very limited at present. The relationship between multicomponent systems, even for binary gaseous systems, and the diffusivities of individual sorbates is not well understood. Equilibrium equations and mass-transfer coefficients can not typically be obtained theoretically. A general solution for multicomponent ion exchange and adsorption, which includes hydrodynamic dispersion, mass-transfer effects, interference effects, and nonlinear complex isotherms, are still not available from the literature.

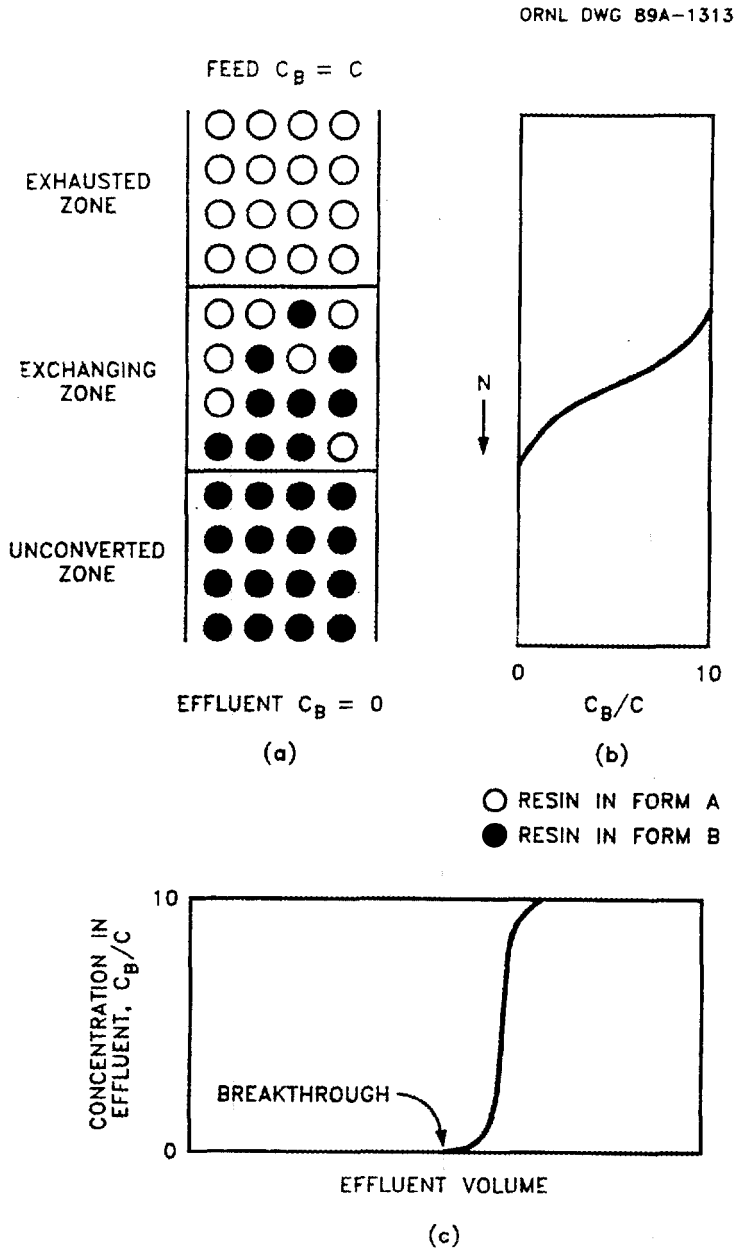

Figure 1. Performance of an ion-exchange column: (a) the exhausted, the exchanging, and the unconverted zones in the column; (b) the axial concentration profile inside the column and (c) the resulting breakthrough curve.

Source: Helfferich, F., *Angew. Chem. Internat. Edit.*, 7 (8), 1962, 440-53.

The decontamination of radioactive waste solutions using zeolites has been studied since the 1950s (Dyer and Keir, 1984). Unfortunately, very few fundamental studies have been performed, and it has been difficult to make use of much of the literature because of the lack of standardized procedures and theoretical bases. The picture presented in the literature for diffusion in zeolites is confusing, conflicting, and/or inconsistent with theory. Therefore, more fundamental studies are needed to aid in the development of models for zeolite ion-exchange systems.

Multicomponent ion exchange in zeolites may be represented by the following chemical reaction equation (Breck, 1974):

$$(g_A+g_E)\,B_{(z)}^{g_B^+} + g_B\,A_{(s)}^{g_A^+} + g_B\,E_{(s)}^{g_E^+} \rightleftharpoons (g_A + g_E)B_{(s)}^{g_B^+} + g_B\,A_{(z)}^{g_A^+} + g_B\,E_{(z)}^{g_E^+}\,, \tag{1}$$

where g_A, g_B, and g_E are the charges of the exchanging cations A, B, and E, and the subscripts z and s refer to the zeolite and solution phases, respectively. The equivalent fractions of the exchanging cation A in the solution and zeolite are defined by

$$A_s = g_A c_A / (g_A c_A + g_B c_B + g_E c_E) \tag{2}$$

and

$$A_z = \frac{\textit{equivalents of exchanging cation A}}{\textit{total equivalents of cations in the zeolite}}\,, \tag{3}$$

where c_A, c_B, and c_E are the concentrations of the ions A, B, and E respectively, in the equilibrium solution. The ion-exchange isotherm is a plot of A_z as a function of A_s at a given temperature. The preference of the zeolite for one of two ions is expressed by the separation factor defined as:

$$\alpha_{A,B} = \frac{A_z B_s}{B_z A_s} \tag{4}$$

If g_A, g_B, and g_E are each equal to one, uni-univalent ion exchange is said to occur. If these variables are each equal to two, di-divalent exchange is occurring. If they are unequal, multivalent ion exchange is occurring, etc.

A model that describes the behavior of ion exchange in packed beds must predict the uptake curve that results from ion-exchange material becoming loaded with the solute. This involves solving liquid and solid phase mass balances along with equilibrium equations. A brief description of solid-liquid multicomponent model development is given below. Since the majority of the models have been developed for carbon adsorption, both adsorption and zeolite ion exchange references have been included. These processes are mathematically equivalent if the ion-exchange process is relatively fast, and solutes diffuse independently.

2.1 Equilibrium Behavior

The complexity and diversity of the mechanisms of single and multicomponent ion-exchange equilibrium behavior have led to the development of a large number of equations, both theoretical and empirical in nature. Useful reviews of this area (Soldatov and Bichknova, 1980; Myers and Byington, 1986; Shallcross et al., 1988) are available. The most frequently used models are the binary Langmuir model,

$$q = \frac{q_s bc}{1+bc} = \frac{ac}{1+bc} \; ; \tag{5}$$

the binary Freundlich model,

$$q = kc^n \; ; \tag{6}$$

and the Dubinin-Polyani model (Ruthven, 1984a; Manes, 1980),

$$\frac{W}{W_o} = \frac{qV_m}{q_sV_m} = \frac{q}{q_s} = \exp\{-kR^2T^2[ln(\frac{c_s}{c})]^2\} . \tag{7}$$

In these equations, q, q_s, c, and c_s are the equilibrium and saturation concentrations in the solid and liquid phases, respectively; and b, n, and k are coefficients fitted to the experimental data. Ideally, k, W_o, and q_s in Equation 7 should be functions of the solid phase only.

These models may be extended in a logical manner to describe multicomponent equilibrium. For instance, the multicomponent Langmuir model is

$$\frac{q_i}{q_{si}} = \frac{b_ic_i}{1+b_1c_1+b_2c_2+\ldots b_mc_m} , \tag{8}$$

and the multicomponent Freundlich equation is

$$\frac{q_i}{q_{si}} = \frac{b_ic_i^{n_i}}{b_1c_1^{n_1}+\ldots\ b_mc_m^{n_m}} . \tag{9}$$

The coefficients, b_i and n_i, are obtained from binary isotherm data.

The Dubinin-Polyani potential theory, a theory for single component gas adsorption, was modified by Bering et al. (1963) to apply to binary mixtures. The multicomponent form of the Dubinin-Polyani equation (Ruthven, 1984a) for liquids is

$$\frac{(q_1+q_2+\ldots)V_m}{W_o} = \exp(-k\phi^2), \tag{10}$$

where

$$q_s = W_o / V_m ,$$

$$V_m = X_1 \overline{V}_1 + X_2 \overline{V}_2 + \ldots ,$$

$$\frac{1}{\sqrt{k}} = \frac{X_1}{\sqrt{k_1}} + \frac{X_2}{\sqrt{k_2}} + \ldots ,$$

and

$$\phi = -RTln(\frac{c_1 + c_2 + \ldots}{c_s}).$$

Equation 10 can be rewritten as

$$\Sigma q_i = \exp\left\{b_0 + b_1 \cdot ln(\Sigma c_i) + b_2 \cdot [ln(\Sigma c_i)]^2\right\} , \tag{11}$$

where

$$b_0 = ln(q_s) - kR^2T^2[ln(c_s)]^2 ,$$

$$b_1 = 2kR^2T^2 ln(c_s) ,$$

and

$$b_2 = -kR^2T^2 .$$

A Langmuir-Freundlich equation (Ruthven, 1984a) has also been used to describe multicomponent systems:

$$\frac{q_i}{q_{s_i}} = \frac{b_i c_i^{n_i}}{1 + b_1 c_1^{n_1} + b_2 c_2^{n_2} + \cdots} . \tag{12}$$

A general empirical equation has been developed to mathematically describe many multicomponent systems (Wankat, 1986):

$$q_i = \frac{a_{i0} C_i^{b_{i0}}}{a_i + \sum_{j=1}^{m} a_{ij} C_{ij}^{b_{ij}}}. \tag{13}$$

Equation 13 includes some well-known relationships as special cases. For $b_{i0}=b_{ij}=a_i=1$, it becomes the Langmuir equation. The Freundlich equation is obtained when $a_i=0$, and the Langmuir-Freundlich equation when $a_i=1$. This empirical correlation has been successfully used to fit experimental adsorption data for two and three organic solutes (Mansour et al., 1982). Unfortunately, it requires relatively large amounts of data to calculate the model coefficients for systems with several components.

The Ideal Adsorbed Solution Theory (IAST) model is based on the Gibbs adsorption equation and only requires single-solute data to predict multicomponent equilibrium. When the binary Freundlich adsorption isotherm equation is substituted into the IAST model, the following equation can be obtained for modeling purposes (Crittenden et al., 1985):

$$c_{i,k} = \frac{q_{i,k}}{\sum_{j=k}^{m} q_{j,k}} \left(\frac{\sum_{j=k}^{m} \frac{q_{j,k}}{n_j}}{\frac{k_i}{n_i}} \right)^{\frac{1}{n_i}} \quad for\ i = 1\ to\ m\ . \tag{14}$$

The IAST model has been simplified to use average, or lumped, isotherm constants allowing its application to complex mixtures of many solutes. However, this simplified competitive adsorption model, has limited applications over broad concentration ranges and is not accurate for many applications (Sengupta and Paul, 1985; Chakravarti and Sengupta, 1983).

Published reports of isotherms for zeolites usually fall into three groups: extension of gaseous adsorption isotherm equations, the Dubinin-Polyani potential theory, and thermodynamic methods (Singhal, 1978). The simple gaseous model isotherms (Langmuir, etc.) have been found to be accurate for some zeolite systems, but they are often not

applicable (Ruthven et al., 1973). The Polanyi potential theory has been applied to carbon adsorption of organic mixtures from aqueous mixtures (Speth, 1986) and has been found to apply to zeolites in many instances (Breck, 1974).

The rigorous thermodynamic approach has received attention in recent years. Equilibrium for an ideal system is estimated using the relative separations factor defined in Equation 4. When the system is not ideal, activity coefficients must be added for both the liquid and/or solid phases. Several thermodynamic formulations have been developed to evaluate activity coefficients for ternary systems using soils and resin exchangers (Myers and Byington, 1985; Shallcross et al., 1988). The activity coefficients for the liquid phases are often calculated using the extended Debye-Huckel equation or Pitzer equation. The Wilson equation has traditionally been used to calculate solid phase activity coefficients. Difficulties have occurred with predicting nonideal behaviors of ionic components in the solid phase. All existing models of ion-exchange equilibrium presently utilize at least some experimental data (Shallcross, 1988).

Historically, thermodynamic approaches have been found to be of limited utility when applied to ion exchange in zeolites (Franklin and Townsend, 1985; Townsend, 1986; Kaul and Sweed, 1984; Ruthven and Goddard, 1986). Most recently, Perona (1992) developed a method for predicting multicomponent equilibrium by using the Pitzer equation to calculate the liquid phase activity coefficients and binary equilibria data to calculate Wilson interaction parameters for the solid phase activity coefficients. He found that the Wilson interaction parameters could not be obtained directly from equilibrium quotients.

While attempts to develop competitive equilibrium models have met with moderate success, researchers are presently limited to extending new theoretical models, modifying existing models to account for observed abnormalities, or developing empirical equations

based on experimental data to predict multicomponent equilibria (Weber and Smith, 1987). In this study, the standard equilibrium models will be tested against experimental isotherm data. These models will be modified as necessary to accurately predict the experimental data.

2.2 Mass-transfer Mechanisms

Various mathematical models with different degrees of complexities have been used to describe multicomponent ion-exchange/adsorption processes. Basically, they can be classified into the following three major categories: 1) staged equilibrium models, 2) interference theory, and 3) rate equation models. The rate equation models are the most realistic and will be discussed in this report. These consist of mass balances on each species in the bulk fluid and particle phases. They generally consider external (fluid) mass transfer, intraparticle diffusion, and equilibrium equations.

Commercial zeolites consist of small crystals of zeolite pelleted with a clay binder. Such solids have a heterogenous pore structure, and the kinetics are governed by three distinct diffusional resistances (shown conceptually in Figure 2): film diffusion from the bulk liquid to the pellet surface, diffusion through the macropores of the pellet, and diffusion within the micropores of the zeolite crystals. The relative importance of the resistances depends on the materials involved and on the specific operating conditions (Ruthven and Loughlin, 1972).

Mass-transfer coefficients can be obtained from experimental data and/or correlations. Both methods are used to determine film mass-transfer coefficients. Although molecular diffusion theory-based, empirical, and semi-empirical correlations are available for predicting

ORNL DWG 89A-1315

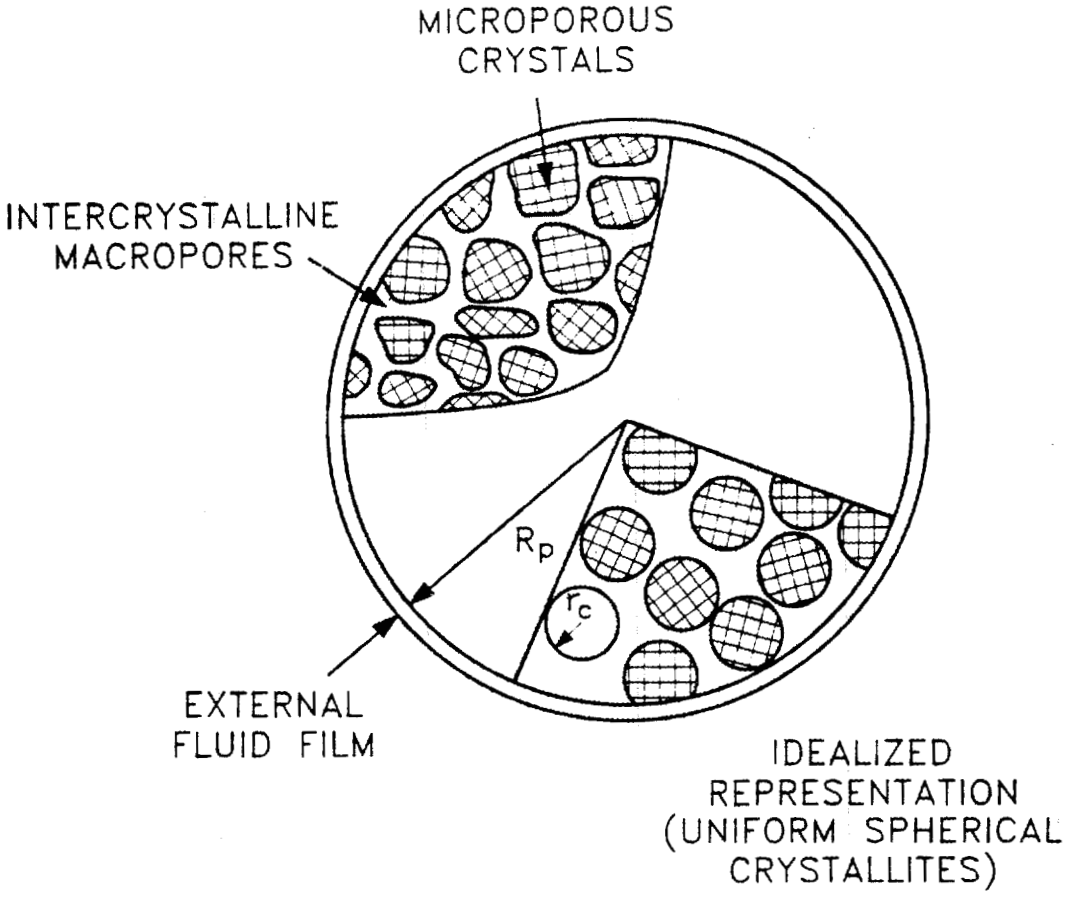

Figure 2. Schematic diagram of a composite pellet showing the three principal resistances to mass transfer.

Source: Ruthven, D. M., *Principles of Adsorption and Adsorption Processes*, John Wiley & Sons, New York, 1984.

macropore diffusion coefficients, they tend to be inaccurate for complex liquid mixtures (Ruthven, 1984a). As a result, macropore diffusion coefficients tend to be calculated by modeling experimental data. Micropore diffusion coefficients for zeolites must be obtained by modeling experimental data.

Several versions of the rate equation model have been used to model zeolites and activated carbon to obtain values for diffusion coefficients. The homogenous diffusion model assumes that the particle is a homogeneous solid through which diffusion can be modeled by a single solid-phase diffusivity. Several researchers have used this model to successfully predict zeolite ion exchange (Rosen, 1952; Prazniak and Byers, 1987; Garg and Ruthven, 1974; Liapis and Crosser, 1982; Ruthven and Doetsch, 1979; Hsu and Hayes, 1981; Weber and Smith, 1987; Dominguez, et al., 1991).

The heterogeneous diffusion model assumes that diffusion in the particle occurs by macropore diffusion through the voids of the porous binder and micropore diffusion in the zeolite crystals. The micropore diffusion mechanism is assumed to be solid diffusion only because molecular species in zeolite crystals should never be free from force fields associated with the pore walls. For liquid systems, macropore diffusion can be due to molecular diffusion and/or surface diffusion.

The frequently used pore diffusion, surface diffusion and combined diffusion models are special cases of the heterogeneous diffusion model. They assume that intraparticle mass-transfer resistance is due to macropore diffusion only.

The pore diffusion model pictures the sorbate diffusing in the pore voids, and adsorption occurs at the surface of the zeolite crystal. The pore diffusion model has been widely used to simulate the behavior of activated carbon particles (Liapis and Rippin, 1977; Fritz, et al., 1981) and, in some cases, for synthetic zeolites (Teo and Ruthven, 1986).

Although pore diffusivities have been reported that predict experimental uptake data, the values were often higher than molecular diffusivities, which is physically impossible (Fritz, 1978; Furusawa and Smith, 1973, 1974; Spahn and Schlunder, 1975; Raghavan and Ruthven, 1984; Carter and Husain, 1974; Nagel et al., 1987). Researchers generally addressed this by assuming that surface diffusion was also contributing to macropore diffusion or that micropore diffusion was significant. No studies were found to validate either assumption.

In the surface diffusion model, mass transport occurs on the surface of the pore walls by molecules jumping between adjacent adsorption sites. The surface diffusion model can be treated theoretically as the homogeneous diffusion model, with the assumption that accumulation of adsorbate within the solids is negligible. When both pore and surface diffusion are taken into account in the model, it is usually called "combined diffusion."

The Glueckauf model uses a linear driving force approximation to describe the diffusion within the particle. The linear driving force approximation model assumes that the intraparticle diffusion may be reduced to a linear mass transport mechanism in which the mass-transfer rate is proportional to the difference in concentrations at the outer surface and the bulk of the particle. This approach has been shown to work well in many instances, but it tends to break down in the case of a liquid phase system with two diffusion resistances (micropore-macropore) and significant intraparticle holdup within the macropores (Ruthven, 1984b).

Models for the heterogenous diffusion model have been developed that assume macropore and micropore diffusion occur in series (Weber and Smith, 1987; Smith and Weber, 1988; Sun and Meunier, 1991; Kapoor and Yang, 1988) or in parallel (Komiyama and Smith, 1974; Nagel et al., 1987). The assumption that macropore and micropore diffusion occurs in series results in coupled partial differential equations involving time and spatial

variables. Recently, several authors (Do and Rice, 1986; Akulov and Ustinov, 1981; Liaw et al., 1979; Rice, 1982; Rice et al., 1983; Doong and Yang; 1987; Cen and Yang, 1986; Kapoor and Yang; 1988) have simplified the mathematics for adsorption processes by assuming that the intraparticle concentration profiles have parabolic shapes. The parabolic concentration profile produces a mass-transfer rate equation with a linear driving force and gives the same mass-transfer coefficient that Glueckauf's equation does (Liaw, et al., 1979)

Although micropore and surface diffusivities are known to vary with sorbate concentration (Ruthven; 1984a), many zeolite models have assumed that they are constant. Models which account for this phenomena use Darken's equation (Garg and Ruthven, 1974; Ruthven and Lee, 1981; Moon and Lee, 1983). Pore diffusivities are usually assumed to be independent of concentration.

Multicomponent models are usually extended from those applied to single component systems, and the competitive effects are most often accounted for through the multicomponent adsorption isotherm. Such work has been done using the film-homogeneous diffusion (Crittenden and Weber, 1978; Fritz et al., 1981; Merk et al., 1980; Thacker et al., 1981, 1983; Takeuchi and Suzuki, 1983; Mathews and Su, 1983; Larson and Tien, 1984; Liang and Weber, 1985; Carter and Husain, 1974), film-pore diffusion (Liapis and Rippin, 1977, 1978; Fritz et al., 1981; Merk et al., 1980; Liapis and Litchfield, 1981; Larson and Tien, 1984; Crittenden et al., 1986), and film-heterogeneous diffusion models with macropore and micropore diffusion (Fritz et al., 1981; Merk et al., 1980; Weber and Smith, 1987; Smith and Weber, 1988; Sun and Meunier, 1991; Kapoor and Yang, 1988; Nagel et al., 1987). In a limited number of cases, models were compared for both single- and multi-component system data. In most cases, single component diffusivities could not be used to predict multicomponent data.

Differences between the kinetic behavior in single-solute and multicomponent systems have also been interpreted as being due to solute interactions during external mass transfer (Mathews, 1975; Liang and Weber, 1985) or intraparticle diffusion (Marutovsky and Bulow, 1987; Fritz et al., 1981; Merk et al., 1980; Moon and Lee, 1986; and Barba, et al., 1983). In these cases, cross-term diffusional coefficients are added to account for solute interactions. Most researchers assume that the cross-term diffusional coefficients do not have to be taken into account because of a study which showed that the off-diagonal terms are two orders of magnitude smaller than the diagonal terms for effective pore diffusivities for dilute solutions (Liapis and Litchfield, 1981).

The results of zeolite modeling reported in the literature to date has been rather confusing. However, this confusion is not unexpected since many researchers have looked at only one model when evaluating a single set of experimental data to estimate intraparticle diffusivities. These researchers tend to assume that a given model represents the mass-transfer mechanisms if effective diffusivities for predicting experimental data can be found which predict experimental data. Most researchers who have modeled dual intraparticle mass transfer simultaneously varied both the macropore and micropore diffusivities to determine which values predict data. Only Doong and Yang (1987) reported verifying their model by varying the size of crystals and pellets.

Ma and Ho (1974) is the only literature reference that measured diffusion in both zeolite powders and pellets to independently determine macropore and micropore diffusivities. Their results from single-component gaseous adsorption tests with Linde 13X zeolites indicated that macropore diffusivities were on the order of 10^{-2} cm^2/s and micropore diffusivities were on the order of 10^{-11} cm^2/s. Even though the macropore diffusivities were nine orders of magnitude higher, they significantly affected the mass transfer resistance.

Diffusivities that accurately predicted the adsorption data were also obtained for the solid diffusion model, but they were an order of magnitude higher than the true micropore diffusivities.

Since there is so much confusion about multicomponent diffusion in zeolites, the present study will obtain experimental uptake data for single and multi-component solute systems for chabazite zeolite. Zeolite crystals and pelletized particles will both be evaluated. A variety of rate equation models will be tested to determine which most accurately predicts experimental data. Models will be evaluated to determine which mass-transfer mechanisms must be accounted for, whether intraparticle diffusivities are concentration dependent, and if cross-term diffusion coefficients are needed to predict multicomponent ion exchange.

2.3 Methods of Solution

Due to the complexity and nonlinearity of ion-exchange equations, analytical solutions are generally impossible and models must be solved by numerical methods. Three different types of algorithms have typically been used to solve ion exchange models: (1) finite difference, (2) orthogonal collocation, and (3) finite elements.

Finite-difference schemes have traditionally been a popular approach to solving equations that describe separation or reaction phenomena. They are relatively easy to program on a computer and there is an abundance of literature on their application to almost any type of problem involving partial differential equations.

Within the past 10 to 15 years, methods of weighted residuals, particularly orthogonal collocation (Finlayson, 1972; Villadsen and Michelsen, 1978), have been used to solve partial differential equations (PDEs). It has been used as the state-of-the-art numerical method for solving ion exchange equations (Noll et al., 1992) since Liapis and coworkers (1978, 1980) used orthogonal collocation to discretize both the bulk- and particle-phase equations for an

adsorption model. The resulting ordinary differential equations (ODEs) are often solved using a Runge-Kutta method.

If the kinetics equations result in stiff equations, and the solution has a steep gradient, orthogonal collocation may not be suitable. Using a global polynomial to approximate a complicated mass-transfer process may also result in a high order polynomial that has oscillation problems. In these cases, finite difference, finite elements, or orthogonal collocation on finite elements may be more appropriate numerical methods (Finlayson, 1980).

In recent studies involving stiff equations, the orthogonal collocation method has been used for the particle-phase equations and either finite element or orthogonal collocation on finite elements for the bulk-phase equations (Yu and Wang, 1986; Gu et al., 1990). The resulting ODEs were solved using the implicit Gear's method for stiff equations. Mansour (1982) and Sun and Meunier (1991) have successfully modeled stiff systems using the finite difference methods for both the bulk- and particle-phase equations.

In the present study, the method of orthogonal collocation will be used to model multicomponent ion exchange in zeolites. The resulting ODEs will be solved using the implicit Gear's method.

3. EXPERIMENTAL

The experimental portion of this study consists of three phases: (1) equilibrium studies, (2) mass-transfer studies, and (3) ion-exchange column studies. The first phase includes determination of the equilibrium isotherms for single and multicomponent cations in aqueous solutions. In the second phase, the controlling mass-transfer mechanisms were determined for these solutions under various conditions. Finally, experimental breakthrough curves were obtained for various sizes of experimental columns to verify the results from mathematical models.

3.1 Materials

Chabazite zeolite, an aluminosilicate mineral, is available both in natural (e.g., Tenneco Specialty Minerals, TSM-300) and synthetic (e.g., Union Carbide Ionsiv IE-90 or IE-96) form. Structurally, chabazite consists of stacked, double six-membered ring prisms, interconnected through four rings, in a cubic, close-paced array (Ruthven, 1984a; Breck, 1974). Repetition of the stacking of prisms produces 11 x 6.6 Å cylindrical cavities, joined to adjacent cavities through six eight-membered rings with 4.1 x 3.7 Å free diameters as shown in Figure 3. The eight-membered rings have free apertures of 4.3 Å, and six-membered rings have 2.6-Å diameters. The neutralizing cation mainly coordinates to water molecules in the eight-membered rings. It is coordinated only to the oxygen in the double six-membered ring. As a result, the six-membered rings are not usually active in ion exchange (Passaglia, 1978).

Samples of the zeolite crystals (Ionsiv IE-90, lot 9146820010) and composite pellets (Ionsiv IE-96, lot 939685090015) were used in this study. The Ionsiv IE-90 zeolite crystals were shipped as 24-μm irregularly shaped particles in the hydrogen form and were converted to the sodium form before use. The Ionsiv IE-96 pellets, produced by pelletizing Ionsiv

ORNL DWG 89A-1316R

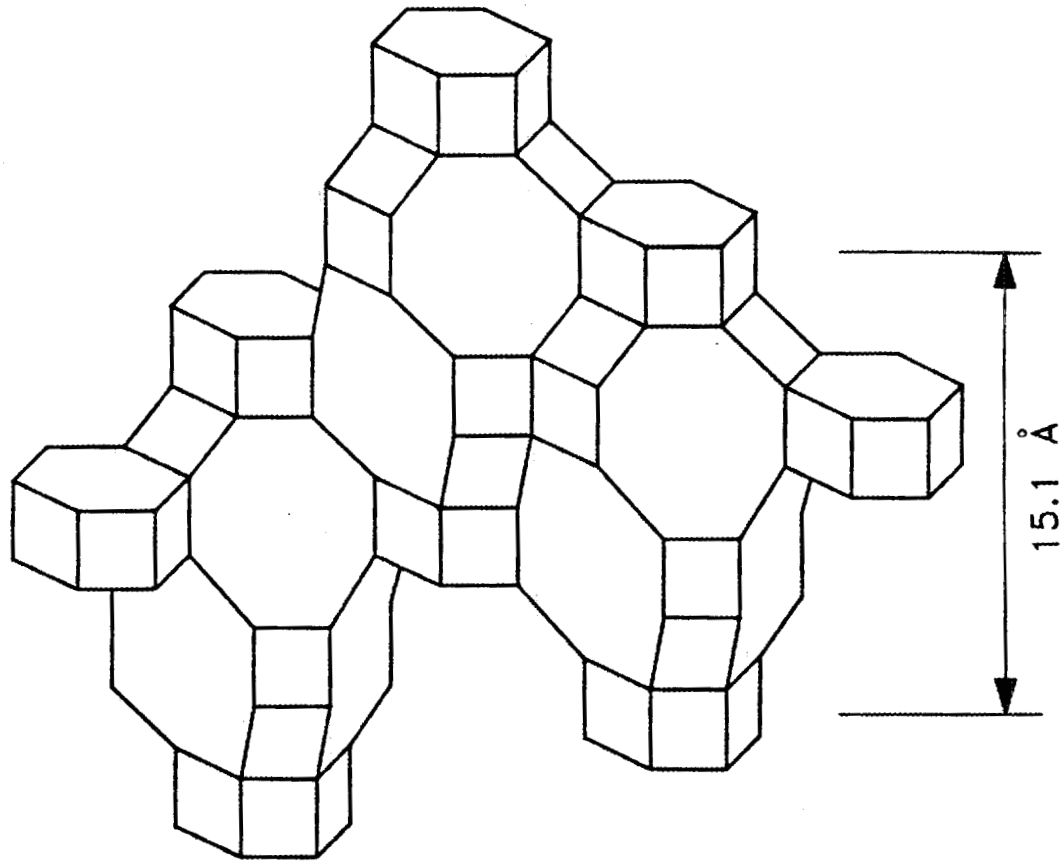

Figure 3. Schematic representation showing the framework structures of chabazite zeolite. To translate the schematic diagram into the actual structure, a Si or Al is placed at each vertex and an 0 at or near the center of each line.

Source: Ruthven, D. M., *Principles of Adsorption and Adsorption Processes*, John Wiley & Sons, New York, 1984.

IE-90 in a clay binder and converting to the sodium form, were shipped in the hydrated form as 20- to 50-mesh (840- to 297-μm) irregularly shaped particles.

The IE-96 sample was screened to size prior to use; 83% of the material was 30- to 35-mesh (590 to 500 μm). This sieve fraction was used in all tests unless otherwise indicated. Smaller particle sizes were obtained for intracrystalline mass-transfer experiments by crushing and screening the pellets. Some tests were performed with particles as small as 48 μm.

The average composition of Ionsiv IE-96 is given in Table 3 (Fennelly, 1991). The physical properties are given in Table 4 for general information. Only the bulk density was used in modeling studies. The physical properties of the zeolite crystals and pellets were determined by Martin Marietta Energy Systems Analytical Chemistry Groups. Typically, only single measurements were taken. In a limited number of cases, 2 to 4 measurements were obtained. In these cases, the standard deviations are reported below.

The surface areas were determined by Brunauer, Emmett, and Teller (BET) Surface Area measurements, and the pore-size distribution for Ionsiv IE-96 was obtained by mercury porosimetry. Standard deviations of 18% and 13% were obtained, respectively. The pore-size distribution for Ionsiv IE-90 could not be accurately measured by mercury porosimetry. The pore diameter was estimated from literature values of the free aperture of chabazite crystals (Breck, 1974; Ruthven, 1984a). Mercury porosimetry measurements were used to determine the bulk density of single particles. Mercury and helium porosimetry results were used to determine real densities of the particles. Standard deviations of 2 to 4% were obtained for density measurements.

Simulated wastewater solutions were used in the experimental tests. The solutions were prepared by dissolving various concentrations of $SrCl_2 \bullet 6H_2O$, CsCl, $CaCl_2$, and $MgCl_2 \bullet 6H_2O$ in distilled water. The solutions containing strontium and cesium were also

Table 3. Average composition of Ionsiv IE-96 zeolite

Metal Oxide	Composition (wt %)[a]
Na_2O	7.9
K_2O	1.0
MgO	0.8
CaO	1.2
BaO	0.1
SiO_2	67.4
Al_2O_3	17.3
FeO	4.0
TiO	0.2

[a] Anhydrous basis.

Source: Fennelly, D., personal communication, Union Carbide, 308 Harper Drive, Morrestown, NJ, 1988.

Table 4. Physical properties of Ionsiv IE-90 and IE-96 zeolite

Property	IE-90	IE-96
Bulk Density, g/cm^3	0.726	1.39
Real Density, g/cm^3	1.85	2.05
Porosity, %	61	32
Avg. Pore Diameter, microns	0.00043	0.050
Max. Pore Diameter, microns	—	10.0
Avg. Particle Radius, microns	12.22	273
Surface Area, m^2/g	306	360
Moisture Content, wt%	7.4 - 7.9	6.9 - 7.9
Cation Form	H[a]	Na

[a] As received from manufacturer. Converted to Na form before use.

spiked with ^{85}Sr and ^{137}Cs tracers, respectively. The aqueous solution chemistry was varied to determine the effects of multicomponent ion exchange in the zeolite. The calcium and magnesium concentrations in the simulated wastewaters were the same as the ORNL process wastewater, but the strontium and cesium concentrations were increased so that residual concentrations in the equilibrated solutions could be accurately measured with available analytical equipment. Both the number and position of cation sites in zeolites depend rather strongly on temperature and degree of hydration (Society of Chemical Industry, 1968). The temperature of the solutions was held constant at 24 to 25°C in all tests. In order to eliminate the effects of hydration, the zeolite samples were preconditioned with deionized water. Zeolite samples were washed with four bed volumes of deionized water in a column to remove fines and air dried prior to use. The water content of the preconditioned samples is listed in Table 4.

3.2 Analytical Methods

Calcium, sodium, and magnesium concentrations in the aqueous solutions were measured by a Varian Techtron, Model 1000 atomic adsorption (AA) spectrometer. Cesium and strontium concentrations in the aqueous solutions were measured by gamma counting of ^{137}Cs and ^{85}Sr tracers using a Canberra, Series 90, NaI detector for single isotopes and a Ge detector for multiple isotopes. The strontium results were also periodically checked by AA. The detection limit of the AA unit is approximately 0.05 mg/L (2.5×10^{-6} meq/mL) for calcium, 0.005 mg/L (4.1×10^{-7} meq/mL) for magnesium, 0.007 mg/L (3.0×10^{-7} meq/mL) for sodium, and 0.05 mg/L (1.1×10^{-6} meq/mL) for strontrium. Cesium solutions used in these tests varied from 0.1 meq/mL nonradioactive cesium (traced with ^{137}Cs) to tracer levels of ^{137}Cs. The detection limits for these solutions, based on counting the ^{137}Cs, ranged from about 0.1 mg/L (7.5×10^{-7} meq/mL) to about 1.2×10^{-4} mg/L (9.2×10^{-10} meq/mL). For

strontium, the initial concentrations ranged from 0.2 meq/mL natural strontium (traced with ^{85}Sr) to tracer levels of ^{85}Sr, and the corresponding detection limits ranged from 0.05 mg/L (1.1×10^{-6} meq/mL) to 3.3×10^{-7} mg/L (7.6×10^{-12} meq/mL). The concentration of cations in the zeolite were calculated from mass balances using the initial and final solution concentrations.

3.3 Experimental Equipment

All ion-exchange capacity tests were performed in batch reactors. Samples were mixed for 24 h on a Labquake, Labindustries, Inc., rocking shaker at 25 cycles/min and centrifuged in a Sorvall, Model RC-5, before being analyzed.

Equilibrium data were obtained from batch and column reactors. Column tests were performed by recirculating solution through the system shown in Figure 4.

Kinetic tests were performed using a batch reactor. The batch reactor, shown in Figure 5, is a Carberry-type reactor (Ruthven, 1984a) that was constructed at ORNL. It consisted of a 5.2-cm diam baffled vessel with a 2.6-cm wide, 1.2-cm high glass impeller. The four 0.5-cm wide, 0.5-cm deep baffles were located at 90° angles. The system was operated with 80 mL of solution and 0.05 g of zeolite (both Ionsiv IE-90 and IE-96 were tested). A 100-mesh stainless-steel envelope that was 3.2-cm wide and 2.5-cm high was attached to the impeller. The one-particle thick bed of zeolite was placed inside the envelope so that liquid could adequately flow around the particles. Impeller speeds were varied between 500 and 1000 rpm.

Column tests were made using short-bed columns (SBC), which have immediate breakthrough, and standard long-bed columns (LBC) where the bed is deep enough so that

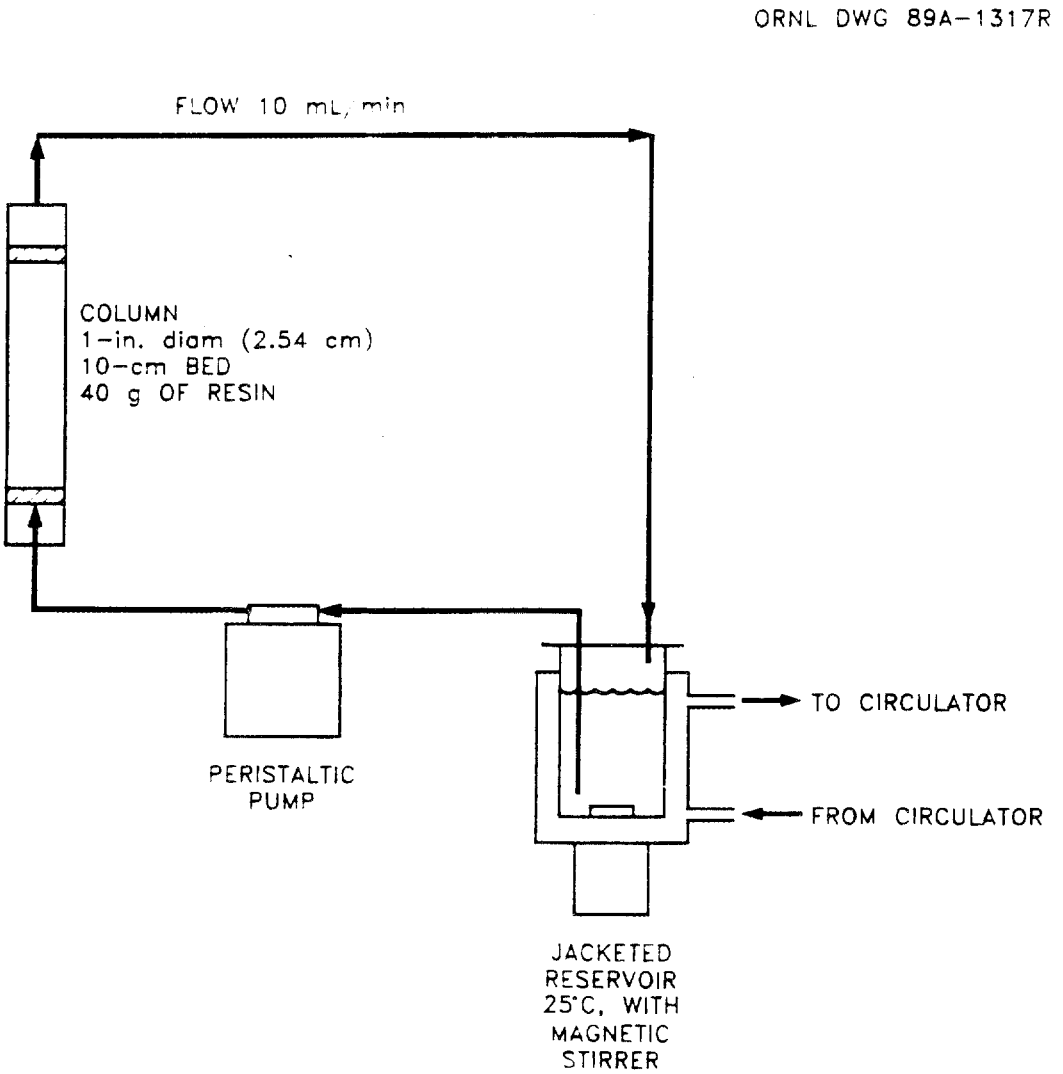

Figure 4. Schematic of experimental system for column isotherm tests.

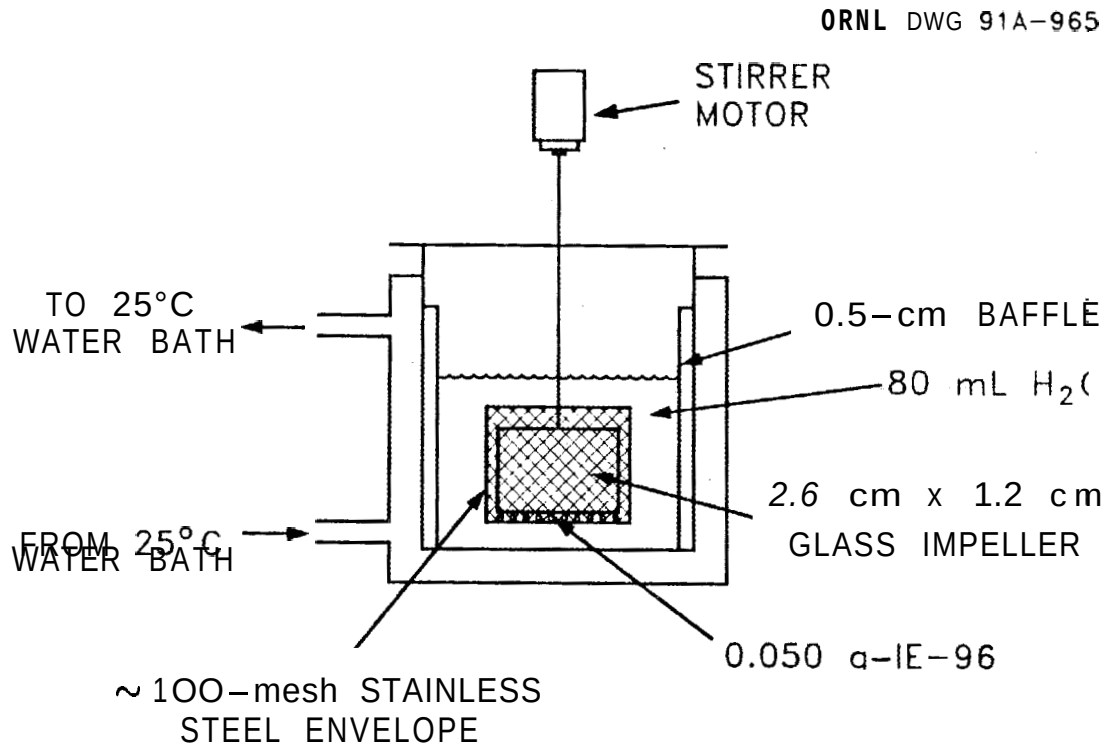

Figure 5. Schematic of batch reactor for mass-transfer experiments.

immediate breakthrough will not occur. The SBC was a 1-cm diam column that contained 1 g zeolite Ionsiv IE-96, which resulted in a bed depth of 1.6 cm. The column was operated with flow rates ranging between 3 and 12 mL/min, resulting in column residence times of 0.22 to 0.06 min, respectively.

Three sizes of LBC were tested. A 1-cm diam column contained 2- or 3-g zeolite Ionsiv IE-96, which resulted in a bed depth of 3.8 or 4.5 cm, respectively. The columns were operated with flow rates ranging between 0.5 and 8.5 mL/min. Larger columns (1.5- and 2.5-cm diam) that had bed depths of up to 11.4 cm were also tested.

4. ION-EXCHANGE CAPACITY STUDIES

The ion-exchange capacities of Ionsiv IE-90 and Ionsiv IE-96 were determined using the procedure developed by Tenneco Specialty Minerals (1988), a vendor of natural zeolites. The zeolite was contacted three times with 20 mL/g of 2 meq/mL NaCl overnight to ensure that it was in the sodium form. The zeolite was then washed three times by mixing with 20 mL/g of deionized water for 30 min. The washed zeolite was dried overnight at 110 °C. The zeolite was then contacted with 20 mL/g of 0.2 meq/mL exchange solution for 24 h. The mixture was weighed, centrifuged for 30 min at 5000 relative centrifugal force (rcf), and the supernate was decanted and analyzed by AA for sodium.

The exchange capacities of Ionsiv IE-90 and IE-96 were determined for $(NH_4)_2SO_4$, CsCl, $SrCl_2$, and a CsCl-$SrCl_2$ mixture. The tests were performed in triplicate, and the averaged results are given in Table 5. These tests indicate that Ionsiv IE-96 has a cation-exchange capacity of 2.8 meq/g when the solution phase does not contain cesium and 3.2 meq/g when cesium is present. Similarly, the Ionsiv IE-90 has an exchange capacity of 3.4 meq/g when cesium is present and 2.9 meq/g when cesium is not present. These values are somewhat higher than the reported values of 2.22 meq/g (Dyer and Keir; 1989) for Ionsiv IE-96 and 2.62 meq/g for Ionsiv IE-95 (Carl and Leonard; 1987), but less than the maximum possible value of 3.6 meq/g calculated from the chemical formula (Carl and Leonard; 1987).

The difference in the exchange capacity of IE-90 and IE-96 should be reflective of the amount of binder present in Ionsiv IE-96. These results indicate that Ionsiv IE-96 contains 5% binder. These results are consistent with those expected by the vendor (Fennelly, 1991).

Exchange capacity variations are not uncommon since zeolite ion exchange is complicated by ion-sieve, steric, and electrostatic forces within the zeolite pores (Barrer and

Table 5. Cation exchange capacity of Ionsiv IE-90 and IE-96 zeolite

Exchange solution	Ionsiv IE-90 capacity (meq/g)	Ionsiv IE-96 capacity (meq/g)	Ionsiv IE-90 standard deviation	Ionsiv IE-96 standard deviation
0.2 *N* CsCl	3.36	3.15	0.02	0.02
0.2 *N* $SrCl_2$	2.86	2.77	0.03	0.01
0.2 *N* $(NH_4)_2SO_4$	3.01	2.86	0.02	0.00
0.1 *N* CsCl + 0.1 *N* $SrCl_2$	3.35	3.21	0.01	0.03

Klinowski, 1972; Franklin et al., 1986). The results from this study indicate that certain sites in chabazite zeolite are available to cesium, but are not available for calcium, magnesium, or strontium exchange. Since some sites are not available for ion exchange with the latter cations, the effective exchange capacity of the zeolite is lowered. The dehydrated Ca, Cs, Mg, Na, and Sr cations have diameters (Dean, 1985) of 1.98, 3.38, 1.30, 1.90, and 2.26 Å, respectively. Ammonium has a critical diameter of greater than 3.8 Å (NH_3 has a diameter of 3.8 Å) (Breck et al., 1956). Since the eight-membered rings of chabazites have free operation of 4.3 Å, all of the ions in their dehydrated forms should be able to enter the zeolite cavities and eight-membered rings. Since the six-membered rings have diameters of 2.6 Å, only cesium should not be able to enter these smaller rings because of steric effects. However, Passaglia (1978) found that the six-membered rings are not active in ion exchange. In their hydrated form, none of the cations could enter the zeolite cavities.

To pass through the eight-membered rings, the ions must shed some of their waters of hydration. Two forces determine whether an ion will become dehydrated and enter a site on the zeolite: (1) the negative pole of attraction in the zeolite framework pulling the cation towards the site; and (2) the hydration energy inhibiting water stripping from the cation and, hence, causing its migration to the site. The hydration energy increases with ionic potential (charge/radius) of the cation and the attractive force increases with the charge density of the framework of the zeolite (Passaglia, 1978). Since cesium has the lowest charge (Baes and Mesmer, 1976) and a large radius, it should release its water of hydration and enter the chabazite more easily than the other competing ions. All experiments discussed in the remainder of this report are consistent with these findings.

5. EQUILIBRIUM STUDIES

Equilibrium studies were performed in two phases. In the first phase, various experimental conditions were evaluated to determine their impact on the resulting isotherms. Based on the results of theses studies, a standard experimental procedure was developed for obtaining binary and multicomponent isotherm data. The experimental data are given in Appendix A and are summarized below.

5.1 Impact of Experimental Conditions

Several references have reported that the experimental method used in equilibrium studies affects the isotherm for multicomponent systems. They have indicated that complex equilibrium behavior will occur if multicomponent feed solutions, multivalent cations, or high solution concentrations are used (Sherman, 1978; Ausikaitis, 1984; Loizidou and Townsend, 1987; Barri and Rees, 1980a; Cremers, 1977; Crittenden and Weber, 1978).

Because of the problems described in the literature, three different experimental methods were compared for use in this study: (1) batch tests in which the volume and concentration of the solution phase were held constant and the mass of solids was varied, (2) batch tests in which the solution concentration was varied and the mass of solids was held constant, and (3) column tests in which the amount of solids was held constant and the solution concentration was varied (See Figure 4). Binary Sr-Na and Cs-Na and ternary Sr-Cs-Na isotherms were obtained by each method. Some tests were repeated using the first experimental method at different initial solution concentrations (the relative concentration of cations was held constant) for several binary and multicomponent systems.

Column tests were performed by recirculating solution through the system shown in Figure 4. Typical examples of the solids loading as a function of time are shown in

Figure 6. These results indicate that mixing for 24h is more than adequate time for reaching equilibrium.

All batch test samples were mixed for 24 h on a Labquake, Labindustries, Inc., rocking shaker at 25 cycles/min and centrifuged at 5,000 rcf for 30 min before being analyzed. The batch tests were performed in triplicate and averaged to obtain the equilibrium concentrations.

The results are summarized in Table 6 and in Figures 7 through 10. The isotherms obtained by each experimental method for the binary and ternary systems are shown in Figures 7 and 8, respectively. The strontium isotherm for the Sr-Na and Sr-Cs-Na systems obtained by experimental method (1) are shown in Figure 9, and the isotherms for the Sr-Cs-Ca-Mg-Na system obtained by method (1) for two initial solution concentrations are shown in Figure 10.

A statistical analysis was performed on the individual experimental data to determine if the experimental method significantly affected the isotherm results. The analysis was performed using the Statistical Analysis System (SAS) computer program (version VMS SAS Production Release 5.18) developed by SAS Institute, Inc. The SAS program used a regression procedure to evaluate a two-way, unbalanced analysis of variance using the Scheffe's test for variability (SAS, 1985).

This analysis indicated that there was statistically no difference between the batch and column methods when the initial solution concentration was varied. However, there were differences between isotherms obtained by these two methods and those obtained by the batch method when the solids concentration was varied and the solution concentration remained constant. This held true for both monovalent-monovalent and divalent-monovalent ion exchange. The data for the binary and ternary systems showed similar trends.

Table 6. Experimental conditions for equilibrium method tests using Ionsiv EE-96

Run number	Experimental method	Exchanging cations	Amount of solids, (g)	Volume of solution (mL)	Feed comp. (*N*)
SR-1	Batch	Sr-Na	0.47	2.2 to 2.2	2.3E-06 to 0.41 Sr
SR-4	Batch	Cs-Na	0.47	2.0 to 2.1	1.0E-09 to 0.20 Cs
SR-6	Batch	Sr-Cs-Na	0.47	2.0 to 2.2	2.3E-06 to 0.43 Sr
SR-25	Batch	Sr-Na	0.005 to 0.4	10.0	2.0E-03 Sr
SR-27	Batch	Cs-Na	0.005 to 0.4	10.0	1.0E-03 Cs
SR-26	Batch	Sr-Cs-Na	0.005 to 0.4	10.0	2.0E-03 Sr, 1.0E-03 Cs
SR-23	Batch	Sr-Cs-Ca-Mg-Na	0.005 to 0.4	10.0	2.0E-03 Sr, 1.0E-03 Cs, 1.9E-03 Ca, 9.1E-04Mg
SR-34	Batch	Sr-Cs-Ca-Mg-Na	0.005 to 0.2	10.0	5.0E-04 Sr, 2.3E-04 Cs, 5.0E-4 Ca, 2.3E-04 Mg
SR-2	Column	Sr-Na	40.0	166.4	2.3E-06 to 0.43 Sr
SR-3	Column	Cs-Na	40.0	165.6	1.0E-09 to 0.20 Cs
SR-5	Column	Sr-Cs-Na	40.0	166.5	2.3E-06 to 0.43 Sr, 1.0E-09 to 0.50 Cs

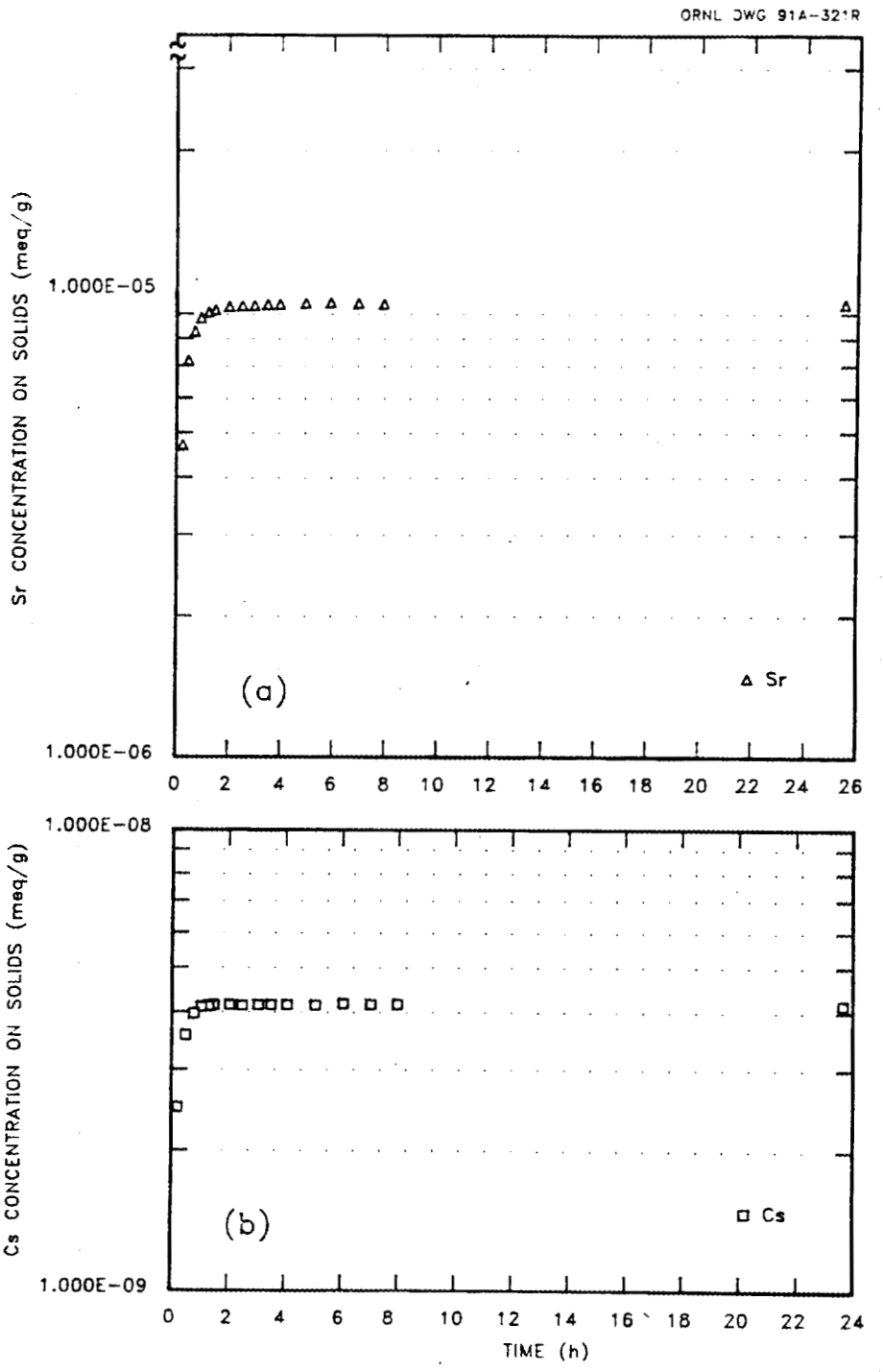

Figure 6. Experimental data from column isotherm test using Ionsiv IE-96: (a) Sr-Na and (b) Cs-Na.

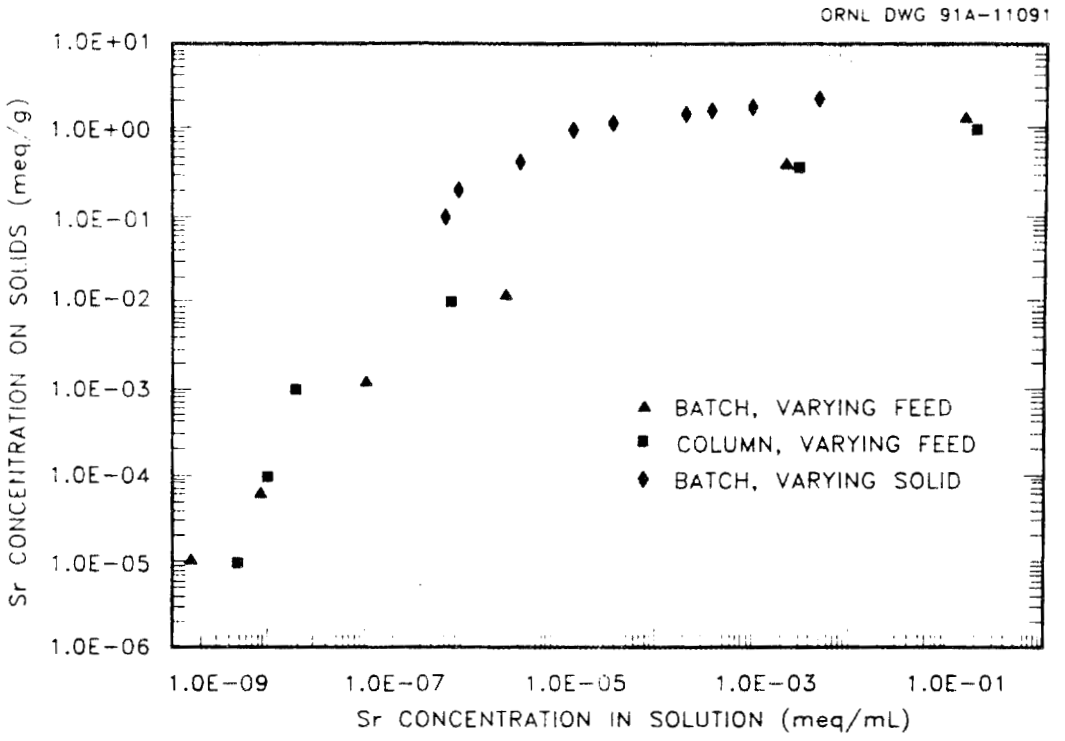

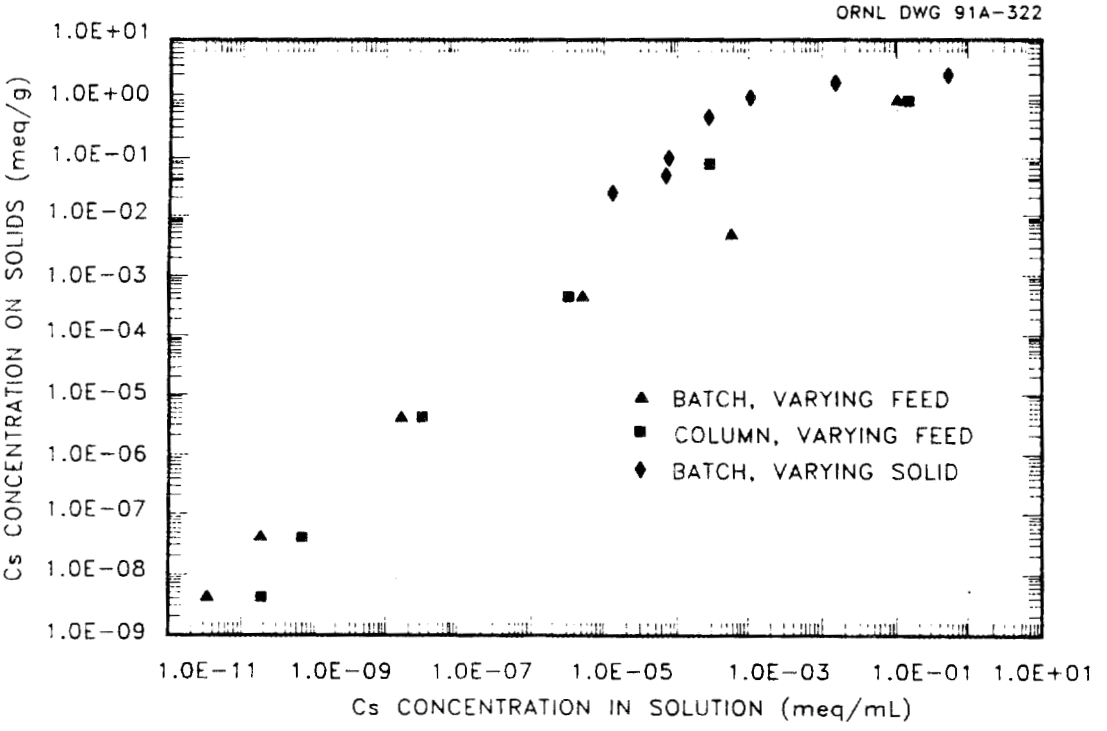

Figure 7. The effect of experimental method on binary exchange with Ionsiv IE-96: (a) Sr-Na isotherm and (b) Cs-Na isotherm.

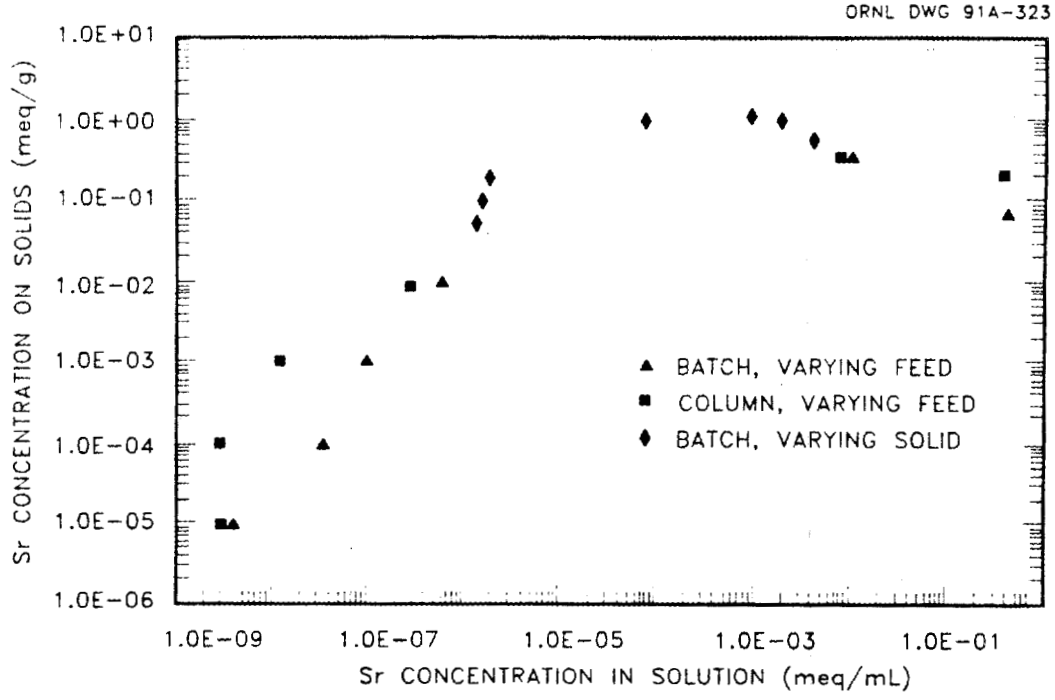

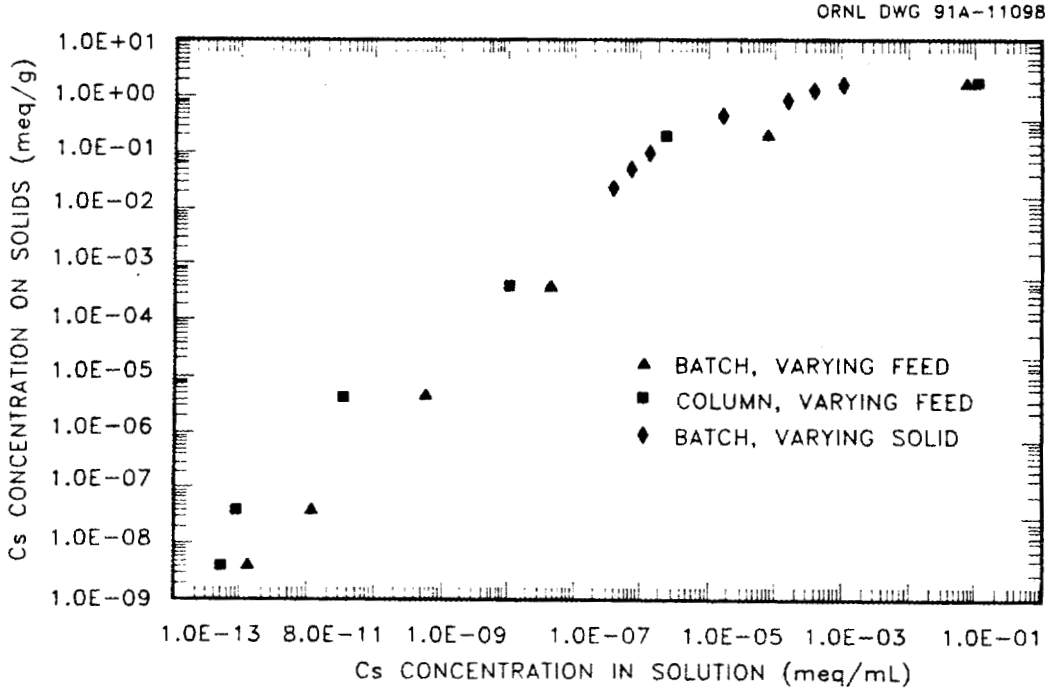

Figure 8. The effect of experimental method on ternary Sr-Cs-Na ion exchange with Ionsiv IE-96: (a) Sr isotherm and (b) Cs isotherm.

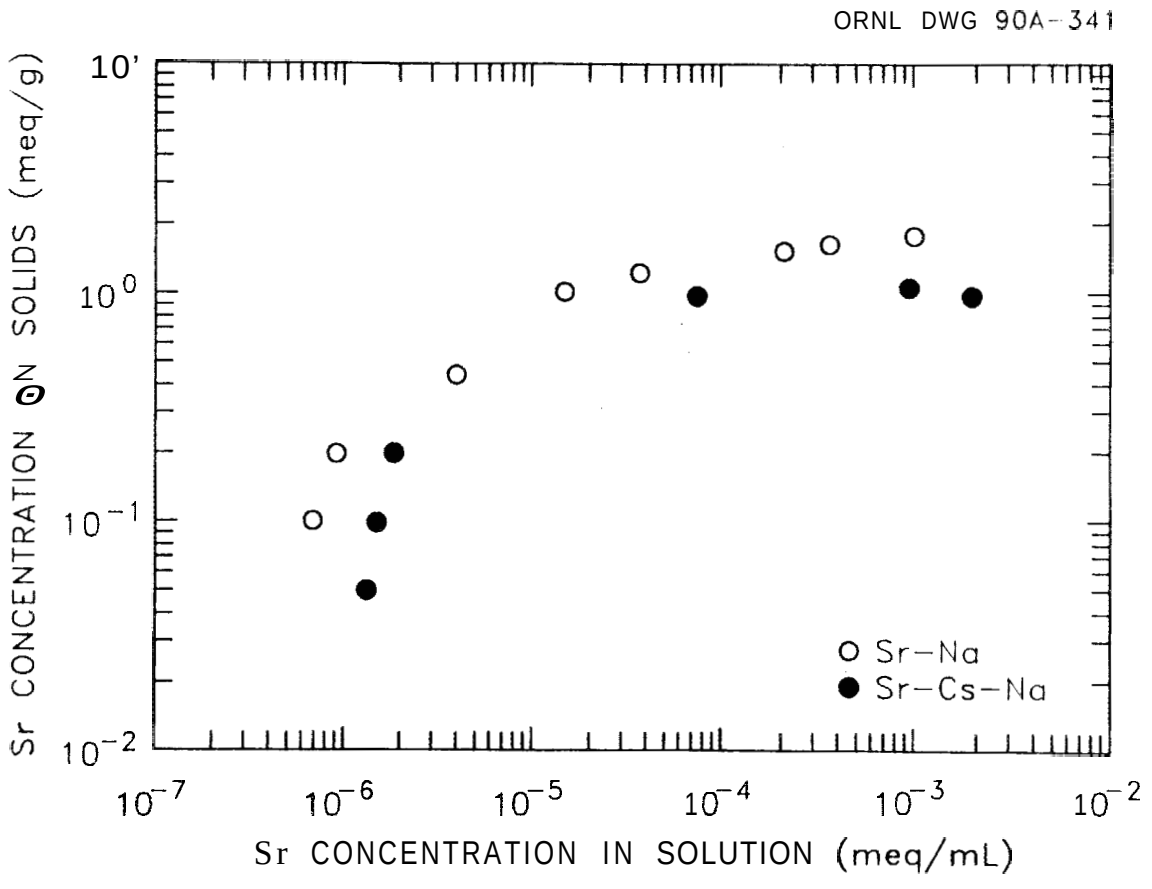

Figure 9. Strontium isotherms for binary and ternary systems using Ionsiv IE-96.

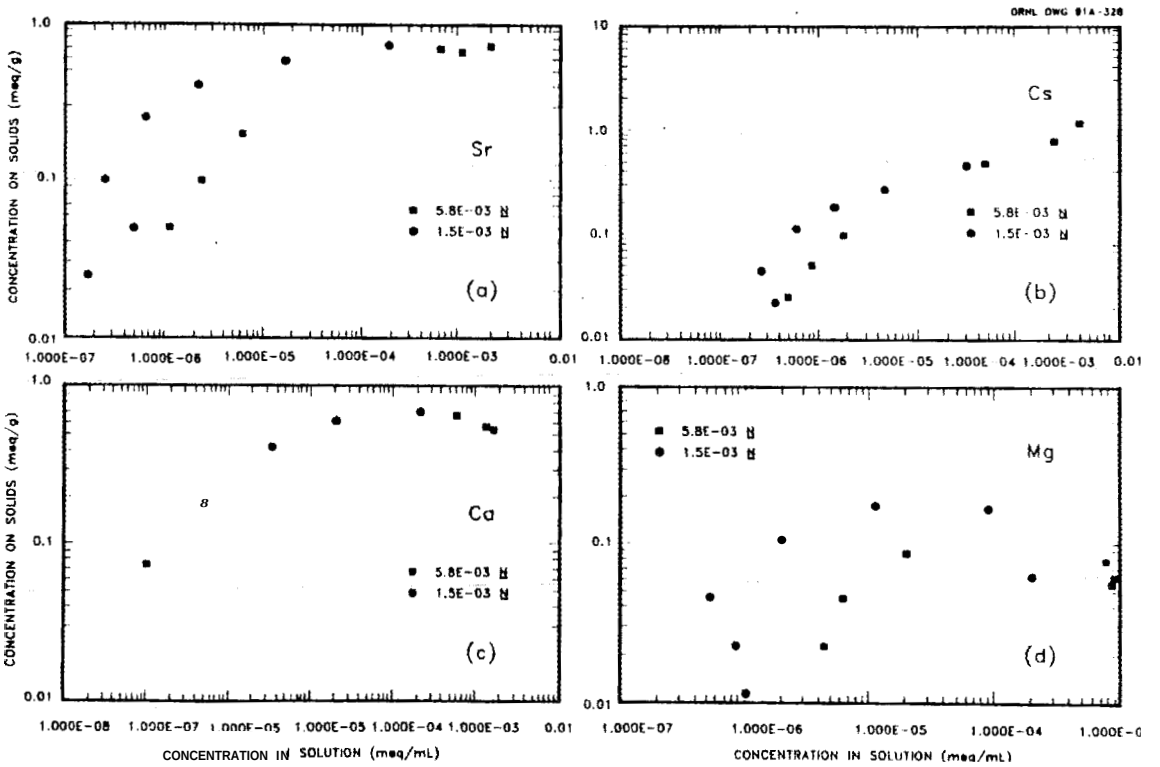

Figure 10. Effect of initial solution concentration on Sr-Cs-Ca-Mg-Na ion exchange with Ionsiv IE-96: (a) Sr isotherm; (b) Cs isotherm; (c) Ca isotherm and (d) Mg isotherm.

The results indicate that the initial concentration of cations, the total solution concentration, and the solid-to-liquid ratio will effect the equilibrium results for multicomponent systems. These data are consistent with earlier findings for nonideal multicomponent ion-exchange systems (Cremmers, 1977; Sherman, 1978; Ausikaitis, 1984; Loizidou and Townsend; 1987; Barri and Rees, 1980a).

Based on the results from these tests, a standard method was adopted for obtaining isotherms for modeling purposes. A batch process was used in which the solution phase volume was held constant at 10 mL and the solids concentration was varied between 0.002 and 0.4 g. The zeolite was washed with distilled water until the solution contained approximately 2 mg/L Na and air dried prior to use. The solution and solids were contacted for 24 h to obtain each isotherm point. The initial concentrations of the exchanging cations in the solution phase were equal to the values listed in Table 7. This is consistent with the methods used by previous researchers who noted experimental effects on isotherm results (Sherman, 1978; Singhal, 1978; Loizidou and Townsend, 1987; Barri and Rees, 1980b).

5.2 Binary and Multicomponent Isotherms

The isotherm data obtained from the standard method described in Section 5.1 are summarized in Table 8 and in Figures 11 and 12. The binary systems are shown in Figure 11, while the multicomponent systems are in Figure 12. Figure 12 has isotherms for both IE-90 and IE-96. Triplicate samples were analyzed to obtain each isotherm point. Standard deviations were typically less than 1%. However, the repeatability was considerably worse for samples with concentrations near the detection limits of the analytical equipment. The maximum standard deviation of all samples was 110%, and the average was 7%. Equilibrium was reached quickly, that is, greater than 90% equilibrium in less than 1 h and at least 99.7%

Table 7. Initial solution phase concentration for isotherm tests

Cation	Concentration (*N*)
Sr	2.0E-03
Cs	1.0E-03
Ca	2.0E-03
Mg	8.0E-04
Na	0

Table 8. Summary of equilibrium data using standard equilibrium method

Run	Exchanging cations	Liquids to solids ratio (mL/g)	Total solution concentration *N*		Na concentration in solution phase, *N*		Solids loading
			Initial[a]	Final[b]	Measured	Calculated	meq/g[c]
SR-25	Sr-Na	1953	2.00E-03	2.08E-03	9.88E-04	8.99E-04	1.76
		993	2.00E-03	2.13E-03	1.76E-03	1.64E-03	1.63
		846	2.00E-03	—[d]	—	—	1.51
		612	2.00E-03	—	—	—	1.20
		504	2.00E-03	2.24E-03	2.23E-03	1.98E-03	1.00
		216	2.00E-03	—	—	—	0.43
		99	2.00E-03	2.28E-03	2.28E-03	2.00E-03	0.20
		50	2.00E-03	2.35E-03	2.35E-06	2.00E-03	0.10
SR-27	Cs-Na	1925	1.00E-03	1.02E-03	8.77E-04	8.58E-04	1.66
		1014	1.00E-03	1.03E-03	1.02E-03	9.91E-04	1.00
		500	1.00E-03	1.03E-03	1.03E-03	1.00E-03	0.50
		99	1.00E-03	1.10E-03	1.10E-03	1.00E-03	0.10
		50	1.00E-03	1.12E-03	1.12E-03	1.00E-03	0.05
		25	1.00E-03	1.29E-03	1.29E-03	1.00E-03	0.03
SR-17	Ca-Na	3498	1.93E-03	—	—	—	1.69
		1318	1.93E-03	—	—	—	1.42
		901	2.10E-03	—	—	—	1.46
		667	1.93E-03	—	—	—	1.24
		478	2.10E-03	—	—	—	1.00
SR-18	Mg-Na	2484	8.18E-04	—	—	—	0.82
		2206	8.40E-04	—	—	—	1.06
		1274	8.18E-04	—	—	—	0.71
		1012	8.40E-04	—	—	—	0.78
		508	8.40E-04	—	—	—	0.43

Table 8 (continued)

Run	Exchanging cations	Liquids to Solids ratio/mL/g	Total Solution Concentration, *N*		Na concentration in solution phase, *N*		Solids loading
			Initial[a]	Final[b]	Measured	Calculated	meq/g[c]
SR-23	Sr-Cs-Ca-Mg-Na	1955	5.76E-03	5.89E-03	1.36E-03	1.27E-03	2.49
		1012	5.76E-03	5.73E-03	1.96E-03	2.03E-03	2.05
		504	5.76E-03	5.74E-03	3.71E-03	3.76E-03	1.89
		99	5.76E-03	5.49E-03	5.46E-03	5.73E-03	0.57
		50	5.76E-03	5.53E-03	5.52E-03	5.75E-03	0.29
		25	5.76E-03	5.47E-03	5.46E-03	5.75E-03	0.14
SR-35[e]	Sr-Cs-Ca-Mg-Na	2612	5.88E-3	-	-	-	2.27
		1337	5.88E-3	-	-	-	2.40
		893	5.88E-3	-	-	-	2.25
		542	5.88E-3	-	-	-	2.06
		220	5.88E-3	-	-	-	1.25
		110	5.88E-3	-	-	-	0.65
		55	5.88E-3	-	-	-	0.32

[a] Total cation concentration in feed.
[b] Total cation concentration in solution phase at equilibrium.
[c] Based on total solids (zeolite crystal plus clay binder). Solid material is Ionsiv IE-96 unless otherwise noted.
[d] Sodium concentration not measured.
[e] Ionsiv IE-90 used.

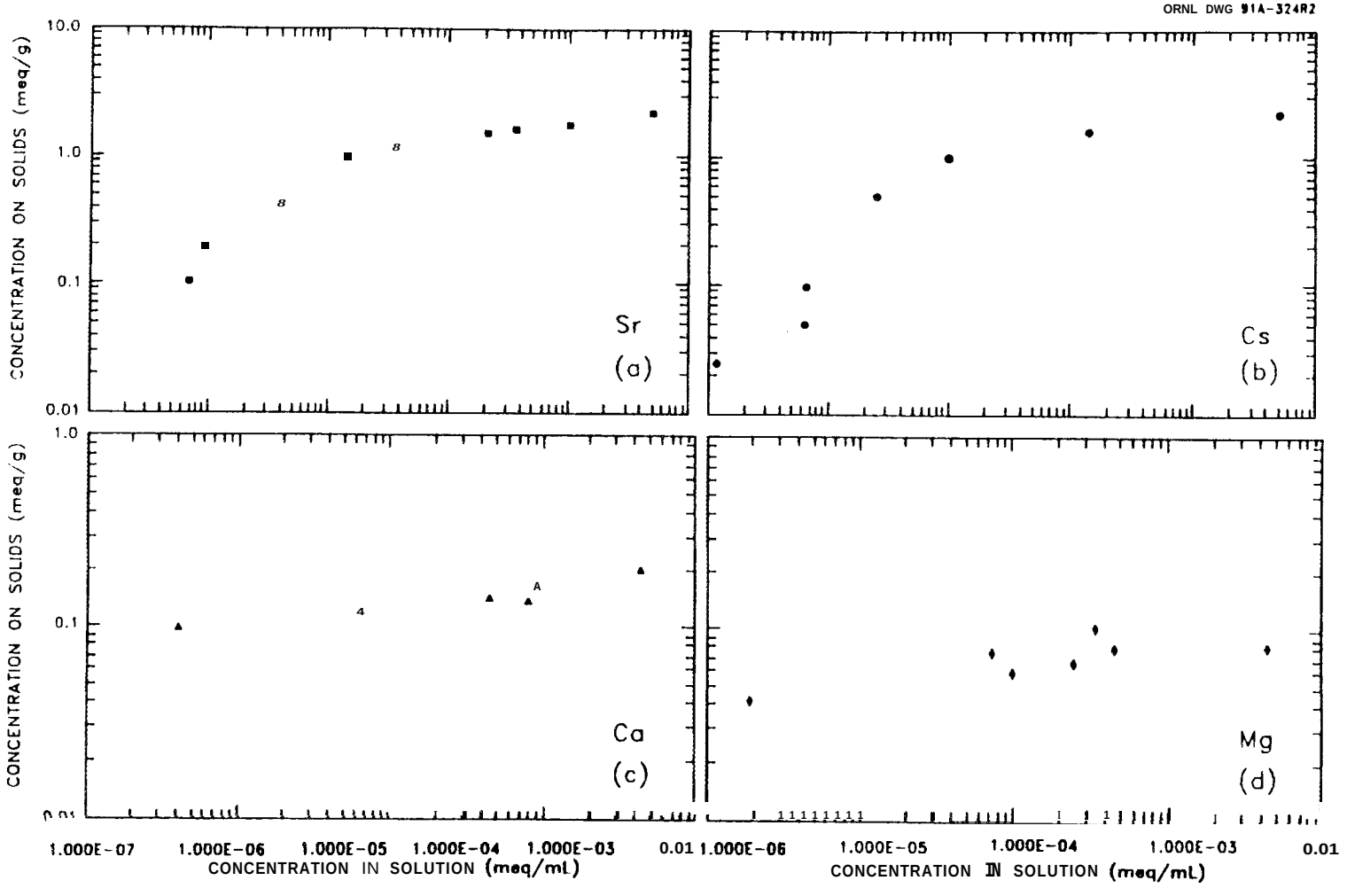

Figure 11. Isotherms for binary exchange with **Ionsiv IE-% (a) Sr-Na; (b) Cs-Na; (c) Ca-Na and (d) Mg-Na.**

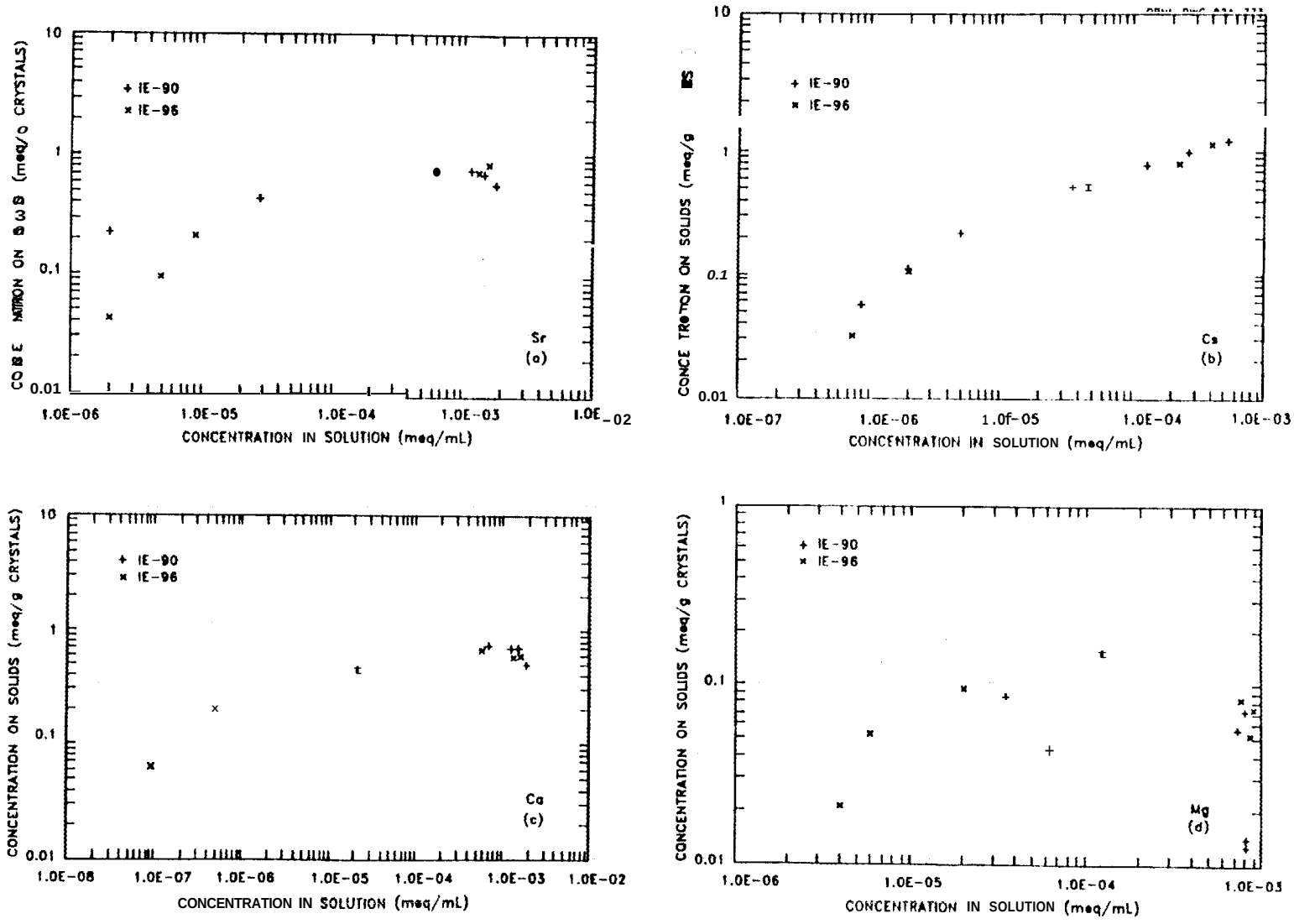

Figure 12. Isotherms for Sr-Cs-Ca-Mg-Na ion exchange.

equilibrium after 5 h. Maximum zeolite loadings of 96% of the total ion-exchange capacities were obtained in the equilibrium tests. Mass balances were performed on the solution phase to ensure that stoichiometry of exchange was established. Experimental errors were typically less than 10%. Therefore, the possibility of complications due to adsorption is eliminated.

The data indicate that Ionsiv IE-96 has the following selectivity order Cs>Sr>Ca>Mg>Na and that the zeolite is selective for the entering cations over sodium for the solution composition range tested. The binary isotherms are "favorable" for uptake of the sorbates.

In the multicomponent systems, the shapes of the isotherms for the cation with the highest selectivity were similar to those of the corresponding binary isotherms. However, cation interactions affected the isotherms for the cations with lower selectivities, and these cations were displaced when the solution concentration increased relative to the available exchange sites. This occurrence was more pronounced with decreasing selectivity and resulted in a magnesium isotherm with a convex shape. Slight displacement of strontium and calcium occurred at the highest loadings tested. Figure 12 shows that the isotherms for IE-90 and IE-96 are not significantly different when the amount of binder in IE-90 is taken into account. Therefore, the same isotherm equations will be used for both materials.

5.3 Isotherm Equations

Standard isotherm equations were used to model the data. The binary data were modeled using Equations 5-7. The Dubinin-Polyani equation was solved for k and q_s by substituting values for R, T, and c_s into Equation 7. Values for c_s, the solubility of the salt in water, were obtained from the literature (Nemeth, 1975): 15.9 meq/mL for calcium, 11.4 meq/mL for cesium, 11.4 for magnesium, and 7.0 for strontium.

The constants for the binary isotherm equations were determined from the isotherm data by multiple linear regression analyses using SAS (1985). The coefficient of determination, commonly called R^2, or the error variance was used to determine the adequacy of the model. The coefficient of determination measures how much variation in the dependent variable is due to the model. It is the ratio of the sums of squares of error due to the model divided by the sum of the squares for the total error (Afifi and Azen, 1979). An estimate of the error variance is the error sum of squares divided by the error degrees of freedom.

The coefficients and R^2 values for each binary isotherm model are given in Table 9. An example of how well the models fit the strontium binary isotherm is shown in Figure 13. The results indicate that all of the models fit the data. The Langmuir model, the best equation for fitting the data for all four systems, as is shown in Figure 14.

In theory, k and q_s calculated from Equation 7 should be independent of the exchanging cation (Noll, 1992). However, the ideal application of this theory requires that both the exchange material and cation be completely nonpolar. The nonidealities in the systems tested account for the variability of the coefficients.

Turning to the multicomponent systems, isotherm equations were tested for the equilibrium data that had been obtained experimentally. Predictive models were obtained using the multicomponent Langmuir, Freundlich, Langmuir-Freundlich, and the IAST models. When the coefficients for the binary isotherms were substituted into Equations 8, 9, 10, 11, 12, and 14, the results did not accurately predict the experimental multicomponent data.

These results indicate that the multicomponent data in this study cannot be predicted from binary data using standard isotherms. Rigorous thermodynamic or empirical equations

Table 9. Model parameters for binary isotherms

Model	Coefficient	Units	Binary isotherm			
			Sr-Na	Cs-Na	Ca-Na	Mg-Na
Langmuir[a]	a	mL/g	173,702	157,009	456,942	481,696
	b	mL/meq	98,176	68,574	221,015	610,790
	R^2	—	0.95	0.94	0.67	0.78
Freundlich[b]	k	mL/meq	18.81	55.98	3.050	1.696
	n	—	0.3183	0.4399	0.0926	0.0977
	R^2	—	0.84	0.80	0.92	0.65
Dubinin-Polyani[c]	q_m	meq/q	6.24	13.3	1.27	2.28
	k	—	3.92E-08	5.00E-08	1.18E-08	1.13E-08
	R^2	—	0.90	0.87	0.70	0.88

[a] See Equation 5.
[b] See Equation 6.
[c] See Equation 7.

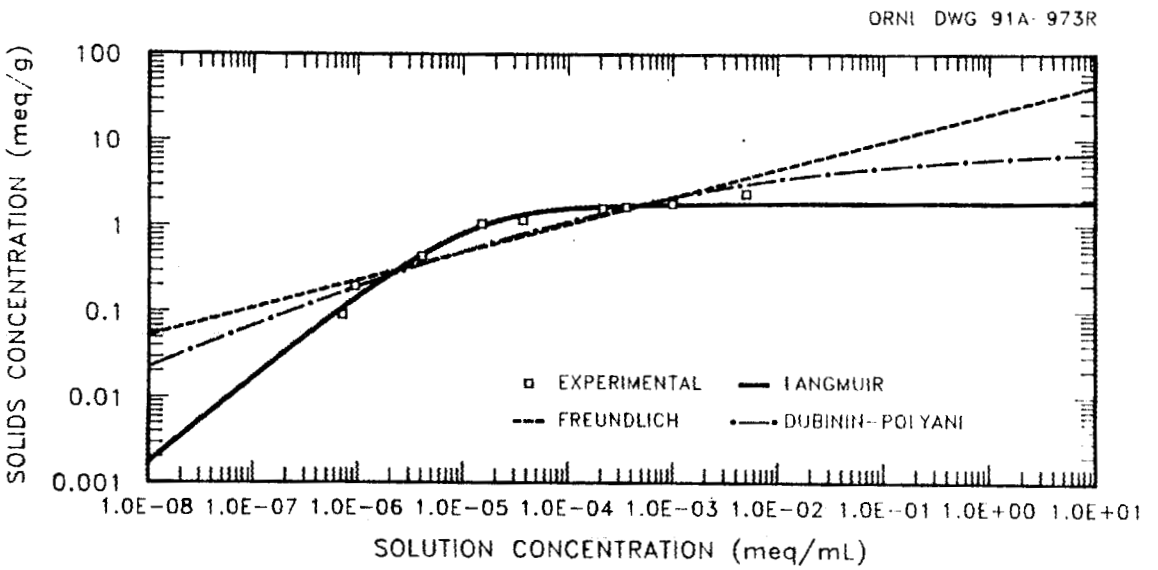

Figure 13. Example models for binary Sr-Na ion-exchange isotherm with Ionsiv IE-96.

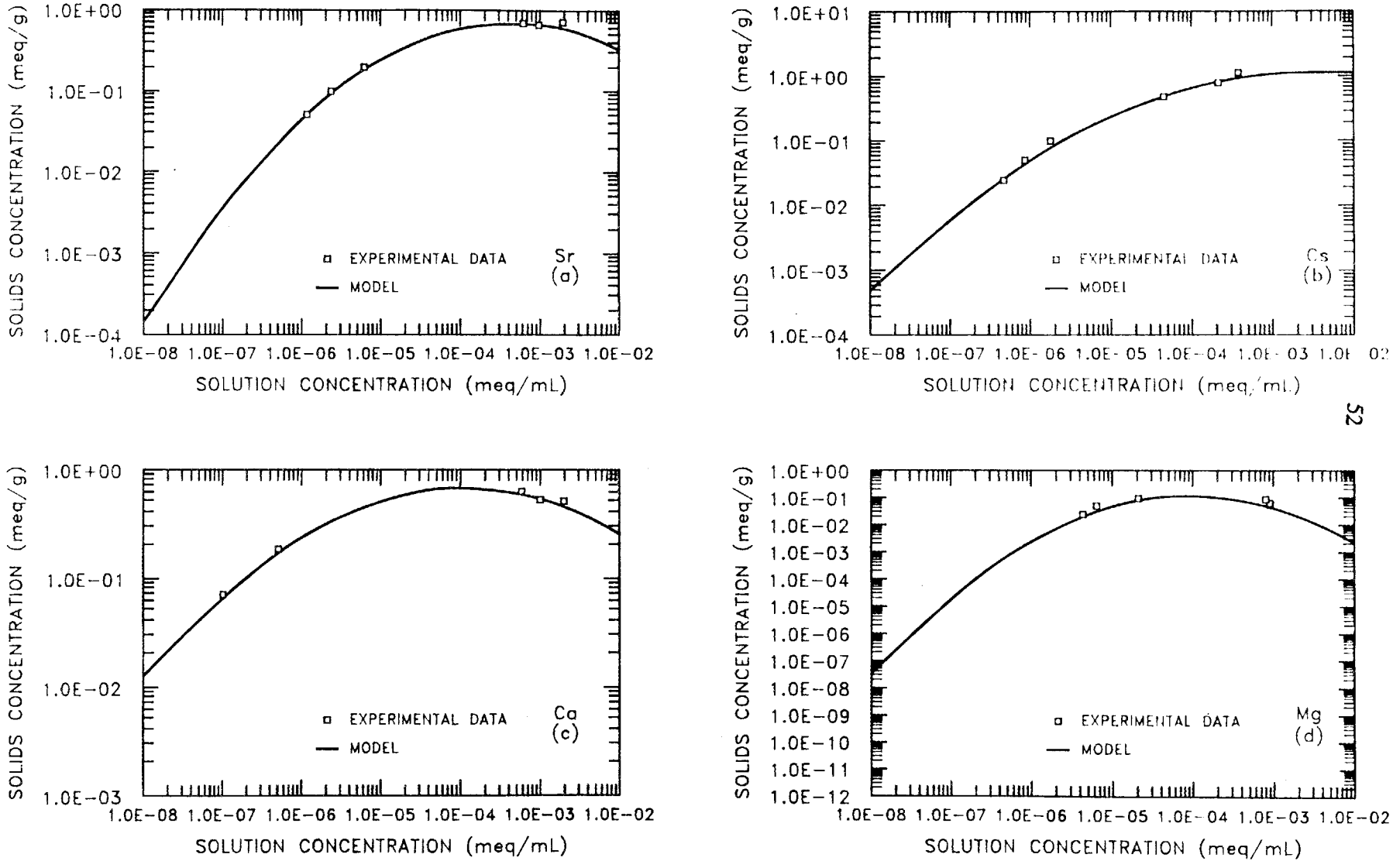

Figure 14. Langmuir models for the binary data with Ionsiv IE-96: (a) strontium isotherm; (b) cesium isotherm; (c) calcium isotherm and (d) magnesium isotherm.

will be required to model the multicomponent data. Both approaches were evaluated in this study.

Several empirical equations were fit to the multicomponent equilibrium data. The constants for these equations were determined by linear or nonlinear regression subroutines using the SAS computer program (SAS, 1985). The equations tested had the basic forms of Equations 8, 9, 12, and 13. A modified version of the Dubinin-Polyani equation was also tested:

$$q_i = exp\{b_0 + b_1 \times ln(c_i) + b_2 \times [ln(c_i)]^2\}. \tag{15}$$

The Dubinin-Polyani equation was solved for b_0, b_1, and b_2. This form of the equation is referred to as the modified Dubinin-Polyani equation in the remainder of this report. If the systems are ideal, Equations 10, 11, and 15 should be equal, resulting in the relationships between q_s, k, b_0, b_1, and b_2 given in Equation 11. However, the values for the k calculated by the two methods were off by an order of magnitude. This is not surprising since the Dubinin-Polyani theory could not account for the nonidealities associated with the binary systems. Typical examples of empirical fits to the data are shown in Figure 15.

Of the equations tested, Equation 15 fit the data most accurately with the least number of experimentally determined coefficients. The parameters for this equation are listed in Table 10. The resulting models are shown in Figure 16. The modified Dubinin-Polyani isotherm equation is semi-empirical, but it is theoretically sound since the Dubinin-Polyani model has a thermodynamic basis. It is a simple equation that can be modeled with a minimum amount of experimental data. The author considers it to be superior to Equation 13 which has been used by the majority of researchers to date to model highly nonlinear isotherms. This preference exists because Equation 13 is an empirical equation that requires

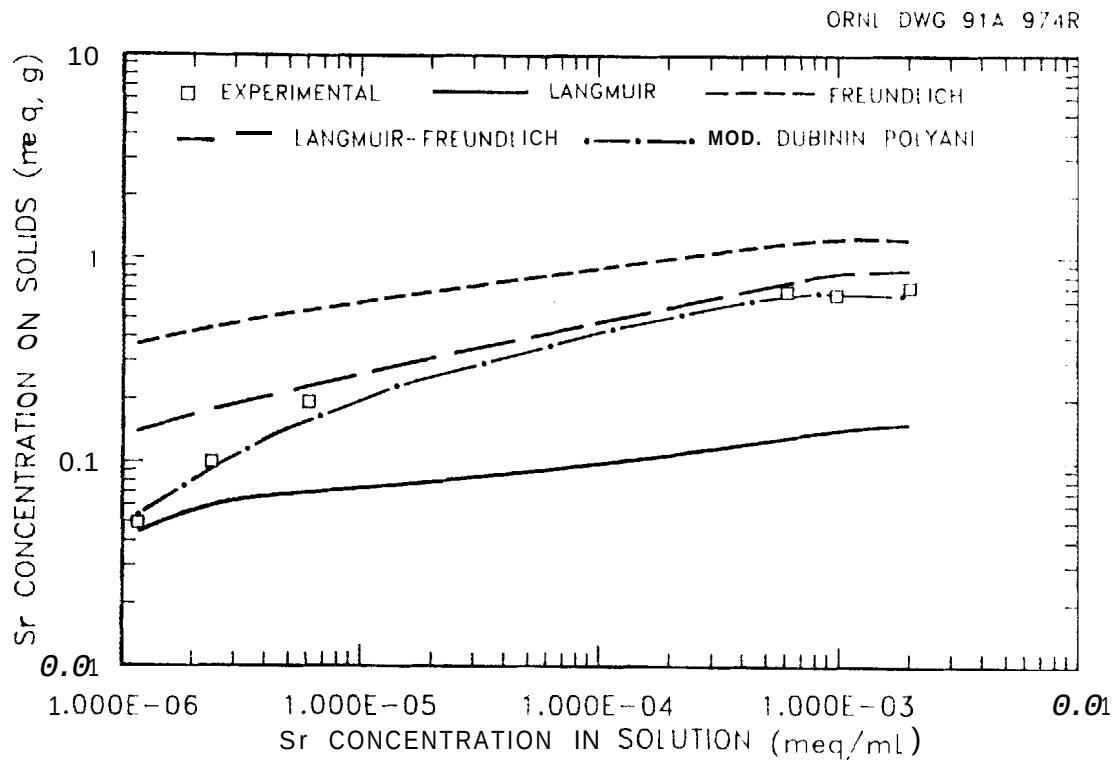

Figure 15. Example models for Sr isotherm for Sr-Cs-Ca-Mg-Na ion exchange with Ionsiv IE-%.

Table 10. Parameters for modified Dubinin-Polyani isotherm equation

Isotherm	Coefficients[a]			
	b_0	b_1	b_2	R^2
Sr isotherm	-4.742	-1.157	-0.07507	0.99
Cs isotherm	-1.532	-0.5890	-0.05002	0.99
Ca isotherm	-4.212	-0.8560	-0.04703	1.00
Mg isotherm	-17.28	-3.345	-0.1818	0.93

[a] See Equation 15.

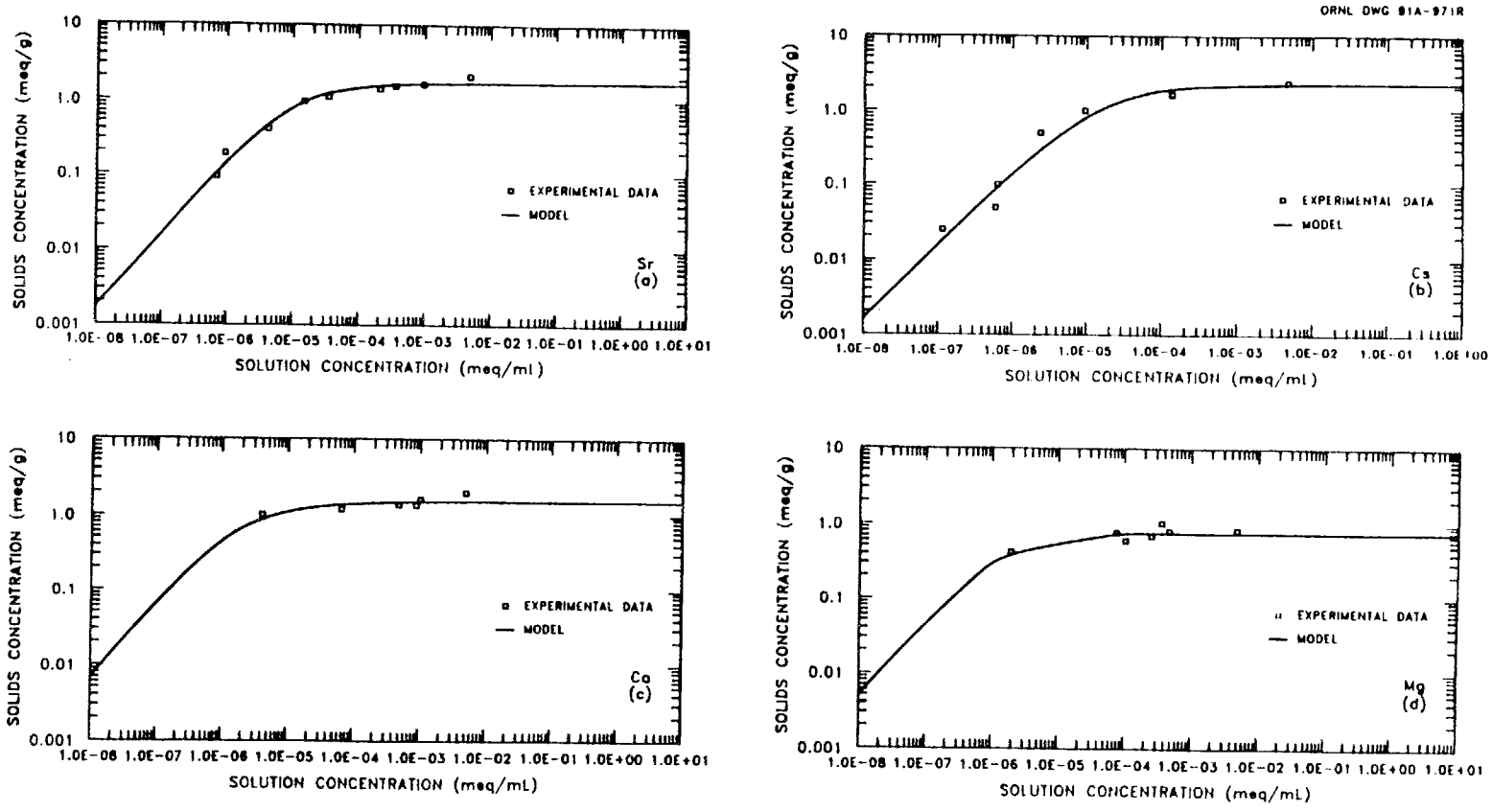

Figure 16. Modified Dubinin-Polyani models for the multicomponent data with Ionsiv IE-96: (a) strontium isotherm; (b) cesium isotherm; (c) calcium isotherm and (d) magnesium isotherm.

12 coefficients to model each isotherm for the Na-Cs-Sr-Ca-Mg system (compared to 3 for the modified Dubinin-Polyani equation).

The rigorous thermodynamic approach for predicting multicomponent equilibrium for this system has been taken by Perona (1992). The Pitzer equation was used to predict the liquid phase activity coefficients, and solid phase activity coefficients were calculated using the Wilson equation. The model is discussed in detail in Section 2.1. The error variance for Perona's model and the modified Dubinin-Polyani model are given in Table 11. Perona's model is more elaborate and does not predict the experimental data as accurately as the modified Dubinin-Polyani model . Therefore, the modified Dubinin-Polyani equation will be used in this study to evaluate a wide variety of mathematical models to determine the mass transfer mechanisms which affect the kinetics of multicomponent zeolite systems. The author recommends that Perona's model be tested in appropiate kinetics models in future studies.

Table 11. Error variances for multicomponent equilibrium models

Cation	Error Variance	
	Dubinin-Polyani model	Perona model
Sr	0.0071	0.21
Cs	0.034	0.15
Ca	0.000035	0.81
Mg	0.028	0.054

6. BATCH REACTOR KINETIC STUDIES

Experimental studies of the kinetics of ion exchange and adsorption processes can be performed in columns or batch reactors. Batch reactors have the advantage of being able to easily control the film mass-transfer resistance by the stirrer speed. At high stirrer speeds, the film mass transfer is usually assumed to be negligible (Ruthven, 1984a). (This will be supported for the present experimental system in Section 8.) Elimination of one mass-transfer mechanism simplifies the models required to determine intraparticle mass-transfer coefficients. The eliminated factors are generally easily estimated in the context of column operation and are introduced at that stage of the design. Therefore, kinetics experiments for this study were performed in the batch reactor system shown in Figure 5.

6.1 Experimental Results

Batch reactor tests were made with single- and multicomponent solutions containing Cs, Sr, Ca, and/or Mg using Ionsiv IE-90 and IE-96. Uptake data for Ionsiv IE-90, zeolite crystals, were taken to determine the impact of micropore diffusion. Experiments with Ionsiv IE-96 were made to model uptake curves from pelletized particles where both macropore and micropore diffusion occur.

The experimental data for the batch reactor kinetic experiments are given in Appendix B and are summarized in Table 12. Impeller speeds varied between 500 and 1000 rpm. Since impeller speeds did not impact the uptake rates, most experiments were performed at 750 rpm.

Experimental data from the batch reactor are summarized in Figures 17 and 18. Figure 17 shows the calcium uptake curves for different particle sizes of Ionsiv IE-96. The uptake

Table 12. Summary of batch reactor kinetic experiments

Run number	Type system	Type zeolite	Particle diameter (μm)	Solution volume (mL)	Solids weight (g)	Stirrer speed (rpm)	Initial solution concentration (meq/L)				Solids loading (meq/g)
							Sr	Cs	Ca	Mg	
SK−38	Batch	IE−90	24.00	80.45	0.0463	750.00				0.84	0.899
SK−26	Batch	IE−90	24.00	79.98	0.0471	750.00		1.01			1.630
SK−21	Batch	IE−90	24.00	80.22	0.0473	750.00			2.27		2.233
SK−39	Batch	IE−90	24.00	80.15	0.4660	750.00	1.89				1.807
SK−40	Batch	IE−90	24.00	79.96	0.0463	750.00	2.07	1.00	2.06	0.88	1.865
SK−22	Batch	IE−96	48.00	80.16	0.0478	750.00			2.34		1.840
SK−11	Batch	IE−96	545.00	80.66	0.0473	500.00			1.97		1.699
SK−9	Batch	IE−96	545.00	80.00	0.0477	1000.00			2.03		1.807
SK−14	Batch	IE−96	545.00	80.09	0.0474	750.00			1.00		1.561
SK−15	Batch	IE−96	545.00	80.28	0.0192	750.00			0.99		1.698
SK−41	Batch	IE−96	545.00	79.84	0.0468	750.00			1.92		1.516
SK−19	Batch	IE−96	545.00	80.52	0.0473	750.00				0.82	0.599
SK−18	Batch	IE−96	545.00	80.36	0.0472	750.00		1.01			1.591
SK−16	Batch	IE−96	545.00	80.46	0.0473	750.00	2.04				1.773
SK−34	Batch	IE−96	545.00	79.74	0.0471	750.00	2.05	1.00	2.35	0.89	1.965

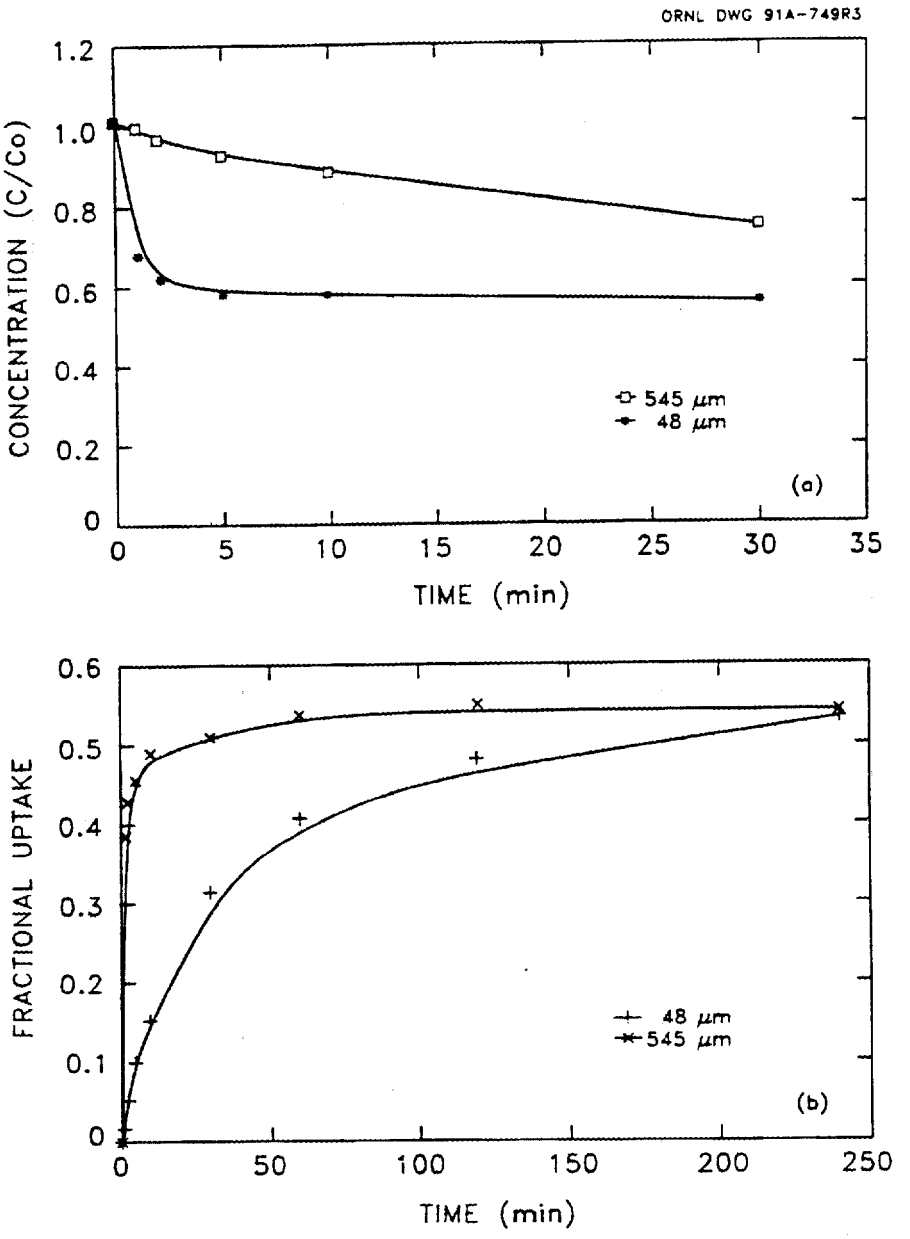

Figure 17. Effect of particle size on uptake rate for a batch reactor using $CaCl_2$ feed and Ionsiv IE-96: (a) solution phase and (b) solids phase.

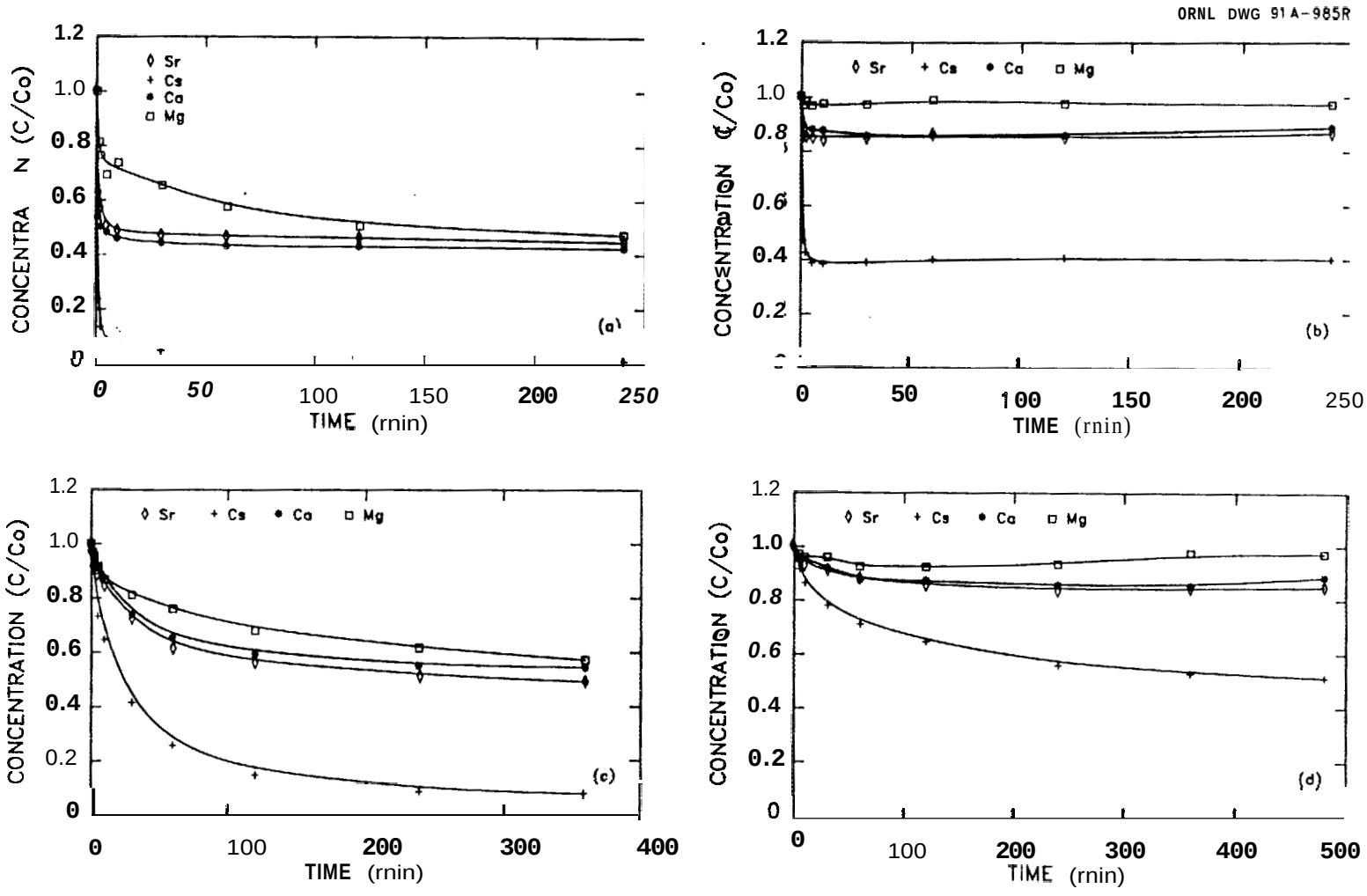

Figure 18. Uptake rates for batch reactor tests: (a) IE-90 binary systems; (b) IE-90 multicomponent system; (c) IE-96 binary systems and (d) IE-96 multicomponent system.

rate for the 48-μm diam particles was significantly faster than for the 545-μm diam particles. Since the uptake curves were a function of particle size, macropore diffusion significantly contributes to the mass-transfer resistance for Ionsiv IE-96 chabazite pellets. Figure 18 shows uptake curves with IE-90 and IE-96 for both the binary and multicomponent systems. The curves in Figure 18 fit the trends which would be expected based on the results of isotherm experiments and Figure 17. Uptake rates for the 24-μm Ionsiv IE-90 particles are significantly faster than for the 545-μm IE-96 particles. The loading for each cation is lower in the multicomponent system than in the binary systems. The selectivity for the cations is Cs>Sr>Ca>Mg>Na.

6.2 Data Evaluation

If the uptake curves in batch reactors are not a function of the stirrer speed, the film mass-transfer coefficient is usually assumed to be negligible. Ruthven (1984a) reports that this assumption is not always valid, particularly for Carberry-type batch reactors, such as the one used in this study, where the relative speed of the particles to the solution is unknown.

Although impeller speeds in this study were varied between 500 and 1000 rpm without an impact on the uptake rates, an effort was undertaken to evaluate the film mass-transfer coefficients for this system to address the above concerns.

Film mass-transfer coefficients are traditionally determined from correlations available in the literature or from modeling experimental data. Unfortunately, these correlations may been obtained experimentally from media that are significantly different from ion-exchange material (Liu and Weber, 1981; Ruthven, 1984a; Weber and Smith, 1987). Surface topography and roughness of an ion-exchange material, as well as column operating conditions, can have an impact on the value obtained for the film mass-transfer coefficients. Furthermore, no standardized criteria have been established for determining which correlation

may be best for a given system, except for hydrodynamic conditions. The applicability of such correlations for a given situation must be verified.

Film mass-transfer correlations for batch reactors have been developed using relationships based on the particle-liquid slip velocity, the relative velocity between the liquid and particles. Since the slip velocity is hard to measure, most correlations have been developed assuming a relationship between the slip velocity and the terminal velocity of free falling particles or the power input to the stirrer. Some of the more widely used correlations for batch reactors are listed below (Letterman et al., 1974; Sherwood et al., 1975; Treybal, 1980).

Treybal (1980) suggests using a correlation based on the stirrer power input:

$$Sh = 2 + 0.47 Re_p^{0.62} \left(d_i/d_t\right)^{0.17} Sc^{0.36}. \tag{16}$$

Letterman et al. (1974) suggest using one of two correlations that are based on the Gilliland-Sherwood and Froessling equations for stirrer power input, respectively:

$$Sh = 0.77 \left[\frac{P(2R_p)^4 \rho_l^{\,3}}{\mu^3}\right]^{0.159} Sc^{1/3} \tag{17}$$

and

$$Sh = 2 + 0.64 \left[\frac{P(2R_p)^4 \rho_l^{\,3}}{\mu^3}\right]^{0.197} Sc^{1/3}. \tag{18}$$

Sherwood et al. (1975) suggest using an equation developed by Ranz and Marshall (1952) that is based on the mass-transfer rates for freely falling solid spheres to calculate k_f,

$$Sh = 2.0 + 0.6\, Sc^{1/3}\, Re^{1/2}, \tag{19}$$

where the Reynolds Number is based on the terminal velocity of free-falling particles:

$$Re = \frac{G(2R_p)^3 \rho_l |\rho - \rho_l|}{18\mu^2}.$$

Researchers have indicated that film mass-transfer dominates the initial uptake rate in batch reactors (McKay and Bino, 1988; Furusawa and Smith, 1973). Since the initial portion of the uptake curve is insensitive to intraparticle mass transfer, it can be modeled by evaluating the equations for film mass transfer.

Mass balances performed on each solute in the liquid phase leads to the following relationship (Ruthven, 1984a):

$$\frac{\partial c_i}{\partial t} + \rho \left(\frac{1-\varepsilon}{\varepsilon}\right) \frac{\partial \overline{q_i}}{\partial t} = 0. \tag{20}$$

The mass transfer from the liquid phase to the solid phase is modeled by the mass transfer across the liquid film surrounding the ion-exchange particles (Ruthven, 1984a):

$$\frac{\partial \overline{q_i}}{\partial t} = \frac{3}{\rho R_p} k_{fi} (c_{di} - c_{si}). \tag{21}$$

Since the initial portion of the uptake curve is insensitive to intraparticle mass transfer, the value of k_f can be obtained by solving Equations 20 and 21 assuming c_s and $\partial c/\partial t$ are zero as t approaches zero. Under these conditions,

$$k_{fi} = -\left(\frac{\varepsilon}{1-\varepsilon}\right) \frac{R_p}{3} \frac{\Delta(c_{di}/c_{0i})}{\Delta t} \Big|_{t=0}. \tag{22}$$

This approach to determining k_f is often known as the initial slope method.

The film mass-transfer coefficients estimated using the correlations given in Equations 16-19 and Equation 22 are shown in Table 13. The correlations predicted k_f values in the

Table 13. Film mass-transfer coefficients for the batch reactor

Cation	Exchanger	Particle size (μm)	k_f (cm/s)					
			Treybal (Eq. 16)	Gilliland-Sherwood (Eq. 17)	Froessling (Eq. 18)	Sherwood, et al. (Eq. 19)	Binary data (Eq. 22)	Multicomponent data (Eq. 22)
Ca	IE-90	24	0.013	0.057	0.047	0.013	0.051	0.013
Sr	IE-90	24	0.013	0.057	0.047	0.013	0.071	0.060
Mg	IE-90	24	0.012	0.054	0.045	0.012	0.022	0.0041
Cs	IE-90	24	0.019	0.075	0.065	0.019	0.085	0.016
Ca	IE-96	545	0.0011	0.018	0.012	0.0090	0.021	0.0039
Sr	IE-96	545	0.0011	0.018	0.012	0.0090	0.018	0.0039
Mg	IE-96	545	0.0010	0.017	0.012	0.0086	0.010	0.0075
Cs	IE-96	545	0.0015	0.024	0.016	0.0120	0.026	0.0064

range of 0.001 to 0.02 cm/s for 545-μm diam particles and 0.01 to 0.08 cm/s for 24-μm diam particles. The Treybal correlation predicted substantially lower values than the other equations for the larger particles, but resulted in similar predictions for 24-μm particles.

Analysis of experimental data using Equation 22 resulted in values from 0.01 to 0.09 cm/s for binary systems and 0.004 to 0.06 cm/s for the multicomponent system. The experimentally derived k_f values were a function of the cation present and particle size. The correlations tended to underpredict k_f by factors up to 10, and the Gilliland-Sherwood correlation (Equation 17) agreed best with experimental data (Equation 22) for the binary data, while the Treybal correlation (Equation 16) agreed best with the multicomponent data. The relative magnitudes of the k_f values were consistently predicted as a function of particle size and cation present in the solution. These results indicate that correlations should be adequate for predicting mass-transfer coefficients in batch reactors.

Diffusivities can be converted to mass-transfer coefficients by (Ruthven, 1984a):

$$k_{ci} = \frac{5D_{ci}}{r_c}, \tag{23}$$

and

$$k_{pi} = \frac{5D_{pi}}{R_p} . \tag{24}$$

Typical effective micropore diffusivities in liquid systems is 10^{-6} - 10^{-10} cm^2/s; macropore diffusivities are on the order of 10^{-5} to 10^{-7} cm^2/s (Ruckenstein et al., 1971). The zeolites used in these tests had a particle radius of 0.0273 cm and a crystal radius of 0.0012 cm. Macropore mass-transfer coefficients could be on the order of 10^{-3} to 10^{-5} cm/s, and micropore mass-transfer coefficients should be on the order of 10^{-3} to 10^{-7} cm/s. Since film

mass-transfer coefficients are 10^{-1} to 10^{-2}, film mass transfer is not likely to significantly contribute to mass-transfer resistance in the batch reactor systems. This will be verified in Section 8.

7. MODEL DEVELOPMENT

Mathematical models were developed for the batch reactor systems tested in this study. The homogenous diffusion model was developed for diffusion in Ionsiv IE-90, zeolite crystals. Several versions of the heterogenous diffusion model were developed for Ionsiv IE-96, zeolite crystals pelletized in a clay binder. These generally accounted for both micro- and macropore intraparticle resistances in the zeolite pellet.

Ion exchange is considered for a finite bath reactor with liquid containing a number of dissolved components diffusing into particles which are suspended in the liquid by agitation so that the liquid has free access to them. The liquid concentration is assumed to be uniform throughout the reactor, except for the thin liquid film immediately surrounding the particles. The zeolite is modeled as an assembly of spherical macroporous adsorbent particles comprised of small spherical microporous particles of uniform size.

All the mathematical models assume that the ion-exchange rate is much faster than the rate of diffusion. Therefore, the reaction rate does not significantly affect the kinetics of the system. The system is isothermal (Liapis and Crosser, 1982). Local equilibrium is assumed to exist between the liquid and solid at the particle surface and at the pore surfaces in the macropores. The Langmuir isotherm is used to represent the equilibrium relationship for binary systems, and the modified Dubinin-Polyani model (Equation 15) is used for the multicomponent system. Mutual interactions that might occur in the multicomponent case are taken into account only through the isotherm equation.

Several parameters were varied to determine their applicability to the chabazite system. These included mass transfer across a stagnant film of liquid surrounding each particle, intraparticle diffusion (macro- and micropore diffusion) occurring in parallel and series, and

the concentration dependence of diffusivities. The models are developed in detail in Appendixes D and E and are summarized below.

7.1 Homogenous Diffusion Model

The homogenous diffusion model assumes that the particle is a homogeneous solid through which diffusion can be modeled by a single solid-phase diffusivity. Diffusion in the zeolite crystal is assumed to follow Fick's law. The differential mass balance for each species i in the crystal gives:

$$\frac{\partial q_i}{\partial t} = \frac{1}{r^2}\frac{\partial}{\partial r}\left(r^2 D_{ci}\frac{\partial q_i}{\partial r}\right). \tag{25}$$

If the micropore diffusivity is concentration dependent, it follows Darken's law:

$$D_{ci} = D_{0i}\frac{d\ln c_{si}}{d\ln q_i}, \tag{26}$$

where D_0 is independent of concentration. For the Langmuir isotherm, Equation 5, this gives:

$$D_{ci} = \frac{D_{0i}}{\left(1 - \frac{b_i q_i}{a_i}\right)}. \tag{27}$$

For the modified Dubinin-Polyani isotherm, Equation 15,

$$D_{ci} = \frac{D_{0i}}{\sqrt{b_{1i}^2 - 4b_{2i}(b_{0i} - \ln q_i)}} \tag{28}$$

is obtained.

The overall mass balance leads to:

One boundary condition is set because the symmetry of the system:

$$\frac{\partial c_{di}}{\partial t} + \frac{3\rho(1-\varepsilon)}{\varepsilon r_c^3}\frac{\partial}{\partial t}\int_0^{r_c} q_i r^2 dr = 0. \tag{29}$$

$$\frac{\partial q_i}{\partial r} = 0 \quad at\ r = 0. \tag{30}$$

A material balance at the particle surface leads to the second boundary condition:

$$\frac{\partial}{\partial t}\int_0^{r_c} q_i r^2 dr = \frac{k_{fi} r_c^2}{\rho}(c_{di} - c_{si}). \tag{31}$$

Also, c_s is in equilibrium with the solid at the particle surface. If film mass transfer is insignificant, c_s becomes equal to c_d. Under these conditions, q at r_c is in equilibrium with c_d. The initial conditions are:

$$c_{di} = c_{0i},\ c_{si} = q_i = 0 \quad at\ t = 0. \tag{32}$$

Equations 25 through 32 can be rewritten in dimensionless form by letting $C = c/c_0$, $Q = q/q_0$, and $\bar{r} = r/r_c$, where q_0 is in equilibrium with c_0:

$$\frac{\partial Q_i}{\partial t} = \frac{1}{r_c^2 \bar{r}^2}\frac{\partial}{\partial \bar{r}}\left(\bar{r}^2 D_{ci}\frac{\partial Q_i}{\partial \bar{r}}\right) \tag{33}$$

for the solid phase mass balance;

$$D_{ci} = \frac{D_{0i}}{\left(1 - \frac{b_i Q_i q_{0i}}{a_i}\right)} \tag{34}$$

for the Langmuir isotherm;

$$D_{ci} = \frac{D_{0i}}{\sqrt{b_{1i}^2 - 4b_{2i}[b_{0i} - \ln(Q_i q_{0i})]}} \tag{35}$$

for the modified Dubinin-Polyani isotherm;

$$\frac{\partial C_{di}}{\partial t} = \frac{-3\rho(1 - \varepsilon)q_{0i}}{\varepsilon c_{0i}} \frac{\partial}{\partial t}\int_0^1 Q_i \bar{r}^2 d\bar{r} \tag{36}$$

for the overall mass balance; and

$$\frac{\partial Q_i}{\partial \bar{r}} = 0 \quad at\ \bar{r} = 0, \tag{37}$$

$$\frac{\partial}{\partial t}\int_0^1 Q_i \bar{r}^2 d\bar{r} = \frac{k_{fi} c_{0i}}{\rho r_c q_{oi}}(C_{di} - C_{si}), \tag{38}$$

and

$$C_{di} = 1,\ C_{si} = Q_i = 0 \quad at\ t = 0 \tag{39}$$

for the boundary and initial conditions, respectively.

Equations 33 through 39 are in a form that is amenable to numerical solution using orthogonal collocation to convert the PDEs into ODEs, and solving ODEs by numerical methods (Friedman, 1984). The set of nonlinear algebraic equations and ODEs were solved using a program written in Fortran IV language and run on a VAX computer system at ORNL.

The double precision program for the numerical method includes four major parts: (1) main program for the input, output, and the definition of the normalized terms; (2) subroutines for the orthogonal collocation procedure; (3) a subroutine for the calculation of equilibrium; and (4) subroutines for solving ODEs. The orthogonal collocation subroutines used were published by Villadsen and Michelsen (1978), Finlayson (1980), and Carnahan

(1969). The set of ODEs were solved using the August 13, 1981, version of Livermore Solver for Ordinary Differential Equations (LSODE). LSODE is a public domain software package which is based on the Gear's stiff integration algorithm (Hindmarsh, 1980). The absolute and relative tolerances of LSODE were set at 10^{-5}. An example program is given in Appendix G.

7.2 Heterogenous Diffusion Models

This model is the same as the model discussed in Section 7.1 except that dual rather than single intraparticle diffusion is assumed to occur in the zeolite particle. The rate of diffusion in the solid phase is assumed to be governed by both micropore and macropore diffusion. Micropore diffusion occurs in the zeolite crystals, and macropore diffusion occurs in the pores of the binder. Models are developed assuming these processes occur in parallel in Section 7.2.1 and in series Section 7.2.2.

7.2.1 Parallel Macropore and Micropore Diffusion.

The differential mass balance in the solid phase gives:

$$\frac{\varepsilon_p}{\rho}\frac{\partial c_{pi}}{\partial t} + (1-\varepsilon_p)\frac{\partial q_i}{\partial t} = \frac{1}{R^2}\frac{\partial}{\partial R}\left[R^2\left((1-\varepsilon_p)D_{ci}\frac{\partial q_i}{\partial R} + \frac{\varepsilon_p D_{pi}}{\rho}\frac{\partial c_{pi}}{\partial R}\right)\right] . \quad (40)$$

The overall mass balance leads to:

$$\frac{\partial c_{di}}{\partial t} + \frac{3\rho(1-\varepsilon)}{\varepsilon R_p^3}\frac{\partial}{\partial t}\int_0^{R_p}[(1-\varepsilon_p)q_i + \frac{\varepsilon_p}{\rho}c_{pi}]R^2 dR = 0 . \quad (41)$$

The boundary condition at R = 0 is:

$$\frac{\partial c_{pi}}{\partial R} = \frac{\partial q_i}{\partial R} = 0 \quad (42)$$

because of symmetry. The material balance at the particle surface leads to:

$$\frac{\partial}{\partial t}\int_0^{R_p}[(1-\varepsilon_p)q_i + \frac{\varepsilon_p}{\rho}c_{pi}]R^2dR = \frac{k_{fi}R_p^2}{\rho}(c_{di} - c_{si}). \tag{43}$$

The liquid concentrations, c_s and c_p, are in equilibrium with the solid at the particle surface and the surfaces of the pores, respectively. If film mass transfer is insignificant, c_s becomes equal to c_d. Under these conditions, Equation 43 reduces to:

$$\frac{3}{R_p^3}\frac{\partial}{\partial t}\int_0^{R_p}[(1-\varepsilon_p)q_i + \frac{\varepsilon_p}{\rho}c_{pi}]R^2dR = -\frac{\varepsilon}{(1-\varepsilon)\rho}\frac{\partial c_{di}}{\partial t}, \tag{44}$$

where q at R_p is in equilibrium with c_d. The initial conditions are:

$$c_{di} = c_{0i},\ c_{pi} = c_{si} = q_i = 0 \quad at\ t = 0. \tag{45}$$

Equations 40 through 45 can be rewritten in dimensionless form by letting $C = c/c_0$, $Q = q/q_0$, and $\bar{R} = R/R_p$, where q_0 is in equilibrium with c_{p0}:

$$\xi_i\frac{\partial C_{pi}}{\partial t} + \frac{\partial Q_i}{\partial t} = \frac{1}{R_p^2\overline{R^2}}\frac{\partial}{\partial \bar{R}}\left[\overline{R^2}\left(D_{ci}\frac{\partial Q_i}{\partial \bar{R}} + \xi_i D_{pi}\frac{\partial C_{pi}}{\partial \bar{R}}\right)\right] \tag{46}$$

for the solid phase mass balance where

$$\xi_i = \frac{\varepsilon_p c_{0i}}{(1-\varepsilon_p)\rho q_{0i}}; \tag{47}$$

$$\frac{\partial C_{di}}{\partial t} = -(1-\varepsilon_p)D_{si}\frac{\partial}{\partial t}\int_0^1(Q_i + \xi_i C_{pi})\overline{R^2}d\bar{R} \tag{48}$$

for the overall mass balance;

$$\frac{\partial C_{pi}}{\partial \overline{R}} = \frac{\partial Q_i}{\partial \overline{R}} = 0 \quad at\ \overline{R} = 0, \tag{49}$$

$$\frac{\partial}{\partial t}\int_0^1 (Q_i + \xi_i C_{pi})\overline{R}^2 d\overline{R} = \frac{k_{gi}}{D_{gi}(1-\varepsilon_p)}(C_{di}-C_{si}) \quad at\ \overline{R} = 1, \tag{50}$$

or

$$\frac{\partial}{\partial t}\int_0^1 (\frac{Q_i}{\xi_i} + C_{pi})\overline{R}^2 d\overline{R} = -\frac{\varepsilon}{3\varepsilon_p(1-\varepsilon)}\frac{\partial C_{di}}{\partial t} \tag{51}$$

if film mass transfer is negligible, and

$$C_{di} = 1,\ C_{si} = C_{pi} = Q_i = 0 \quad at\ t = 0 \tag{52}$$

for the boundary and initial conditions, respectively.

If D_c is concentration dependent, Equation 33 or 34 is incorporated into Equations 40 and 46. The PDEs in Equations 46 through 52 were converted into ODEs by orthogonal collocation. The resulting set of ODEs was solved by LSODE in a similar manner to the homogenous diffusion model described in Section 7.1.

7.2.2 Series Macropore and Micropore Diffusion.

Mass balances performed on each solute in the liquid phase leads to the following relationship:

$$\frac{\partial c_{di}}{\partial t} + \frac{\rho(1-\varepsilon)}{\varepsilon}\frac{\partial \overline{\overline{q}}_i}{\partial t} = 0, \tag{53}$$

where

$$\frac{\partial \overline{\overline{q}}_i}{\partial t} = \frac{3(1-\varepsilon_p)}{R_p^3}\int_0^{R_p} R^2 \frac{\partial \overline{q}_i}{\partial t} dR + \frac{3\varepsilon_p}{\rho R_p^3}\int_0^{R_p} R^2 \frac{\partial c_{pi}}{\partial t} dR. \tag{54}$$

The equations that represent mass transfer within the solid are:

$$\frac{\partial \overline{\overline{q}}_i}{\partial t} = \frac{3}{\rho R_p} k_{fi} (c_{di} - c_{pi}), \tag{55}$$

$$\frac{1}{R^2}\frac{\partial}{\partial R}\left(R^2 D_{pi}\frac{\partial c_{pi}}{\partial R}\right) = \frac{\partial c_{pi}}{\partial t} + \frac{\rho(1-\varepsilon_p)}{\varepsilon_p}\frac{\partial \overline{q}_i}{\partial t}, \tag{56}$$

where

$$\frac{\partial \overline{q}_i}{\partial t} = \frac{3}{r_c^3}\int_0^{r_c} r^2 \frac{\partial q_i}{\partial t} dr, \tag{57}$$

and

$$\frac{\partial q_i}{\partial t} = \frac{1}{r^2}\frac{\partial}{\partial r}\left(r^2 D_{ci}\frac{\partial q_i}{\partial r}\right). \tag{58}$$

If film mass transfer is insignificant, Equation 55 is replaced with $c_d = c_p$ at $R = R_p$.

The boundary conditions are:

$$\frac{\partial c_{pi}}{\partial R} = \frac{\partial \overline{q}_i}{\partial R} = \frac{\partial q_i}{\partial r} = 0 \ at \ R = 0, \ r = 0. \tag{59}$$

The initial conditions are:

$$c_{di} = c_{0i}, \ c_{pi} = q_i = 0 \quad at \ t = 0. \tag{60}$$

Equations 53 through 60 can be rewritten in dimensionless form as $C = c/c_0$, $Q = q/q_0$, $\overline{Q} = \overline{q}/q_0$, $\overline{\overline{Q}} = \overline{\overline{q}}/q_0$, $\overline{r} = r/r_c$, and $\overline{R} = R/R_p$, where q_0 is in equilibrium with c_{p0}:

$$\frac{\partial C_{di}}{\partial t} + \frac{\rho(1-\varepsilon)q_{0i}}{\varepsilon c_{0i}} \frac{\partial \overline{\overline{Q}}_i}{\partial t} = 0, \tag{61}$$

where

$$\frac{\partial \overline{\overline{Q}}_i}{\partial t} = 3(1 - \varepsilon_p)\int_0^1 \overline{R^2} \frac{\partial \overline{Q}_i}{\partial t} d\overline{R} + \frac{3\varepsilon_p c_{0i}}{\rho q_{0i}} \int_0^1 \overline{R^2} \frac{\partial C_{pi}}{\partial t} d\overline{R} \tag{62}$$

for the overall mass balance. The mass-transfer equations become:

$$\frac{\partial \overline{\overline{Q}}_i}{\partial t} = \frac{3c_{0i}k_{fi}}{\rho R_p q_{0i}} (C_{di} - C_{pi}), \tag{63}$$

$$\frac{1}{R_p^2\,\overline{R^2}} \frac{\partial}{\partial \overline{R}} \left(\overline{R^2}\, D_{pi} \frac{\partial C_{pi}}{\partial \overline{R}} \right) = \frac{\partial C_{pi}}{\partial t} + \frac{\rho(1-\varepsilon_p)q_{0i}}{\varepsilon_p c_{0i}} \frac{\partial \overline{Q}_i}{\partial t} \tag{64}$$

where

$$\frac{\partial \overline{Q}_i}{\partial t} = 3\int_0^1 \frac{\partial Q_i}{\partial t} \overline{r^2} d\overline{r}, \tag{65}$$

and

$$\frac{\partial Q_i}{\partial t} = \frac{1}{r_c^2 \overline{r^2}} \frac{\partial}{\partial \overline{r}} \left(\overline{r^2} D_{ci} \frac{\partial Q_i}{\partial \overline{r}} \right). \tag{66}$$

If film mass transfer is insignificant, Equation 63 is replaced with $C_d = C_p$ at $\overline{R} = 1$. Because of symmetry,

$$\frac{\partial C_{pi}}{\partial \overline{R}} = \frac{\partial \overline{Q}_i}{\partial \overline{R}} = \frac{\partial Q_i}{\partial \overline{r}} = 0 \ at\ \overline{R} = 0,\ \overline{r} = 0. \tag{67}$$

The initial conditions are:

$$C_{di} = 1,\ C_{pi} = Q_i = 0 \quad at\ t = 0. \tag{68}$$

The assumption that macropore and micropore diffusion occurs in series results in coupled PDEs involving time and spatial variables. Recently, several authors (Do and Rice, 1986; Akulov and Ustinov, 1981; Liaw et al., 1979; Rice, 1982; Rice et al., 1983; Doong and Yang, 1987; Cen and Yang, 1986; Kapoor and Yang; 1988) have simplified the mathematics by assuming that the concentration profiles in the zeolite crystals have parabolic shapes. This type of profile has been shown to be valid for binary sorption or desorption, but may not be valid for multicomponent ion exchange where ion competition occurs. If the zeolite crystal has a parabolic profile,

$$q_i = a_{0i} + a_{2i} r^2 \ where\ a_{2i} = \frac{5}{2r_c^2}(q_i|_{r_c} - \overline{q_i}), \tag{69}$$

Equations 57 and 58 become

$$\frac{\partial \overline{q_i}}{\partial t} = \frac{15D_{ci}}{r_c^2}(q_i|_{r=r_c} - \overline{q_i}). \tag{70}$$

Equations 65 and 66 become

$$\frac{\partial \overline{Q_i}}{\partial t} = \frac{15D_{ci}}{r_c^2}(Q_i|_{\bar{r}=1} - \overline{Q_i}). \tag{71}$$

If D_c is concentration dependent, Equation 34 or 35 is incorporated into Equations 58, 66, 70, and 71. Equations 61 through 71 were solved orthogonal collocation to convert the PDEs into ODEs. The resulting set of ODEs were solved by LSODE in a similar manner to the homogenous diffusion model described in Section 7.1.

7.2.3 Macropore Diffusivity Equations.

The D_p given in Equations 40, 46, 56, and 64 is an effective diffusivity. Macropore diffusivities may be due to four transport mechanisms (Ruthven, 1984a): molecular diffusion, Knudsen diffusion, Poiseuille flow, and surface diffusion. For liquid systems, diffusion due to molecular and/or surface diffusion might be expected. If the transport within the macropores occurs only by molecular diffusion, the pore diffusivity is given by

$$D_p = \frac{D_l}{\tau} \tag{72}$$

where the tortuosity factor, τ, is introduced to allow for the fact that the diffusion path through zeolite pores is greater than that of straight round tubes. Values of τ usually ranges from 2 to 6 for zeolites (Ruthven, 1984a). Values less than two indicate surface diffusion of intracrystalline diffusion is contributing to mass transfer. If surface diffusion significantly contributes to macropore diffusion, molecular and surface diffusion will occur in parallel. The effective macropore diffusivity will then be

$$D_p = \frac{D_l}{\tau} + D_s. \tag{73}$$

The surface diffusivity is generally found to be concentration dependent (Ruthven, 1984a). It was assumed to follow Darken's equation (Equations 27 and 28 for the Langmuir and modified Dubinin-Polyani equilibrium equations, respectively).

Experimental data were modeled to obtain values for D_p in Equations 40, 46, 56, and 64. Equation 73 was also substituted into Equations 40, 46, 56, and 64 assuming a tortuosity factor of two and using liquid diffusivities obtained from the literature. In the latter case, the parameter D_s was varied to obtain model results that fit the experimental data. The results of the modeling evaluation are discussed in Section 8.

8. MODELING RESULTS

The batch reactor kinetic data shown in Figure 18 were evaluated to obtain diffusivities using each of the models developed in Section 7. The calculated values for the diffusivities are given in Tables 14-16. Examples of the model results are given in Figures 19-23. The diffusivities listed in Tables 14-16 resulted in uptake curves that had standard deviations (Noll, 1992) of 1 to 4% where the standard deviation is defined as

$$\sigma = \frac{1}{N}\sum_{j=1}^{N}\left[\left(\frac{c_{j,exp} - c_{j,cal}}{c_0}\right)^2\right]^{0.5} . \tag{74}$$

These values are well within the limits of accuracy for diffusivities reported in the literature. Typical standard deviations for film mass-transfer coefficients are +\- 30%, while intraparticle diffusivity ranges are +/- 3-8% (Balzli, et al., 1978).

The Ionsiv IE-90, zeolite crystal, data were modeled using the homogenous diffusion model developed in Section 7.1 to determine the micropore diffusivities. Micropore diffusivities were obtained for both single- and multicomponent systems. The variables evaluated to determine their impact on micropore diffusivities included film mass-transfer resistance and the concentration dependence of diffusivities. The resulting diffusivities are listed in Table 14.

The effective diffusivities obtained when D_c was assumed to be constant ranged between 10^{-9} and 10^{-11} cm^2/s for single-component systems. These effective micropore diffusivities accurately predicted the experimental data as shown in Figure 19 (a). The effective micropore diffusivities generated from modeling single-component data did not

Table 14. Micropore diffusivities for Ionsiv IE-90

	Binary system		Multicomponent system	
	$D_{c,eff}$[a] (cm^2/s)	$D_{c,o}$[b] (cm^2/s)	$D_{c,eff}$ (cm^2/s)	$D_{c,o}$ (cm^2/s)
Sr	1.5E-9	6.4E-10	1.5E-9	6.4E-10
Cs	9.5E-9	4.5E-10	3.0E-9	4.5E-10
Ca	3.0E-9	9.0E-10	3.0E-10	9.0E-10
Mg	6.0E-11	1.8E-10	5.0E-10	1.8E-10

[a] Assumes micropore diffusion is not a function of solute concentration in the solid phase.
[b] Corrected diffusivity assuming micropore diffusion is a function of solute concentration in the solid phase.

Table 15. Effective micropore diffusivities for Ionsiv IE-96

	$D_{c,eff}$[a] (cm^2/s)	$D_{c,o}$[b] (cm^2/s)
Sr	1.5E-8	6.4E-9
Cs	8.0E-9	4.0E-9
Ca	9.0E-9	4.0E-9
Mg	6.0E-9	3.0E-9

[a] Assumes that micropore diffusion is not a function of solute concentration in the solid phase.
[b] Corrected diffusivity assuming micropore diffusion is a function of solute concentration in the solid phase.

Table 16. Macropore diffusivities for Ionsiv IE-96[a]

	Binary system		Multicomponent system	
	$D_{p,eff}$[b] (cm^2/s)	$D_{s,o}$[c] (cm^2/s)	$D_{p,eff}$ (cm^2/s)	$D_{s,o}$ (cm^2/s)
Sr	2.8E-4	6.0E-9	5.0E-5	6.0E-9
Cs	9.0E-4	4.0E-9	1.5E-4	4.0E-9
Ca	2.0E-4	3.0E-9	6.0E-5	3.0E-9
Mg	1.4E-4	3.5E-9	1.0E-3	3.5E-9

[a] Obtained from the series heterogenous diffusion model using the micropore diffusivities listed in Table 14.
[b] Assumes a single diffusion coefficient describes macropore diffusion.
[c] Corrected surface diffusivity assuming liquid and surface diffusion contribute to pore diffusion.

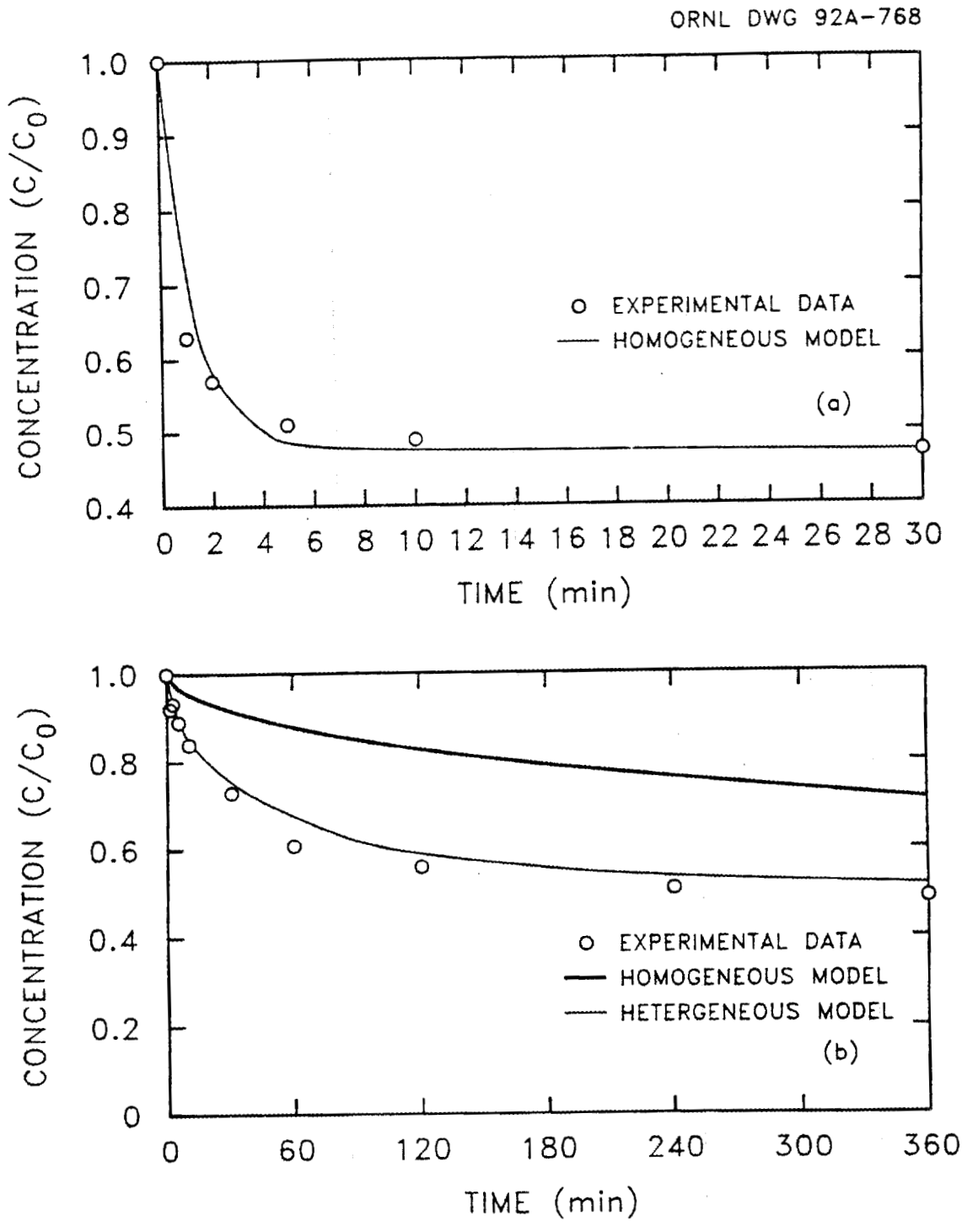

Figure 19. Models of Sr-Na uptake curves: (a) Ionsiv IE-90 using $D_{c,eff}$ or $D_{c,o}$ and (b) Ionsiv IE-96 using $D_{c,eff}$ from Ionsiv IE-90 data.

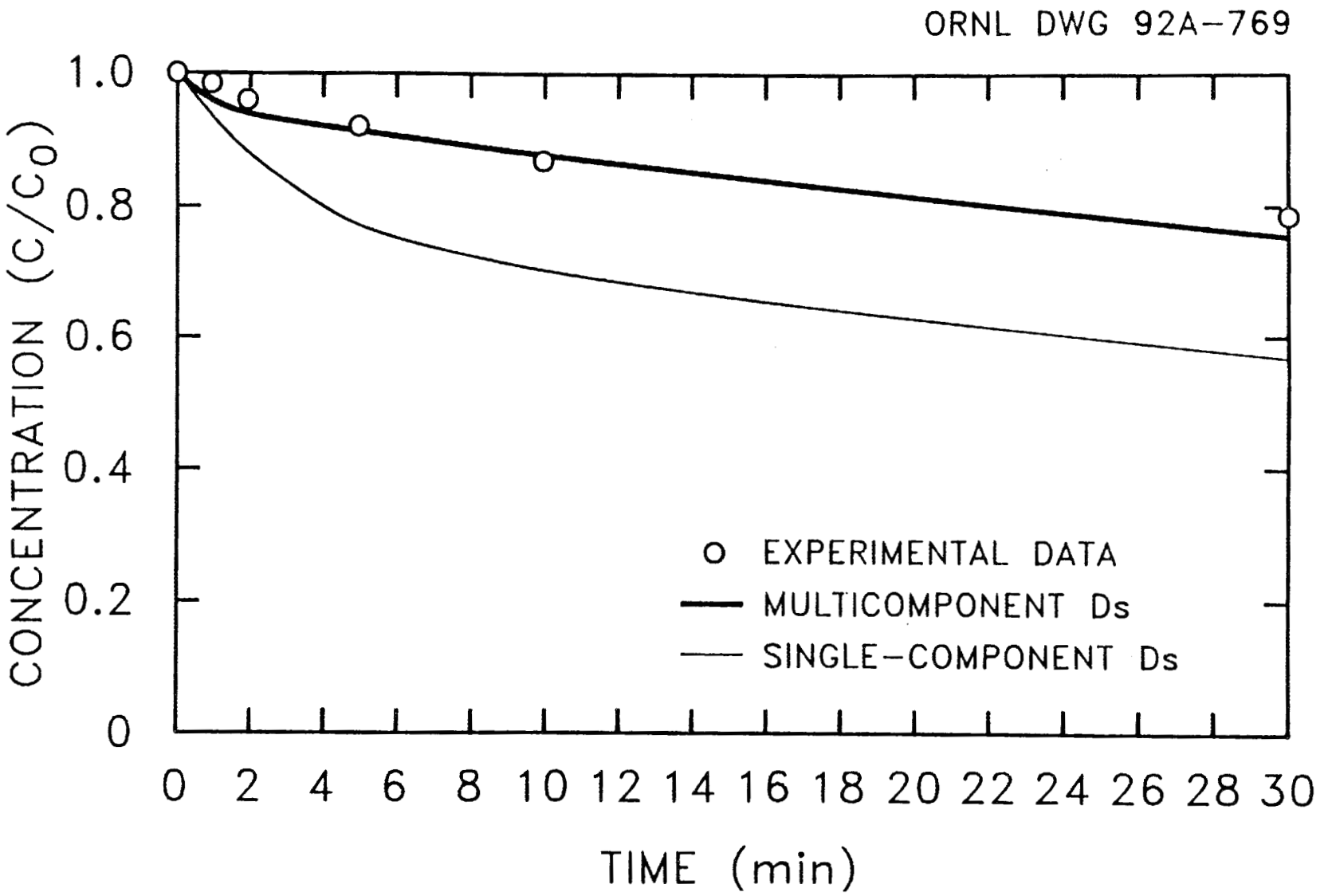

Figure 20. Models of Sr uptake curve for Sr-Cs-Ca-Mg-Na ion exchange using effective diffusivities obtained from single- and multicomponent data.

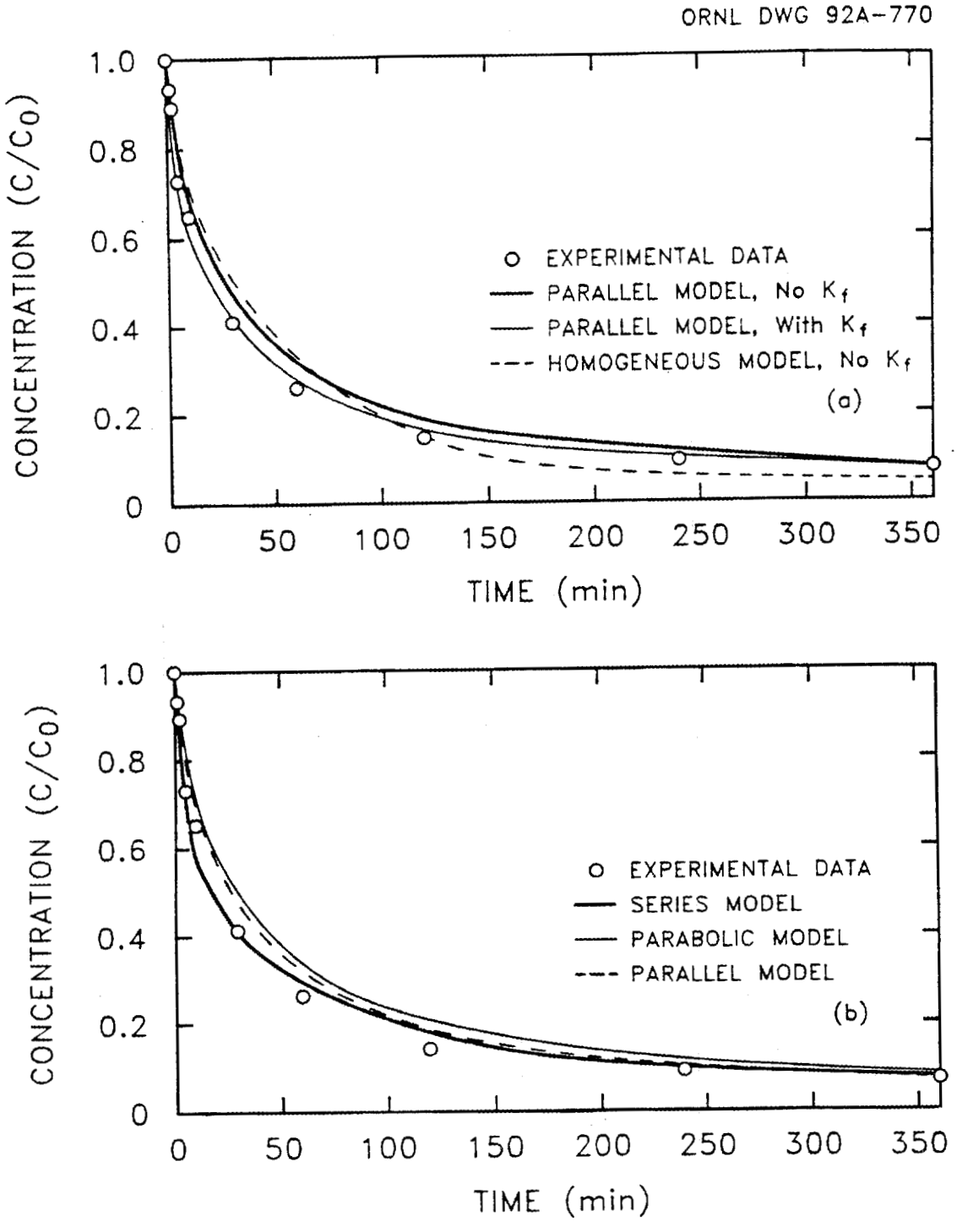

Figure 21. Models of Cs-Na uptake curves for Ionsiv IE-96: (a) effect of film mass transfer and (b) effect of heterogenous model assumptions.

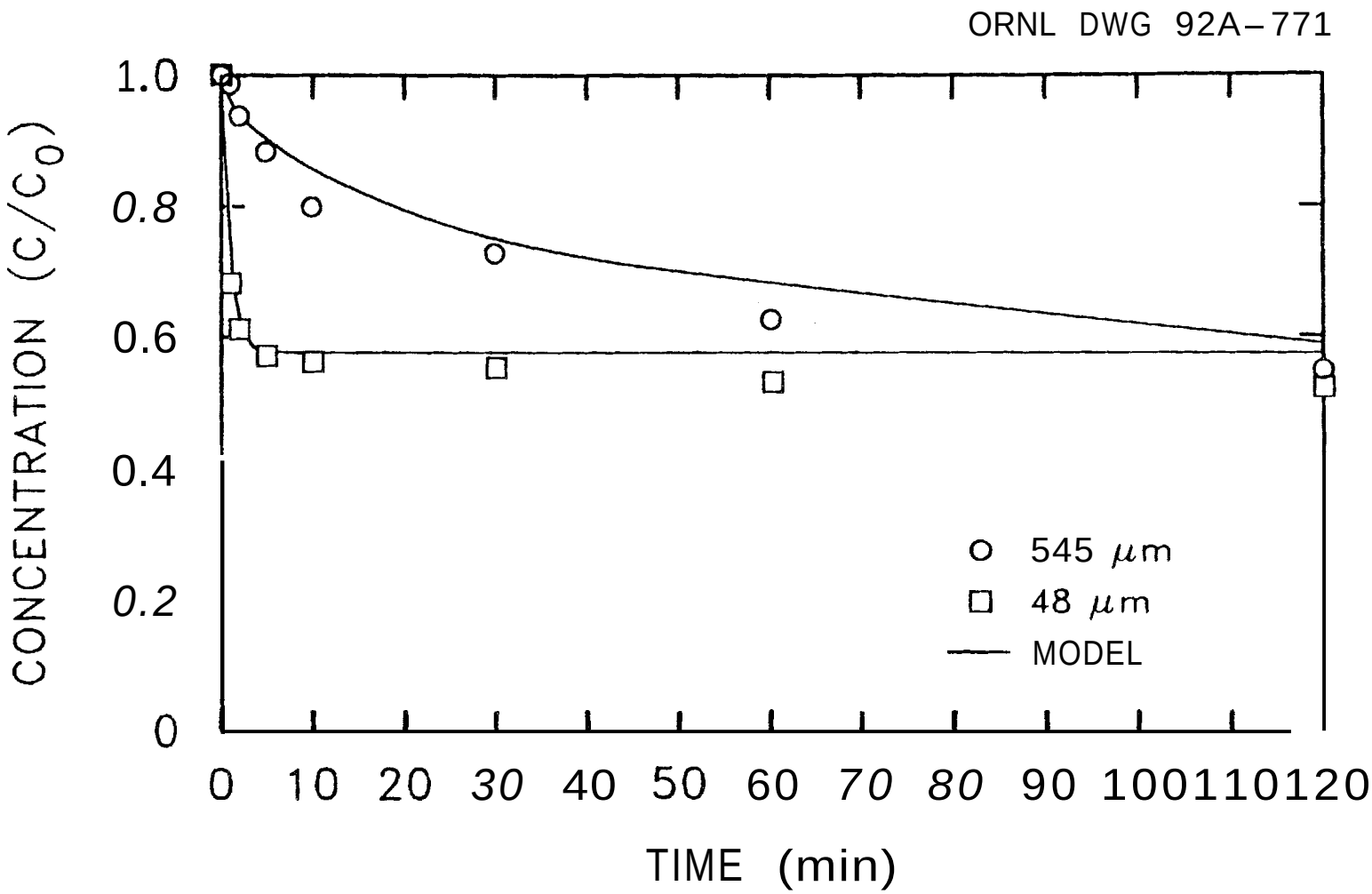

Figure 22. Effect of particle size on models for Ca-Na uptake curves using Ionsiv IE-96.

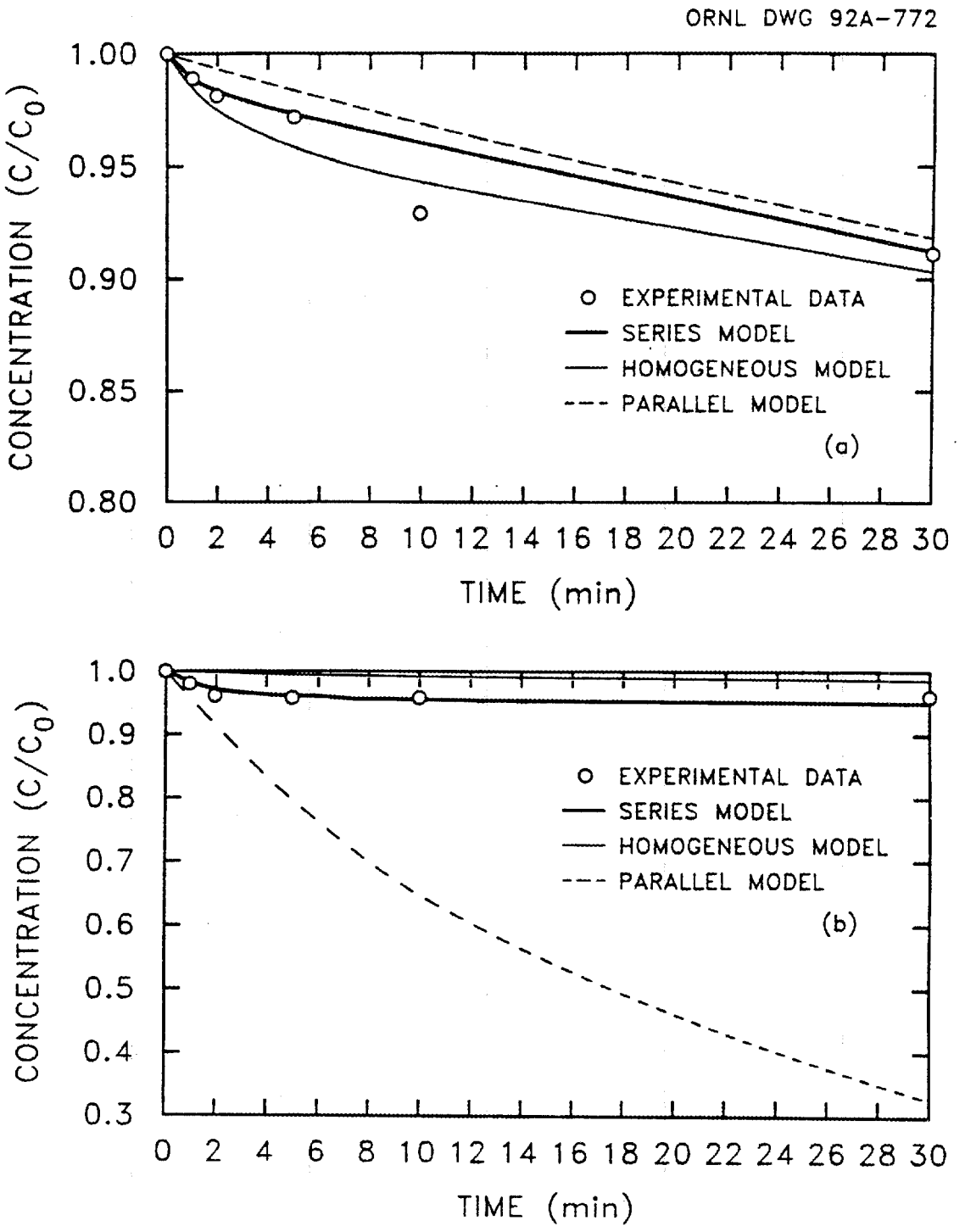

Figure 23. Models of Sr-Cs-Ca-Mg-Na ion exchange using Ionsiv IE-96: (a) strontium and (b) magnesium.

accurately predict multicomponent uptake curves for Ionsiv IE-90 as shown in Figure 20. However, effective micropore diffusivities were obtained which accurately modeled the multicomponent data (also shown in Figure 20). The effective micropore diffusivities for multicomponent Ionsiv IE-90 ranged between 10^{-9} to 10^{-10} cm^2/s. This indicates that the diffusivities are concentration-dependent or that cross-term diffusivities must be added to account for solute interactions.

When Darken's equation (Equations 26-28) was incorporated into the model to account for the concentration dependence of solid-phase diffusion, corrected micropore diffusivities were obtained that accurately modeled both the single- and multicomponent data. These values were between 2×10^{-10} and 9×10^{-10} cm^2/s, which is approximately an order of magnitude different than the effective diffusivities obtained from the constant-diffusivity model. The diffusivities agree with Ruckenstein's (1971) values for micropore diffusivities for liquids in zeolites which range between 10^{-6} and 10^{-10} cm^2/s .

The film mass-transfer coefficients listed in Table 13 for Equation 22 were used to model the single-component uptake curves. The inclusion of film mass transfer did not impact the results of the homogenous diffusion model for the single component systems. Since modeling results from the single-component systems indicated that film mass transfer was not significant, it was dropped from the models for all multicomponent systems.

Effective macropore diffusivities for liquids in zeolites are typically on the order of 10^{-5} to 10^{-7} cm^2/s (Ruckenstein et al., 1971). Since these values are up to five orders of magnitude higher than the micropore diffusivities, the micropore diffusivities obtained for the zeolite crystals were used in the homogenous diffusion model in an attempt to predict the uptake curves for Ionsiv IE-96 particles (zeolite crystals in a porous binder). The model significantly underpredicted the uptake rate, as shown in Figure 19 (b). This result indicates that pore

diffusion significantly contributes to the mass transfer in zeolite particles and it must be accounted for through an effective solid diffusivity in the homogenous diffusion model or the heterogenous diffusion model.

Effective solid diffusivities were obtained that accurately predicted the uptake data in Ionsiv IE-96 for both the single- and multicomponent systems. Solid diffusivities were obtained from models which assumed concentration-dependent diffusion equations (Equations 34-35) and constant diffusvities. The values are listed in Table 15. An example of the model results is shown in Figure 21 (a). Effective diffusivities obtained when the diffusion was assumed to be concentration independent were approximately twice as high as those obtained for corrected diffusivities that accounted for concentration effects. Both were an order of magnitude higher than the corresponding micropore diffusivities obtained for Ionsiv IE-90.

Various versions of the heterogenous diffusion model (developed in Section 7.2) were successfully used to predict the uptake curves for the single-component systems. This is consistent with literature findings (Ma and Ho, 1974; Neretnieks, 1976). The micropore diffusivities listed in Table 14, obtained from the Ionsiv IE-90 data, were used to predict the effective pore diffusivities listed in Table 16. The resulting curves are shown in Figure 21. The results were basically the same when macropore and micropore diffusion was assumed to occur in parallel or in series. The assumption that the concentration profile in the zeolite crystal had a parabolic profile also gave an accurate prediction. Film mass-transfer resistance did not effect the model results. The models also predicted the uptake profiles for various particle sizes, as shown in Figure 22.

Similar attempts were made to model the multicomponent data for Ionsiv IE-96. Typical results are shown in Figure 23. Effective diffusivities were found that would predict

the experimental data using the homogenous diffusion model, but the results did not fit the data as well as those from IE-90 or single component IE-96 systems.

The heterogenous diffusion models did not give the same results for multicomponent systems. The concentration profile in the zeolite crystals were not parabolic for the components which were displaced during multicomponent exchange. The model would not converge under these circumstances. The model that assumed that macropore and micropore diffusion occurred in parallel predicted the data for strongly held components rather well. However, it did not accurately predict the data for weakly held components. Typical examples are the strontium and magnesium uptake curves shown in Figure 23 (a) and (b), respectively. The heterogenous diffusion model, which assumed that macropore and micropore diffusion occurred in series, accurately predicted the uptake curves for all components (Figure 23).

The effective macropore diffusivities obtained from single- and multicomponent Ionsiv IE-96 were different, but all values were on the order of 10^{-4} cm^2/s. These values and liquid diffusivities obtained from the literature were used in Equation 72 to calculate tortuosity factors for the chabazite zeolite. The Nernst-Haskell equation (Reid et al., 1987) was used to calculate molecular diffusvities of 1.2×10^{-5} cm^2/s for strontium, 1.9×10^{-5} cm^2/s for cesium, 1.3×10^{-5} cm^2/s for calcium, and 1.3×10^{-5} cm^2/s for magnesium. This resulted in tortuosity factors well below 0.1. This indicates that both surface and molecular diffusion contribute to pore diffusion as discussed in Section 7.2.3.

Equation 73 was substituted into Equations 40, 46, 56, and 64 to represent surface and molecular diffusion occurring in parallel in the macropores, followed by micropore diffusion occurring in series. The liquid diffusivities obtained from the literature and a tortuosity factor of two were used to model the Ionsiv IE-96 data. The parameter D_s was varied to obtain

model results that fit the experiment. The resulting values were on the order of 10^{-9} cm^2/s, one order of magnitude higher than the corrected micropore diffusivities. The surface diffusivity values were the same for both single and multicomponent systems as shown in Table 16.

These results indicate that effective diffusivities that vary by orders of magnitude can be obtained and can be used in a wide variety of mathematical models to predict ion exchange in chabazite zeolite. However, the resulting effective diffusivities can be physically unrealistic and do not account for multicomponent interactions. The true mass-transfer mechanisms are macropore and micropore diffusion occurring in series. Both surface and molecular diffusion contribute to macropore diffusion. When the correct diffusion mechanisms are used, concentration-dependent micropore and surface diffusivities coupled with nonlinear equilibrium equations adequately predict multicomponent interactions. The introduction of cross-term diffusional coefficients to account for solute interactions was not necessary.

The results of this study increases the understanding of why the results of zeolite studies reported in the literature are so confusing. Most researchers have looked at a few models to predict a limited amount of experimental data. These researchers tend to assume that a given model represents the mass-transfer mechanisms if effective diffusivities can be found to predict experimental data. Most researchers who have modeled dual intraparticle mass-transfer simultaneously varied both the macropore and micropore diffusivities to determine values that predict experimental data. They have not verified their models with both single- and multicomponent data using various sizes of crystals and pellets. This study shows that such limited testing of zeolite systems can result in erroneous conclusions about the mass-transfer mechanisms.

9. VALIDATION WITH COLUMN DATA

Liapis and Rippin (1977 and 1978), Liapis and Litchfield (1980), Balzli et al. (1978), Mathews (1975), Crittenden (1975), Fritz et al., (1981), Merk et al., (1980), and Moon and Lee (1986) have shown that diffusivities obtained from batch tests can be used to model ion-exchange columns for single- and multicomponent systems. Nevertheless, ion-exchange column data were taken to qualitatively verify the batch reactor data evaluated in this study.

Experiments were run with two types of ion-exchange columns described in Section 3.3: SBC and LBC. The SBC are designed to be short enough that immediate breakthrough occurs. According to the designers (Liu and Weber, 1981; Weber and Smith, 1987; Weber and Wang, 1987), the SBC has the advantage of being able to evaluate both of film and intraparticle mass-transfer mechanisms with a single set of data. The initial stage of the SBC breakthrough curve is dominated by film transfer and is insensitive to intraparticle mass transfer. Therefore, the effects of film mass transfer can be obtained by evaluating the initial experimental data, and the intraparticle mass-transfer coefficients can be determined by evaluating the latter part of the breakthrough curve. The LBC is a standard ion-exchange column that is long enough to prevent immediate breakthrough from occurring. It is more representative of the type of system that would be installed in an operating facility.

9.1 Experimental Results

The experimental data is given in Appendix C. The runs are summarized in Table 17, and typical data are shown in Figures 24, 25, and 26. Figure 24 shows the effect of flow rate and particle size variations on the initial portion of the SBC breakthrough curves for 545-μm diam Ionsiv IE-96 with calcium chloride ($CaCl_2$) feed. Figure 25 shows the single- and

Table 17. Summary of column ion-exchange experiments

Run number	Type system	Type zeolite	Particle diameter (μm)	Solution volume (mL)	Solids weight (g)	Column diameter (cm)	Bed height (cm)	Flow rate (mL/min)	Initial solution concentration (meq/L) Sr	Cs	Ca	Mg	Solids loading (meq/g)
SK-7	SBC[1]	IE-96	194.00	1883.00	1.0003	1.00	1.60	8.56			1.95		1.801
SK-6	SBC	IE-96	385.00	1885.00	1.0018	1.00	1.60	8.57			1.92		1.638
SK-2	SBC	IE-96	545.00	1335.00	1.0014	1.00	1.60	5.70			1.99		1.454
SK-5	SBC	IE-96	545.00	1974.00	1.0021	1.00	1.60	3.20			1.82		1.588
SK-4	SBC	IE-96	545.00	1910.00	1.0022	1.00	1.60	11.60			1.94		1.553
SK-31	SBC	IE-96	545.00	4749.00	0.9222	1.00	1.60	8.50			2.03		1.859
SK-33	SBC	IE-96	545.00	1900.00	0.9224	1.00	1.60	8.60		1.00			1.454
SK-30	SBC	IE-96	545.00	1874.00	0.9228	1.00	1.60	8.60				0.83	0.555
SK-29	SBC	IE-96	545.00	1880.00	0.9235	1.00	1.60	8.50	1.84				1.631
SK-35	SBC	IE-96	545.00	4806.00	0.9276	1.00	1.60	8.60	0.53	0.25	0.58	0.23	2.129
SK-44	SBC	IE-96	545.00	3398.00	0.9220	1.00	1.60	8.60	2.03	1.00	1.94	1.09	2.056
SK-36	LBC[2]	IE-96	545.00	3738.00	2.3052	1.00	3.80	8.60			2.22		1.831
SK-37	LBC	IE-96	545.00	4322.00	2.3061	1.00	3.80	8.30		0.28			1.768
SK-45	LBC	IE-96	545.00	3015.00	3.0017	1.00	4.50	0.50	2.10	1.00	2.01	0.81	2.035
MV-10	LBC	IE-96	545.00	3200.00	3.0030	1.00	4.50	1.00	2.10	1.00	2.01	0.95	2.206
SK-47	LBC	IE-96	545.00	10039.00	10.0330	1.50	7.20	2.08	2.01	1.00	1.95	0.85	2.053
SK-48	LBC	IE-96	545.00	46225.00	44.8000	2.50	11.40	5.80	2.07	1.00	2.14	0.83	2.471

[1]SBC = Short Bed Column
[2]LBC = Long Bed Column

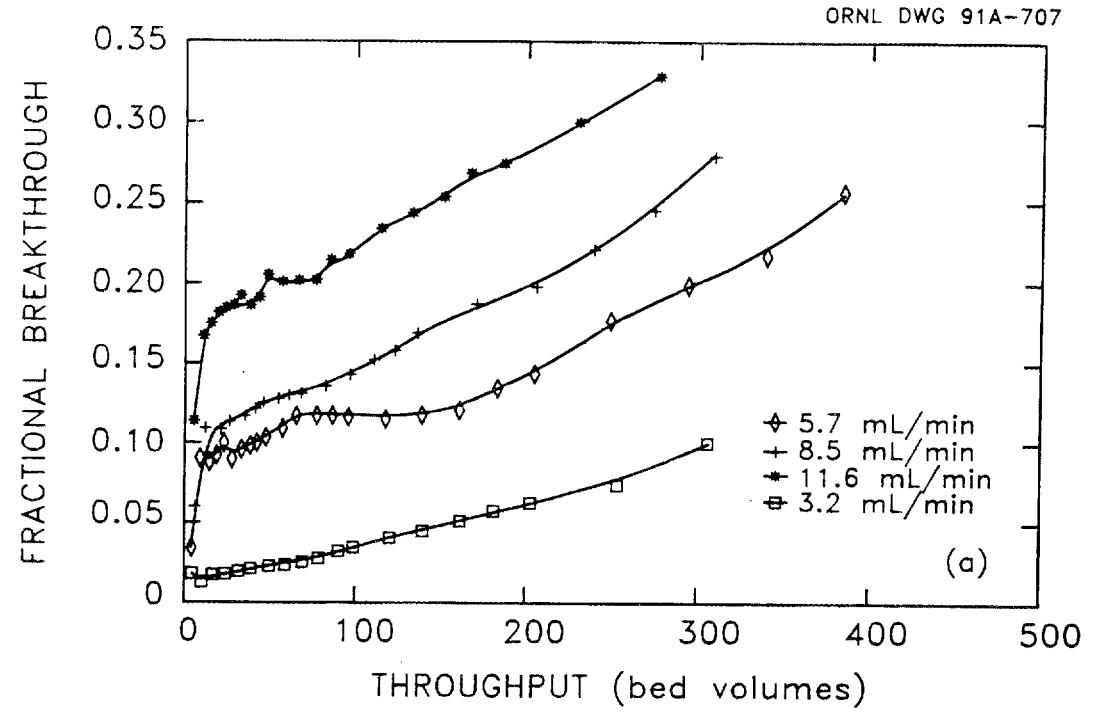

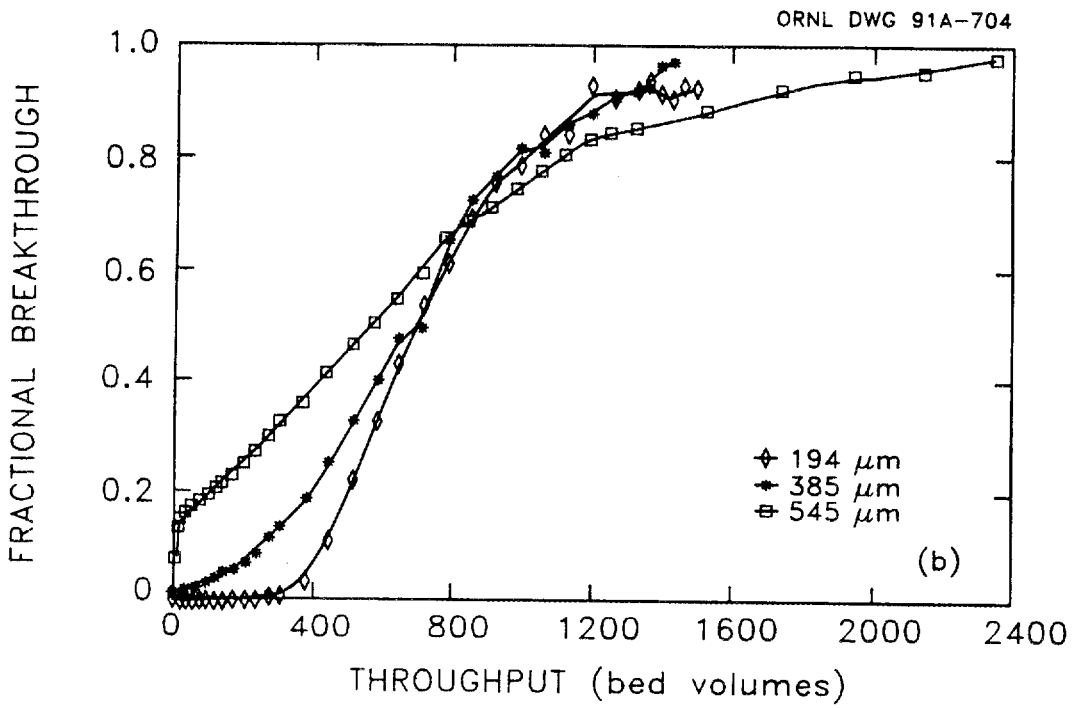

Figure 24. Effect of experimental conditions on breakthrough curves for short-bed column with $CaCl_2$ feed and Ionsiv IE-96: (a) flow rate and (b) particle size.

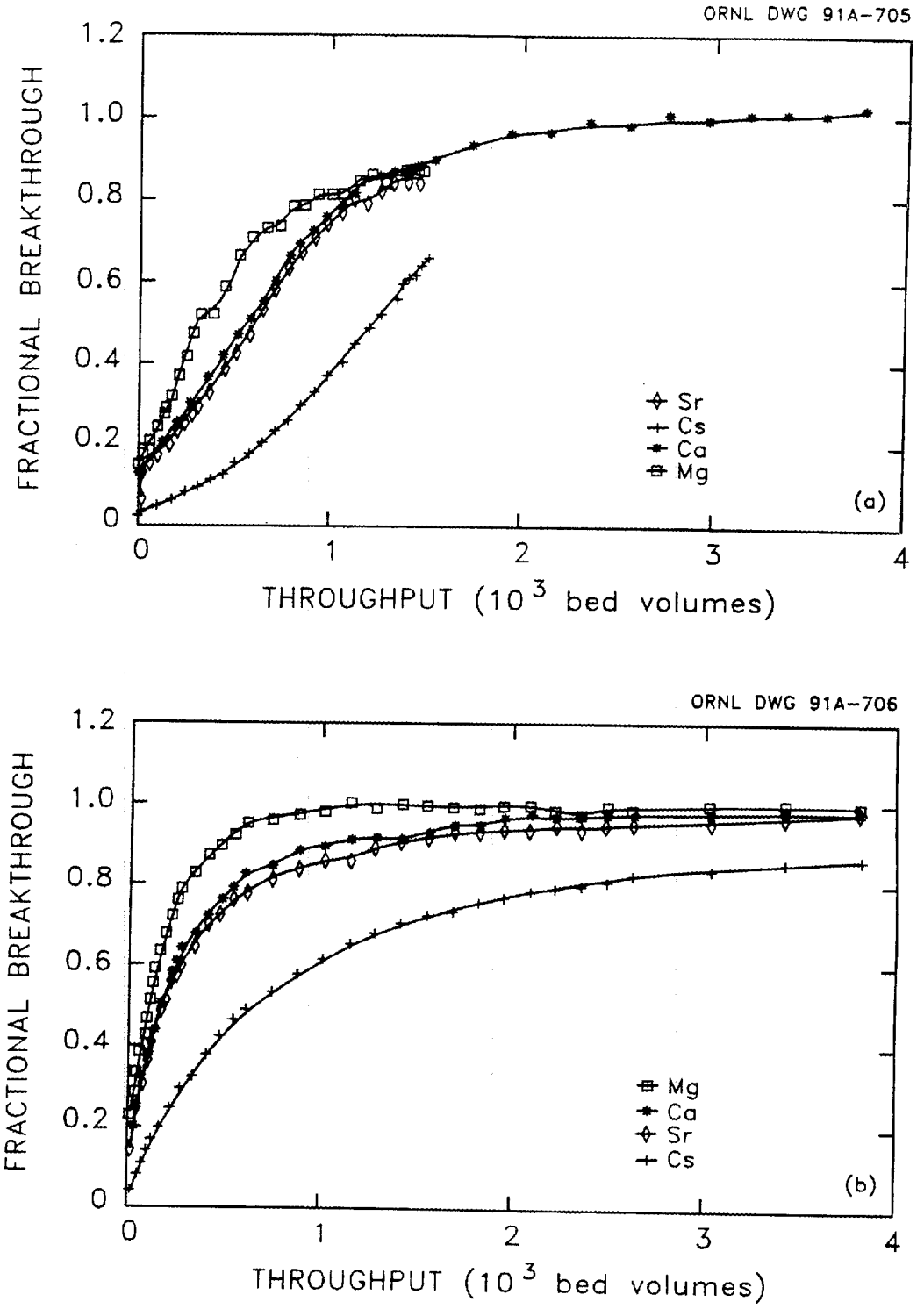

Figure 25. Breakthrough curves for short-bed adsorber: (a) single-component system and (b) multicomponent system.

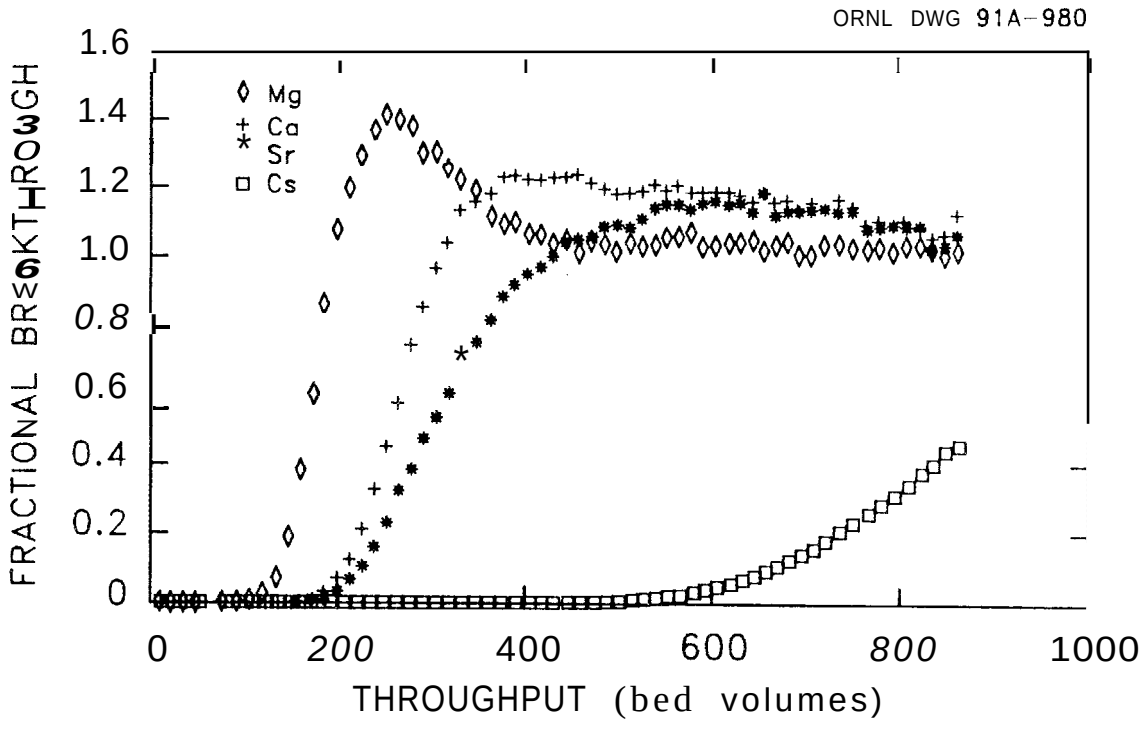

Figure 26. Breakthrough curves for long-bed ion-exchange column with multicomponent feed.

multicomponent SBC breakthrough curves for 545-μm diam Ionsiv IE-96 at a flow rate of 8.5 mL/min. Figure 26 is a typical example of breakthrough curves for the multicomponent for 545-μm diam Ionsiv IE-96 at a flow rate of 8.6 mL/min in a LBC.

Figure 24 shows that the kinetics are slower for larger-sized particles. Since the breakthrough curves are impacted by particle size, macropore intraparticle mass-transfer resistance is significant. These results are consistent with the uptake curves for different particle sizes of Ionsiv IE-96 obtained in the batch reactor tests (Figure 17).

These curves also show that chabazite zeolite has a selectivity of Cs>Sr>Ca>Mg>Na. This is consistent with the equilibrium tests and batch reactor results. The slopes of the SBC and LBC breakthrough curves for all cations were also steeper for the multicomponent system than for the single-component systems. Similar trends were seen in the batch reactor tests. Figures 17 and 18 showed that both the slope and the equilibrium values for the uptake curves in the batch reactor system were affected by the particle size and by the number of components in the system.

Displacement of Mg and Ca by Sr and Cs resulted in fractional breakthroughs in excess of one for Mg and Ca in Figure 26. Similar trends were obtained for the multicomponent Ionsiv IE-96 batch reactor tests (Figure 18). This was not seen for the binary systems or for the Ionsiv IE-90 batch reactor data.

9.2 Data Evaluation

The ion-exchange column data can be impacted by the film mass-transfer coefficients and intraparticles diffusivities. The intraparticle diffusivities should be the same as those obtained in the batch reactor studies. However, the film mass-transfer coefficients should be significantly lower than those obtained from batch reactors. Film mass-transfer coefficients

for columns can be obtained from evaluation of SBC or from correlations. Both were evaluated in this study.

Correlations developed for film mass transfer in columns contain relationships between the dimensionless Reynolds (Re), Schmidt (Sc), and Sherwood (Sh) Numbers. Some of the more widely used correlations are listed below (Weber and Smith, 1987; Ruthven, 1984a; Teo and Ruthven, 1986).

A correlation was developed for packed beds by Williamson et al., (1963) for 0.08 <Re <125 and 150 <Sc <1300:

$$Sh = 2.4\ \varepsilon\ Re^{0.34} Sc^{0.42}. \tag{75}$$

Wilson and Geankoplis (1966) developed a similar correlation for 0.0016 <ϵRe <55 and 950 <Sc <70,000,

$$Sh = 1.09\,\varepsilon^{-2/3}\ Re^{1/3}\ Sc^{1/3}\ . \tag{76}$$

Ohaski et al. (1981) developed:

$$Sh = 2+1.58\ Re^{0.4}\ Sc^{1/3}\ for\ 0.001<Re<5.8, \tag{77}$$

$$Sh = 2+1.21\ Re^{0.5}\ Sc^{1/3}\ for\ 5.8<Re<500, \tag{78}$$

and

$$Sh = 2 + 0.59\ Re^{0.6}\ Sc^{1/3}\ for\ Re>500. \tag{79}$$

Gnielinsk (Roberts et al., 1985) developed the following correlation for 1 <Re <10,000 and 0.6 <Sc <10,000:

$$Sh = \left[2 + \left(Sh_L^2 + Sh_T^2\right)^{0.5}\right]\ [1 + 1.5\ (1-\varepsilon)]\ , \tag{80}$$

where

$$Sh_L = 0.644 Re^{1/2} Sc^{1/3}$$

and

$$Sh_T = 0.037 Re^{0.8} Sc / [1 + 2.443 Re^{-0.1} (Sc^{2/3} - 1)].$$

Kataoka et al. (1972) developed an equation for $Re[\varepsilon/(1-\varepsilon)]<100$

$$Sh = 1.85 [(1-\varepsilon)/\varepsilon]^{1/3} Re^{1/3} Sc^{1/3}. \tag{81}$$

Dwivedi-Upadhyay (1977) found that for 0.01 <Re <15,000,

$$Sh = (1/\varepsilon) [0.765 (\varepsilon Re)^{0.18} + 0.365 (\varepsilon Re)^{0.614}] Sc^{1/3} . \tag{82}$$

The correlation developed by Ranz and Marshall (1952),

$$Sh = 2.0 + 0.6 Sc^{1/3} Re^{1/2} \tag{83}$$

is based on mass-transfer rates for freely falling solid spheres. Wakao and Funazki (1978) developed

$$Sh = 2.0 + 1.1 Sc^{1/3} Re^{0.6} \tag{84}$$

by correcting previous correlations for axial dispersion (Ruthven, 1984a) for $3 < Re < 10^4$.

Since the initial portion of the SBC breakthrough curve is dominated by film mass transfer, the film mass-transfer coefficient can be obtained from film mass-transfer model. Mass balances performed on each solute in the liquid phase leads to the following relationship (Ruthven, 1984a):

$$D_z \frac{\partial^2 c}{\partial z^2} = v \frac{\partial c}{\partial z} + \frac{\partial c}{\partial t} + \rho \left(\frac{1-\varepsilon}{\varepsilon} \right) \frac{\partial \bar{q}}{\partial t} . \tag{85}$$

The mass transfer from the liquid phase to the solid phase is modeled by the mass transfer across the liquid film surrounding the ion-exchange particles (Ruthven, 1984a):

$$\frac{\partial \bar{q}}{\partial t} = \frac{3}{\rho R_p} k_f (c_d - c_s), \tag{86}$$

Since the initial portion of the uptake curve is insensitive to intraparticle mass transfer, the value of k_f can be obtained by solving Equations 84 and 85 assuming D_z, c_s, and dc/dt are zero as t approaches zero. Under these conditions,

$$k_f = -\frac{\upsilon R_p \varepsilon}{3L(1-\varepsilon)} ln\left[\frac{c_d}{c_0}\right]. \tag{87}$$

Figure 24 shows that varying the flow rate from 3.2 to 11.6 mL/min significantly impacted the SBC breakthrough curves. This indicates that film mass transfer has a significant effect in these ranges. After approximately 2000 min, the curves converged, indicating that film mass transfer has less of an effect after initial breakthrough. This is consistent with previous findings for the SBC (Weber and Smith, 1987; Liu and Weber, 1981; Weber and Wang; 1987), and indicates that evaluating the initial part of the breakthrough curves by Equation 86 should be an appropriate method of determining film mass-transfer coefficients for these systems.

Film mass-transfer coefficients were estimated using the correlations given in Equations 75-84 and using Equation 87 for the SBC data for both binary and multicomponent systems. Typical results for 545-μm diam particles are summarized in Table 18. The correlations predicted k_f values for the binary systems in the range of 0.001 to 0.008 cm/s with an average of 0.004 cm/s. Analysis of experimental data using Equation 87 resulted in values from 0.004 to 0.009 cm/s for the binary systems.

Diffusivities can be converted to mass-transfer coefficients by using Equations 23 and 24 (Ruthven, 1984a). Typical micropore diffusivities given in Section 8 are 10^{-10} cm^2/s;

Table 18. Film mass-transfer coefficients for the short-bed column

Cation	Flow rate (mL/min)	k_f (cm/s)									
		Williamson, et al. (Eq. 74)	Wilson & Geankoplis (Eq. 75)	Ohaski, et al. (Eq. 76-78)	Gnielinsk (Eq. 79)	Kataoka et al. (Eq. 80)	Dwivedi-Upadhyay (Eq. 81)	Ranz & Marshall (Eq. 82)	Wakao & Funazkii (Eq. 83)	Binary Data (Eq. 86)	Multicomponent Data (Eq. 86)
Ca	8.6	0.0047	0.0042	0.0037	0.0031	0.0036	0.0036	0.0028	0.0028	0.0067	0.0052
Sr	8.6	0.0047	0.0037	0.0035	0.0028	0.0033	0.0032	0.0026	0.0026	0.0071	0.0053
Mg	8.6	0.0045	0.0041	0.0035	0.0030	0.0035	0.0034	0.0026	0.0026	0.0042	0.0038
Cs	8.6	0.0052	0.0048	0.0043	0.0036	0.0041	0.0041	0.0032	0.0032	0.0086	0.0081
Ca	3.2	0.0035	0.0029	0.0026	0.0022	0.0026	0.0026	0.0018	0.0017	0.039	—[a]
Ca	11.6	0.0052	0.0047	0.0041	0.0032	0.0040	0.0040	0.0032	0.0032	0.0070	—

[a] Indicates not measured.

effective macropore diffusivities are on the order of 10^{-4} cm^2/s. The particles in these tests had a particle radius of 0.0273 cm and a crystal radius of 0.0012 cm. Effective macropore mass-transfer coefficients are on the order of 10^{-3} cm/s, and micropore mass transfer coefficients are on the order of 10^{-8} cm/s. Therefore, film mass transfer could significantly contribute to mass-transfer resistance in the column systems.

Film mass-transfer coefficients calculated for multicomponent data were slightly lower than the corresponding values for binary systems. This trend is consistent with results seen in tests for removing organics from wastewaters using activated carbon (Smith and Weber, 1988). The correlations tended to underpredict k_f for both binary and multicomponent data by factors up to two, and the Williamson correlation tended to agree best with experimental data for both systems. This is consistent with the trend seen in batch reactor data. The results indicate that standard correlations are accurate for chabazite zeolites.

10. SUMMARY

Zeolites have had limited application as ion exchangers in the past. As a result the equilibrium and kinetic properties of zeolites have been neglected, and only minimal information has been published in this area (Townsend, 1986). To date, most multicomponent equilibrium data have been fit using empirically derived equations. The kinetics, even for simple single-component zeolite systems, are not well understood. The literature is filled with confusing, and often conflicting, explanations of multicomponent zeolite data.

This study examined multicomponent ion exchange from an aqueous solution to a chabazite zeolite. Single component equilibrium data were adequately modeled by the Langmuir equation. Multicomponent equilibrium data were not accurately modeled by standard isotherm equations. A semi-empirical equation, based on the Dubinin-Polyani theory for gaseous sorption in zeolites, was used to model the multicomponent data. This equation can be used to model multicomponent systems will a minimal amount of experimental data.

Experimental kinetic data were taken in a batch reactor using zeolite crystals and zeolite particles (crystals plus binder) to determine the mass-transfer mechanisms which significantly affect multicomponent ion exchange in chabazite zeolites. The micropore diffusivities, on the order of 10^{-10} cm^2/s, were the most significant mass-transfer resistance. The effective macropore diffusivity, typically 10^{-4} cm^2/s, also significantly contributed to mass transfer resistance in the zeolite particles. Film mass transfer did not significantly contribute to the mass-transfer resistance.

The values obtained for the effective macropore diffusivities were two orders of magnitude higher than expected from liquid diffusivities. Mathematical modeling determined that liquid diffusion plus surface diffusion significantly contributed to macropore diffusion. Models indicated that surface diffusivities were on the order of 10^{-9} cm^2/s.

This study showed that several simplified mathematical models can be used to predict the experimental uptake data (both single- and multicomponent systems). These include assuming that diffusivities in the solid are independent of concentration, macropore and micropore diffusion occur in parallel or in series, the concentration profile inside the zeolite crystal is parabolic, and solutes diffuse independently. Effective diffusivities could be obtained that would predict experimental data for most of these models. However, single-component diffusivities could not be used to predict multicomponent diffusivities, and many of the resulting values were physically impossible. The results were similar to those obtained in several literature references that employed simple models to predict zeolite and carbon adsorption data.

Only the most rigorous model predicted multicomponent batch reactor data using physically realistic diffusivities obtained from single-component batch reactor data. This model incorporated parallel molecular diffusion and surface diffusion occurring in series with micropore diffusion in the zeolite crystal. The surface and micropore diffusivities where concentration dependent and followed Darken's equation. Solute interactions were accounted for in multicomponent equilibrium equations and concentration dependency of the solid diffusivities. Column data were evaluated qualitatively and were determined to be consistent with batch reactor data.

Recommendations for future studies include more detailed evaluation of the column data presented in this study (see Appendix F). The PDEs, which modeled batch reactor systems, were solved by converting to ODEs using orthogonal collocation and using LSODE to solve the resulting set of stiff ODEs. For multicomponent systems, this method was very slow. LSODE would not converge unless test values for the diffusivities were very carefully selected. Future studies should consider alternative numerical methods such as orthogonal

collocation coupled with finite elements, finite differences, or finite elements (discussed in Section 2.3).

A semi-empirical multicomponent isotherm was developed in this study. The equation accurately predicted equilibrium data used in this study. However, it is recommended that the accuracy of the isotherm equation be determined for a wider range of data. It is also recommended that thermodynamic models, such as the one developed by Perona (1992), continue to be developed and incorporated into the kinetics models.

BIBLIOGRAPHY

BIBLIOGRAPHY

Akulov, A. K., and Ustinov, E. A. *Russ. J. Phys. Chem.*, 55, 509, 1981.

Ausikaitis, J. P. *Fundamentals of Adsorption*, AIChE, New York, 1984, 49-63.

Afifi, A. A., and Azen, S. P. *Statistical Analysis. A Computer Oriented Approach*, Academic Press, New York, 1979.

Baes, C. F., and Mesmer, R. E. *The Hydrolysis of Cations*, John Wiley and Sons, 1976.

Balzli, M. W., et al. *Trans IChemE*, 56, 1978, 145-56.

Barba, D., et al. *Chem. Eng. J.*, 26, 1983, 33.

Barrer, R. M., and Klinowski, J. *J. Chem. Soc. Faraday Trans.* 1, 9, 1972, 1956-63.

Barri, S. A. I., and Rees, L. V. C. *J. Chromatogr.*, 201, 1980a, 21.

Barri, S. A. I., and Rees, L. V. C. *Solution Behavior of Surfactants: Theoretical and Applied Aspects*, Vol. 2., Plenum Press, New York, 1980b, 1477-86.

Bering, B. P., et al. *Dokl. Akad. Nauk. USSR*, 153(1), 1963, 129.

Breck, D. W. *Zeolite Molecular Sieves*, John Wiley & Sons, New York, 1974.

Breck, D. W., et al. *J. Amer. Chem. Soc.*, 78(23), 1956, 5966.

Carl, D. E., and Leonard, I. M. DOE/NE/44139--25, Est Valley Nuclear Services, West Valley, New York, February 1987.

Carnahan, B. *Applied Numerical Methods*, John Wiley & Sons, New York, 1969.

Carter, J. W., and Husain, H. *Chem. Eng. Sci.*, 29, 1974, 267-73.

Cen, P. I., and Yang, R. T. *AIChE J.*, 32(10), 1986, 1635-64.

Chakravarti, A. K., and Sengupta, M. *J. Indian Chem. Soc.*, LX, 1983, 1124-28.

Cremers, A. *Molecular Sieves-II*, J. R. Katzer, ed., ACS Symp. Series, 40, Washington, DC, 1977, 179-93.

Crittenden, J. C. Thesis, University of Michigan, Ann Arbor, Michigan, 1975.

Crittenden, J. C. et al. *J. Water Poll. Cont. Fed.*, 52(11), 1980, 2780-95.

Crittenden, J. C. et al. *Environ. Sci. Technol.*, 19(11), 1985, 1037-43.

Crittenden, J. C. et al. *Water Resources Research*, 22(3), 1986, 271-84.

Crittenden, J. C. and Weber, Jr., W. J. *ASCE Env. Eng. Div.*, 104(EE6), 1978, 1175-1195.

Dean, J. A. ed., *Lange's Handbook of Chemistry*, McGraw-Hill, New York, 1985, 3-121 to 3-126.

Do, D. D., and Rice, R. G. *AIChE J.*, 32(1), 1986, 149-54.

Dominguez, J. A., et al. *1991 Annual AIChE Meeting*, Los Angeles, California, October, 1991.

Doong, S. J., and Yang, R. T. *AIChE J.*, 33(6), 1987, 1045-49.

Dwivedi, P. N., and Upadhyay, S. N. *Ind. Eng. Chem. Proc. Des. and Dev.*, 16, 1977, 157-65.

Dyer, A., and Keir, D. *Zeolites*, 4, 1984, 215-7.

Dyer, A., and Keir, D. *J. Radioanalytical and Nuclear Chemistry*, Articles, 132(2), 1989, 423-441.

Fennelly, D. personal communication, Union Carbide, 308 Harper Drive, Morristown, NJ, 1991.

Finlayson, B. A. *The Method of Weighted Residuals and Variational Principles*, Academic Press, New York, 1972.

Finlayson, B. A. *Nonlinear Analysis in Chemical Engineering*, McGraw-Hill, New York, 1980.

Franklin, K. R., and Townsend, R. P. *J. Chem. Soc. Faraday Trans.*, 1, 81, 1985, 1071-86, 3127-41.

Franklin, K. R., et al. *New Developments in Zeolite Science and Technology*, Proceedings of the 7th International Zeolite Conference, Y. Murakami, A. Iijima, and J. W. Ward, eds., Elsevier Science Publishing Company, Inc., 1986, 289-296.

Friedman, G. "Mathematical Modeling of Multicomponent Adsorption in Batch and Fixed-Bed Reactors," Michigan Technological University, Houghton, MI, 1984.

Fritz, W. Dissertation, Universitat Karlsruhe, 1978.

Fritz, W. et al. *Chem. Eng. Sci.*, 36, 1981, 731-741.

Furusawa, T., and Smith, J. M. *Ind. Eng. Chem. Fundam.*, 12(2), 1973, 197-203.

Furusawa, T., and Smith, J. M. *AIChE J.*, 20, 1974, 88.

Garg, D. R., and Ruthven, D. M. *Chem. Eng. Sci.*, 29, 1974, 571-81.

Gierke, J. S. et al. *Water Resources Research*, 26(7), 1990, 1529-47.

Gu, et al. *AIChE J.*, 36(5), 1990, 784-8.

Harris, M. T., and Byers, C. H. ORNL/TM-10735, Oak Ridge National Laboratory, Oak Ridge, TN, 1988.

Helfferich, F. *Angew. Chem. Internat. Edit.*, 7(8), 1962, 440-53.

Hindmarsh, A. C. *LSODE: Livermore Solver For Ordinary Differential Equations*, Lawrence Livermore Laboratory, P. O. Box 808, Livermore, CA, 1980.

Hsu, L.-K. P., and Hayes, H. W. *AIChE J.*, 27(1), 1981, 81-91.

Kapoor, A., and Yang, R. T. DOE/MC/22060-2649, State University of New York at Buffalo, Buffalo, New York, February 1988.

Kataoka, T. et al. *Chem. Eng. Japan*, 5, 1972, 132-6.

Kaul, B. K. and Sweed, N. H. *Fundamentals of Adsorption*, AIChE, New York, 1984, 249-58.

Komiyama, H., and Smith, J. M. *AIChE J.*, 20(4), 1974, 728-34.

Larson, A. C., and Tien, C. *Chem. Eng. Communications*, 27, 1984, 359-79.

Letterman, R. D. et al. *Journal WPCF*, 46(11), 1974, 2536-2546.

Liang, S., and Weber, Jr., W. J. *Chem. Eng. Commun.*, 35, 1985, 49-61.

Liapis, A. I., and Crosser, O. K. *Chem. Eng. Sci.*, 37(6), 1982, 958-61.

Liapis, A. I., and Litchfield, R. J. *Chem. Eng. Sci.*, 35, 1980, 2366-69.

Liapis, A. I., and Litchfield, R. J. *Trans. Inst. Chem. Eng.*, 59, 1981, 122-24.

Liapis, A. I., and Rippin, D. W. T. *Chem. Eng. Sci.*, 32, 1977, 619-27.

Liapis, A. I., and Rippin, D. W. T. *Chem. Eng. Sci.*, 33, 1978, 593.

Liaw, C. H. et al. *AIChE J.*, 25, 1979, 376.

Liu, K. T., and Weber, W. J. *Journal WPCF*, 53(10), 1981, 1541-50.

Loizidou, M., and Townsend, R. P. *Zeolites*, 7(2), 1987.

Ma, Y. H., and Ho, S. Y. *AIChE J.*, 20(2), 1974, 279-84.

Manes, M. *Activated Carbon Adsorption of Organics from the Aqueous Phase, Volume 1*, I. H. Suffet and M. J. McGuire, eds., Ann Arbor Science Publishers, Inc., Michigan, 1980, 42-64.

Mansour, A. et al. *AIChE J.*, 28, (5), 1982, 765-72.

Marutovsky, R. M., and Bulow, M. *Zeolites*, 7, 1987, 111-14.

Mathews, A. P. Thesis, University of Michigan, Ann Arbor, Michigan, 1975.

Mathews, A. P., and Su, C. A. *Envir. Progress*, 2(4)1983 , 257-61.

McKay, G., and Bino, M. J. *Wat. Res.*, 22(3), 1988, 279-286.

Merk, W., Fritz, W., and Schlunder, E. U. *Chem. Eng. Sci.*, 36, 1980, 743-57.

Michelsen, M. L., and Villadsen, M. L. *Chem. Engr. J.*, 4, 1972, 64-8.

Moon, H., and Lee, W. K. *J. of Colloid and Interface Science*, 96(1), 1983, 162-71.

Moon, H., and Lee, W. K. *Chem. Eng. Sci.*, 41(8), 1986, 1995-2004.

Myers, A. L., and Byington, V. A. *Ion-Exchange: Science and Technology*, Rodrigues, A. E., ed., NATO ASI Series E 107, Martinus Nijhoff Publishers, Boston, 1986, 119-45.

Nagel, G. et al. *Chem. Eng. Sci.*, 42(1), 1987, 143-53.

Nemeth, B. A. *Chemical Tables*, John Wiley and Sons, New York, 1975.

Noll, K. E. et al. *Adsorption Technology for Air and Water Pollution Control*, Lewis Publishers, Inc., Chelsea, Michigan, 1992.

Ohaski, H. et al. *J. Chem. Eng. Japan*, 14, 1981, 433-8.

Palekar, M. G and Rjadhyaksha, R. A. *Chem. Eng. Sci.*, 41(3), 1986, 463-8.

Passaglia, E. *Natural Zeolites: Occurrences, Properties, and Use*, Pergamon Press, New York, 1978, 45-52.

Perona, J. J. *1992 Annual AIChE Meeting*, Miami, Florida, November, 1992.

Prazniak, J. K. and Byers, C. H. ORNL/TM-10327, Oak Ridge National Laboratory, Oak Ridge, TN, 1987.

Raghavan, N. S., and Ruthven, D. M. *Chem. Eng. Sci.*, 39(7/8), 1984, 1201-12.

Ranz, W. E., and Marshall, W. R. *Chem. Eng. Prog.*, 48, 1952, 173.

Reid, R. C. et al. *The Properties of Gases and Liquids*, McGraw-Hill, New York, 1987.

Rice, R. G. *Chem. Eng. Sci.*, 37, 1982, 83.

Rice, R. G. et al. *Chem. Eng. Commun.*, 1983.

Robinson, S. M., and Parrott, J. R. ORNL/TM-10836, Oak Ridge National Laboratory, Oak Ridge, TN, 1988.

Robinson, S. M. et al. ORNL/TM-11426, Oak Ridge National Laboratory, Oak Ridge, TN, 1991.

Rosen, J. B. *J. Chem. Phys.*, 20, 1952, 387.

Ruckenstein, E. et al. *Chem. Eng. Sci.*, 26, 1971, 1305-1318.

Ruthven, D. M. *Principles of Adsorption and Adsorption Processes*, John Wiley & Sons, New York, 1984a.

Ruthven, D. M. *Fundamentals of Adsorption*, AIChE, New York, 1984b, 739-41.

Ruthven, D. M. et al. *Chem. Engr. Sc.*, 28, 1973, 701-9.

Ruthven, D. M., and Doetsch, I. H. *J. Chem. Soc. Faraday I* 75, 1979, 2406.

Ruthven, D. M., and Goddard, M. *Zeolites*, 6, 1986, 275-82.

Ruthven, D. M., and Lee, L. K. *AIChE J.*, 27(4), 1981, 654-663.

Ruthven, D. M., and Loughlin, K. F. *Can. J. Chem. Engng*, 50, 1972, 550.

SAS Institute, Inc. SAS® *User's Guide: Statistics*, Version 5 Edition, Cary, NC, 1985, 403-433.

Sengupta, M., and Paul, T. B. *Reactive Polymers*, 3, 1985, 217-229.

Shallcross, D. C., Hermann, C. C., and McCoy, B. J. *Chem. Eng. Sci.*, 43(2), 1988, 79-288.

Sherman, J. D. *AIChE Symposium Series*, 74(179), 1978.

Sherwood, T. K. et al. *Mass Transfer*, McGraw-Hill, New York, 1975, 220-224.

Singhal, A. K. *AIChE Symposium Series*, 74(179), 1978, 36-41.

Smith, E. H., and Weber, Jr., W. J. *Environ. Sci. Technol.*, 22(3), 1988, 313-321.

Society of Chemical Industry, *Molecular Sieves*, London, 1968.

Soldatov, V. S., and Bichknova, V. A. *Separ. Sci.*, 15, 1980, 89-110.

Spahn, H., and Schlunder, E. U. *Chem. Eng. Sci.*, 30, 1975, 529.

Speth, T. F. Masters Thesis, Michigan Technology University, 1986.

Sun, L. M., and Meunier, F. *AIChE J.*, 37(2), 1991, 244-54.

Takeuchi, Y., and Suzuki, Y. *Fundamentals of Adsorption*, A. L. Meyers and G. Belfort, Eds., Eng. Found. Conf., New York, New York, 1983.

Tan, H. K. S. *Chem. Engr.*, 91(26), 1984, 57-61.

Tenneco Specialty Minerals, personnel communications, 1988.

Teo, W. K., and Ruthven, D. M. *Ind. Eng. Chem. Process Des. Dev.*, 25, 1986, 17-21.

Thacker, W. E., et al. *Water Resources Center Research Report 161*, Univ. of Illinois, Urbana, Ill., 1981.

Thacker, W. E. et al. *J. Amer. Water Works Assoc.*, 75(3), 1983, 144-149.

Treybal, R. E., *Mass-Transfer Operations*, McGraw-Hill, New York, 1980, 603.

Townsend, R. P. *Pure & Appl. Chem.*, 58(10), 1986, 1259-66.

Villadsen, J., and Michelsen, M. L. *Solution of Differential Equation Models by Polynomial Approximation*, Prentice-Hall, Inc., New Jersey, 1978.

Wakao, N., and Funazkri, T. *Chem. Eng. Sci.*, 33, 1978, 1375.

Wankat, P. C. *Large-Scale Adsorption and Chromatography*, Vol. 1, CRC Press, 1986.

Weber, Jr., W. J., and Liang, S. *Environ. Prog.*, 2(3), 1983, 167-75.

Weber, Jr., W. J., and Smith, E. H. *Environ. Sci. Technol.*, 21(11), 1987, 1040-50.

Weber, Jr., W. J., and Wang, C. K. *Environ. Sci. Technol.*, 21(11), 1987, 1096-1102.

Williamson, J. E. et al. *Ind. and E. C. Fund.*, 2, 1963, 126-9.

Wilson, E. J., and Geankoplis, C. J. *Ind. Eng. Chem. Fund.*, 5, 1966, 9-12.

Yu, Q., and Wang, N. *Sep. and Purification Methods*, 15(2), 1986, 127-58.

APPENDIXES

Appendix A. EQUILIBRIUM DATA

Table A.1. Equilibrium Data for Run SR−1

Run Number	Sample Number	Run Type	Liquid Volume (mL)	Solids Mass (g)	Elapsed Time (h)	Initial Solution Sr Conc. (meg/mL)	Final Solution Sr Conc. (meg/mL)	Final Solids Sr Conc. (meq/g)
SR−1	1	Batch	2.15	4.690E−01	24.00	2.30E−06	1.51E−09	1.04E−05
SR−1	2	Batch	2.16	4.700E−01	24.00	1.32E−05	8.18E−09	6.06E−05
SR−1	3	Batch	2.18	4.700E−01	24.00	2.26E−04	1.04E−07	1.21E−03
SR−1	4	Batch	2.20	4.700E−01	24.00	2.26E−03	3.03E−06	1.23E−02
SR−1	5	Batch	2.30	4.700E−01	24.00	8.32E−02	2.82E−03	3.94E−01
SR−1	6	Batch	2.40	4.700E−01	24.00	4.12E−01	1.54E−01	1.32E+00

Table A.2. Equilibrium Data for Run SR-2

Run Number	Sample Number	Run Type	Liquid Volume (mL)	Solids Mass (g)	Elapsed Time (h)	Initial Solution Sr Conc. (meg/mL)	Final Solution Sr Conc. (meg/mL)	Final Solids Sr Conc. (meq/g)
SR-2-1	0	Column	166.40	4.000E+01	0.00	2.30E-06	2.29E-06	0.00E+00
SR-2-1	1	Column	166.40	4.000E+01	0.25	2.30E-06	1.09E-06	4.99E-06
SR-2-1	2	Column	166.40	4.000E+01	0.50	2.30E-06	6.06E-07	7.00E-06
SR-2-1	3	Column	166.40	4.000E+01	0.75	2.30E-06	3.74E-07	7.97E-06
SR-2-1	4	Column	166.40	4.000E+01	1.00	2.30E-06	2.52E-07	8.48E-06
SR-2-1	5	Column	166.40	4.000E+01	1.25	2.30E-06	1.72E-07	8.81E-06
SR-2-1	6	Column	166.40	4.000E+01	1.50	2.30E-06	1.19E-07	9.03E-06
SR-2-1	7	Column	166.40	4.000E+01	2.00	2.30E-06	6.45E-08	9.26E-06
SR-2-1	8	Column	166.40	4.000E+01	2.50	2.30E-06	4.18E-08	9.35E-06
SR-2-1	9	Column	166.40	4.000E+01	3.00	2.30E-06	2.68E-08	9.41E-06
SR-2-1	10	Column	166.40	4.000E+01	3.50	2.30E-06	1.80E-08	9.45E-06
SR-2-1	11	Column	166.40	4.000E+01	4.00	2.30E-06	1.35E-08	9.47E-06
SR-2-1	12	Column	166.40	4.000E+01	5.00	2.30E-06	9.40E-09	9.49E-06
SR-2-1	13	Column	166.40	4.000E+01	6.00	2.30E-06	4.60E-09	9.51E-06
SR-2-1	14	Column	166.40	4.000E+01	7.00	2.30E-06	4.91E-09	9.51E-06
SR-2-1	15	Column	166.40	4.000E+01	8.00	2.30E-06	3.97E-09	9.51E-06
SR-2-1	16	Column	166.40	4.000E+01	23.67	2.30E-06	1.74E-09	9.52E-06
SR-2-2	0	Column	166.40	4.000E+01	0.00	2.30E-05	2.28E-08	9.52E-05
SR-2-2	1	Column	166.40	4.000E+01	0.25	2.30E-05	1.59E-08	9.52E-05
SR-2-2	2	Column	166.40	4.000E+01	0.50	2.30E-05	1.36E-08	9.52E-05
SR-2-2	3	Column	166.40	4.000E+01	0.75	2.30E-05	1.28E-08	9.52E-05
SR-2-2	4	Column	166.40	4.000E+01	1.00	2.30E-05	6.46E-09	9.52E-05
SR-2-2	5	Column	166.40	4.000E+01	1.25	2.30E-05	1.36E-08	9.52E-05
SR-2-2	6	Column	166.40	4.000E+01	1.50	2.30E-05	1.18E-08	9.52E-05
SR-2-2	7	Column	166.40	4.000E+01	2.00	2.30E-05	2.07E-08	9.52E-05
SR-2-2	8	Column	166.40	4.000E+01	2.50	2.30E-05	1.49E-08	9.52E-05
SR-2-2	9	Column	166.40	4.000E+01	3.00	2.30E-05	5.44E-09	9.52E-05
SR-2-2	10	Column	166.40	4.000E+01	3.50	2.30E-05	2.64E-09	9.53E-05
SR-2-2	11	Column	166.40	4.000E+01	4.00	2.30E-05	5.70E-09	9.52E-05
SR-2-2	12	Column	166.40	4.000E+01	5.00	2.30E-05	1.16E-08	9.52E-05
SR-2-2	13	Column	166.40	4.000E+01	6.00	2.30E-05	1.21E-08	9.52E-05
SR-2-2	14	Column	166.40	4.000E+01	7.00	2.30E-05	8.76E-09	9.52E-05
SR-2-2	15	Column	166.40	4.000E+01	8.00	2.30E-05	-2.47E-09	9.53E-05
SR-2-2	16	Column	166.40	4.000E+01	23.67	2.30E-05	7.74E-09	9.52E-05
SR-2-3	0	Column	166.60	4.000E+01	0.00	2.30E-04	4.79E-08	9.54E-04
SR-2-3	1	Column	166.60	4.000E+01	0.25	2.30E-04	1.25E-07	9.53E-04
SR-2-3	2	Column	166.60	4.000E+01	0.50	2.30E-04	1.76E-07	9.53E-04
SR-2-3	3	Column	166.60	4.000E+01	0.75	2.30E-04	1.22E-07	9.53E-04
SR-2-3	4	Column	166.60	4.000E+01	1.00	2.30E-04	1.71E-08	9.54E-04
SR-2-3	5	Column	166.60	4.000E+01	1.25	2.30E-04	1.15E-07	9.53E-04
SR-2-3	6	Column	166.60	4.000E+01	1.50	2.30E-04	1.89E-07	9.53E-04
SR-2-3	7	Column	166.60	4.000E+01	2.00	2.30E-04	1.40E-07	9.53E-04
SR-2-3	8	Column	166.60	4.000E+01	2.50	2.30E-04	1.22E-07	9.53E-04
SR-2-3	9	Column	166.60	4.000E+01	3.00	2.30E-04	4.27E-08	9.54E-04
SR-2-3	10	Column	166.60	4.000E+01	3.50	2.30E-04	5.30E-08	9.54E-04
SR-2-3	11	Column	166.60	4.000E+01	4.00	2.30E-04	-1.32E-07	9.54E-04
SR-2-3	12	Column	166.60	4.000E+01	5.00	2.30E-04	1.71E-08	9.54E-04
SR-2-3	13	Column	166.60	4.000E+01	6.00	2.30E-04	1.20E-08	9.54E-04
SR-2-3	14	Column	166.60	4.000E+01	7.00	2.30E-04	1.97E-08	9.54E-04
SR-2-3	15	Column	166.60	4.000E+01	8.00	2.30E-04	4.27E-09	9.54E-04

Table A.2 (Continued)

Run Number	Sample Number	Run Type	Liquid Volume (mL)	Solids Mass (g)	Elapsed Time (h)	Initial Solution Sr Conc. (meg/mL)	Final Solution Sr Conc. (meg/mL)	Final Solids Sr Conc. (meq/g)
SR-2-3	16	Column	166.60	4.000E+01	23.67	2.30E-04	4.02E-08	9.54E-04
SR-2-4	0	Column	166.80	4.000E+01	0.00	2.28E-03	9.62E-07	9.55E-03
SR-2-4	1	Column	166.80	4.000E+01	0.25	2.28E-03	1.48E-06	9.54E-03
SR-2-4	2	Column	166.80	4.000E+01	0.50	2.28E-03	1.92E-06	9.54E-03
SR-2-4	3	Column	166.80	4.000E+01	0.75	2.28E-03	1.25E-06	9.54E-03
SR-2-4	4	Column	166.80	4.000E+01	1.00	2.28E-03	7.80E-07	9.55E-03
SR-2-4	5	Column	166.80	4.000E+01	1.25	2.28E-03	1.01E-06	9.55E-03
SR-2-4	6	Column	166.80	4.000E+01	1.50	2.28E-03	4.68E-07	9.55E-03
SR-2-4	7	Column	166.80	4.000E+01	2.00	2.28E-03	6.50E-07	9.55E-03
SR-2-4	8	Column	166.80	4.000E+01	2.50	2.28E-03	8.84E-07	9.55E-03
SR-2-4	9	Column	166.80	4.000E+01	3.00	2.28E-03	1.07E-06	9.54E-03
SR-2-4	10	Column	166.80	4.000E+01	3.50	2.28E-03	1.79E-06	9.54E-03
SR-2-4	11	Column	166.80	4.000E+01	4.00	2.28E-03	3.12E-07	9.55E-03
SR-2-4	12	Column	166.80	4.000E+01	5.00	2.28E-03	5.20E-07	9.55E-03
SR-2-4	13	Column	166.80	4.000E+01	6.00	2.28E-03	2.34E-07	9.55E-03
SR-2-4	14	Column	166.80	4.000E+01	7.00	2.28E-03	8.84E-07	9.55E-03
SR-2-4	15	Column	166.80	4.000E+01	8.00	2.28E-03	1.27E-06	9.54E-03
SR-2-4	16	Column	166.80	4.000E+01	23.67	2.28E-03	1.04E-06	9.54E-03
SR-2-5	0	Column	167.00	4.000E+01	0.00	8.72E-02	2.61E-05	3.64E-01
SR-2-5	1	Column	167.00	4.000E+01	0.25	8.72E-02	3.13E-04	3.63E-01
SR-2-5	2	Column	167.00	4.000E+01	0.50	8.72E-02	6.07E-04	3.62E-01
SR-2-5	3	Column	167.00	4.000E+01	0.75	8.72E-02	7.93E-04	3.61E-01
SR-2-5	4	Column	167.00	4.000E+01	1.00	8.72E-02	1.09E-03	3.59E-01
SR-2-5	5	Column	167.00	4.000E+01	1.25	8.72E-02	1.32E-03	3.59E-01
SR-2-5	6	Column	167.00	4.000E+01	1.50	8.72E-02	1.56E-03	3.58E-01
SR-2-5	7	Column	167.00	4.000E+01	2.00	8.72E-02	1.86E-03	3.56E-01
SR-2-5	8	Column	167.00	4.000E+01	2.50	8.72E-02	2.00E-03	3.56E-01
SR-2-5	9	Column	167.00	4.000E+01	3.00	8.72E-02	2.30E-03	3.54E-01
SR-2-5	10	Column	167.00	4.000E+01	3.50	8.72E-02	2.46E-03	3.54E-01
SR-2-5	11	Column	167.00	4.000E+01	4.00	8.72E-02	2.56E-03	3.53E-01
SR-2-5	12	Column	167.00	4.000E+01	5.00	8.72E-02	2.46E-03	3.54E-01
SR-2-5	13	Column	167.00	4.000E+01	6.00	8.72E-02	2.73E-03	3.53E-01
SR-2-5	14	Column	167.00	4.000E+01	7.00	8.72E-02	2.70E-03	3.53E-01
SR-2-5	15	Column	167.00	4.000E+01	8.00	8.72E-02	2.67E-03	3.53E-01
SR-2-5	16	Column	167.00	4.000E+01	23.67	8.72E-02	2.97E-03	3.52E-01
SR-2-6	0	Column	167.50	4.000E+01	0.00	4.34E-01	1.45E-02	1.76E+00
SR-2-6	1	Column	167.50	4.000E+01	0.25	4.34E-01	1.11E-01	1.36E+00
SR-2-6	2	Column	167.50	4.000E+01	0.50	4.34E-01	1.47E-01	1.21E+00
SR-2-6	3	Column	167.50	4.000E+01	0.75	4.34E-01	1.64E-01	1.14E+00
SR-2-6	4	Column	167.50	4.000E+01	1.00	4.34E-01	1.69E-01	1.11E+00
SR-2-6	5	Column	167.50	4.000E+01	1.25	4.34E-01	1.74E-01	1.09E+00
SR-2-6	6	Column	167.50	4.000E+01	1.50	4.34E-01	1.80E-01	1.07E+00
SR-2-6	7	Column	167.50	4.000E+01	2.00	4.34E-01	1.81E-01	1.06E+00
SR-2-6	8	Column	167.50	4.000E+01	2.50	4.34E-01	1.89E-01	1.03E+00
SR-2-6	9	Column	167.50	4.000E+01	3.00	4.34E-01	1.88E-01	1.03E+00
SR-2-6	10	Column	167.50	4.000E+01	3.50	4.34E-01	1.89E-01	1.03E+00
SR-2-6	11	Column	167.50	4.000E+01	4.00	4.34E-01	1.89E-01	1.03E+00
SR-2-6	12	Column	167.50	4.000E+01	5.00	4.34E-01	1.95E-01	1.01E+00
SR-2-6	13	Column	167.50	4.000E+01	6.00	4.34E-01	1.89E-01	1.03E+00
SR-2-6	14	Column	167.50	4.000E+01	7.00	4.34E-01	1.95E-01	1.01E+00

Table A.2 (Continued)

Run Number	Sample Number	Run Type	Liquid Volume (mL)	Solids Mass (g)	Elapsed Time (h)	Initial Solution Sr Conc. (meg/mL)	Final Solution Sr Conc. (meg/mL)	Final Solids Sr Conc. (meq/g)
SR-2-6	15	Column	167.50	4.000E+01	8.00	4.34E-01	1.99E-01	9.89E-01
SR-2-6	16	Column	167.50	4.000E+01	23.67	4.34E-01	2.04E-01	9.68E-01

Table A.3. Equilibrium Data for Run SR-3

Run Number	Sample Number	Run Type	Liquid Volume (mL)	Solids Mass (g)	Elapsed Time (h)	Initial Solution Cs Conc. (meg/mL)	Final Solution Cs Conc. (meg/mL)	Final Solids Cs Conc. (meq/g)
SR-3-1	0	Column	165.58	4.000E+01	0.00	1.00E-09	1.00E-09	0.00E+00
SR-3-1	1	Column	165.58	4.000E+01	0.25	1.00E-09	4.37E-10	2.33E-09
SR-3-1	2	Column	165.58	4.000E+01	0.50	1.00E-09	1.96E-10	3.33E-09
SR-3-1	3	Column	165.58	4.000E+01	0.75	1.00E-09	8.85E-11	3.77E-09
SR-3-1	4	Column	165.58	4.000E+01	1.00	1.00E-09	4.90E-11	3.94E-09
SR-3-1	5	Column	165.58	4.000E+01	1.25	1.00E-09	3.02E-11	4.01E-09
SR-3-1	6	Column	165.58	4.000E+01	1.50	1.00E-09	2.04E-11	4.05E-09
SR-3-1	7	Column	165.58	4.000E+01	2.00	1.00E-09	1.15E-11	4.09E-09
SR-3-1	8	Column	165.58	4.000E+01	2.50	1.00E-09	6.61E-12	4.11E-09
SR-3-1	9	Column	165.58	4.000E+01	3.00	1.00E-09	4.91E-12	4.12E-09
SR-3-1	10	Column	165.58	4.000E+01	3.50	1.00E-09	3.56E-12	4.12E-09
SR-3-1	11	Column	165.58	4.000E+01	4.00	1.00E-09	3.73E-12	4.12E-09
SR-3-1	12	Column	165.58	4.000E+01	5.00	1.00E-09	2.84E-12	4.13E-09
SR-3-1	13	Column	165.58	4.000E+01	6.00	1.00E-09	2.05E-12	4.13E-09
SR-3-1	14	Column	165.58	4.000E+01	7.00	1.00E-09	2.25E-12	4.13E-09
SR-3-1	15	Column	165.58	4.000E+01	8.00	1.00E-09	1.69E-12	4.13E-09
SR-3-1	16	Column	165.58	4.000E+01	23.42	1.00E-09	9.52E-13	4.14E-09
SR-3-2	0	Column	165.59	4.000E+01	0.00	1.00E-08	1.08E-11	4.14E-08
SR-3-2	1	Column	165.59	4.000E+01	0.25	1.00E-08	9.02E-12	4.14E-08
SR-3-2	2	Column	165.59	4.000E+01	0.50	1.00E-08	8.29E-12	4.14E-08
SR-3-2	3	Column	165.59	4.000E+01	0.75	1.00E-08	7.83E-12	4.14E-08
SR-3-2	4	Column	165.59	4.000E+01	1.00	1.00E-08	9.48E-12	4.14E-08
SR-3-2	5	Column	165.59	4.000E+01	1.25	1.00E-08	9.30E-12	4.14E-08
SR-3-2	6	Column	165.59	4.000E+01	1.50	1.00E-08	6.08E-12	4.14E-08
SR-3-2	7	Column	165.59	4.000E+01	2.00	1.00E-08	7.64E-12	4.14E-08
SR-3-2	8	Column	165.59	4.000E+01	2.50	1.00E-08	6.45E-12	4.14E-08
SR-3-2	9	Column	165.59	4.000E+01	3.00	1.00E-08	9.67E-12	4.14E-08
SR-3-2	10	Column	165.59	4.000E+01	3.50	1.00E-08	3.68E-12	4.14E-08
SR-3-2	11	Column	165.59	4.000E+01	4.00	1.00E-08	1.03E-11	4.14E-08
SR-3-2	12	Column	165.59	4.000E+01	5.00	1.00E-08	2.85E-12	4.14E-08
SR-3-2	13	Column	165.59	4.000E+01	6.00	1.00E-08	5.25E-12	4.14E-08
SR-3-2	14	Column	165.59	4.000E+01	7.00	1.00E-08	9.02E-12	4.14E-08
SR-3-2	15	Column	165.59	4.000E+01	8.00	1.00E-08	8.47E-12	4.14E-08
SR-3-2	16	Column	165.59	4.000E+01	23.67	1.00E-08	8.75E-12	4.14E-08
SR-3-3	0	Column	165.61	4.000E+01	0.00	1.00E-06	6.00E-10	4.14E-06
SR-3-3	1	Column	165.61	4.000E+01	0.25	1.00E-06	9.49E-10	4.14E-06
SR-3-3	2	Column	165.61	4.000E+01	0.50	1.00E-06	3.24E-10	4.14E-06
SR-3-3	3	Column	165.61	4.000E+01	0.75	1.00E-06	4.99E-10	4.14E-06
SR-3-3	4	Column	165.61	4.000E+01	1.00	1.00E-06	4.53E-10	4.14E-06
SR-3-3	5	Column	165.61	4.000E+01	1.25	1.00E-06	7.56E-10	4.14E-06
SR-3-3	6	Column	165.61	4.000E+01	1.50	1.00E-06	1.32E-10	4.14E-06
SR-3-3	7	Column	165.61	4.000E+01	2.00	1.00E-06	7.65E-11	4.14E-06
SR-3-3	8	Column	165.61	4.000E+01	2.50	1.00E-06	3.70E-10	4.14E-06
SR-3-3	9	Column	165.61	4.000E+01	3.00	1.00E-06	3.61E-10	4.14E-06
SR-3-3	10	Column	165.61	4.000E+01	3.50	1.00E-06	2.23E-10	4.14E-06
SR-3-3	11	Column	165.61	4.000E+01	4.00	1.00E-06	3.24E-10	4.14E-06
SR-3-3	12	Column	165.61	4.000E+01	5.00	1.00E-06	3.70E-10	4.14E-06
SR-3-3	13	Column	165.61	4.000E+01	6.00	1.00E-06	2.60E-10	4.14E-06
SR-3-3	14	Column	165.61	4.000E+01	7.00	1.00E-06	4.16E-10	4.14E-06
SR-3-3	15	Column	165.61	4.000E+01	8.00	1.00E-06	3.06E-11	4.14E-06

Table A.3 (Continued)

Run Number	Sample Number	Run Type	Liquid Volume (mL)	Solids Mass (g)	Elapsed Time (h)	Initial Solution Cs Conc. (meg/mL)	Final Solution Cs Conc. (meg/mL)	Final Solids Cs Conc. (meq/g)
SR-3-3	16	Column	165.61	4.000E+01	23.67	1.00E-06	4.90E-10	4.14E-06
SR-3-4	0	Column	165.63	4.000E+01	0.00	1.00E-04	6.14E-08	4.14E-04
SR-3-4	1	Column	165.63	4.000E+01	0.25	1.00E-04	1.44E-08	4.14E-04
SR-3-4	2	Column	165.63	4.000E+01	0.50	1.00E-04	5.12E-08	4.14E-04
SR-3-4	3	Column	165.63	4.000E+01	0.75	1.00E-04	3.10E-08	4.14E-04
SR-3-4	4	Column	165.63	4.000E+01	1.00	1.00E-04	4.66E-08	4.14E-04
SR-3-4	5	Column	165.63	4.000E+01	1.25	1.00E-04	4.02E-08	4.14E-04
SR-3-4	6	Column	165.63	4.000E+01	1.50	1.00E-04	3.19E-08	4.14E-04
SR-3-4	7	Column	165.63	4.000E+01	2.00	1.00E-04	2.45E-08	4.14E-04
SR-3-4	8	Column	165.63	4.000E+01	2.50	1.00E-04	-2.33E-08	4.14E-04
SR-3-4	9	Column	165.63	4.000E+01	3.00	1.00E-04	3.83E-08	4.14E-04
SR-3-4	10	Column	165.63	4.000E+01	3.50	1.00E-04	6.14E-09	4.14E-04
SR-3-4	11	Column	165.63	4.000E+01	4.00	1.00E-04	6.14E-08	4.14E-04
SR-3-4	12	Column	165.63	4.000E+01	5.00	1.00E-04	2.64E-08	4.14E-04
SR-3-4	13	Column	165.63	4.000E+01	6.00	1.00E-04	2.55E-08	4.14E-04
SR-3-4	14	Column	165.63	4.000E+01	7.00	1.00E-04	5.03E-08	4.14E-04
SR-3-4	15	Column	165.63	4.000E+01	8.00	1.00E-04	3.47E-08	4.14E-04
SR-3-4	16	Column	165.63	4.000E+01	23.67	1.00E-04	3.28E-08	4.14E-04
SR-3-5	0	Column	165.75	4.000E+01	0.00	2.00E-02	9.20E-06	8.28E-02
SR-3-5	1	Column	165.75	4.000E+01	0.25	2.00E-02	8.84E-06	8.28E-02
SR-3-5	2	Column	165.75	4.000E+01	0.50	2.00E-02	3.13E-06	8.29E-02
SR-3-5	3	Column	165.75	4.000E+01	0.75	2.00E-02	2.02E-06	8.29E-02
SR-3-5	4	Column	165.75	4.000E+01	1.00	2.00E-02	3.68E-06	8.29E-02
SR-3-5	5	Column	165.75	4.000E+01	1.25	2.00E-02	3.68E-06	8.29E-02
SR-3-5	6	Column	165.75	4.000E+01	1.50	2.00E-02	3.31E-06	8.29E-02
SR-3-5	7	Column	165.75	4.000E+01	2.00	2.00E-02	9.76E-06	8.28E-02
SR-3-5	8	Column	165.75	4.000E+01	2.50	2.00E-02	9.57E-06	8.28E-02
SR-3-5	9	Column	165.75	4.000E+01	3.00	2.00E-02	6.07E-06	8.28E-02
SR-3-5	10	Column	165.75	4.000E+01	3.50	2.00E-02	6.44E-06	8.28E-02
SR-3-5	11	Column	165.75	4.000E+01	4.00	2.00E-02	1.47E-06	8.29E-02
SR-3-5	12	Column	165.75	4.000E+01	5.00	2.00E-02	5.15E-06	8.29E-02
SR-3-5	13	Column	165.75	4.000E+01	6.00	2.00E-02	3.50E-06	8.29E-02
SR-3-5	14	Column	165.75	4.000E+01	7.00	2.00E-02	7.36E-07	8.29E-02
SR-3-5	15	Column	165.75	4.000E+01	8.00	2.00E-02	3.31E-06	8.29E-02
SR-3-5	16	Column	165.75	4.000E+01	23.08	2.00E-02	9.20E-07	8.29E-02
SR-3-6	0	Column	167.00	4.000E+01	0.00	2.00E-01	-6.20E-07	8.35E-01
SR-3-6	1	Column	167.00	4.000E+01	0.25	2.00E-01	2.35E-05	8.35E-01
SR-3-6	2	Column	167.00	4.000E+01	0.50	2.00E-01	5.14E-05	8.35E-01
SR-3-6	3	Column	167.00	4.000E+01	0.75	2.00E-01	5.89E-05	8.35E-01
SR-3-6	4	Column	167.00	4.000E+01	1.00	2.00E-01	-4.71E-05	8.35E-01
SR-3-6	5	Column	167.00	4.000E+01	1.25	2.00E-01	8.86E-05	8.35E-01
SR-3-6	6	Column	167.00	4.000E+01	1.50	2.00E-01	3.47E-05	8.35E-01
SR-3-6	7	Column	167.00	4.000E+01	2.00	2.00E-01	1.09E-04	8.35E-01
SR-3-6	8	Column	167.00	4.000E+01	2.50	2.00E-01	2.34E-04	8.34E-01
SR-3-6	9	Column	167.00	4.000E+01	3.00	2.00E-01	3.01E-04	8.34E-01
SR-3-6	10	Column	167.00	4.000E+01	3.50	2.00E-01	4.79E-04	8.33E-01
SR-3-6	11	Column	167.00	4.000E+01	4.00	2.00E-01	6.11E-04	8.32E-01
SR-3-6	12	Column	167.00	4.000E+01	5.00	2.00E-01	8.23E-04	8.32E-01
SR-3-6	13	Column	167.00	4.000E+01	6.00	2.00E-01	1.06E-03	8.31E-01
SR-3-6	14	Column	167.00	4.000E+01	7.00	2.00E-01	1.15E-03	8.30E-01

Table A.3 (Continued)

Run Number	Sample Number	Run Type	Liquid Volume (mL)	Solids Mass (g)	Elapsed Time (h)	Initial Solution Cs Conc. (meg/mL)	Final Solution Cs Conc. (meg/mL)	Final Solids Cs Conc. (meq/g)
SR-3-6	15	Column	167.00	4.000E+01	8.00	2.00E-01	1.16E-03	8.30E-01
SR-3-6	16	Column	167.00	4.000E+01	23.67	2.00E-01	1.26E-03	8.30E-01

Table A.4. Equilibrium Data for Run SR−4

Run Number	Sample Number	Run Type	Liquid Volume (mL)	Solids Mass (g)	Elapsed Time (h)	Initial Solution Cs Conc. (meg/mL)	Final Solution Cs Conc. (meg/mL)	Final Solids Cs Conc. (meq/g)	Final Solution Na Conc. (meg/mL)
SR−4	1	Batch	2.01	4.68E−01	24.00	1.00E−09	3.39E−13	4.28E−09	6.89E−04
SR−4	2	Batch	2.00	4.67E−01	24.00	1.00E−08	1.10E−12	4.28E−08	1.22E−03
SR−4	3	Batch	2.00	4.69E−01	24.00	1.00E−06	1.58E−10	4.27E−06	4.94E−04
SR−4	4	Batch	2.00	4.70E−01	24.00	1.00E−04	4.16E−08	4.25E−04	5.43E−04
SR−4	5	Batch	2.00	4.70E−01	24.00	2.00E−02	3.20E−06	8.51E−02	2.14E−02
SR−4	6	Batch	2.04	4.71E−01	24.00	2.00E−01	1.27E−03	8.62E−01	2.25E−01

Table A.5. Equilibrium Data for Run SR-5

Run Number	Sample Number	Run Type	Liquid Volume (mL)	Solids Mass (g)	Elapsed Time (h)	Initial Solution Sr Conc. (meg/mL)	Final Solution Sr Conc. (meg/mL)	Final Solids Sr Conc. (meq/g)	Initial Solution Cs Conc. (meg/mL)	Final Solution Cs Conc. (meg/mL)	Final Solids Cs Conc. (meq/g)
SR-5-1	0	Column	166.40	4.000E+01	0.00	2.28E-06	2.28E-06	2.25E-22	1.00E-09	1.00E-09	-2.00E-25
SR-5-1	1	Column	166.40	4.000E+01	0.25	2.28E-06	1.16E-06	4.67E-06	1.00E-09	4.02E-10	2.49E-09
SR-5-1	2	Column	166.40	4.000E+01	0.50	2.28E-06	5.62E-07	7.16E-06	1.00E-09	1.41E-10	3.57E-09
SR-5-1	3	Column	166.40	4.000E+01	0.75	2.28E-06	3.01E-07	8.24E-06	1.00E-09	4.91E-11	3.96E-09
SR-5-1	4	Column	166.40	4.000E+01	1.00	2.28E-06	1.74E-07	8.77E-06	1.00E-09	1.94E-11	4.08E-09
SR-5-1	5	Column	166.40	4.000E+01	1.25	2.28E-06	1.12E-07	9.03E-06	1.00E-09	9.80E-12	4.12E-09
SR-5-1	6	Column	166.40	4.000E+01	1.50	2.28E-06	7.40E-08	9.19E-06	1.00E-09	5.43E-12	4.14E-09
SR-5-1	7	Column	166.40	4.000E+01	2.00	2.28E-06	3.39E-08	9.35E-06	1.00E-09	2.57E-12	4.15E-09
SR-5-1	8	Column	166.40	4.000E+01	2.50	2.28E-06	2.12E-08	9.40E-06	1.00E-09	1.91E-12	4.15E-09
SR-5-1	9	Column	166.40	4.000E+01	3.00	2.28E-06	1.90E-08	9.41E-06	1.00E-09	2.05E-12	4.15E-09
SR-5-1	10	Column	166.40	4.000E+01	3.50	2.28E-06	1.22E-08	9.44E-06	1.00E-09	1.12E-12	4.16E-09
SR-5-1	11	Column	166.40	4.000E+01	4.00	2.28E-06	9.20E-09	9.45E-06	1.00E-09	1.16E-12	4.16E-09
SR-5-1	12	Column	166.40	4.000E+01	5.00	2.28E-06	5.44E-09	9.47E-06	1.00E-09	7.81E-13	4.16E-09
SR-5-1	13	Column	166.40	4.000E+01	6.00	2.28E-06	3.66E-09	9.48E-06	1.00E-09	5.43E-13	4.16E-09
SR-5-1	14	Column	166.40	4.000E+01	7.00	2.28E-06	2.67E-09	9.48E-06	1.00E-09	4.24E-13	4.16E-09
SR-5-1	15	Column	166.40	4.000E+01	8.00	2.28E-06	2.42E-09	9.48E-06	1.00E-09	7.02E-13	4.16E-09
SR-5-1	16	Column	166.40	4.000E+01	23.58	2.28E-06	1.13E-09	9.49E-06	1.00E-09	1.06E-13	4.16E-09
SR-5-2	0	Column	166.40	4.000E+01	0.00	2.28E-05	1.18E-08	9.49E-05	1.00E-08	6.63E-13	4.16E-08
SR-5-2	1	Column	166.40	4.000E+01	0.25	2.28E-05	7.50E-09	9.49E-05	1.00E-08	1.66E-12	4.16E-08
SR-5-2	2	Column	166.40	4.000E+01	0.50	2.28E-05	6.49E-09	9.49E-05	1.00E-08	3.25E-12	4.16E-08
SR-5-2	3	Column	166.40	4.000E+01	0.75	2.28E-05	7.03E-09	9.49E-05	1.00E-08	1.66E-12	4.16E-08
SR-5-2	4	Column	166.40	4.000E+01	1.00	2.28E-05	6.11E-09	9.49E-05	1.00E-08	8.62E-13	4.16E-08
SR-5-2	5	Column	166.40	4.000E+01	1.25	2.28E-05	5.14E-09	9.49E-05	1.00E-08	1.46E-12	4.16E-08
SR-5-2	6	Column	166.40	4.000E+01	1.50	2.28E-05	5.08E-09	9.49E-05	1.00E-08	2.85E-12	4.16E-08
SR-5-2	7	Column	166.40	4.000E+01	2.00	2.28E-05	7.08E-09	9.49E-05	1.00E-08	4.64E-13	4.16E-08
SR-5-2	8	Column	166.40	4.000E+01	2.50	2.28E-05	7.52E-09	9.49E-05	1.00E-08	1.26E-12	4.16E-08
SR-5-2	9	Column	166.40	4.000E+01	3.00	2.28E-05	5.10E-09	9.49E-05	1.00E-08	2.25E-12	4.16E-08
SR-5-2	10	Column	166.40	4.000E+01	3.50	2.28E-05	8.98E-09	9.49E-05	1.00E-08	4.64E-13	4.16E-08

Table A.5 (Continued)

Run Number	Sample Number	Run Type	Liquid Volume (mL)	Solids Mass (g)	Elapsed Time (h)	Initial Solution Sr Conc. (meg/mL)	Final Solution Sr Conc. (meg/mL)	Final Solids Sr Conc. (meq/g)	Initial Solution Cs Conc. (meg/mL)	Final Solution Cs Conc. (meg/mL)	Final Solids Cs Conc. (meq/g)
SR-5-2	11	Column	166.40	4.000E+01	4.00	2.28E-05	3.23E-09	9.49E-05	1.00E-08	1.66E-12	4.16E-08
SR-5-2	12	Column	166.40	4.000E+01	5.00	2.28E-05	8.98E-10	9.49E-05	1.00E-08	6.63E-13	4.16E-08
SR-5-2	13	Column	166.40	4.000E+01	6.00	2.28E-05	5.20E-09	9.49E-05	1.00E-08	6.63E-14	4.16E-08
SR-5-2	14	Column	166.40	4.000E+01	7.00	2.28E-05	3.73E-09	9.49E-05	1.00E-08	1.06E-12	4.16E-08
SR-5-2	15	Column	166.40	4.000E+01	8.00	2.28E-05	3.98E-10	9.49E-05	1.00E-08	1.26E-12	4.16E-08
SR-5-2	16	Column	166.40	4.000E+01	23.67	2.28E-05	4.20E-09	9.49E-05	1.00E-08	1.26E-12	4.16E-08
SR-5-3	0	Column	166.40	4.000E+01	0.00	2.28E-04	3.11E-08	9.49E-04	1.00E-06	1.66E-10	4.16E-06
SR-5-3	1	Column	166.40	4.000E+01	0.25	2.28E-04	2.77E-09	9.49E-04	1.00E-06	4.64E-11	4.16E-06
SR-5-3	2	Column	166.40	4.000E+01	0.50	2.28E-04	2.71E-08	9.49E-04	1.00E-06	-1.33E-11	4.16E-06
SR-5-3	3	Column	166.40	4.000E+01	0.75	2.28E-04	-2.73E-09	9.49E-04	1.00E-06	2.06E-10	4.16E-06
SR-5-3	4	Column	166.40	4.000E+01	1.00	2.28E-04	6.97E-08	9.49E-04	1.00E-06	1.46E-10	4.16E-06
SR-5-3	5	Column	166.40	4.000E+01	1.25	2.28E-04	-2.98E-09	9.49E-04	1.00E-06	2.65E-10	4.16E-06
SR-5-3	6	Column	166.40	4.000E+01	1.50	2.28E-04	2.60E-09	9.49E-04	1.00E-06	8.62E-11	4.16E-06
SR-5-3	7	Column	166.40	4.000E+01	2.00	2.28E-04	4.14E-08	9.49E-04	1.00E-06	2.65E-11	4.16E-06
SR-5-3	8	Column	166.40	4.000E+01	2.50	2.28E-04	-1.79E-09	9.49E-04	1.00E-06	-1.33E-11	4.16E-06
SR-5-3	9	Column	166.40	4.000E+01	3.00	2.28E-04	-7.11E-09	9.49E-04	1.00E-06	1.06E-10	4.16E-06
SR-5-3	10	Column	166.40	4.000E+01	3.50	2.28E-04	1.21E-08	9.49E-04	1.00E-06	1.26E-10	4.16E-06
SR-5-3	11	Column	166.40	4.000E+01	4.00	2.28E-04	-6.77E-09	9.49E-04	1.00E-06	2.65E-11	4.16E-06
SR-5-3	12	Column	166.40	4.000E+01	5.00	2.28E-04	1.73E-08	9.49E-04	1.00E-06	2.65E-11	4.16E-06
SR-5-3	13	Column	166.40	4.000E+01	6.00	2.28E-04	2.68E-09	9.49E-04	1.00E-06	6.63E-11	4.16E-06
SR-5-3	14	Column	166.40	4.000E+01	7.00	2.28E-04	-1.16E-08	9.49E-04	1.00E-06	2.65E-11	4.16E-06
SR-5-3	15	Column	166.40	4.000E+01	8.00	2.28E-04	1.74E-08	9.49E-04	1.00E-06	6.63E-12	4.16E-06
SR-5-3	16	Column	166.40	4.000E+01	23.67	2.28E-04	-6.60E-09	9.49E-04	1.00E-06	-1.33E-11	4.16E-06
SR-5-4	0	Column	166.40	4.000E+01	0.00	2.28E-03	1.26E-07	9.49E-03	1.00E-04	2.65E-09	4.16E-04
SR-5-4	1	Column	166.40	4.000E+01	0.25	2.28E-03	2.21E-07	9.49E-03	1.00E-04	6.63E-09	4.16E-04
SR-5-4	2	Column	166.40	4.000E+01	0.50	2.28E-03	3.18E-07	9.49E-03	1.00E-04	6.63E-09	4.16E-04
SR-5-4	3	Column	166.40	4.000E+01	0.75	2.28E-03	3.15E-07	9.49E-03	1.00E-04	1.46E-08	4.16E-04
SR-5-4	4	Column	166.40	4.000E+01	1.00	2.28E-03	-2.06E-08	9.49E-03	1.00E-04	4.64E-09	4.16E-04

Table A.5 (Continued)

Run Number	Sample Number	Run Type	Liquid Volume (mL)	Solids Mass (g)	Elapsed Time (h)	Initial Solution Sr Conc. (meg/mL)	Final Solution Sr Conc. (meg/mL)	Final Solids Sr Conc. (meq/g)	Initial Solution Cs Conc. (meg/mL)	Final Solution Cs Conc. (meg/mL)	Final Solids Cs Conc. (meq/g)
SR-5-4	5	Column	166.40	4.000E+01	1.25	2.28E-03	3.66E-07	9.49E-03	1.00E-04	8.62E-09	4.16E-04
SR-5-4	6	Column	166.40	4.000E+01	1.50	2.28E-03	7.47E-08	9.49E-03	1.00E-04	8.62E-09	4.16E-04
SR-5-4	7	Column	166.40	4.000E+01	2.00	2.28E-03	2.19E-07	9.49E-03	1.00E-04	1.06E-08	4.16E-04
SR-5-4	8	Column	166.40	4.000E+01	2.50	2.28E-03	1.27E-07	9.49E-03	1.00E-04	6.63E-10	4.16E-04
SR-5-4	9	Column	166.40	4.000E+01	3.00	2.28E-03	-7.26E-08	9.49E-03	1.00E-04	1.26E-08	4.16E-04
SR-5-4	10	Column	166.40	4.000E+01	3.50	2.28E-03	3.18E-07	9.49E-03	1.00E-04	6.63E-09	4.16E-04
SR-5-4	11	Column	166.40	4.000E+01	4.00	2.28E-03	1.27E-07	9.49E-03	1.00E-04	-1.33E-09	4.16E-04
SR-5-4	12	Column	166.40	4.000E+01	5.00	2.28E-03	2.19E-07	9.49E-03	1.00E-04	1.26E-08	4.16E-04
SR-5-4	13	Column	166.40	4.000E+01	6.00	2.28E-03	1.23E-07	9.49E-03	1.00E-04	8.62E-09	4.16E-04
SR-5-4	14	Column	166.40	4.000E+01	7.00	2.28E-03	3.17E-07	9.49E-03	1.00E-04	8.62E-09	4.16E-04
SR-5-4	15	Column	166.40	4.000E+01	8.00	2.28E-03	4.11E-07	9.49E-03	1.00E-04	1.66E-08	4.16E-04
SR-5-4	16	Column	166.40	4.000E+01	23.42	2.28E-03	2.70E-07	9.49E-03	1.00E-04	6.63E-09	4.16E-04
SR-5-5	0	Column	166.40	4.000E+01	0.00	8.72E-02	4.87E-06	3.63E-01	5.00E-02	1.66E-06	2.08E-01
SR-5-5	1	Column	166.40	4.000E+01	0.25	8.72E-02	1.17E-03	3.58E-01	5.00E-02	4.64E-06	2.08E-01
SR-5-5	2	Column	166.40	4.000E+01	0.50	8.72E-02	3.13E-03	3.50E-01	5.00E-02	8.62E-06	2.08E-01
SR-5-5	3	Column	166.40	4.000E+01	0.75	8.72E-02	4.87E-03	3.43E-01	5.00E-02	5.64E-06	2.08E-01
SR-5-5	4	Column	166.40	4.000E+01	1.00	8.72E-02	5.72E-03	3.39E-01	5.00E-02	1.66E-06	2.08E-01
SR-5-5	5	Column	166.40	4.000E+01	1.25	8.72E-02	6.29E-03	3.37E-01	5.00E-02	2.65E-06	2.08E-01
SR-5-5	6	Column	166.40	4.000E+01	1.50	8.72E-02	6.52E-03	3.36E-01	5.00E-02	7.62E-06	2.08E-01
SR-5-5	7	Column	166.40	4.000E+01	2.00	8.72E-02	7.16E-03	3.33E-01	5.00E-02	3.65E-06	2.08E-01
SR-5-5	8	Column	166.40	4.000E+01	2.50	8.72E-02	7.23E-03	3.33E-01	5.00E-02	6.63E-07	2.08E-01
SR-5-5	9	Column	166.40	4.000E+01	3.00	8.72E-02	7.38E-03	3.32E-01	5.00E-02	2.65E-06	2.08E-01
SR-5-5	10	Column	166.40	4.000E+01	3.50	8.72E-02	7.40E-03	3.32E-01	5.00E-02	1.66E-06	2.08E-01
SR-5-5	11	Column	166.40	4.000E+01	4.00	8.72E-02	7.40E-03	3.32E-01	5.00E-02	5.64E-06	2.08E-01
SR-5-5	12	Column	166.40	4.000E+01	5.00	8.72E-02	7.60E-03	3.31E-01	5.00E-02	-3.31E-06	2.08E-01
SR-5-5	13	Column	166.40	4.000E+01	6.00	8.72E-02	7.43E-03	3.32E-01	5.00E-02	3.65E-06	2.08E-01
SR-5-5	14	Column	166.40	4.000E+01	7.00	8.72E-02	7.64E-03	3.31E-01	5.00E-02	6.63E-07	2.08E-01
SR-5-5	15	Column	166.40	4.000E+01	8.00	8.72E-02	7.44E-03	3.32E-01	5.00E-02	-3.31E-07	2.08E-01

Table A.5 (Continued)

Run Number	Sample Number	Run Type	Liquid Volume (mL)	Solids Mass (g)	Elapsed Time (h)	Initial Solution Sr Conc. (meg/mL)	Final Solution Sr Conc. (meg/mL)	Final Solids Sr Conc. (meq/g)	Initial Solution Cs Conc. (meg/mL)	Final Solution Cs Conc. (meg/mL)	Final Solids Cs Conc. (meq/g)
SR-5-5	16	Column	166.40	4.000E+01	24.75	8.72E-02	7.64E-03	3.31E-01	5.00E-02	2.65E-06	2.08E-01
SR-5-6	0	Column	166.50	4.000E+01	0.00	4.34E-01	4.01E-02	1.67E+00	5.00E-01	2.70E-05	2.12E+00
SR-5-6	1	Column	166.50	4.000E+01	0.25	4.34E-01	3.05E-01	5.49E-01	5.00E-01	4.05E-02	1.95E+00
SR-5-6	2	Column	166.50	4.000E+01	0.50	4.34E-01	3.44E-01	3.84E-01	5.00E-01	1.26E-01	1.59E+00
SR-5-6	3	Column	166.50	4.000E+01	0.75	4.34E-01	3.58E-01	3.25E-01	5.00E-01	1.31E-01	1.57E+00
SR-5-6	4	Column	166.50	4.000E+01	1.00	4.34E-01	3.65E-01	2.95E-01	5.00E-01	1.22E-01	1.61E+00
SR-5-6	5	Column	166.50	4.000E+01	1.25	4.34E-01	3.64E-01	2.97E-01	5.00E-01	1.19E-01	1.62E+00
SR-5-6	6	Column	166.50	4.000E+01	1.50	4.34E-01	3.74E-01	2.54E-01	5.00E-01	1.14E-01	1.64E+00
SR-5-6	7	Column	166.50	4.000E+01	2.00	4.34E-01	3.74E-01	2.56E-01	5.00E-01	1.14E-01	1.64E+00
SR-5-6	8	Column	166.50	4.000E+01	2.50	4.34E-01	3.77E-01	2.42E-01	5.00E-01	1.12E-01	1.65E+00
SR-5-6	9	Column	166.50	4.000E+01	3.00	4.34E-01	3.79E-01	2.33E-01	5.00E-01	1.12E-01	1.65E+00
SR-5-6	10	Column	166.50	4.000E+01	3.50	4.34E-01	3.85E-01	2.09E-01	5.00E-01	1.13E-01	1.64E+00
SR-5-6	11	Column	166.50	4.000E+01	4.00	4.34E-01	3.83E-01	2.16E-01	5.00E-01	1.14E-01	1.64E+00
SR-5-6	12	Column	166.50	4.000E+01	5.00	4.34E-01	3.86E-01	2.05E-01	5.00E-01	1.13E-01	1.65E+00
SR-5-6	13	Column	166.50	4.000E+01	6.00	4.34E-01	3.83E-01	2.18E-01	5.00E-01	1.13E-01	1.65E+00
SR-5-6	14	Column	166.50	4.000E+01	7.00	4.34E-01	3.86E-01	2.03E-01	5.00E-01	1.11E-01	1.65E+00
SR-5-6	15	Column	166.50	4.000E+01	8.00	4.34E-01	3.90E-01	1.85E-01	5.00E-01	1.21E-01	1.61E+00
SR-5-6	16	Column	166.50	4.000E+01	23.67	4.34E-01	3.93E-01	1.72E-01	5.00E-01	1.19E-01	1.62E+00

Table A.6. Equilibrium Data for Run SR−6

Run Number	Sample Number	Run Type	Liquid Volume (mL)	Solids Mass (g)	Elapsed Time (h)	Initial Solution Sr Conc. (meg/mL)	Final Solution Sr Conc. (meg/mL)	Final Solids Sr Conc. (meq/g)	Initial Solution Cs Conc. (meg/mL)	Final Solution Cs Conc. (meg/mL)	Final Solids Cs Conc. (meq/g)	Final Solution Na Conc. (meg/mL)
SR−6	1	Batch	1.99	4.69E−01	24.00	2.28E−06	3.54E−09	9.68E−06	1.00E−09	1.29E−12	4.24E−09	4.47E−04
SR−6	2	Batch	1.99	4.72E−01	24.00	2.28E−05	3.57E−08	9.60E−05	1.00E−08	1.15E−11	4.21E−08	5.09E−04
SR−6	3	Batch	1.99	4.70E−01	24.00	2.28E−04	9.69E−08	9.66E−04	1.00E−06	5.46E−10	4.23E−06	6.18E−04
SR−6	4	Batch	1.99	4.71E−01	24.00	2.28E−03	5.70E−07	9.65E−03	1.00E−04	4.21E−08	4.23E−04	2.83E−03
SR−6	5	Batch	2.02	4.68E−01	24.00	8.72E−02	7.97E−03	3.42E−01	5.00E−02	7.94E−05	2.15E−01	1.35E−01
SR−6	6	Batch	2.17	4.72E−01	24.00	4.34E−01	4.20E−01	6.61E−02	5.00E−01	1.01E−01	1.84E+00	4.44E−01

Table A.7. Equilibrium Data for Run SR−17

Run Number	Sample Number	Run Type	Liquid Volume (mL)	Solids Mass (g)	Elapsed Time (h)	Initial Solution Ca Conc. (meg/mL)	Final Solution Ca Conc. (meg/mL)	Final Solids Ca Conc. (meq/g)
SR−17	1	Batch	10.09	1.12E−02	24.00	2.10E−03	4.87E−04	1.46E+00
SR−17	2	Batch	10.05	2.10E−02	24.00	2.10E−03	4.06E−06	1.00E+00
SR−17	3	Batch	10.09	9.21E−02	24.00	2.10E−03	1.25E−06	2.30E−01
SR−17	4	Batch	10.18	1.86E−01	24.00	2.10E−03	1.25E−06	1.17E−01
SR−17	5	Batch	10.18	2.61E−01	24.00	2.10E−03	1.25E−06	6.00E−02

Table A.8. Equilibrium Data for Run SR−18

Run Number	Sample Number	Run Type	Liquid Volume (mL)	Solids Mass (g)	Elapsed Time (h)	Initial Solution Mg Conc. (meg/mL)	Final Solution Mg Conc. (meg/mL)	Final Solids Mg Conc. (meq/g)
SR−18	1	Batch	9.98	4.15E−03	24.00	8.40E−04	3.81E−04	1.12E+00
SR−18	2	Batch	10.00	9.87E−03	24.00	8.40E−04	7.62E−05	7.80E−01
SR−18	3	Batch	9.97	1.96E−02	24.00	8.40E−04	1.92E−06	4.27E−01
SR−18	4	Batch	9.98	6.56E−01	24.00	8.40E−04	2.06E−07	9.00E−02
SR−18	5	Batch	9.99	1.87E−01	24.00	8.40E−04	2.06E−07	4.67E−02

Table A.9. Equilibrium Data for Run SR−23

Run Number	Sample Number	Run Type	Liquid Volume (mL)	Solids Mass (g)	Elapsed Time (h)	Initial Solution Sr Conc. (meg/mL)	Final Solution Sr Conc. (meg/mL)	Final Solids Sr Conc. (meq/g)	Initial Solution Cs Conc. (meg/mL)	Final Solution Cs Conc. (meg/mL)	Final Solids Cs Conc. (meq/g)	Initial Solution Ca Conc. (meg/mL)	Final Solution Ca Conc. (meg/mL)	Final Solids Ca Conc. (meq/g)	Initial Solution Mg Conc. (meg/mL)	Final Solution Mg Conc. (meg/mL)	Final Solids Mg Conc. (meq/g)	Final Solution Na Conc. (meg/mL)
SR−23	1	Batch	9.961	5.07E−03	24.00	2.00E−03	1.63E−03	7.30E−01	1.00E−03	4.03E−04	1.17E+00	1.85E−03	1.58E−03	5.25E−01	9.12E−04	9.14E−04	6.25E−02	1.36E−03
SR−23	2	Batch	9.988	9.83E−03	24.00	2.00E−03	1.35E−03	6.64E−01	1.00E−03	2.25E−04	7.88E−01	1.85E−03	1.31E−03	5.44E−01	9.12E−04	8.88E−04	5.74E−02	1.97E−03
SR−23	3	Batch	9.985	1.98E−02	24.00	2.00E−03	6.27E−04	6.92E−01	1.00E−03	4.67E−05	4.80E−01	1.85E−03	5.75E−04	6.42E−01	9.12E−04	7.83E−04	7.94E−02	3.71E−03
SR−23	4	Batch	10.003	1.01E−01	24.00	2.00E−03	6.24E−06	1.98E−01	1.00E−03	1.82E−06	9.93E−02	1.85E−03	4.99E−07	1.84E−01	9.12E−04	2.05E−05	8.86E−02	5.46E−03
SR−23	5	Batch	10.015	2.01E−01	24.00	2.00E−03	2.39E−06	1.00E−01	1.00E−03	8.78E−07	5.02E−02	1.85E−03	4.99E−07	9.28E−02	9.12E−04	6.37E−06	4.54E−02	5.52E−03
SR−23	6	Batch	10.047	4.01E−01	24.00	2.00E−03	1.17E−06	5.02E−02	1.00E−03	4.86E−07	2.51E−02	1.85E−03	4.99E−07	4.64E−02	9.12E−04	4.49E−06	2.28E−02	5.47E−03

Table A.10. Equilibrium Data for Run SR−25

Run Number	Sample Number	Run Type	Liquid Volume (mL)	Solids Mass (g)	Elapsed Time (h)	Initial Solution Sr Conc. (meg/mL)	Final Solution Sr Conc. (meg/mL)	Final Solids Sr Conc. (meq/g)	Final Solution Na Conc. (meg/mL)
SR−25	1	Batch	9.960	0.0051	24.00	2.00E−03	1.10E−03	1.76E+00	9.87E−04
SR−25	2	Batch	9.964	0.0100	24.00	2.00E−03	3.63E−04	1.63E+00	1.77E−03
SR−25	3	Batch	9.981	0.0198	24.00	2.00E−03	1.49E−05	1.00E+00	2.23E−03
SR−25	4	Batch	9.984	0.1012	24.00	2.00E−03	9.36E−07	1.97E−01	2.28E−03
SR−25	5	Batch	9.994	0.1997	24.00	2.00E−03	6.95E−07	1.00E−01	2.35E−03
SR−25	6	Batch	10.069	0.4011	24.00	2.00E−03	2.00E−06	5.02E−02	2.39E−03

Table A.11. Equilibrium Data for Run SR−26

Run Number	Sample Number	Run Type	Liquid Volume (mL)	Solids Mass (g)	Elapsed Time (h)	Initial Solution Sr Conc. (meg/mL)	Final Solution Sr Conc. (meg/mL)	Final Solids Sr Conc. (meq/g)	Initial Solution Cs Conc. (meg/mL)	Final Solution Cs Conc. (meg/mL)	Final Solids Cs Conc. (meq/g)	Final Solution Na Conc. (meg/mL)
SR−26	1	Batch	10.011	0.0049	24.00	2.00E−03	1.53E−03	9.65E−01	1.00E−03	4.05E−04	1.23E+00	1.14E−03
SR−26	2	Batch	10.007	0.0100	24.00	2.00E−03	9.59E−04	1.05E+00	1.00E−03	1.61E−04	8.44E−01	2.02E−03
SR−26	3	Batch	10.002	0.0201	24.00	2.00E−03	7.53E−05	9.57E−01	1.00E−03	1.67E−05	4.89E−01	3.11E−03
SR−26	4	Batch	10.003	0.1012	24.00	2.00E−03	1.88E−06	1.98E−01	1.00E−03	1.24E−06	9.88E−02	3.38E−03
SR−26	5	Batch	10.002	0.2016	24.00	2.00E−03	1.53E−06	9.92E−02	1.00E−03	6.75E−07	4.96E−02	3.42E−03
SR−26	6	Batch	10.029	0.4011	24.00	2.00E−03	1.33E−06	5.00E−02	1.00E−03	3.70E−07	2.50E−02	3.45E−03

Table A.12. Equilibrium Data for Run SR−27

Run Number	Sample Number	Run Type	Liquid Volume (mL)	Solids Mass (g)	Elapsed Time (h)	Initial Solution Cs Conc. (meg/mL)	Final Solution Cs Conc. (meg/mL)	Final Solids Cs Conc. (meq/g)	Final Solution Na Conc. (meg/mL)
SR−27	1	Batch	10.073	0.0052	24.00	1.00E−03	1.43E−04	1.66E+00	8.77E−04
SR−27	2	Batch	10.002	0.0098	24.00	1.00E−03	9.93E−06	1.01E+00	1.02E−03
SR−27	3	Batch	10.002	0.0200	24.00	1.00E−03	2.48E−06	4.99E−01	1.03E−03
SR−27	4	Batch	10.006	0.1013	24.00	1.00E−03	6.58E−07	9.87E−02	1.10E−03
SR−27	5	Batch	10.004	0.2030	24.00	1.00E−03	6.30E−07	4.92E−02	1.12E−03
SR−27	6	Batch	10.008	0.4032	24.00	1.00E−03	1.20E−07	2.48E−02	1.29E−03

Table **A.13. Equilibrium Data for** Run **SR–34**

Run Number	Sample Number	Run Type	Liquid Volume (mL)	Solids Mars (g)	Elapsed Time (h)	Initial Solution Sr Conc. (meg/mL)	Final Solution Sr Conc. (meg/mL)	Final Solids Sr Conc. (meq/g)	Initial Solution Cs Conc. (meg/mL)	Final Solution Cs Conc. (meg/mL)	Final Solids Cs Conc. (meq/g)	Initial Solution Ca Conc. (meg/mL)	Final Solution Ca Conc. (meg/mL)	Final Solids Ca Conc. (meq/g)	Initial Solution Mg Conc. (meg/mL)	Final Solution Mg Conc. (meg/mL)	Final Solids Mg Conc. (meq/g)
SR–34	1	Batch	9.942	0.0042	24.00	4.98E-04	1.86E-04	7.38E-01	2.27E-04	2.90E-05	4.68E-01	4.99E-04	2.10E-04	6.81E-01	2.2%–04	2.02E-04	6.31E-02
SR-34	2	Batch	10.009	0.0081	24.00	4.98E-04	1.69E-05	5.96E-01	2.27E-04	4.68E-06	2.7.X–01	4.9%–04	1.94E-05	5.94E-01	2.2%–04	9.10E-05	1.71E-01
SR–34	3	Batch	10.063	0.0122	24.00	4.98E-04	2.21E-06	4.11E-01	2.27E-04	1.46E-06	1.87E-01	4.9%–04	3.24E-06	4.11E-01	2.2%–04	1.13E-05	1.80E-01
SR–34	4	Batch	9.963	0.0198	24.00	4.9813–04	6.47E-07	2.52E-01	2.27E-04	5.98E-07	1.14E-01	1.9%–04	3.24E-06	2.51E-01	2.2%–04	2.06E-06	1.15E-01
SR-34	5	Batch	9.998	0.0498	24.00	4.98E-04	2.58E-07	9.99E-02	2.27E-04	2.60E-07	4.54E-02	4.9%–04	3.24E-06	9.94E-02	2.29E-04	5.38E-07	4.58E-02
SR–34	6	Batch	9.965	0.0997	24.00	4.98E-04	4.9.X–07	4.97E-02	2.27E-04	3.58E-07	2.26E-02	4.99E-04	3.24E-06	4.95E-02	2.2%–04	8.53E-07	2.28E-02
SR–34	7	Batch	10.000	0.1991	24.00	4.98E-04	1.69E-07	2.50E-02	2.27E-04	1.07E-07	1.14E-02	4.99E-04	3.24E-06	2.49E-02	2.2%–04	1.06E-06	1.14E-02

Table A.14. Equilibrium Data for Run SR−35

Run Number	Sample Number	Run Type	Liquid Volume (mL)	Solids Mass (g)	Elapsed Time (h)	Initial Solution Sr Conc. (meg/mL)	Final Solution Sr Conc. (meg/mL)	Final Solids Sr Conc. (meq/g)	Initial Solution Cs Conc. (meg/mL)	Final Solution Cs Conc. (meg/mL)	Final Solids Cs Conc. (meq/g)	Initial Solution Ca Conc. (meg/mL)	Final Solution Ca Conc. (meg/mL)	Final Solids Ca Conc. (meq/g)	Initial Solution Mg Conc. (meg/mL)	Final Solution Mg Conc. (meg/mL)	Final Solids Mg Conc. (meq/g)
SR−35	1	Batch	10.052	0.0038	24.00	2.01E−03	1.79E−03	5.72E−01	1.00E−03	5.33E−04	1.22E+00	2.05E−03	1.85E−03	5.03E−01	8.22E−04	8.31E−04	2.38E−02
SR−35	2	Batch	10.053	0.0075	24.00	2.01E−03	1.48E−03	7.11E−01	1.00E−03	2.67E−04	9.80E−01	2.05E−03	1.52E−03	7.09E−01	8.22E−04	8.21E−04	4.65E−03
SR−35	3	Batch	10.069	0.0113	24.00	2.01E−03	1.18E−03	7.39E−01	1.00E−03	1.28E−04	7.79E−01	2.05E−03	1.25E−03	7.15E−01	8.22E−04	8.08E−04	1.27E−02
SR−35	4	Batch	10.067	0.0186	24.00	2.01E−03	6.30E−04	7.48E−01	1.00E−03	3.54E−05	5.23E−01	2.05E−03	6.90E−04	7.36E−01	8.22E−04	7.19E−04	5.62E−02
SR−35	5	Batch	10.116	0.0463	24.00	2.01E−03	2.83E−05	4.33E−01	1.00E−03	4.97E−06	2.17E−01	2.05E−03	2.24E−05	4.42E−01	8.22E−04	1.24E−04	1.53E−01
SR−35	6	Batch	10.238	0.0923	24.00	2.01E−03	2.01E−06	2.23E−01	1.00E−03	2.19E−06	1.11E−01	2.05E−03	2.92E−06	2.27E−01	8.22E−04	3.57E−05	8.72E−02
SR−35	7	Batch	10.214	0.1845	24.00	2.01E−03	3.99E−06	1.11E−01	1.00E−03	1.04E−06	5.53E−02	2.05E−03	9.22E−06	1.14E−01	8.22E−04	6.26E−05	4.21E−02

Appendix B. BATCH KINETIC DATA

Table B.1. Batch Reactor Operating Conditions

Run Number	Type System	Type Zeolite	Particle Size (μm)	Solution Volume (mL)	Solids Weight (g)	Stirrer Speed (rpm)	Initial Solution Concentration (meq/L)				Solids Loading (meq/g)
							Sr	Cs	Ca	Mg	
SK-38	Batch	IE-90	24	80.45	0.0463	750				0.84	0.899
SK-26	Batch	IE-90	24	79.98	0.0471	750		1.01			1.630
SK-21	Batch	IE-90	24	80.22	0.0473	750			2.27		2.233
SK-39	Batch	IE-90	24	80.15	0.4660	750	1.89				1.807
SK-28	Batch	IE-90	24	80.62	0.0473	750	0.59	0.25	0.59	0.21	2.320
SK-40	Batch	IE-90	24	79.96	0.0463	750	2.07	1.00	2.06	0.88	1.865
SK-42	Batch	IE-96	24	80.16	0.0477	750			1.93		1.519
SK-11	Batch	IE-96	545	80.66	0.0473	500			1.97		1.699
SK-9	Batch	IE-96	545	80.00	0.0477	1000			2.03		1.807
SK-14	Batch	IE-96	545	80.09	0.0474	750			1.00		1.561
SK-15	Batch	IE-96	545	80.28	0.0192	750			0.99		1.698
SK-41	Batch	IE-96	545	79.84	0.0468	750			1.92		1.516
SK-19	Batch	IE-96	545	80.52	0.0473	750				0.82	0.599
SK-18	Batch	IE-96	545	80.36	0.0472	750		1.01			1.591
SK-16	Batch	IE-96	545	80.46	0.0473	750	2.04				1.773
SK-34	Batch	IE-96	545	79.74	0.0471	750	2.05	1.00	2.35	0.89	1.965
SK-24	Batch	IE-96	545	80.24	0.0474	750	0.55	0.25	0.57	0.21	1.968

Table B.2. Single Component Batch Reactor Data for Ionsiv IE−90

Time	SK−39 Sr (meq/mL)	SK−26 Cs (meq/mL)	SK−21 Ca (meq/mL)	SK−38 Mg (meq/mL)
0	1.89E−03	1.01E−03	2.27E−03	8.40E−04
1	1.18E−03	2.36E−04	1.22E−03	6.80E−04
2	1.08E−03	1.37E−04	1.14E−03	6.41E−04
5	9.58E−04	8.01E−05	1.09E−03	5.77E−04
10	9.18E−04	1.17E−04	1.03E−03	6.15E−04
30	8.85E−04	4.84E−05	9.94E−04	5.45E−04
60	8.74E−04	6.26E−05	9.67E−04	4.79E−04
120	8.63E−04	4.93E−05	9.69E−04	4.22E−04
240	8.37E−04	4.73E−05	9.59E−04	3.94E−04
360	8.55E−04	4.71E−05	9.57E−04	3.43E−04
480	8.37E−04			3.23E−04

Table B.3. Multicomponent Component Batch Reactor Data for Ionsiv IE−90

Time	SK−40 Sr (meq/mL)	SK−40 Cs (meq/mL)	SK−40 Ca (meq/mL)	SK−40 Mg (meq/mL)
0	2.07E−03	1.00E−03	2.06E−03	8.78E−04
1	1.77E−03	4.69E−04	1.83E−03	8.47E−04
2	1.76E−03	4.22E−04	1.84E−03	8.58E−04
5	1.75E−03	3.85E−04	1.81E−03	8.47E−04
10	1.72E−03	3.80E−04	1.80E−03	8.54E−04
30	1.75E−03	3.84E−04	1.76E−03	8.49E−04
60	1.78E−03	3.98E−04	1.76E−03	8.66E−04
120	1.75E−03	4.01E−04	1.76E−03	8.53E−04
240	1.79E−03	4.00E−04	1.82E−03	8.49E−04
360	1.80E−03	4.04E−04	1.81E−03	8.60E−04
480	1.82E−03	4.09E−04	1.81E−03	8.81E−04

Table B.4. Single Component Batch Reactor Data for Ionsiv IE−96

Time	SK−16 Sr (meq/mL)	SK−18 Cs (meq/mL)	SK−41 Ca (meq/mL)	SK−19 Mg (meq/mL)
0	2.04E−03	1.01E−03	1.91E−03	8.13E−04
1	1.88E−03	9.35E−04	1.88E−03	7.90E−04
2	1.90E−03	8.94E−04	1.83E−03	7.76E−04
5	1.81E−03	7.37E−04	1.76E−03	7.47E−04
10	1.72E−03	6.52E−04	1.67E−03	7.05E−04
30	1.48E−03	4.16E−04	1.41E−03	6.60E−04
60	1.25E−03	2.57E−04	1.25E−03	6.16E−04
120	1.14E−03	1.46E−04	1.13E−03	5.48E−04
240	1.04E−03	8.58E−05	1.05E−03	4.96E−04
360	9.96E−04	7.31E−05	1.03E−03	4.61E−04
480			1.03E−03	

Table B.5. Multicomponent Component Batch Reactor Data for Ionsiv IE−96

Time	SK−34 Sr (meq/mL)	SK−34 Cs (meq/mL)	SK−34 Ca (meq/mL)	SK−34 Mg (meq/mL)
0	2.05E−03	1.00E−03	2.35E−03	8.91E−04
1	2.03E−03	9.82E−04	2.32E−03	8.72E−04
2	2.01E−03	9.58E−04	2.28E−03	8.57E−04
5	1.99E−03	9.18E−04	2.16E−03	8.51E−04
10	1.90E−03	8.66E−04	2.26E−03	8.54E−04
30	1.87E−03	7.82E−04	2.16E−03	8.55E−04
60	1.80E−03	7.11E−04	2.05E−03	8.22E−04
120	1.75E−03	6.42E−04	2.05E−03	8.21E−04
240	1.71E−03	5.57E−04	2.01E−03	8.29E−04
360	1.73E−03	5.28E−04	2.00E−03	8.68E−04
480	1.74E−03	5.12E−04	2.07E−03	8.67E−04

Appendix C. COLUMN KINETIC DATA

Table C.1. Column Operating Conditions

Run Number	Type System	Type Zeolite	Particle Size (μm)	Solution Volume (mL)	Solids Weight (g)	Column Diameter (cm)	Bed Height (cm)	Flow Rate (mL/min)	Initial Solution Concentration (meq/L)				Solids Loading (meq/g)
									Sr	Cs	Ca	Mg	
SK-7	SBA	IE-96	194	1883.00	1.0003	1	1.6	8.56			1.95		1.801
SK-6	SBA	IE-96	385	1885.00	1.0018	1	1.6	8.57			1.92		1.638
SK-2	SBA	IE-96	545	1335.00	1.0014	1	1.6	5.7			1.99		1.454
SK-5	SBA	IE-96	545	1974.00	1.0021	1	1.6	3.2			1.82		1.588
SK-4	SBA	IE-96	545	1910.00	1.0022	1	1.6	11.6			1.94		1.553
SK-31	SBA	IE-96	545	4749	0.9222	1	1.6	8.5			2.03		1.859
SK-33	SBA	IE-96	545	1900	0.9224	1	1.6	8.6		1.00			1.454
SK-30	SBA	IE-96	545	1874	0.9228	1	1.6	8.6				0.83	0.555
SK-29	SBA	IE-96	545	1880	0.9235	1	1.6	8.5	1.84				1.631
SK-35	SBA	IE-96	545	4806	0.9276	1	1.6	8.6	0.53	0.25	0.58	0.23	2.129
SK-44	SBA	IE-96	545	3398	0.9220	1	1.6	8.6	2.03	1.00	1.94	1.09	2.056
SK-36	Column	IE-96	545	3738	2.3052	1	3.8	8.6			2.22		1.831
SK-37	Column	IE-96	545	4322	2.3061	1	3.8	8.3		0.28			1.768
SK-45	Column	IE-96	545	3015	3.0017	1	4.5	0.5	2.10	1.00	2.01	0.81	2.035
MV-10	Column	IE-96	545	3200	3.0030	1	4.5	1	2.10	1.00	2.01	0.95	2.206
SK-47	Column	IE-96	545	10039	10.0330	1.5	7.2	2.08	2.01	1.00	1.95	0.85	2.053
SK-48	Column	IE-96	545	46225	44.8000	.5	11.4	5.8	2.07	1.00	2.14	0.83	2.471

Table C.2. Single Component Short Bed Column Kinetic Tests

SK-29 Sr (mL)	SK-29 Sr (meq/mL)	SK-33 Cs (mL)	SK-33 Cs (meq/mL)	SK-31 Ca (mL)	SK-31 Ca (meq/mL)	SK-30 Mg (mL)	SK-30 Mg (meq/mL)
8	1.25E-04	8	2.43E-05	8	1.49E-04	8	1.24E-04
17	2.29E-04	17	3.10E-05	16	2.65E-04	17	1.34E-04
25	2.41E-04	25	3.41E-05	25	2.87E-04	26	1.38E-04
33	2.49E-04	33	3.77E-05	33	2.93E-04	34	1.45E-04
42	2.48E-04	42	3.95E-05	41	3.02E-04	43	1.45E-04
50	2.57E-04	50	3.81E-05	50	3.14E-04	52	1.54E-04
59	2.63E-04	59	4.08E-05	58	3.21E-04	60	1.59E-04
67	2.72E-04	67	4.13E-05	66	3.29E-04	69	1.64E-04
75	2.79E-04	75	4.28E-05	75	3.41E-04	78	1.71E-04
84	2.83E-04	84	4.49E-05	83	3.47E-04	86	1.77E-04
101	2.97E-04	101	4.73E-05	100	3.59E-04	103	1.81E-04
118	3.09E-04	118	5.01E-05	116	3.76E-04	121	1.93E-04
134	3.20E-04	134	5.19E-05	133	3.91E-04	138	2.10E-04
152	3.36E-04	152	5.58E-05	150	4.08E-04	156	2.24E-04
168	3.53E-04	168	5.85E-05	167	4.29E-04	173	2.37E-04
211	3.74E-04	211	6.10E-05	209	4.55E-04	217	2.58E-04
253	4.17E-04	253	6.95E-05	251	5.00E-04	263	3.00E-04
296	4.51E-04	296	7.91E-05	294	5.45E-04	304	3.42E-04
338	4.98E-04	338	8.55E-05	336	6.02E-04	348	3.87E-04
381	5.36E-04	381	9.16E-05	379	6.55E-04	391	4.22E-04
467	6.04E-04	467	1.10E-04	464	7.24E-04	479	4.28E-04
552	6.97E-04	552	1.26E-04	550	8.35E-04	566	4.78E-04
638	7.76E-04	638	1.53E-04	639	9.36E-04	654	5.42E-04
724	8.56E-04	724	1.75E-04	721	1.02E-03	740	5.78E-04
810	9.65E-04	810	2.04E-04	807	1.11E-03	828	5.97E-04
896	1.06E-03	896	2.30E-04	893	1.21E-03	915	6.02E-04
984	1.15E-03	984	2.58E-04	979	1.33E-03	1002	6.38E-04
1068	1.23E-03	1068	2.93E-04	1065	1.39E-03	1089	6.43E-04
1154	1.28E-03	1154	3.26E-04	1151	1.44E-03	1176	6.64E-04
1240	1.35E-03	1240	3.65E-04	1237	1.51E-03	1262	6.65E-04
1326	1.40E-03	1326	3.99E-04	1323	1.58E-03	1349	6.66E-04
1411	1.46E-03	1411	4.42E-04	1409	1.64E-03	1436	6.89E-04
1496	1.44E-03	1496	4.79E-04	1495	1.69E-03	1522	7.01E-04
1582	1.50E-03	1582	5.14E-04	1581	1.71E-03	1608	6.83E-04
1667	1.53E-03	1667	5.52E-04	1667	1.73E-03	1694	6.97E-04
1710	1.56E-03	1710	5.87E-04	1925	1.79E-03	1737	7.12E-04
1752	1.54E-03	1752	6.01E-04	2183	1.87E-03	1780	7.13E-04
1795	1.57E-03	1795	6.09E-04	2444	1.92E-03	1823	7.13E-04
1837	1.53E-03	1837	6.30E-04	2698	1.93E-03	1866	7.09E-04
1880	1.61E-03	1880	6.50E-04	2956	1.98E-03	1874	7.18E-04
				3213	1.97E-03		
				3470	2.01E-03		
				3727	1.99E-03		
				3983	2.00E-03		
				4240	2.01E-03		
				4495	2.01E-03		
				4749	2.04E-03		

Table C.3. Single Component Short Bed Column Calcium Kinetic Tests

SK-2 Ca (mL)	SK-2 Ca (meq/mL)	SK-4 Ca (mL)	SK-4 Ca (meq/mL)	SK-5 Ca (mL)	SK-5 Ca (meq/mL)	SK-6 Ca (mL)	SK-6 Ca (meq/mL)	SK-7 Ca (mL)	SK-7 Ca (meq/mL)
5	6.78E-05	6	2.19E-04	6	3.20E-05	8	4.16E-06	8	4.99E-07
11	1.79E-04	12	3.23E-04	12	2.22E-05	17	2.37E-05	17	4.99E-07
17	1.76E-04	18	3.37E-04	18	2.99E-05	26	2.78E-05	25	4.99E-07
23	1.84E-04	24	3.51E-04	25	3.06E-05	34	3.36E-05	34	4.99E-07
29	1.99E-04	30	3.56E-04	31	3.29E-05	43	3.73E-05	42	4.99E-07
36	1.79E-04	36	3.59E-04	37	3.49E-05	51	4.06E-05	51	4.99E-07
42	1.92E-04	42	3.70E-04	44	3.80E-05	60	4.41E-05	60	4.99E-07
48	1.98E-04	48	3.60E-04	50	4.05E-05	68	4.74E-05	68	4.99E-07
54	2.00E-04	54	3.67E-04	56	4.28E-05	77	4.84E-05	77	4.99E-07
60	2.08E-04	60	3.98E-04	63	4.36E-05	86	5.05E-05	85	4.99E-07
72	2.18E-04	72	3.87E-04	75	4.49E-05	103	6.02E-05	103	4.99E-07
84	2.32E-04	84	3.89E-04	88	4.79E-05	120	6.47E-05	120	4.99E-07
96	2.34E-04	96	3.90E-04	101	5.25E-05	137	7.22E-05	137	4.99E-07
109	2.34E-04	108	4.13E-04	114	5.91E-05	155	8.06E-05	155	4.99E-07
120	2.31E-04	119	4.21E-04	126	6.37E-05	172	8.68E-05	172	4.99E-07
148	2.28E-04	143	4.53E-04	152	7.61E-05	215	1.02E-04	215	4.99E-07
176	2.35E-04	166	4.73E-04	178	8.19E-05	258	1.28E-04	258	4.99E-07
204	2.42E-04	189	4.91E-04	204	9.31E-05	301	1.61E-04	302	4.99E-07
232	2.70E-04	212	5.19E-04	230	1.05E-04	344	2.10E-04	345	7.02E-06
259	2.87E-04	235	5.28E-04	256	1.15E-04	388	2.59E-04	388	1.98E-05
314	3.51E-04	292	5.78E-04	321	1.33E-04	474	3.42E-04	474	6.77E-05
371	3.95E-04	349	6.35E-04	386	1.83E-04	560	4.74E-04	561	2.06E-04
427	4.32E-04	405	6.92E-04	451	2.41E-04	647	6.16E-04	647	4.21E-04
484	5.09E-04	462	7.38E-04	516	3.11E-04	730	7.59E-04	733	6.26E-04
541	6.03E-04	519	8.10E-04	582	3.97E-04	814	9.09E-04	818	8.33E-04
598	7.26E-04	631	8.76E-04	712	5.64E-04	900	9.49E-04	904	1.04E-03
655	7.94E-04	744	9.95E-04	843	8.28E-04	987	1.25E-03	990	1.18E-03
711	8.81E-04	856	1.13E-03	973	1.04E-03	1073	1.39E-03	1076	1.35E-03
768	8.63E-04	968	1.20E-03	1104	1.27E-03	1160	1.47E-03	1161	1.47E-03
824	1.07E-03	1080	1.28E-03	1234	1.46E-03	1245	1.57E-03	1247	1.53E-03
881	1.17E-03	1191	1.36E-03	1365	1.50E-03	1331	1.56E-03	1332	1.63E-03
938	1.29E-03	1303	1.38E-03	1495	1.62E-03	1417	1.64E-03	1417	1.64E-03
994	1.31E-03	1414	1.45E-03	1625	1.61E-03	1503	1.69E-03	1502	1.81E-03
1051	1.47E-03	1524	1.43E-03	1756	1.72E-03	1588	1.74E-03	1588	1.76E-03
1108	1.53E-03	1635	1.56E-03	1821	1.73E-03	1673	1.76E-03	1671	1.80E-03
1136	1.57E-03	1690	1.53E-03	1886	1.85E-03	1716	1.77E-03	1714	1.82E-03
1165	1.56E-03	1745	1.60E-03	1951	1.77E-03	1757	1.85E-03	1756	1.78E-03
1193	1.61E-03	1800	1.61E-03	1974	1.77E-03	1800	1.86E-03	1798	1.76E-03
1221	1.63E-03	1855	1.62E-03			1842	1.83E-03	1840	1.81E-03
1250	1.68E-03	1910	1.55E-03			1885	1.73E-03	1883	1.80E-03
1261	1.56E-03								
1273	1.73E-03								
1284	1.58E-03								
1295	1.68E-03								
1307	1.74E-03								
1312	1.70E-03								
1318	1.72E-03								
1324	1.72E-03								
1329	1.72E-03								
1335	1.71E-03								

Table C.4. Multicomponent Short Bed Column Kinetic Tests

Run Number	Volume (mL)	Sr (meq/mL)	Cs (meq/mL)	Ca (meq/mL)	Mg (meq/mL)
SK-44	9	2.89E-04	4.11E-05	2.79E-04	2.50E-04
SK-44	17	4.10E-04	6.56E-05	4.27E-04	3.10E-04
SK-44	26	5.02E-04	7.84E-05	4.97E-04	3.67E-04
SK-44	34	5.64E-04	9.33E-05	5.59E-04	4.26E-04
SK-44	43	6.27E-04	1.09E-04	6.40E-04	4.23E-04
SK-44	52	6.90E-04	1.24E-04	6.87E-04	4.68E-04
SK-44	60	7.44E-04	1.39E-04	7.42E-04	5.14E-04
SK-44	68	7.91E-04	1.48E-04	8.02E-04	5.66E-04
SK-44	77	8.29E-04	1.68E-04	8.49E-04	6.08E-04
SK-44	86	8.91E-04	1.82E-04	9.16E-04	6.55E-04
SK-44	103	9.92E-04	2.00E-04	9.74E-04	6.97E-04
SK-44	120	1.05E-03	2.24E-04	1.06E-03	7.48E-04
SK-44	137	1.14E-03	2.48E-04	1.14E-03	7.95E-04
SK-44	154	1.17E-03	2.71E-04	1.19E-03	8.40E-04
SK-44	171	1.23E-03	2.98E-04	1.25E-03	8.73E-04
SK-44	214	1.33E-03	3.32E-04	1.32E-03	9.14E-04
SK-44	258	1.44E-03	3.82E-04	1.41E-03	9.63E-04
SK-44	300	1.48E-03	4.27E-04	1.48E-03	9.89E-04
SK-44	343	1.56E-03	4.69E-04	1.54E-03	1.02E-03
SK-44	386	1.59E-03	4.95E-04	1.62E-03	1.05E-03
SK-44	472	1.67E-03	5.43E-04	1.65E-03	1.07E-03
SK-44	558	1.72E-03	5.85E-04	1.73E-03	1.08E-03
SK-44	644	1.76E-03	6.23E-04	1.75E-03	1.09E-03
SK-44	729	1.76E-03	6.61E-04	1.78E-03	1.11E-03
SK-44	815	1.82E-03	6.88E-04	1.79E-03	1.10E-03
SK-44	900	1.85E-03	7.08E-04	1.77E-03	1.11E-03
SK-44	985	1.86E-03	7.30E-04	1.82E-03	1.10E-03
SK-44	1070	1.91E-03	7.42E-04	1.86E-03	1.10E-03
SK-44	1156	1.91E-03	7.61E-04	1.85E-03	1.09E-03
SK-44	1240	1.92E-03	7.72E-04	1.89E-03	1.10E-03
SK-44	1325	1.92E-03	7.91E-04	1.91E-03	1.11E-03
SK-44	1410	1.94E-03	7.97E-04	1.89E-03	1.09E-03
SK-44	1495	1.92E-03	8.07E-04	1.90E-03	1.07E-03
SK-44	1578	1.95E-03	8.17E-04	1.91E-03	1.10E-03
SK-44	1662	1.96E-03	8.33E-04	1.92E-03	1.09E-03
SK-44	1913	1.96E-03	8.41E-04	1.91E-03	1.10E-03
SK-44	2162	1.99E-03	8.66E-04	1.94E-03	1.11E-03
SK-44	2411	2.02E-03	8.76E-04	1.93E-03	1.10E-03
SK-44	2659	2.02E-03	9.03E-04	1.96E-03	1.09E-03
SK-44	2906	2.03E-03	9.06E-04	1.97E-03	1.10E-03
SK-44	3153	2.05E-03	9.10E-04	1.93E-03	1.10E-03

Table C.4 (Continued)

Run Number	Volume (mL)	Sr (meq/mL)	Cs (meq/mL)	Ca (meq/mL)	Mg (meq/mL)
SK−44	3398	2.06E−03	9.21E−04	1.96E−03	1.09E−03
SK−44	3641	2.06E−03	9.23E−04	1.94E−03	1.08E−03
SK−44	3886	2.05E−03	9.28E−04	1.96E−03	1.10E−03
SK−44	4130	2.06E−03	9.36E−04	1.94E−03	1.10E−03
SK−44	4374	2.03E−03	9.47E−04	1.97E−03	1.08E−03
SK−44	4618	2.03E−03	9.65E−04	1.94E−03	1.09E−03
SK−35	8	2.28E−05	5.15E−06	1.56E−05	3.25E−05
SK−35	17	6.08E−05	8.10E−06	6.11E−05	3.38E−05
SK−35	26	6.48E−05	8.38E−06	5.79E−05	3.47E−05
SK−35	34	6.79E−05	8.69E−06	6.25E−05	3.52E−05
SK−35	42	6.82E−05	9.07E−06	6.11E−05	3.57E−05
SK−35	51	6.97E−05	9.68E−06	6.43E−05	3.83E−05
SK−35	59	7.02E−05	9.75E−06	6.49E−05	3.90E−05
SK−35	68	7.12E−05	9.99E−06	6.65E−05	3.91E−05
SK−35	76	7.35E−05	1.07E−05	6.57E−05	3.96E−05
SK−35	85	7.67E−05	1.10E−05	6.89E−05	4.03E−05
SK−35	102	7.77E−05	1.16E−05	7.54E−05	4.17E−05
SK−35	119	8.16E−05	1.29E−05	8.29E−05	4.43E−05
SK−35	136	8.36E−05	1.39E−05	8.86E−05	4.58E−05
SK−35	153	8.78E−05	1.42E−05	9.94E−05	4.85E−05
SK−35	170	9.08E−05	1.52E−05	1.03E−04	4.97E−05
SK−35	213	9.33E−05	1.72E−05	1.12E−04	4.84E−05
SK−35	256	1.02E−04	2.01E−05	1.23E−04	5.69E−05
SK−35	299	1.10E−04	2.24E−05	1.31E−04	6.35E−05
SK−35	343	1.18E−04	2.57E−05	1.42E−04	7.08E−05
SK−35	386	1.25E−04	2.92E−05	1.55E−04	7.65E−05
SK−35	473	1.44E−04	3.42E−05	1.63E−04	7.19E−05
SK−35	560	1.64E−04	4.12E−05	1.92E−04	9.46E−05
SK−35	647	1.84E−04	4.94E−05	2.28E−04	1.15E−04
SK−35	734	2.05E−04	5.75E−05	2.42E−04	1.35E−04
SK−35	821	2.24E−04	6.63E−05	2.75E−04	1.54E−04
SK−35	908	2.48E−04	7.36E−05	3.06E−04	1.72E−04
SK−35	998	2.64E−04	8.13E−05	2.92E−04	1.88E−04
SK−35	1083	2.87E−04	8.76E−05	3.32E−04	2.01E−04
SK−35	1170	2.99E−04	9.37E−05	3.60E−04	2.08E−04
SK−35	1257	3.19E−04	1.03E−04	3.80E−04	2.18E−04
SK−35	1344	3.36E−04	1.06E−04	3.96E−04	2.24E−04
SK−35	1431	3.42E−04	1.12E−04	4.04E−04	2.31E−04
SK−35	1518	3.46E−04	1.18E−04	4.19E−04	2.32E−04
SK−35	1605	3.62E−04	1.20E−04	4.39E−04	2.33E−04
SK−35	1692	3.69E−04	1.28E−04	4.55E−04	2.40E−04

Table C.4 (Continued)

Run Number	Volume (mL)	Sr (meq/mL)	Cs (meq/mL)	Ca (meq/mL)	Mg (meq/mL)
SK−35	1953	3.88E−04	1.34E−04	4.47E−04	2.38E−04
SK−35	2214	4.10E−04	1.45E−04	5.12E−04	2.42E−04
SK−35	2475	4.33E−04	1.56E−04	5.37E−04	2.37E−04
SK−35	2734	4.53E−04	1.62E−04	5.41E−04	2.38E−04
SK−35	2993	4.59E−04	1.71E−04	5.57E−04	2.34E−04
SK−35	3253	4.67E−04	1.76E−04	5.72E−04	2.35E−04
SK−35	3512	4.74E−04	1.83E−04	5.78E−04	2.35E−04
SK−35	3771	4.85E−04	1.87E−04	6.14E−04	2.15E−04
SK−35	4030	4.89E−04	1.92E−04	5.90E−04	2.27E−04
SK−35	4289	5.05E−04	1.96E−04	5.94E−04	2.24E−04
SK−35	4548	5.06E−04	1.98E−04	5.96E−04	2.24E−04
SK−35	4806	4.92E−04	2.00E−04	5.86E−04	2.21E−04

Table C.5. Single Component Long Bed Column Kinetic Tests

SK−36 Volume (mL)	SK−36 Ca (meq/mL)	SK−37 Volume (mL)	SK−37 Ca (meq/mL)
8	3.16E−07	8	2.86E−06
16	4.94E−06	16	1.02E−05
24	7.67E−06	25	1.08E−05
33	6.85E−06	33	1.29E−05
41	8.76E−06	41	1.35E−05
48	8.48E−06	50	1.32E−05
57	7.94E−06	58	1.43E−05
65	9.85E−06	66	1.61E−05
73	9.03E−06	75	1.26E−05
82	9.85E−06	83	1.32E−05
99	1.09E−05	99	1.61E−05
116	1.18E−05	116	1.58E−05
133	1.26E−05	133	1.67E−05
150	1.67E−05	150	1.93E−05
167	1.86E−05	166	1.82E−05
185	1.94E−05	183	1.82E−05
202	1.72E−05	200	2.05E−05
219	1.91E−05	216	2.38E−05
236	1.94E−05	233	2.20E−05
254	2.18E−05	250	2.29E−05
297	2.54E−05	292	2.76E−05
341	3.41E−05	333	2.94E−05
384	3.68E−05	379	3.47E−05
428	4.06E−05	417	3.47E−05
471	4.74E−05	459	4.11E−05
515	5.80E−05	501	4.47E−05
559	6.92E−05	543	4.91E−05
603	7.55E−05	585	5.32E−05
647	8.91E−05	627	6.35E−05
692	1.08E−04	668	6.70E−05
781	1.29E−04	752	8.24E−05
871	1.78E−04	836	1.05E−04
961	2.35E−04	920	1.27E−04
1051	3.00E−04	1003	1.66E−04
1142	3.99E−04	1087	2.07E−04
1233	4.86E−04	1171	2.59E−04
1325	6.07E−04	1288	3.15E−04
1416	7.08E−04	1339	3.82E−04
1507	8.25E−04	1422	4.44E−04
1599	9.74E−04	1506	5.11E−04

Table C.5 (Continued)

SK−36 Volume (mL)	SK−36 Ca (meq/mL)	SK−37 Volume (mL)	SK−37 Ca (meq/mL)
1780	1.16E−03	1673	6.19E−04
1955	1.29E−03	1839	7.92E−04
2124	1.45E−03	2006	8.71E−04
2289	1.56E−03	2173	1.04E−03
2446	1.70E−03	2338	1.18E−03
2668	1.71E−03	2587	1.30E−03
2869	1.81E−03	2836	1.30E−03
3055	1.91E−03	3084	1.54E−03
3226	1.88E−03	3333	1.54E−03
3379	1.95E−03	3581	1.62E−03
3519	1.93E−03	3828	1.59E−03
3624	1.96E−03	4075	1.59E−03
3738	1.93E−03	4322	1.74E−03

Table C.6. Multicomponent Long Bed Column Kinetic Tests

Run Number	Volume (mL)	Sr (meq/mL)	Cs (meq/mL)	Ca (meq/mL)	Mg (meq/mL)
SK−45	62	7.54E−07	0.00E+00	0.00E+00	6.91E−07
SK−45	121	7.54E−07	0.00E+00	0.00E+00	6.68E−07
SK−45	181	7.54E−07	0.00E+00	0.00E+00	7.14E−07
SK−45	241	7.54E−07	0.00E+00	0.00E+00	9.65E−07
SK−45	300	7.54E−07	0.00E+00	0.00E+00	6.68E−07
SK−45	359	7.54E−07	0.00E+00	0.00E+00	1.17E−06
SK−45	418	7.54E−07	0.00E+00	0.00E+00	3.50E−06
SK−45	477	7.54E−07	0.00E+00	0.00E+00	2.24E−05
SK−45	536	7.54E−07	0.00E+00	0.00E+00	7.87E−05
SK−45	594	5.77E−06	0.00E+00	1.52E−06	2.07E−04
SK−45	653	1.55E−05	0.00E+00	2.98E−05	3.84E−04
SK−45	712	3.86E−05	0.00E+00	9.84E−05	5.89E−04
SK−45	777	1.01E−04	0.00E+00	2.66E−04	8.24E−04
SK−45	828	2.18E−04	0.00E+00	5.06E−04	1.05E−03
SK−45	887	3.38E−04	0.00E+00	8.10E−04	1.17E−03
SK−45	944	5.11E−04	0.00E+00	1.12E−03	1.23E−03
SK−45	1001	7.27E−04	0.00E+00	1.54E−03	1.25E−03
SK−45	1058	9.44E−04	0.00E+00	1.91E−03	1.22E−03
SK−45	1116	1.16E−03	0.00E+00	2.28E−03	1.17E−03
SK−45	1173	1.38E−03	0.00E+00	2.57E−03	1.09E−03
SK−45	1231	1.57E−03	0.00E+00	2.68E−03	1.02E−03
SK−45	1288	1.65E−03	0.00E+00	2.73E−03	1.07E−03
SK−45	1346	1.82E−03	0.00E+00	2.72E−03	9.58E−04
SK−45	1403	1.97E−03	0.00E+00	2.69E−03	9.19E−04
SK−45	1461	2.10E−03	0.00E+00	2.67E−03	9.26E−04
SK−45	1520	2.20E−03	8.38E−08	2.62E−03	9.17E−04
SK−45	1577	2.21E−03	1.43E−07	2.59E−03	9.12E−04
SK−45	1635	2.30E−03	2.67E−07	2.55E−03	9.04E−04
SK−45	1693	2.29E−03	4.29E−07	2.59E−03	9.05E−04
SK−45	1750	2.34E−03	1.07E−06	2.59E−03	8.90E−04
SK−45	1807	2.33E−03	1.74E−06	2.54E−03	8.90E−04
SK−45	1865	2.44E−03	2.87E−06	2.53E−03	8.77E−04
SK−45	1922	2.41E−03	4.15E−06	2.52E−03	8.50E−04
SK−45	1980	2.41E−03	5.99E−06	2.49E−03	8.61E−04
SK−45	2038	2.40E−03	1.01E−05	2.47E−03	8.71E−04
SK−45	2095	2.36E−03	1.45E−05	2.41E−03	8.47E−04
SK−45	2153	2.43E−03	1.97E−05	2.41E−03	8.47E−04
SK−45	2211	2.41E−03	2.87E−05	2.41E−03	8.47E−04
SK−45	2268	2.41E−03	3.80E−05	2.41E−03	8.31E−04
SK−45	2325	2.44E−03	4.89E−05	2.45E−03	8.24E−04
SK−45	2382	2.43E−03	6.36E−05	2.50E−03	8.52E−04

Table C.6 (Continued)

Run Number	Volume (mL)	Sr (meq/mL)	Cs (meq/mL)	Ca (meq/mL)	Mg (meq/mL)
SK−45	2439	2.44E−03	8.23E−05	2.50E−03	8.72E−04
SK−45	2496	2.45E−03	1.06E−04	2.49E−03	8.50E−04
SK−45	2552	2.45E−03	1.22E−04	2.47E−03	8.38E−04
SK−45	2609	2.44E−03	1.50E−04	2.48E−03	8.52E−04
SK−45	2666	2.40E−03	1.78E−04	2.41E−03	8.55E−04
SK−45	2723	2.39E−03	2.07E−04	2.39E−03	8.27E−04
SK−45	2780	2.39E−03	2.35E−04	2.39E−03	8.55E−04
SK−45	2838	2.35E−03	2.69E−04	2.39E−03	8.62E−04
SK−45	2894	2.30E−03	3.04E−04	2.39E−03	8.43E−04
SK−45	2953	2.31E−03	3.45E−04	2.41E−03	8.27E−04
SK−45	3011	2.27E−03	3.84E−04	2.41E−03	8.54E−04
MV−10	41	0.00E+00	3.47E−08	0.00E+00	2.79E−06
MV−10	85	0.00E+00	0.00E+00	0.00E+00	2.71E−06
MV−10	130	0.00E+00	1.72E−08	0.00E+00	2.46E−06
MV−10	177	0.00E+00	2.09E−07	0.00E+00	2.71E−06
MV−10	226	0.00E+00	1.59E−08	0.00E+00	2.71E−06
MV−10	276	0.00E+00	3.34E−08	0.00E+00	2.88E−06
MV−10	327	0.00E+00	0.00E+00	0.00E+00	4.41E−06
MV−10	376	0.00E+00	1.97E−07	0.00E+00	9.46E−06
MV−10	426	0.00E+00	1.33E−08	0.00E+00	2.73E−05
MV−10	476	0.00E+00	0.00E+00	0.00E+00	6.85E−05
MV−10	523	0.00E+00	8.98E−08	5.99E−06	1.82E−04
MV−10	569	0.00E+00	1.11E−07	1.58E−05	3.64E−04
MV−10	616	0.00E+00	3.14E−08	3.47E−05	5.74E−04
MV−10	663	0.00E+00	2.17E−08	7.42E−05	8.24E−04
MV−10	710	0.00E+00	0.00E+00	1.44E−04	1.03E−03
MV−10	757	0.00E+00	0.00E+00	2.48E−04	1.14E−03
MV−10	804	0.00E+00	0.00E+00	4.24E−04	1.24E−03
MV−10	850	0.00E+00	0.00E+00	6.56E−04	1.31E−03
MV−10	897	0.00E+00	5.66E−08	9.02E−04	1.35E−03
MV−10	944	0.00E+00	0.00E+00	1.16E−03	1.33E−03
MV−10	990	0.00E+00	0.00E+00	1.50E−03	1.32E−03
MV−10	1037	0.00E+00	1.30E−07	1.72E−03	1.25E−03
MV−10	1083	0.00E+00	1.43E−07	1.95E−03	1.25E−03
MV−10	1129	0.00E+00	1.36E−09	2.09E−03	1.20E−03
MV−10	1176	1.56E−07	2.35E−07	2.29E−03	1.17E−03
MV−10	1233	1.56E−07	1.76E−07	2.33E−03	1.14E−03
MV−10	1291	1.56E−07	3.01E−07	2.38E−03	1.07E−03
MV−10	1337	1.04E−06	2.67E−07	2.48E−03	1.05E−03
MV−10	1383	1.04E−06	5.77E−07	2.49E−03	1.05E−03
MV−10	1431	1.04E−06	8.03E−07	2.46E−03	1.02E−03

Table C.6 (Continued)

Run Number	Volume (mL)	Sr (meq/mL)	Cs (meq/mL)	Ca (meq/mL)	Mg (meq/mL)
MV−10	1480	3.26E−06	1.05E−06	2.46E−03	1.02E−03
MV−10	1529	3.71E−06	1.43E−06	2.48E−03	9.90E−04
MV−10	1577	3.71E−06	2.11E−06	2.48E−03	1.00E−03
MV−10	1626	8.59E−06	3.53E−06	2.50E−03	9.64E−04
MV−10	1674	9.03E−06	4.47E−06	2.45E−03	1.00E−03
MV−10	1723	9.03E−06	5.91E−06	2.41E−03	9.89E−04
MV−10	1772	1.84E−05	7.96E−06	2.38E−03	9.68E−04
MV−10	1820	1.88E−05	1.06E−05	2.39E−03	9.94E−04
MV−10	1869	1.92E−05	1.38E−05	2.40E−03	9.84E−04
MV−10	1914	3.88E−05	1.73E−05	2.44E−03	9.89E−04
MV−10	1960	3.92E−05	2.31E−05	2.41E−03	1.01E−03
MV−10	2005	3.92E−05	2.59E−05	2.43E−03	1.01E−03
MV−10	2051	0.00E+00	3.45E−05	2.39E−03	1.02E−03
MV−10	2097	0.00E+00	3.95E−05	2.39E−03	9.85E−04
MV−10	2143	0.00E+00	4.81E−05	2.40E−03	9.90E−04
MV−10	2188	0.00E+00	5.60E−05	2.40E−03	9.96E−04
MV−10	2234	0.00E+00	6.70E−05	2.38E−03	1.00E−03
MV−10	2279	0.00E+00	7.87E−05	2.34E−03	1.00E−03
MV−10	2325	0.00E+00	9.30E−05	2.38E−03	9.74E−04
MV−10	2370	0.00E+00	1.07E−04	2.34E−03	9.91E−04
MV−10	2416	0.00E+00	1.26E−04	2.35E−03	9.98E−04
MV−10	2461	0.00E+00	1.40E−04	2.30E−03	9.62E−04
MV−10	2507	0.00E+00	1.55E−04	2.33E−03	9.63E−04
MV−10	2552	0.00E+00	1.80E−04	2.31E−03	9.90E−04
MV−10	2609	0.00E+00	2.06E−04	2.35E−03	9.93E−04
MV−10	2655	0.00E+00	2.28E−04	2.31E−03	9.80E−04
MV−10	2711	0.00E+00	2.55E−04	2.20E−03	9.78E−04
MV−10	2757	0.00E+00	2.82E−04	2.23E−03	9.85E−04
MV−10	2810	0.00E+00	3.08E−04	2.23E−03	9.72E−04
MV−10	2861	0.00E+00	3.36E−04	2.23E−03	9.89E−04
MV−10	2909	0.00E+00	3.71E−04	2.24E−03	9.88E−04
MV−10	2956	0.00E+00	3.97E−04	2.14E−03	9.77E−04
MV−10	3003	0.00E+00	4.36E−04	2.15E−03	9.59E−04
MV−10	3050	0.00E+00	4.53E−04	2.27E−03	9.74E−04
SK−47	2E+02	0.00E+00	0.00E+00	0.00E+00	8.31E−07
SK−47	4E+02	0.00E+00	0.00E+00	0.00E+00	5.81E−07
SK−47	6E+02	0.00E+00	0.00E+00	0.00E+00	7.63E−07
SK−47	8E+02	0.00E+00	0.00E+00	0.00E+00	5.59E−07
SK−47	1E+03	0.00E+00	0.00E+00	0.00E+00	5.59E−07
SK−47	1E+03	0.00E+00	0.00E+00	0.00E+00	7.40E−07
SK−47	1E+03	0.00E+00	0.00E+00	0.00E+00	1.97E−06

Table C.6 (Continued)

Run Number	Volume (mL)	Sr (meq/mL)	Cs (meq/mL)	Ca (meq/mL)	Mg (meq/mL)
SK−47	2E+03	0.00E+00	0.00E+00	0.00E+00	1.11E−05
SK−47	2E+03	0.00E+00	0.00E+00	0.00E+00	6.02E−05
SK−47	2E+03	0.00E+00	0.00E+00	0.00E+00	1.87E−04
SK−47	2E+03	3.09E−08	0.00E+00	8.78E−08	3.91E−04
SK−47	2E+03	9.12E−06	0.00E+00	1.37E−06	6.27E−04
SK−47	2E+03	3.38E−05	0.00E+00	2.27E−06	8.55E−04
SK−47	3E+03	9.07E−05	0.00E+00	5.64E−06	1.07E−03
SK−47	3E+03	1.91E−04	0.00E+00	1.11E−05	1.18E−03
SK−47	3E+03	4.42E−04	0.00E+00	1.86E−05	1.24E−03
SK−47	3E+03	5.39E−04	0.00E+00	2.78E−05	1.28E−03
SK−47	3E+03	7.22E−04	0.00E+00	3.66E−05	1.24E−03
SK−47	4E+03	9.61E−04	0.00E+00	4.54E−05	1.19E−03
SK−47	4E+03	1.17E−03	0.00E+00	5.18E−05	1.11E−03
SK−47	4E+03	1.39E−03	0.00E+00	5.76E−05	1.06E−03
SK−47	4E+03	1.60E−03	0.00E+00	6.17E−05	1.03E−03
SK−47	4E+03	1.79E−03	0.00E+00	6.38E−05	9.92E−04
SK−47	5E+03	1.91E−03	0.00E+00	6.32E−05	9.51E−04
SK−47	5E+03	2.03E−03	0.00E+00	6.37E−05	9.43E−04
SK−47	5E+03	2.10E−03	0.00E+00	6.28E−05	9.19E−04
SK−47	6E+03	2.41E−03	1.49E−06	5.96E−05	8.77E−04
SK−47	6E+03	2.42E−03	2.40E−06	5.82E−05	8.75E−04
SK−47	7E+03	2.46E−03	4.64E−06	5.88E−05	8.82E−04
SK−47	7E+03	2.49E−03	7.02E−06	5.95E−05	8.66E−04
SK−47	7E+03	2.48E−03	1.10E−05	5.81E−05	8.62E−04
SK−47	7E+03	2.50E−03	1.77E−05	5.84E−05	9.00E−04
SK−47	7E+03	2.55E−03	2.37E−05	5.94E−05	8.87E−04
SK−47	7E+03	2.55E−03	3.31E−05	5.87E−05	8.88E−04
SK−47	8E+03	2.54E−03	4.23E−05	5.92E−05	8.83E−04
SK−47	8E+03	2.55E−03	5.60E−05	5.84E−05	8.71E−04
SK−47	8E+03	2.51E−03	6.95E−05	5.73E−05	8.71E−04
SK−47	8E+03	2.52E−03	8.76E−05	5.79E−05	8.66E−04
SK−47	8E+03	2.55E−03	1.05E−04	5.79E−05	8.50E−04
SK−47	9E+03	2.53E−03	1.28E−04	5.74E−05	8.66E−04
SK−47	9E+03	2.44E−03	1.50E−04	5.56E−05	8.76E−04
SK−47	9E+03	2.48E−03	1.75E−04	5.68E−05	8.70E−04
SK−47	9E+03	2.44E−03	2.01E−04	5.63E−05	8.69E−04
SK−47	9E+03	2.49E−03	2.24E−04	5.76E−05	8.65E−04
SK−47	9E+03	2.48E−03	2.46E−04	5.70E−05	8.68E−04
SK−47	1E+04	2.43E−03	2.83E−04	5.59E−05	8.71E−04
SK−47	1E+04	2.45E−03	3.09E−04	5.57E−05	8.67E−04
SK−47	1E+04	2.36E−03	3.45E−04	5.44E−05	8.63E−04

Table C.6 (Continued)

Run Number	Volume (mL)	Sr (meq/mL)	Cs (meq/mL)	Ca (meq/mL)	Mg (meq/mL)
SK−48	925	0.00E+00	2.70E−06	0.00E+00	0.00E+00
SK−48	1842	0.00E+00	3.58E−07	0.00E+00	0.00E+00
SK−48	2746	0.00E+00	2.99E−06	0.00E+00	0.00E+00
SK−48	3639	0.00E+00	1.63E−06	0.00E+00	0.00E+00
SK−48	4526	0.00E+00	5.14E−06	0.00E+00	0.00E+00
SK−48	5404	0.00E+00	0.00E+00	0.00E+00	0.00E+00
SK−48	6273	0.00E+00	8.46E−07	0.00E+00	0.00E+00
SK−48	7131	0.00E+00	6.51E−07	0.00E+00	0.00E+00
SK−48	7980	0.00E+00	1.63E−07	0.00E+00	0.00E+00
SK−48	8831	0.00E+00	1.43E−06	0.00E+00	0.00E+00
SK−48	9714	0.00E+00	1.53E−06	4.14E−06	6.84E−06
SK−48	10602	3.08E−06	0.00E+00	2.99E−05	4.93E−05
SK−48	11504	5.49E−05	8.46E−07	1.27E−04	2.09E−04
SK−48	12390	9.43E−05	2.70E−06	3.18E−04	5.25E−04
SK−48	13264	1.90E−04	2.11E−06	5.68E−04	9.37E−04
SK−48	14136	2.91E−04	1.92E−06	8.43E−04	1.39E−03
SK−48	15004	4.32E−04	5.53E−07	1.15E−03	1.90E−03
SK−48	15866	5.87E−04	8.46E−07	1.57E−03	2.59E−03
SK−48	16727	7.81E−04	1.04E−06	2.01E−03	3.32E−03
SK−48	17602	9.92E−04	0.00E+00	2.42E−03	3.99E−03
SK−48	18486	1.23E−03	0.00E+00	2.61E−03	4.30E−03
SK−48	19381	1.45E−03	1.53E−06	2.72E−03	4.49E−03
SK−48	20273	1.63E−03	7.48E−07	2.71E−03	4.47E−03
SK−48	21163	1.80E−03	0.00E+00	2.68E−03	4.41E−03
SK−48	22047	1.86E−03	0.00E+00	2.57E−03	4.24E−03
SK−48	22918	1.93E−03	1.82E−06	2.50E−03	4.12E−03
SK−48	23779	2.06E−03	2.80E−06	2.50E−03	4.13E−03
SK−48	24634	2.03E−03	0.00E+00	2.40E−03	3.95E−03
SK−48	25488	2.09E−03	1.63E−06	2.42E−03	3.98E−03
SK−48	26375	2.13E−03	2.21E−06	2.40E−03	3.96E−03
SK−48	27275	2.23E−03	0.00E+00	2.42E−03	4.00E−03
SK−48	28178	2.18E−03	1.72E−06	2.32E−03	3.82E−03
SK−48	29073	2.20E−03	1.43E−06	2.35E−03	3.88E−03
SK−48	29958	2.24E−03	4.65E−06	2.38E−03	3.93E−03
SK−48	30827	2.22E−03	9.43E−07	2.29E−03	3.78E−03
SK−48	31687	2.25E−03	1.33E−06	2.31E−03	3.81E−03
SK−48	32536	2.23E−03	6.60E−06	2.30E−03	3.79E−03
SK−48	33384	2.28E−03	9.53E−06	2.36E−03	3.89E−03
SK−48	34242	2.24E−03	1.35E−05	2.30E−03	3.80E−03
SK−48	35111	2.27E−03	2.59E−05	2.34E−03	3.87E−03
SK−48	35974	2.25E−03	2.66E−05	2.30E−03	3.79E−03

Table C.6 (Continued)

Run Number	Volume (mL)	Sr (meq/mL)	Cs (meq/mL)	Ca (meq/mL)	Mg (meq/mL)
SK−48	36847	2.28E−03	4.56E−05	2.33E−03	3.84E−03
SK−48	37714	2.26E−03	6.03E−05	2.29E−03	3.77E−03
SK−48	38584	2.25E−03	6.40E−05	2.28E−03	3.76E−03
SK−48	39436	2.31E−03	8.60E−05	2.29E−03	3.77E−03
SK−48	40276	2.24E−03	1.02E−04	2.26E−03	3.72E−03
SK−48	41114	2.23E−03	1.21E−04	2.28E−03	3.76E−03
SK−48	41952	2.25E−03	1.41E−04	2.28E−03	3.76E−03
SK−48	42804	2.22E−03	1.72E−04	2.28E−03	3.75E−03
SK−48	43653	2.21E−03	1.96E−04	2.27E−03	3.75E−03
SK−48	44513	2.20E−03	2.34E−04	2.28E−03	3.75E−03
SK−48	45374	2.18E−03	2.76E−04	2.19E−03	3.62E−03
SK−48	46225	2.21E−03	3.07E−04	2.24E−03	3.70E−03

Appendix D. ORTHOGONAL COLLOCATION NUMERICAL METHODS

Orthogonal collocation is a method of weighted residuals that converts PDEs to a system of ODEs (Villadsen and Michelsen, 1978; Finlayson, 1980). In the orthogonal collocation method, the unknown solution to the spatial derivatives in the PDEs are approximated by orthogonal polynomials. The coefficients of the polynomials are adjusted so that the substitution of the polynomials results in zero error at the roots of the orthogonal polynomials. Thus, orthogonal collocation replaces spatial derivatives with matrices and reduces the PDEs to ODEs.

In this study, the collocation points are chosen to be the roots of the Jacobi orthogonal polynomials. The solution at these points is computed by solving N simultaneous equations that result from substitution of the trial function into the differential equation where N is the number of arbitrary collocation points in the trial function.

Depending on the system definition, the trial functions can be selected as symmetrical or asymmetrical Jacobi polynomials. The symmetrical Jacobi polynomial trail function (Finlayson, 1980) is defined as:

$$G(\eta,\bar{t}) = G(1,\bar{t}) + (1-\eta^2)\sum_{i=1}^{MC} a_i(\bar{t})P_{i-1}(\eta^2), \tag{88}$$

where the polynomials are defined to be orthogonal by

$$\int_0^1 W(\eta^2)P_k(\eta^2)P_m(\eta^2)\eta^{a-1}d\eta = 0 \quad k \le m - 1, \tag{89}$$

where MC is the number of arbitrary collocation points in the trial polynomials for half of a symmetrical system; $W(\eta^2) = (\eta^2)^\alpha(1 - \eta^2)^\beta$ where α and β are 0 or 1; and a = 1, 2, or 3 for planar, cylindrical, or spherical geometry respectively. The spatial derivatives are replaced with the following matrices:

$$\frac{dG}{d\eta}\Big|_{\eta_j} = \sum_{i=1}^{MC} A_{ji}^{\eta} G_i, \tag{90}$$

and

$$\frac{d^2G}{d\eta^2}\Big|_{\eta_j} = \sum_{i=1}^{MC} B_{ji}^{\eta} G_i \ . \tag{91}$$

The spatial integral is replaced with:

$$\int_0^1 G d\eta = \sum_{i=1}^{MC} W_i^{\eta} G_i. \tag{92}$$

Once the weighting function and number of collation points are chosen and the system geometry is defined, the location of the collation points and values for the constants are automatically defined.

The asymmetrical Jacobi polynomial trail function (Finlayson, 1980) is

$$U(\lambda,\tau) = (1 - \lambda)U(0,\bar{t}) + \lambda U(1,\bar{t})$$

$$+ \lambda(1-\lambda)\sum_{i=1}^{NC} a_i(\bar{t}) P_{i-1}(\lambda) \tag{93}$$

where the polynomials are defined by

$$\int_0^1 W(\lambda)P_k(\lambda)P_m(\lambda)\lambda^{a-1}d\lambda = 0 \quad k \le m - 1 \tag{94}$$

with NC equaling the numerical of collocation points for an asymmetrical system; $W(\lambda) = (\lambda)^{\alpha}(1 - \beta)$, where α, β, and a are the same as in the symmetrical system. The spatial derivatives are replaced with the following matrices:

$$\frac{dU}{d\lambda}\Big|_{\lambda_j} = \sum_{i=1}^{NC} A_{ji}^{\lambda} U_i \ , \tag{95}$$

and

$$\frac{d^2U}{d\lambda^2}\Big|_{\lambda_j} = \sum_{i=1}^{NC} B_{ji}^{\lambda} U_i \ . \tag{96}$$

The spatial integral is replaced with

$$\int_0^1 U d\lambda = \sum_{i=1}^{NC} W_i^{\lambda} U_i. \tag{97}$$

The orthogonal collocation subroutines used were published by Villadsen and Michaelson (1978). These subroutines solve the unsymmetric shifted Legendre polynomials for A^{λ}, B^{λ}, W^{λ}, and F^{λ} where F is the vector containing the roots of the polynomial. The resulting values were converted to solutions for the symmetric Legendre polynomials using equations derived by Michelsen and Villadsen (1972) and Finlayson (1980):

$$A_{ji}^{r} = 2.0 \ F_j^{r} \ A_{ji}^{\lambda}, \tag{98}$$

$$B_{ji}^{r} = 4.0 \ F_j^{\lambda} \ B_{ji}^{\lambda} + 2.0 \ a \ A_{ji}^{\lambda}, \tag{99}$$

$$F_j^{r} = \sqrt{F_j^{\lambda}}, \tag{100}$$

and

$$W_j^{r} = \sum_{i=1}^{MC} \frac{1}{2i-2+a} \left((F_j^{r})^{2i-2} \right)^{-1}, \tag{101}$$

where a = 1, 2, or 3 for planar, cylindrical, or spherical geometries, respectively.

Appendix E. MODELS FOR ION EXCHANGE IN BATCH REACTORS

Sets of PDEs were developed in Section 7 for various diffusion models for ion exchange in zeolites in batch reactor systems. The orthogonal collocation equations developed in Appendix D for symmetrical systems can be used to convert the PDEs to sets of ODEs that can be solved by standard numerical methods. The resulting ODEs contain functions which are dependent on the concentration in the zeolite at collocation points located across the particle radius.

E.1 Homogenous Diffusion Model with Constant Diffusivities.

The PDEs for the homogenous diffusion model were derived for several different cases in Section 7.1. If the micropore diffusivity is assumed to be constant and film mass transfer is taken into account, Equations 33 through 39 for component m become:

$$\frac{\partial Q_m}{\partial t} = \frac{D_{cm}}{r_c^2}\nabla^2 Q_m \tag{102}$$

for the solid phase mass balance;

$$\frac{\partial C_{dm}}{\partial t} = \frac{-3\rho(1-\varepsilon)q_{0m}}{\varepsilon c_{0m}}\frac{\partial}{\partial t}\int_0^1 Q_m \bar{r}^2 d\bar{r} \tag{103}$$

for the overall mass balance; and

$$\frac{\partial Q_m}{\partial \bar{r}} = 0 \quad at\ \bar{r} = 0, \tag{104}$$

$$\frac{\partial}{\partial t}\int_0^1 Q_m \bar{r}^2 d\bar{r} = \frac{k_{fm}c_{0m}}{\rho r_c q_{0m}}(C_{dm} - C_{sm}), \tag{105}$$

and

$$C_{dm} = 1,\ C_{sm} = Q_m = 0 \quad at\ t = 0, \tag{106}$$

for the boundary and initial conditions, respectively.

The application of orthogonal collocation to Equations 102 through 106 produces a set of ODEs. The solid phase mass balance becomes

$$\frac{dQ_{mj}}{dt} = \frac{D_{cm}}{r_c^2}\sum_{i=1}^{MC} B_{ji}^r Q_{mi} \tag{107}$$

where m is the subscript denoting the exchanging component, and MC is the number of collocation points across the zeolite crystal radius. Equation 107 is used to produce MC-1 solid phase mass balances, one for each collocation point across the zeolite crystal (excluding the surface collocation point) represented by j = 1 to MC-1. The overall phase mass balance becomes

$$\frac{dC_{dm}}{dt} = -D_{gm}\sum_{i=1}^{MC} W_i^r \frac{dQ_{mi}}{dt}. \tag{108}$$

The boundary condition given in Equation 105 becomes:

$$\frac{d}{dt}\sum_{i=1}^{MC} W_i^r Q_{mi} = \frac{k_{gm}}{D_{gm}}(C_{dm} - C_{sm}). \tag{109}$$

This equation can be rearranged to solve for dQ_{mMC}/dt at the particle surface:

$$\frac{dQ_{mMC}}{dt} = \frac{k_{gm}}{D_{gm}W_{MC}^r}(C_{dm} - C_{sm}) - \sum_{i=1}^{MC-1}\frac{W_i^r}{W_{MC}^r}\frac{dQ_{mi}}{dt}. \tag{110}$$

The boundary condition given in Equation 104 is automatically satisfied because of the symmetric Legendre polynomials. The initial conditions are:

Equations 107 through 111 represent a set of m(MC+1) ODEs: (1) one overall mass

$$C_{dm} = 1,\ C_{sm} = Q_{mi} = 0 \quad at\ t = 0\ for\ i = 1,\ MC. \tag{111}$$

balance for each of m components, (2) the MC-1 equations for mass transfer within the particle for m components, and (4) m equations for the mass balances of each component at the particle surface (collocation point MC). The system of equations has m(MC+2) unknowns: C_d for m components, C_s for m components, and MC values of Q_{MC} along the particle radius for m components. The remaining equations required to solve the model are the equilibrium equations for each of m components which couples C_s with Q_{MC} at the particle surface. Equations 107, 108, and 110 and the equilibrium equations were solved using Gear's method.

If film mass transfer is negligible, C_s becomes equal to C_d. Under these conditions Equations 109 and 110 are dropped, and Equation 108 becomes

$$\frac{dC_{dm}}{dt} = \frac{-D_{gm}\sum_{i=1}^{MC-1} W_i^r \frac{dQ_{mi}}{dt}}{D_g m W_{MC}^r \frac{dQ_{mMC}}{dC_{dm}} + 1}. \tag{112}$$

The equilibrium equation now couples C_d with Q_{MC}.

E.2 Homogenous Diffusion Model with Variable Diffusivities.

If the micropore diffusivity is concentration dependent, Equation 33 becomes

$$\frac{\partial Q_m}{\partial t} = \frac{D_{cm}(Q_m)}{r_c^2}\frac{\partial^2 Q_m}{\partial \bar{r}^2} + \frac{2D_{cm}(Q_m)}{r_c^2 \bar{r}}\frac{\partial Q_m}{\partial \bar{r}} + \frac{q_{0m}}{r_c^2}\frac{\partial D_{cm}}{\partial Q_m}\left(\frac{\partial Q_m}{\partial \bar{r}}\right)^2, \tag{113}$$

rather than Equation 102. When Equation 113 is converted to an ODE by orthogonal collocation, it becomes

$$\frac{dQ_{mj}}{dt} = \frac{D_{cm}(Q_{mj})}{r_c^2}\sum_{i=1}^{MC} B_{ji}^r Q_{mi} + \frac{q_{0m}}{r_c^2}\frac{\partial D_{cm}}{\partial Q_{mj}}\left(\sum_{i=1}^{MC} A_{ji}^r Q_{mi}\right)^2. \tag{114}$$

The concentration dependence of the micropore diffusivity is given by Darken's equation, which leads to

$$D_{cm} = \frac{D_{0m}}{\left(1 - \frac{b_m Q_m q_{0m}}{a_m}\right)} \tag{115}$$

for the Langmuir isotherm, and

$$D_{cm} = \frac{D_{0m}}{\sqrt{b_{1m}^2 - 4b_{2m}[b_{0m} - \ln(Q_m q_{0m})]}} \tag{116}$$

for the modified Dubinin-Polyani isotherm. The partial derivatives are

$$\frac{\partial D_{cm}}{\partial Q_m} = \frac{q_{0m} b_m D_{0m}}{a_m\left(1 - \frac{b_m Q_m q_{0m}}{a_m}\right)^2} \tag{117}$$

and

$$\frac{\partial D_{cm}}{\partial Q_m} = \frac{2 b_{2m} D_{0m}}{Q_m}\left\{b_{1m}^2 - 4b_{2m}[b_{0m} - \ln(Q_m q_{0m})]\right\}^{-1.5} \tag{118}$$

for the Langmuir and modified Dubinin-Polyani isotherms. Equation 114 becomes

$$\frac{dQ_{mj}}{dt} = \frac{D_{0m}}{r_c^2}\left(\frac{1}{1 - \frac{b_m Q_{mj} q_{0m}}{a_m}}\right)$$

$$\left[\sum_{i=1}^{MC} B_{ji}^r Q_{mi} + \frac{q_{0m} b_m}{a_m\left(1 - \frac{b_m Q_{mj} q_{0m}}{a_m}\right)}\left(\sum_{i=1}^{MC} A_{ji}^r Q_{mi}\right)^2\right] \tag{119}$$

for the Langmuir isotherm, and

$$\frac{dQ_{mj}}{dt} = \frac{D_{0m}}{r_c^2\sqrt{b_{1m}^2 - 4\,b_{2m}[b_{0m} - \ln(Q_{mj} q_{0m})}}\sum_{i=1}^{MC} B_{ji}^r Q_{mi}$$

$$- \frac{2\,b_{2m} D_{0m}}{r_c^2 Q_{mj}\{b_{1m}^2 - 4\,b_{2m}[b_{0m} - \ln(Q_{mj} q_{0m})]\}^{1.5}}$$

$$\left(\sum_{i=1}^{MC} A_{ji}^r Q_{mi}\right)^2 \tag{120}$$

for the modified Dubinin-Polyani isotherm.

E.3 Heterogenous Parallel Diffusion Model with Constant Diffusivities.

The PDEs for various versions of the heterogenous parallel diffusion model were derived in Section 7.2.1. If the micropore and macropore diffusivities are assumed to be independent of concentration and film mass transfer is taken into account, Equations 46 to 52 are:

$$\xi_m \frac{\partial C_{pm}}{\partial t} + \frac{\partial Q_m}{\partial t} = \frac{1}{R_p^2 \overline{R}^2}\frac{\partial}{\partial \overline{R}}\left[\overline{R}^2\left(D_{cm}\frac{\partial Q_m}{\partial \overline{R}} + \xi_m D_{pm}\frac{\partial C_{pm}}{\partial \overline{R}}\right)\right] \tag{121}$$

for the solid phase mass balance;

$$\frac{\partial C_{dm}}{\partial t} = -(1 - \varepsilon_p) D_{gm} \frac{\partial}{\partial t} \int_0^1 (Q_m + \xi_m C_{pm}) \overline{R}^2 d\overline{R} \tag{122}$$

for the overall mass balance;

$$\frac{\partial C_{pm}}{\partial \overline{R}} = \frac{\partial Q_m}{\partial \overline{R}} = 0 \quad at\ \overline{R} = 0, \tag{123}$$

$$\frac{\partial}{\partial t} \int_0^1 (Q_m + \xi_m C_{pm}) \overline{R}^2 d\overline{R} = \frac{k_{gm}}{D_{gm}} (1-\varepsilon_p)(C_{dm} - C_{sm}) \quad at\ \overline{R} = 1, \tag{124}$$

and

$$C_{dm} = 1,\ C_{sm} = C_{pm} = Q_m = 0 \quad at\ t = 0 \tag{125}$$

for the boundary and initial conditions, respectively.

The application of orthogonal collocation to Equations 121 through 125 produces the following set of ODEs for each component m:

$$\frac{dC_{pmj}}{dt} = \frac{\frac{D_{cm}}{R_p^2} \sum_{i=1}^{PC} B_{ji}^r Q_{mi} + \frac{\xi_m D_{pm}}{R_p^2} \sum_{i=1}^{PC} B_{ji}^r C_{pmi}}{\frac{dQ_{mj}}{dC_{pmj}} + \xi_m} \tag{126}$$

where j = 1 to PC-1 if PC is the total number of collocation points across the zeolite particle radius,

$$\frac{dC_{dm}}{dt} = -(1 - \varepsilon_p) D_{gm} \sum_{i=1}^{PC} W_i^r \frac{d(Q_{mi} + \xi_m C_{pmi})}{dt}, \tag{127}$$

where $C_{pmPC} = C_{sm}$, and

$$\frac{dC_{pmPC}}{dt} = \frac{\dfrac{k_{gm}}{1-\varepsilon_p D_{gm} W^r_{PC}}(C_{dm} - C_{sm}) - \sum_{i=1}^{PC-1} \dfrac{W^r_i}{W^r_{PC}} \dfrac{d(Q_{mi} + \xi_m C_{pmi})}{dt}}{\dfrac{dQ_{mPC}}{dC_{pmPC}} + \xi_m} . \tag{128}$$

The equilibrium equation defines C_{pmj} as a function of Q_{mj} at all collocation points. Therefore, the time dependence of Q_{mj} can be described by substituting the equilibrium equation and Equations 126 and 128 into

$$\frac{dQ_{mj}}{dt} = \frac{dQ_{mj}}{dC_{pmj}} \frac{dC_{pmj}}{dt} \quad for\ j = 1\ to\ PC. \tag{129}$$

The boundary condition given in Equation 123 is automatically satisfied because of the symmetric Legendre polynomials.

Equations 126 through 129 represent a set of m(2PC+1) nonlinear algebraic and ODEs that can be solved for the m(2PC+1) unknowns in a manner similar to that discussed in Section E.1. The initial conditions are

$$C_{dm} = 1,\ C_{pmi} = Q_{mi} = 0 \quad at\ t = 0 \tag{130}$$

for i = 1 to PC.

If film mass transfer is negligible, C_{pmPC} becomes equal to C_{dm}. Under these conditions, Equation 124 becomes:

$$\frac{\partial C_{dm}}{\partial t} = -(1 - \varepsilon_p) D_{gm} \frac{\partial}{\partial t} \int_0^1 (Q_m + \xi_m C_{pm}) \overline{R}^2 d\overline{R} , \tag{131}$$

and Equation 128 changes to

$$\frac{dC_{dm}}{dt} = \frac{-(1-\varepsilon_p)D_{gm}\sum_{i=1}^{PC-1} W_i^r \frac{d(Q_{mi}+\xi_m C_{pmi})}{dt}}{1+(1-\varepsilon_p)D_{gm}W_{PC}^r\left(\frac{dQ_{mPC}}{dC_{dm}}+\xi_m\right)}. \tag{132}$$

E.4 Heterogenous Parallel Diffusion Model with Variable Micropore Diffusivity.

If the micropore diffusivity is assumed to be dependent on the solid phase concentration, Equations 121 and 126 become:

$$\xi_m \frac{\partial C_{pm}}{\partial t} + \frac{\partial Q_m}{\partial t} = \frac{D_{cm}}{R_p^2}\frac{\partial^2 Q_m}{\partial \overline{R}^2} + \frac{2D_{cm}}{R_p^2 \overline{R}}\frac{\partial Q_m}{\partial \overline{R}}$$

$$+ \frac{q_{0m}}{R_p^2}\frac{\partial D_{cm}}{\partial Q_m}\left(\frac{\partial Q_m}{\partial \overline{R}}\right)^2 + \frac{\xi_m D_{pm}}{R_p^2}\frac{\partial^2 C_{pm}}{\partial \overline{R}^2}, \tag{133}$$

and

$$\frac{dC_{pmj}}{dt} = \frac{\frac{D_{cm}}{R_p^2}\sum_{i=1}^{PC} B_{ji}^r Q_{mi}}{\frac{dQ_{mj}}{dC_{pmj}}+\xi_m} + \frac{\frac{q_{0m}}{R_p^2}\frac{\partial D_{cm}}{\partial Q_{mj}}\left(\sum_{i=1}^{PC} A_{ji}^r Q_{mi}\right)^2}{\frac{dQ_{mj}}{dC_{pmj}}+\xi_m}$$

$$+ \frac{\frac{\xi_m D_{pm}}{R_p^2}\sum_{i=1}^{PC} B_{ji}^r C_{pmi}}{\frac{dQ_{mj}}{dC_{pmj}}+\xi_m} \tag{134}$$

respectively, where D_{cm} and the partials of D_{cm} are given by Equations 115 through 118. The equations are solved similarly to those described in Section E.3.

E.5 Heterogenous Series Diffusion Model with Constant Diffusivities.

The PDEs for various versions of the heterogenous series diffusion model were derived in Section 7.2.2. If the micropore and macropore diffusivities are assumed to occur in series and be concentration independent, Equations 61 through 68 can be rewritten in the form given below. The overall mass balance becomes:

$$\frac{\partial C_{dm}}{\partial t} + \frac{\rho(1-\varepsilon)q_{0m}}{\varepsilon c_{0m}} \frac{\partial \overline{\overline{Q_m}}}{\partial t} = 0, \tag{135}$$

where

$$\frac{\partial \overline{\overline{Q_m}}}{\partial t} = 3(1 - \varepsilon_p)\int_0^1 \overline{R^2} \frac{\partial \overline{Q_m}}{\partial t} d\overline{R} + \frac{3\varepsilon_p c_{0m}}{\rho q_{0m}} \int_0^1 \overline{R^2} \frac{\partial C_{pm}}{\partial t} d\overline{R}. \tag{136}$$

The intraparticle mass transfer equations become:

$$\frac{1}{R_p^2\, \overline{R^2}} \frac{\partial}{\partial \overline{R}} \left(\overline{R^2}\, D_{pm} \frac{\partial C_{pm}}{\partial \overline{R}} \right) = \frac{\partial C_{pm}}{\partial t} + \frac{\rho(1-\varepsilon_p)q_{0m}}{\varepsilon_p c_{0m}} \frac{\partial \overline{Q_m}}{\partial t}, \tag{137}$$

where

$$\frac{\partial \overline{Q_m}}{\partial t} = 3\int_0^1 \frac{\partial Q_m}{\partial t} \overline{r^2}\, d\overline{r}, \tag{138}$$

and

$$\frac{\partial Q_m}{\partial t} = \frac{1}{r_c^2 \overline{r^2}} \frac{\partial}{\partial \overline{r}} \left(\overline{r^2} D_{cm} \frac{\partial Q_m}{\partial \overline{r}} \right). \tag{139}$$

The surface of each zeolite crystal is in equilibrium with the liquid concentration in the pore at each collocation point across the particle radius. Since the film mass transfer is insignificant, $C_{dm} = C_{pm}$ at $\overline{R} = 1$. Because of symmetry,

$$\frac{\partial C_{pm}}{\partial \bar{R}} = \frac{\partial \overline{Q_m}}{\partial \bar{R}} = \frac{\partial Q_m}{\partial \bar{r}} = 0 \ at \ \bar{R} = 0, \ \bar{r} = 0. \tag{140}$$

The initial conditions are:

$$C_{dm} = 1, \ C_{pm} = C_{sm} = Q_m = 0 \quad at \ t = 0. \tag{141}$$

Equations 135 to 139 are transformed to ODEs by applying orthogonal collocation using the trial functions for a symmetrical system as described in Appendix D. The mass-transfer equation inside the zeolite crystal becomes:

$$\frac{dQ_{mjk}}{dt} = \frac{D_{cm}}{r_c^2} \sum_{l=1}^{MC} B_{jl}^{r} Q_{mlk}, \tag{142}$$

for j = 1 to MC and k = 1 to PC. In Equation 142, m is component; j is the collocation point along the zeolite crystal radius; and k is the collocation point along the particle radius. MC and PC are the number of collocation points for the zeolite crystal and particle, respectively.

The average concentration in each zeolite crystal is given by:

$$\frac{d\overline{Q_{mk}}}{dt} = 3 \sum_{j=1}^{MC} W_j \frac{dQ_{mjk}}{dt} \tag{143}$$

for each collocation point across the particle radius, that is, k=1 to PC. The macropore mass-transfer equation becomes:

$$\frac{dC_{pmk}}{dt} = \frac{D_{pm}}{R_p^2} \sum_{j=1}^{PC} B_{kj} C_{pmj} - \frac{1}{\xi_m} \frac{d\overline{Q_{mk}}}{dt} \tag{144}$$

where k = 1 to PC - 1. The overall mass balance yields an equation for the bulk solution concentration as a function of time:

$$\frac{dC_{dm}}{dt} = \frac{-\frac{3\varepsilon_p(1-\varepsilon)}{\varepsilon}\left(\sum_{i=1}^{PC}\frac{W_i^r}{\xi_m}\frac{d\overline{Q_{mi}}}{dt} + \sum_{i=1}^{PC-1} W_i^r \frac{dC_{pmi}}{dt}\right)}{1 + \frac{3\varepsilon_p(1-\varepsilon)}{\varepsilon} W_{PC}^r}. \tag{145}$$

The boundary condition given in Equation 139 is met by the selection of a symmetrical trial polynomial.

Equations 142 through 145 represent a set of m x PC x (MC + 1) ODEs: (1) MC equations for mass transfer within the zeolite crystal at each collocation point PC across the particle radius for each of m components, (2) PC - 1 equations for mass transfer in the macropores across the particle radius for each of m components, and (3) m equations for the mass balances of each component at the particle surface (collocation point PC). The system of equations has m x PC x (MC+1) unknowns: C_d for m components, (PC - 1) values of C_p for m components, and MC values of Q along the crystal radius at each of PC particle radial coordinate points for m components. Therefore, Equations 142 through 145 can be used to solve heterogenous series diffusion model.

E.6 Heterogenous Series Diffusion Model with Parabolic Concentration Profile in Zeolite Crystals.

The assumption that macropore and micropore diffusion occurs in series results in coupled partial differential equations involving time and spatial variables as shown in Section E.5. The mathematics can be simplified considerably by assuming that the concentration profiles in the zeolite crystals have parabolic shapes. If we assume that the zeolite crystal has a parabolic profile given by Equation 69, Equations 138 and 139 become

$$\frac{\partial \overline{Q_m}}{\partial t} = \frac{15D_{cm}}{r_c^2}(Q_m|_{r=1} - \overline{Q_m}). \tag{146}$$

Under these conditions, Equations 141 and 142 reduce to

$$\frac{d\overline{Q_{mk}}}{dt} = \frac{15D_{cm}}{r_c^2}(Q_{mk}|_{\bar{r}=1} - \overline{Q_{mk}}) \quad for\ k = 1\ to\ PC. \tag{147}$$

The macropore mass-transfer equation (Equation 144) and the equation for the bulk solution concentration (Equation 145) remain the same.

The introduction of the parabolic profile for the concentration in the zeolite crystal reduces the number of unknowns from m x PC x (MC+1) to 3mPC: the average concentration in the zeolite crystal, the solid concentration at the crystal surface, and the liquid concentration in the pore at each collocation point (k = 1 to PC) for m components. The bulk solution concentration is equal to the pore concentration at the particle surface. The equations required to solve this model are m x PC equations from Equation 146, m x (PC - 1) equations from Equation 144, m equations from Equation 145, and m x PC equations from the equilibrium equation that couples the liquid pore concentration and the solid concentration at the zeolite crystal surface.

E.7 Heterogenous Series Diffusion Model with Variable Diffusivities.

The most rigorous heterogenous diffusion model accounts for micropore and macropore diffusion occurring in series where the macropore diffusivities are a combination of surface and molecular diffusion occurring in parallel. Both the surface and micropore diffusivities are a function of concentration. Under these conditions, Equations 33, 34, and 73 must be substituted into Equations 135 to 139.

The overall mass balance is:

$$\frac{\partial C_{dm}}{\partial t} + \frac{\rho(1-\varepsilon)q_{0m}}{\varepsilon c_{0m}} \frac{\partial \overline{\overline{Q_m}}}{\partial t} = 0 \tag{148}$$

where

$$\frac{\partial \overline{\overline{Q_m}}}{\partial t} = 3(1 - \varepsilon_p)\int_0^1 \overline{R^2} \frac{\partial \overline{Q_m}}{\partial t} d\overline{R} + \frac{3\varepsilon_p c_{0m}}{\rho q_{0m}} \int_0^1 \overline{R^2} \frac{\partial C_{pm}}{\partial t} d\overline{R}. \tag{149}$$

The macropore mass transfer equations become:

$$\frac{1}{R_p^2\,\overline{R^2}} \frac{\partial}{\partial \overline{R}} \left[\overline{R^2} \left(\frac{D_{sm}}{\xi_m} \frac{\partial Q_m}{\partial \overline{R}} \Big|_{\overline{r}=1} + \frac{D_{lm}}{\tau} \frac{\partial C_{pm}}{\partial \overline{R}} \right) \right] =$$

$$\frac{\partial C_{pm}}{\partial t} + \frac{1}{\xi_m} \frac{\partial \overline{Q_m}}{\partial t}, \tag{150}$$

where the concentration dependence of the surface diffusivity is given by Darken's equation, which leads to

$$D_{sm} = \frac{D_{s0m}}{\left(1 - \dfrac{b_m Q_m q_{0m}}{a_m}\right)} \tag{151}$$

for the Langmuir isotherm, and

$$D_{sm} = \frac{D_{s0m}}{\sqrt{b_{1m}^2 - 4b_{2m}[b_{0m} - \ln(Q_m q_{0m})]}} \tag{152}$$

for the modified Dubinin-Polyani isotherm. The micropore mass-transfer equations are:

$$\frac{\partial \overline{Q_m}}{\partial t} = 3\int_0^1 \frac{\partial Q_m}{\partial t} \overline{r}^2 d\overline{r}, \tag{153}$$

and

$$\frac{\partial Q_m}{\partial t} = \frac{D_{cm}}{r_c^2}\frac{\partial^2 Q_m}{\partial \bar{r}^2} + \frac{2D_{cm}}{r_c^2 \bar{r}}\frac{\partial Q_m}{\partial \bar{r}} + \frac{q_{0m}}{\bar{r}_c^2}\frac{\partial D_{cm}}{\partial Q_m}\left(\frac{\partial Q_m}{\partial \bar{r}}\right)^2 , \tag{154}$$

where the concentration dependence of the micropore diffusivity is given by Darken's equation, which leads to

$$D_{cm} = \frac{D_{0m}}{\left(1 - \frac{b_m Q_m q_{0m}}{a_m}\right)} \tag{155}$$

for the Langmuir isotherm, and

$$D_{cm} = \frac{D_{0m}}{\sqrt{b_{1m}^2 - 4b_{2m}[b_{0m} - \ln(Q_m q_{0m})]}} \tag{156}$$

for the modified Dubinin-Polyani isotherm. The partial derivatives are:

$$\frac{\partial D_{cm}}{\partial Q_m} = \frac{q_{0m} b_m D_{0m}}{a_m\left(1 - \frac{b_m Q_m q_{0m}}{a_m}\right)^2} \tag{157}$$

and

$$\frac{\partial D_{cm}}{\partial Q_m} = \frac{2b_{2m} D_{0m}}{Q_m}\left\{b_{1m}^2 - 4b_{2m}[b_{0m} - \ln(Q_m q_{0m})]\right\}^{-1.5} \tag{158}$$

for the Langmuir and modified Dubinin-Polyani isotherms, respectively. The surface of each zeolite crystal is in equilibrium with the liquid concentration in the pore at each point across the particle radius. Since the film mass transfer is insignificant, $C_{dm} = C_{pm}$ at $\bar{R} = 1$. Because of symmetry,

The initial conditions are:

$$\frac{\partial C_{pm}}{\partial \bar{R}} = \frac{\partial \overline{Q_m}}{\partial \bar{R}} = \frac{\partial Q_m}{\partial \bar{r}} = 0 \ at \ \bar{R} = 0, \ \bar{r} = 0. \tag{159}$$

$$C_{dm} = 1, \ C_{pm} = C_{sm} = Q_m = 0 \quad at \ t = 0. \tag{160}$$

Equations 148 to 160 are transformed to ODEs by applying orthogonal collocation using the trial functions for a symmetrical system as described in Appendix D. The mass-transfer equation inside the zeolite crystal becomes:

$$\frac{dQ_{mjk}}{dt} = \frac{D_{cm}}{r_c^2}\sum_{l=1}^{MC} B_{jl}^r Q_{mlk} + \frac{q_{0m}}{r_c^2}\left(\sum_{l=1}^{MC} A_{jl}^r Q_{mlk}\right)^2, \tag{161}$$

for j = 1 to MC and k = 1 to PC. Equations 155 through 158 are used to define the concentration dependence of D_c. The subscriptions in Equation 161 are defined as: m is the component, j is the collocation point along the zeolite crystal radius, and k is the collocation point along the particle radius. MC and PC are the number of collocation points for the zeolite crystal and particle, respectively. The average concentration in each zeolite crystal is given by:

$$\frac{d\overline{Q_{mk}}}{dt} = 3\sum_{j=1}^{MC} W_j \frac{dQ_{mjk}}{dt} \tag{162}$$

for each collocation point across the particle radius, that is, k=1 to PC. The macropore mass-transfer equation becomes:

$$\frac{dC_{pmk}}{dt} = \frac{D_{lm}}{\tau R_p^2}\sum_{j=1}^{PC} B_{kj}C_{pmj} + \frac{D_{sm}}{\xi_m R_p^2}\sum_{j=1}^{PC} B_{kj}Q_{mMCj}$$

$$+ \frac{q\xi_m}{\xi_m R_p^2}\frac{\partial D_s}{\partial Q_{mMCk}}\left(\sum_{j=1}^{PC} A_{kj}Q_{mMCj}\right)^2 - \frac{1}{\xi_m}\frac{d\overline{Q_{mk}}}{dt}, \tag{163}$$

where k = 1 to PC - 1. The overall mass balance yields an equation for the bulk solution concentration as a function of time:

$$\frac{dC_{dm}}{dt} = \frac{\frac{-3\varepsilon_p(1-\varepsilon)}{\varepsilon}\left(\sum_{i=1}^{PC}\frac{W_i^r}{\xi_m}\frac{d\overline{Q_{mi}}}{dt} + \sum_{i=1}^{PC-1} W_i^r\frac{dC_{pmi}}{dt}\right)}{1 + \frac{3\varepsilon_p(1-\varepsilon)}{\varepsilon}W_{PC}^r}. \tag{164}$$

The boundary condition given in Equation 140 is met by the selection of a symmetrical system. The system of equations are solved similarly to those described in Section E.5.

Appendix F. FIXED-BED ION-EXCHANGE COLUMN MODEL

A model that describes the behavior of packed beds of zeolite is illustrated in Figure F.1. It is assumed that the fluid phase containing the components to be sorbed enters the bed at the top and exits from the bottom of the column. It is also assumed that axial dispersion is negligible for the LBC and concentration gradients exist only in the axial direction. Since axial dispersion could be significant for the SBC, the model was developed assuming mass-transfer effects due to macropore and micropore intraparticle diffusion, liquid film diffusion, and axial dispersion. The equations are derived in detail for the heterogenous parallel diffusion model were the diffusivities are assumed to be independent of concentration.

The development of the mathematical model for ion exchange columns is similar to that of the batch system described in Section 7.2.1 except that the concentrations now change in axial direction as well as in the radial direction (Friedman, 1984). Mass balances performed on each solute m leads to the following relationship for mass transfer in the axial direction:

$$D_z \frac{\partial^2 c_{dm}}{\partial z^2} = \upsilon \frac{\partial c_{dm}}{\partial z} + \frac{\partial c_{fm}}{\partial t} + \frac{3\,(1-\varepsilon)\,k_{fm}}{\varepsilon R_p}(c_{dm} - c_{sm})\,. \tag{165}$$

The solid mass balance is given:

$$\frac{\varepsilon_p}{\rho}\frac{\partial c_{pm}}{\partial t} + \frac{\partial q_m}{\partial t} = \frac{1}{R^2}\frac{\partial}{\partial R}\left[R^2\left(D_{cm}\frac{\partial q_m}{\partial R} + \frac{\varepsilon_p D_{pm}}{\rho}\frac{\partial c_{pm}}{\partial R}\right)\right]. \tag{166}$$

The boundary conditions in the radial direction are given by:

$$\frac{\partial c_{pm}}{\partial R} = \frac{\partial q_m}{\partial R} = 0 \quad at\ R = 0\,, \tag{167}$$

and

$$\frac{\partial}{\partial t}\int_0^{R_p}(q_m + \frac{\varepsilon_p}{\rho}c_{pm})R^2 dR = \frac{k_{fm}R_p^2}{\rho}(c_{dm} - c_{sm})\,. \tag{168}$$

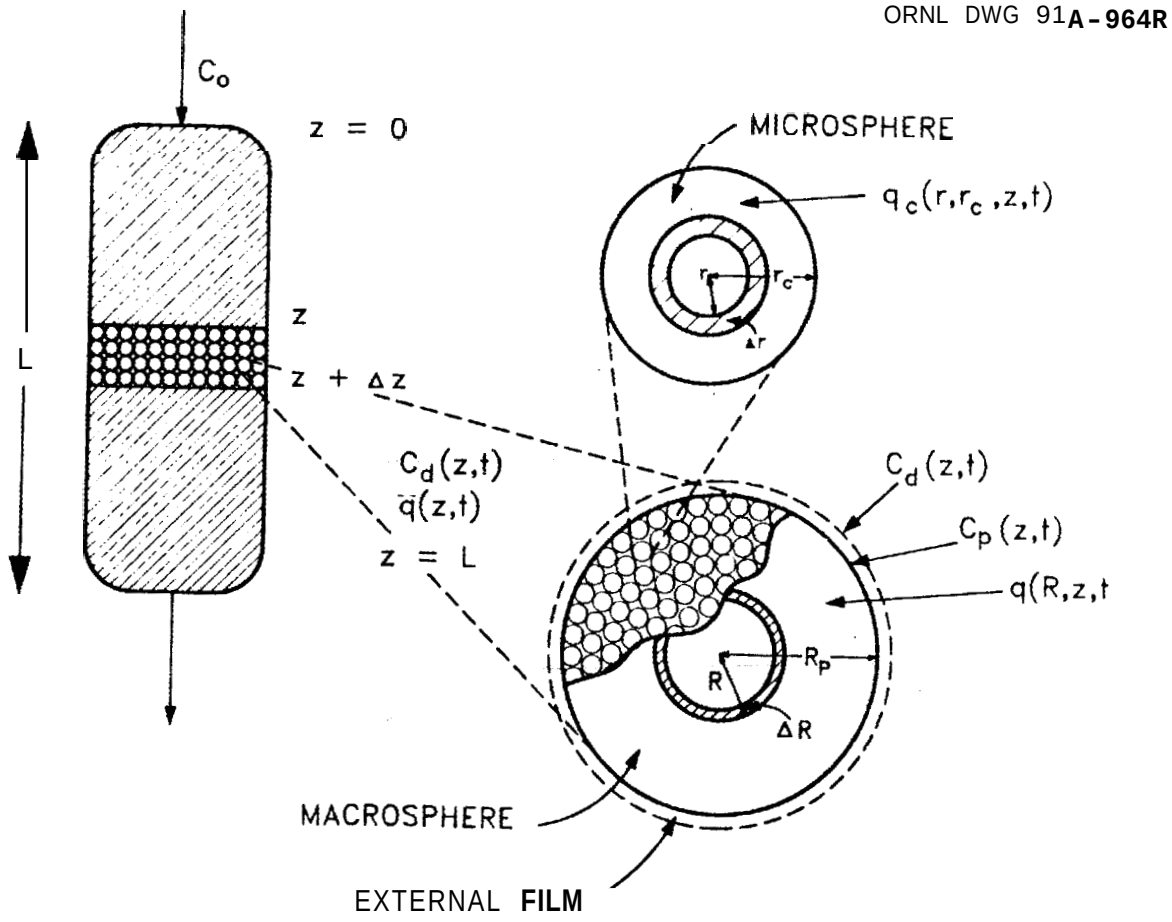

Figure F.1. Schematic representation of fixed-bed adsorption column models with the film, macropore, and micropore diffusion.

The boundary conditions in the axial direction are given by:

$$c_{dm} = c_{0m} + \frac{D_z}{v}\frac{\partial c_{dm}}{\partial z} \quad at\ z = 0 \tag{169}$$

and

$$\frac{\partial c_{dm}}{\partial z} = 0 \quad at\ z = L. \tag{170}$$

The initial conditions are:

$$c_{dm} = c_{pm} = c_{sm} = q_m = 0 \quad at\ t = 0,\ z > 0. \tag{171}$$

Equations 165 through 171 can be rewritten in dimensionless form by letting $C = c/c_0$, $Q = q/q_0$, $Z = z/L$, $\bar{t} = tv/L$ and $\bar{R} = R/R_p$ where q_0 is in equilibrium with c_0:

$$\frac{1}{Pe}\frac{\partial^2 C_{dm}}{\partial Z^2} = \frac{\partial C_{dm}}{\partial Z} + \frac{\partial C_{dm}}{\partial \bar{t}} + 3\ St\ (C_{dm} - C_{sm}), \tag{172}$$

$$\xi_m \frac{\partial C_{pm}}{\partial \bar{t}} + \frac{\partial Q_m}{\partial \bar{t}} = \frac{t_c D_{cm}}{R_p^2}\nabla^2 Q_m + \frac{t_c \xi_m D_{pm}}{R_p^2}\nabla^2 C_{pm}, \tag{173}$$

$$\frac{\partial C_{pm}}{\partial \bar{R}} = \frac{\partial Q_m}{\partial \bar{R}} = 0 \quad at\ \bar{R} = 0, \tag{174}$$

$$\frac{\partial}{\partial \bar{t}}\int_0^1 (Q_m + \xi_m C_{pm})\,\bar{R}^2 d\bar{R} =$$

$$\frac{t_c k_{gm}}{(1 - \varepsilon_p) D_{gm}} (C_{dm} - C_{sm}) \quad at\ \bar{R} = 1, \tag{175}$$

$$C_{dm} = 1 + \frac{1}{Pe}\frac{\partial C_{dm}}{\partial Z} \quad at\ Z = 0, \tag{176}$$

$$\frac{\partial C_{dm}}{\partial Z} = 0 \quad at\ Z = 1, \tag{177}$$

and

$$C_{dm} = C_{pm} = C_{sm} = Q_m = 0 \quad at\ \bar{t} = 0,\ Z > 0. \tag{178}$$

The application of orthogonal collocation to an ion exchange column leads to a series of ODEs that are dependent of the axial and radial location in the column. Figure F.2 gives a sample grid of the orthogonal collocation points which result from two internal collocation points in both the axial and radial directions. There are NC collocation points in the axial direction where NC is equal to the number of internal axial collocation points plus the two boundary points at the entrance and exit of the column. These points are located at the roots of the asymmetrical Jacobi polynomial trial function with a weighting factor of one as described in Appendix D. There are PC collocation point in the radial direction where PC is equal to the number of internal radial collocation points plus the boundary point at the particle surface. These points are located at the roots of the symmetrical Jacobi polynomial trial function with a weighting function of

$(1-r^2)$.

The application of orthogonal collocation to Equations 165 through 170 produces the following set of ODEs:

$$\frac{dC_{dml}}{d\bar{t}} = \sum_{k=1}^{NC}\left(\frac{B_{lk}^{z}}{Pe} - A_{lk}^{z}\right)C_{dmk} - 3St\,(C_{dm} - C_{sm}) \tag{179}$$

for l = 2 to NC-1 in the axial direction,

ORNL DWG 92A-26R

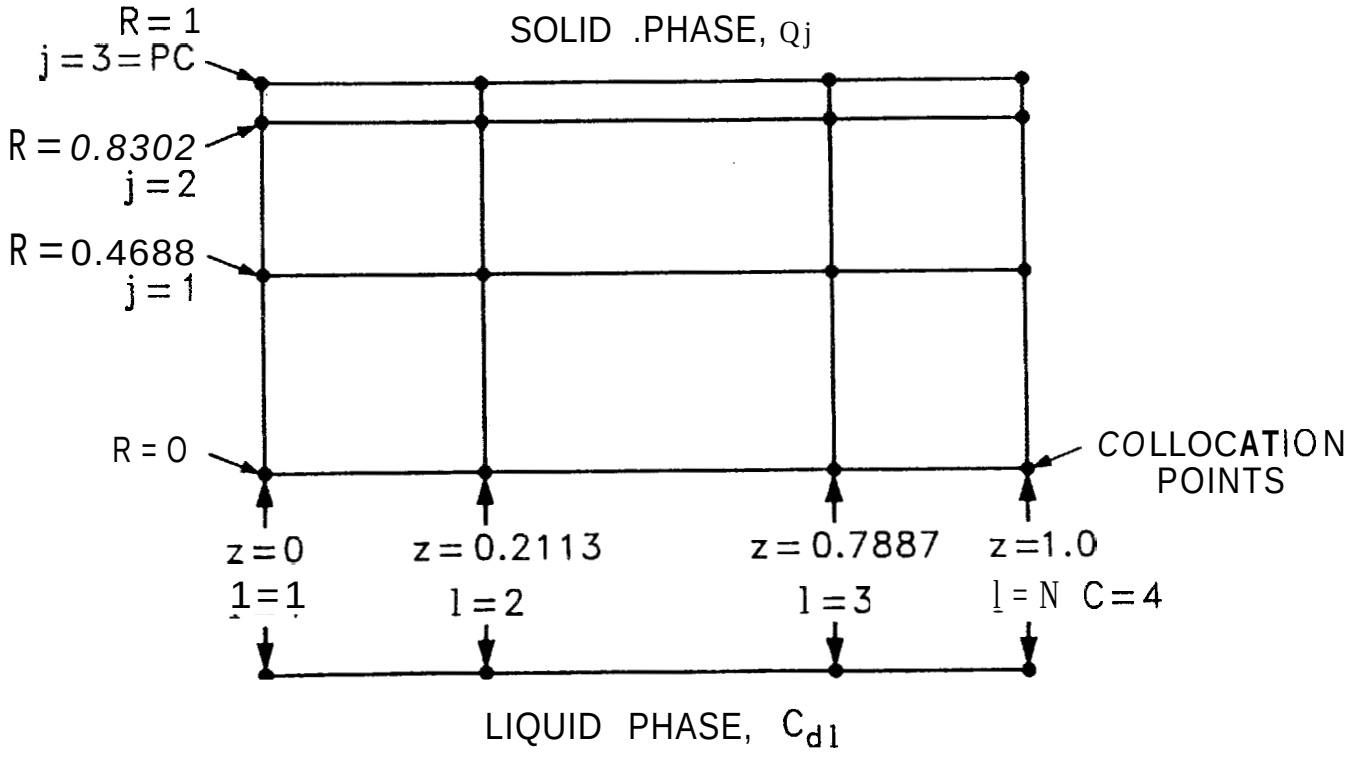

Figure F.2. Location of orthogonal collocation points in the axial and radial directions for two internal points.

$$\frac{d(\xi_m C_{pmlj} + Q_{mlj})}{d\bar{t}} =$$

$$\frac{t_c D_{cm}}{R_p^2}\sum_{i=1}^{PC} B_{ji}^r Q_{mli} + \frac{t_c \xi_m D_{pm}}{R_p^2}\sum_{i=1}^{PC} B_{ji}^r C_{pmli} \tag{180}$$

where j = 1 to PC-1 in the radial direction and l = 2 to NC in the axial direction,

$$\frac{d\,(Q_{mlPC} + \xi_m C_{pmlPC})}{d\bar{t}} = \frac{t_c k_{gm}}{(1 - \varepsilon_p) D_{gm} W_{PC}^r}(C_{dml} - C_{sml})$$

$$-\sum_{i=1}^{PC-1} \frac{W_i^r}{W_{PC}^r}\,\frac{d(Q_{mli} + \xi_m C_{pmli})}{d\bar{t}} \tag{181}$$

where $C_{pmlPC} = C_{sml}$ and l = 2 to NC,

$$\sum_{k=1}^{NC} A_{1k}^z C_{dmk} = Pe(C_{dm1} - 1), \tag{182}$$

and

$$\sum_{k=1}^{NC} A_{NCk}^z C_{dmk} = 0. \tag{183}$$

C_{pmlj} is a function of Q_{mlj} as defined by the equilibrium equation for all collocation points. The boundary condition given in Equation 175 is automatically satisfied because of the symmetric Legendre polynomials.

Equations 179, 182, and 183 can be combined into one equation in which C_{dm1} and C_{dmNC} are eliminated. The resulting equation, Equation 180, Equation 181, and the equilibrium equation represent a set of m(2PC+1)(NC-1) nonlinear algebraic and ODEs which can be solved for the m(2PC+1)(NC-1) unknowns in a manner similar to that discussed in Appendix E.

Appendix G. COMPUTER PROGRAMS

The models derived in Section 7 were converted to ODEs using orthogonal collocation in Appendixes E and F. The resulting sets of nonlinear algebraic equations and ODEs where solved using a program written in Fortran IV language and run on a VAX computer system at ORNL. The program for the numerical method includes four major parts: (1) main program for the input, output, and the definition of the normalized terms; (2) subroutines for the orthogonal collocation procedure; (3) a subroutine for the calculation of equilibrium; and (4) subroutines for solving ODEs.

The set of ordinary differential equations were solved using the August 13, 1981, version of Livermore Solver for Ordinary Differential Equations (LSODE). LSODE is a public domain software package which is based on the Gear's Stiff integration algorithm (Hindmarsh, 1980). A listing of an example computer code is given in this Appendix.

```
C*****************************************************************
C                              DCDP.FOR
C*****************************************************************
C     THIS PROGRAM SOLVES FIRST ORDER PDE'S FOR ION EXCHANGE IN
C     ZEOLITES FOR BATCH REACTORS WITH SERIES PORE AND
C     INTRACTRYSTALLINE MASS TRANSFER WHERE CRYSTAL DIFFUSIVITY
C     IS A FUNCTION OF SOLIDS CONCENTRATION AND PORE DIFFUSIVITY
C     IS DUE TO LIQUID & SURFACE MASS TRANSFER IN PARALLEL
C *
C     PDES ARE CONVERTED TO ODES BY ORTHOGONAL COLLOCATION.
C     COLLOCATION POINTS ARE CALCULATED BY SUBROUTINES FROM
C     MICHELSON AND VILLASEN AND FINLAYSON (COLLOC.FOR FILE)
C *
C     ODES ARE IN SUBROUTINE DERIVS (DPDERIVMS.FOR FILE)
C *
C     LSODE SUBROUTINE IS USED TO SOLVE THE RESULTING ODE'S
C *
C     LANGMUIR ISOTHERM (EQDCDPMS.FOR FILE) IS USED FOR
C    SINGLE COMPONENT SYSTEMS.  MODIFIED DUBININ-POLAYNI ISOTHERM
C     (EPDCDPMM.FOR FILE) IS USED FOR MULTICOMPONENT SYSTEMS.
C *
C     INPUT DATA IN IS DCDPMS.DAT; OUTPUT DATA IS IN OUTDCDPMS.DAT
C *
C     TO RUN PROGRAM ON ORNL SCIENCIFIC AND TECHNICAL COMPUTING
C     VAX, USE "FOR", "LINK", AND "RUN" COMMANDS WHERE "LINK" IS:
C      LINK DCDP,DPDERIVMS,COLLOC,EQDCDPMS,SYS$LIBRARY:CORLIB/LIB
C *
C*****************************************************************
C*****************************************************************
C     VOL=VOLUME SOLUTION, ML
C     GRMS=SORBENT ADDED, GR
C     ROB=SORBENT DENSITY, GR/ML
C     RADC=ZEOLITE CRYSTAL RADIUS, CM
C     RAD=PARTICLE RADIUS, CM
C     EPSP=PARTICLE VOID FRACTION
C     DC=CORRECTED ZEOLITE CRYSTAL DIFFUSIVITY, CM^2/S
C     DL=MOLECULAR DIFFUSIVITY/TOROUSITY FACTOR, CM^2/S
C     DS=CORRECTED SURFACE DIFFUSIVITY, CM^2/S
C     CF=FEED CONCENTRATION, MEQ/ML
C     C0=INITIAL CONCENTRATION, MEQ/ML
C     CREF=REFERENCE CONCENTRATION, MEQ/ML
C     TSTEP=RUN TIME, SEC
C     TDISP=OUTPUT TIME INCREMENT, SEC
C     N=NUMBER OF COLLOCATION POINTS ACROSS PARTICLE RADIUS
C     M=NUMBER OF COLLOCATION POINTS ACROSS CRYSTAL RADIUS
C     NCOMP=NUMBER OF COMPONENTS WHERE:
C         1 FOR Sr       2 FOR Cs       3 FOR Ca        4 FOR Mg
C*****************************************************************
      IMPLICIT REAL*8 (A-H,O-Z)
      COMMON/LAGR/EL1(800,800),EL2(800,800),NT,N,Y(50000),ROB,RADC,
     CRAD,DC(4),Q0(4),NCOMP,W(800),CREF(4),DP(800),XI(4),
     CEPSS,EPSP,Y0(800),EC1(800,800),EC2(800,800),MT,M,WC(800),
     CQSTAR(800),QBAR(800),QBARR(800),DL(4),DS(4)
      DIMENSIONDIF1(800),DIF2(800),DIF3(800),ROOT(800),VECT(800),
```

```
      CAKF(4),DIFC1(800),DIFC2(800),DIFC3(800),ROOTC(800),VECTC(800)
      C,SROOTC(800),TEMP(800),TEMP0(800),
      CYOUT(4),QAVG(4),CMAX(4),CMAXN(4),XOUT1(4),XOUT2(4),XOUT3(4)
      C0(4),CF(4),SROOT(800),RWORK(80000),IWORK(2000),XOUT(4)
       EXTERNAL F,JAC
C
C
C      INPUT PARAMETERS
C
       OPEN(UNIT=5,FILE='DCDPMS.DAT', STATUS='OLD')
       REWIND 5
       READ(5,601)CHAR1,CHAR2,CHAR3,CHAR4,CHAR5,CHAR6,CHAR7
 601   FORMAT(X,7A5)
       READ(5,*) NCOMP,AKF(1),AKF(2),AKF(3),AKF(4),DC(1),DC(2)
       READ(5,*) DC(3),DC(4),DS(1),DS(2),DS(3),DS(4),DL(1),DL(2)
       READ(5,*) DL(3),DL(4),GRMS,VOL,ROB
       READ(5,*) RADC,RAD,EPSP
       READ(5,*) CF(1),CF(2),CF(3),CF(4),C0(1),C0(2),C0(3),C0(4)
       READ(5,*) CREF(1),CREF(2),CREF(3),CREF(4)
       READ(5,*) TSTEP
       READ(5,*) N,M
       READ(5,*) TDISP
       OPEN(UNIT=6,FILE='OUTDCDPMS.DAT', STATUS='NEW')
       WRITE(6,602)CHAR1,CHAR2,CHAR3,CHAR4,CHAR5,CHAR6,CHAR7
 602   FORMAT(X,7A5)
C      CALCULATE VOID FRACTION IN BATCH REACTOR
       EPSS=GRMS/VOL/ROB
C      DETERMINE COLLOCATION CONSTANTS FOR SYMMETRICAL SYSTEM
       A=3.0D0
       N0=0
       N1=1
       AL=1.D0
       BE=0.5D0
       NT=N+N0+N1
       MT=M+N0+N1
       NEQ=NCOMP*MT*NT
       CALL JCOBI (N,N0,N1,AL,BE,DIF1,DIF2,DIF3,ROOT)
       WRITE(6,114),MT,NT
 114   FORMAT(2I3,' COLLOCATION POINTS FOR CRYSTAL RADIUS
      C AND PARTICLE RADIUS, RESPECTIVELY')
       DO 200 I=1,NT
       SROOT(I)=DSQRT(ROOT(I))
 200   CONTINUE
       DO 10 J=1,NT
       DO 5 ID=1,2
       CALL DFOPR (N,N0,N1,J,ID,DIF1,DIF2,DIF3,ROOT,VECT)
       DO 5 I=1,NT
       IF(ID.EQ.1) EL1(J,I)=VECT(I)
       IF(ID.EQ.2) EL2(J,I)=VECT(I)
 5     CONTINUE
 10    CONTINUE
       DO 17 J=1,NT
       DO 15 I=1,NT
       EL2(J,I)=4.0D0*ROOT(J)*EL2(J,I)+2.D0*A*EL1(J,I)
```

```
      EL1(J,I)=2.0D0*DSQRT(ROOT(J))*EL1(J,I)
      CALL WEIGHT(N,N0,N1,A,SROOT,VECT)
      W(J)=VECT(J)

   15 CONTINUE
   17 CONTINUE
      CALL JCOBI (M,N0,N1,AL,BE,DIFC1,DIFC2,DIFC3,ROOTC)
      DO 300 I=1,MT
      SROOTC(I)=DSQRT(ROOTC(I))
  300 CONTINUE
      DO 310 J=1,MT
      DO 305 ID=1,2
      CALL DFOPR (M,N0,N1,J,ID,DIFC1,DIFC2,DIFC3,ROOTC,VECTC)
      DO 305 I=1,MT
      IF(ID.EQ.1) EC1(J,I)=VECTC(I)
      IF(ID.EQ.2) EC2(J,I)=VECTC(I)
  305 CONTINUE
  310 CONTINUE
      DO 317 J=1,MT
      DO 315 I=1,MT
      EC2(J,I)=4.0D0*ROOTC(J)*EC2(J,I)+2.D0*A*EC1(J,I)
      EC1(J,I)=2.0D0*DSQRT(ROOTC(J))*EC1(J,I)
      CALL WEIGHT(M,N0,N1,A,SROOTC,VECTC)
      WC(J)=VECTC(J)
  315 CONTINUE
  317 CONTINUE
C     ASSIGN BOUNDARY AND INITIAL CONDITIONS
      DO 21 I=1,NCOMP
      DO 21 J=1,NT
      TEMP(J+(I-1)*NT)=0.
   21 CONTINUE
      NN=0
      DO 22 K=1,NT
      DO 22 I=1,NCOMP
      NN=NN+1
      TEMP(NN)=CREF(I)
   22 CONTINUE
      CALL QEQUIL(TEMP,TEMP0)
      NN=0
      DO 23 K=1,NT
      DO 23 I=1,NCOMP
      NN=NN+1
      Q0(I)=TEMP0(NN)
   23 CONTINUE
      T=0.0D0
      MM=0
      BTOT=0.0
      DO 25 I=1,NCOMP
      DO 20 K=I,NT
      DO 20 J=1,MT
      MM=MM+1
   20 Y(MM)=C0(I)/Q0(I)
      Y(NCOMP*MT*(NT-1)+I*MT)=CF(I)/CREF(I)
      XI(I)=EPSP*CREF(I)/ROB/Q0(I)/(1-EPSP)
```

```
      BTOT=BTOT+CF(I)*VOL
 25   CONTINUE
C     WRITE OUT INITIAL CONDITIONS AND INPUT PARAMETERS
      WRITE(6,26) CF(1),CF(2),CF(3),CF(4),GRMS,VOL,RAD
 26   FORMAT(' CFs=',E12.4,' ',E12.4,' ',E12.4,' ',E12.4,/,' SOLIDS
     C (GMS)=',E12.4,' VOLUME (ML)=',E12.4,' RADIUS (CM)=',E12.4)
      WRITE(6,228) Q0(1),Q0(2),Q0(3),Q0(4)
 228  FORMAT(' Q0s=',E12.4,' ',E12.4,' ',E12.4,' ',E12.4)
      WRITE(6,226)AKF(1),AKF(2),AKF(3),AKF(4),
     CDC(1),DC(2),DC(3),DC(4)
     C,DS(1),DS(2),DS(3),DS(4),DL(1),DL(2),DL(3),DL(4)
 226  FORMAT(' KFs= ',4D10.3,/,' DCs= ',4D10.3,/,' DSs=',4D10.3
     C,/,' DL/Ts=',4D10.3)
      WRITE(6,124)
 124  FORMAT(/,' TIME, MIN                NORMALIZED SOLUTION
     CCONCENTRATIONS')
      WRITE(6,227)TOUT,Y(NCOMP*MT*(NT-1)+MT),Y(NCOMP*MT*
     C(NT-1)+2*MT),Y(NCOMP*MT*(NT-1)+3*MT),Y(NCOMP*MT
     C*(NT-1)+4*MT)
 227  FORMAT(F12.4,' ',E12.4,' ',E12.4,' ',E12.4,' ',E12.4)
      ENDT=TDISP
      IFLAG=0
C     SET PARAMETERS FOR LSODE TO SOLVE ODEs IN DERIVS SUBROUTINE
      MF=22
      RTOL=1.0D-5
      ATOL=1.0D-5
      ITOL=1
      ITASK=1
      ISTATE=1
      IOPT=1
      LRW=80000
      LIW=2000
      DO 31 L=5,10
      RWORK(L)=0.0
      IWORK(L)=0
 31   CONTINUE
      IWORK(6)=500
 30   CONTINUE
      IF(ENDT.LT.TSTEP.OR.IFLAG.EQ.1) GOTO 35
      ENDT=TSTEP
      IFLAG=1
 35   CONTINUE
      CALL LSODE (F,NEQ,Y,T,ENDT,ITOL,RTOL,ATOL,ITASK,ISTATE,IOPT,
     CRWORK,LRW,IWORK,LIW,JAC,MF)
C     PRINT OUT RESULTS
      DO 37 J=1,NCOMP
      XOUT(J)=Y(NCOMP*MT*(NT-1)+J*MT)
      XOUT1(J)=Y(NCOMP*MT*(NT-2)+J*MT)
      XOUT2(J)=Y(NCOMP*MT*(NT-3)+J*MT)
      XOUT3(J)=Y(NCOMP*MT*(NT-4)+J*MT)
 37   CONTINUE
      TOUT=T/60.
      WRITE(6,40)TOUT,XOUT(1),XOUT(2),XOUT(3),XOUT(4)
 40   FORMAT(/,F12.4,' ',E12.4,' ',E12.4,' ',E12.4,' ',E12.4)
```

```
      IF(ISTATE.LT.0) GOTO 80
      GOTO 90
   80 WRITE(6,85) ISTATE
   85 FORMAT(' ERROR IN LSODE.  ISTATE= ',I3)
      GOTO 510
   90 CONTINUE
      IF(IOUTF.EQ.1) WRITE(5,*)T,XOUT1,XOUT2
      ENDT=ENDT+TDISP
      IF(T.GE.TSTEP) GOTO 510
      IF(IFLAG.EQ.1) GOTO 510
      GOTO 30
  510 CONTINUE
      END
C
C     SUBROUTINES TO CALCULATE DERIVATIVES OF ODES
C
      SUBROUTINE  F (NEQ,T,Y,YDOT)
      IMPLICIT REAL*8 (A-H,O-Z)
      DIMENSION Y(80),YDOT(80)
      CALL DERIVS (NEQ,T,Y,YDOT)
      RETURN
      END
C
C     DUMMY SUBROUTINE NEEDED FOR LSODE WHEN MF=22
      SUBROUTINE JAC (NEQ,T,Y,ML,MU,PD,NROWPD)
      IMPLICIT REAL*8 (A-H,O-Z)
      DIMENSION Y(NEQ),PD(NROWPD,NEQ)
      RETURN
      END
C
C
C
C     SUBROUTINE CONTAINING ODES
C
      SUBROUTINE  DERIVS (NEQ,X,V,YP)
      IMPLICIT REAL*8 (A-H,O-Z)
      COMMON/LAGR/EL1(800,800),EL2(800,800),NT,N,Y(50000),
     1ROB,RADC,RAD,DC(4),Q0(4),NCOMP,W(800),CREF(4),DP(800),XI(4),
     2EPSS,EPSP,Y0(800),EC1(800,800),EC2(800,800),MT,M,WC(800)
     3,QSTAR(800),QBAR(800),QBARR(800),dl(4),ds(4)
      DIMENSION V(50000),YP(50000),CSTAR(800),YSUM(800),WW(800),
     CCSUM(50000),COEF(800),XSUM(800),KFLAG(4),TEST(4),ASUM(800),
     CDSTAR(800),Q(800),BSUM(800),YTEMPC(50000),DSUM(50000),
     CZSUM(800),DA(4),DB(4),DCC(4),VSUM(800),YTEMPS(800)
C     SET MAXIMUM ZEOLITE LOADING CAPACITY
      DCC(1)=2.86D0
      DCC(2)=3.35D0
      DCC(3)=2.86D0
      DCC(4)=2.86D0
      NN=0
C     DETERMINE EQUILIBRIUM VALUES AT PARTICLE AND PORE SURFACES
      DO 2 K=1,NT
      DO 2 I=1,NCOMP
      NN=NN+1
```

```
      CSTAR(NN)=V(NN*MT)*CREF(I)
    2 CONTINUE
      CALL QEQUIL (CSTAR,QSTAR)
      NN=0
      DO 3 K=1,NT
      DO 3 I=1,NCOMP
      NN=NN+1
      QSTAR(NN)=QSTAR(NN)/Q0(I)
    3 CONTINUE
C     CALCULATE MICROPORE ODES
      JJ=0
      KK=0
      DO 20 K=1,NT
      DO 20 I=1,NCOMP
      KK=KK+1
      DO 19 J=1,MT
      JJ=JJ+1
      CSUM(JJ)=0.D0
      DSUM(JJ)=0.D0
      DO 15 L=1,M
      ITEMP1=(K-1)*NCOMP*MT+(I-1)*MT
      CSUM(JJ)=CSUM(JJ)+EC2(J,L)*V(ITEMP1+L)
      DSUM(JJ)=DSUM(JJ)+EC1(J,L)*V(ITEMP1+L)
   15 CONTINUE
      CSUM(JJ)=CSUM(JJ)+EC2(J,mt)*QSTAR(KK)
      DSUM(JJ)=DSUM(JJ)+EC1(J,mt)*QSTAR(KK)
      YTEMPC(JJ)=1.D0-V(JJ)*Q0(I)/DCC(I)
      YP(JJ)=DC(I)/RADC/RADC/YTEMPC(JJ)*(CSUM(JJ)+1.D0/YTEMPC(JJ)*
     CDSUM(JJ)*DSUM(JJ))
   19 CONTINUE
      DSTAR(KK)=YP(JJ)
C     YP(JJ) IS TEMPORARILY USED
   20 CONTINUE
C     CALCULATE AVERAGE ZEOLITE CRYSTAL CONCENTRATIONS AND
C     COORSPONDING ODES
      KKK=0
      NNN=0
      DO 22 K=1,NT
      DO 22 I=1,NCOMP
      NNN=NNN+1
      ASUM(NNN)=0.0
      YSUM(NNN)=0.0
      DO 21 J=1,M
      KKK=KKK+1
      ASUM(NNN)=ASUM(NNN)+WC(J)*V(KKK)
      YSUM(NNN)=YSUM(NNN)+WC(J)*YP(KKK)
   21 CONTINUE
      YSUM(NNN)=YSUM(NNN)+WC(mt)*dstar(NNN)
      ASUM(NNN)=ASUM(NNN)+WC(MT)*QSTAR(NNN)
      KKK=KKK+1
      Q(NNN)=3.D0*YSUM(NNN)
      QBAR(NNN)=3.D0*ASUM(NNN)
   22 CONTINUE
      NQ=NT-1
```

```
      II=0
      DO 60 I=1,NCOMP
      DO 30 J=1,NQ
      VSUM(J)=0.D0
      XSUM(J)=0.D0
      ZSUM(J)=0.D0
 30   CONTINUE
      WW(I)=0.0D0
      BSUM(I)=0.D0
      DO 50 J=1,NQ
      II=II+1
      DO 40 K=1,NT
      KK=KK+1
      ZSUM(J)=ZSUM(J)+EL1(J,K)*QSTAR(((K-1)*NCOMP*MT+I*MT)/MT)
      XSUM(J)=XSUM(J)+EL2(J,K)*QSTAR(((K-1)*NCOMP*MT+I*MT)/MT)
      VSUM(J)=VSUM(J)+EL2(J,K)*V((K-1)*NCOMP*MT+I*MT)
 40   CONTINUE
C     CALCULATE MACROPORE ODES
      ITEMP3=(J-1)*NCOMP*MT+I*MT
      YTEMPS(J)=1.D0-QSTAR(ITEMP3/MT)*Q0(I)/DCC(I)
      YP(ITEMP3)=(DL(I)*VSUM(J)+DS(I)/XI(I)*XSUM(J)/YTEMPS(J)
     C+DS(I)*ZSUM(J)**2/XI(I)/YTEMPS(J)**2)/RAD/RAD
     C-Q(ITEMP3/MT)/XI(I)
C     CALCULATE BULK SOLUTION CONCENTRATION FROM BOUNDARY MASS
C     BALANCE
      WW(I)=WW(I)+W(J)*(Q(ITEMP3/MT)/XI(I)+YP((J-1)*
     CNCOMP*MT+I*MT))
      BSUM(I)=BSUM(I)+W(J)*(QBAR(ITEMP3/MT)*(1.0D0-EPSP)+V((J-1)*
     CNCOMP*MT+I*MT)*EPSP*CREF(I)/Q0(I))
 50   CONTINUE
      YP((NT-1)*NCOMP*MT+I*MT)=-3.D0*EPSP*EPSS*(WW(I)+
     CQ(((NT-1)*NCOMP*MT+I*MT)/MT)/XI(I)*W(NT))/
     C(1.D0+3.D0*EPSP*EPSS*W(NT))
      QBARR(I)=3.D0*(BSUM(I)+W(NT)*(QBAR(((NT-1)
     C*NCOMP*MT+I*MT)/MT)*
     C(1.D0-EPSP)+V((NT-1)*NCOMP*MT+I*MT)*EPSP*CREF(I)/Q0(I)))
      II=II+1
 60   CONTINUE
      RETURN
      END
C
C
C
C     SUBROUTINE FOR BINARY EQUILIBRIUM EQUATIONS
C     LANGMUIR MODEL
C
      SUBROUTINE QEQUIL (X,Q)
      IMPLICIT REAL*8 (A-H,O-Z)
      COMMON/LAGR/EL1(800,800),EL2(800,800),NT,N,Y(50000),ROB,
     CRADC,RAD,DC(4),Q0(4),NCOMP,W(800),CREF(4),DP(800),XI(4)
     C,EPSS,EPSP,Y0(800),EC1(800,800),EC2(800,800),MT,M,WC(800),
     CQSTAR(800),QBAR(800),QBARR(800),ds(4),dl(4)
      DIMENSION X(800),Q(800),A(4),B(4),C(4)
C
```

```
C     SUBROUTINE CALCULATES QSTAR GIVEN C FROM THE
C     EQUILIBRIUM ISOTHERM
      A(1)=173702.D0
      B(1)=98176.D0
      A(2)=157009.D0
      B(2)=68574.D0
      A(3)=456942.D0
      B(3)=221015.D0
      A(4)=481696.D0
      B(4)=610790.D0
      DO 10 J=1,NT
      DO 10 K=1,NCOMP
      Q((J-1)*NT+K)=A(K)*X((J-1)*NT+K)/(1.D0+B(K)*X((J-1)*NT+K))
   10 CONTINUE
      RETURN
      END
C
      SUBROUTINE CEQUIL (Q,C)
      IMPLICIT REAL*8 (A-H,O-Z)
      COMMON/LAGR/EL1(800,800),EL2(800,800),NT,N,Y(50000),ROB,
     CRADC,RAD,DC(4),Q0(4),NCOMP,W(800),CREF(4),DP(4),XI(4)
     C,EPSS,EPSP,Y0(800),EC1(800,800),EC2(800,800),MT,M,WC(800),
     CQSTAR(800),QBAR(800),QBARR(800)
      DIMENSION X(800),Q(800),A(4),B(4),C(4)
C
C     SUBROUTINE CALCULATES CSTAR GIVEN Q FROM THE
C     EQUILIBRIUM ISOTHERM
      A(1)=173702.D0
      B(1)=98176.D0
      A(2)=157009.D0
      B(2)=68574.D0
      A(3)=456942.D0
      B(3)=221015.D0
      A(4)=481696.D0
      B(4)=610790.D0
      DO 5 J=1,NT
      DO 5 K=1,NCOMP
      IF(Q((J-1)*NT+K).LE.0.D0)Q((J-1)*NT+K)=1.D-12
    5 CONTINUE
      DO 10 J=1,NT
      DO 10 K=1,NCOMP
      X((J-1)*NT+K)=A(K)/Q((J-1)*NT+K)-B(K)
      C((J-1)*NT+K)=1.D0/X((J-1)*NT+K)
   10 CONTINUE
      RETURN
      END

      SUBROUTINE DEQUIL (X,DQ)
      IMPLICIT REAL*8 (A-H,O-Z)
      COMMON/LAGR/EL1(800,800),EL2(800,800),NT,N,Y(50000),ROB,
     CRADC,RAD,DC(4),Q0(4),NCOMP,W(800),CREF(4),DP(4),XI(4)
     C,EPSS,EPSP,Y0(800),EC1(800,800),EC2(800,800),MT,M,WC(800),
     CQSTAR(800),QBAR(800),QBARR(800)
      DIMENSION X(800),DQ(800),A(4),B(4),C(4)
```

```
C
C     SUBROUTINE CALCULATES DERIVATIVE OF QSTAR/DT FROM THE
C     EQUILIBRIUM ISOTHERM
      A(1)=173702.D0
      B(1)=98176.D0
      A(2)=157009.D0
      B(2)=68574.D0
      A(3)=456942.D0
      B(3)=221015.D0
      A(4)=481696.D0
      B(4)=610790.D0
      DO 10 J=1,NT
      DO 10 K=1,NCOMP
      DQ((J-1)*NT+K)=A(K)/(1.D0+B(K)*X((J-1)*NT+K))**2
   10 CONTINUE
      RETURN
      END
C
C
C
C     SUBROUTINE FOR MULTICOMPONENT EQUILIBRIUM EQUATIONS
C     MODIFIED DUBININ POLYANI MODEL FOR SR, CA, CS
C     LANGMUIR ISOTHERM MODEL FOR CS
C
      SUBROUTINE QEQUIL (X,Q)
      IMPLICIT REAL*8 (A-H,O-Z)
      COMMON/LAGR/EL1(800,800),EL2(800,800),NT,N,Y(50000),ROB,
     CRADC,RAD,DC(4),Q0(4),NCOMP,W(800),CREF(4),DP(4),XI(4),
     CEPSS,EPSP,Y0(800),EC1(800,800),EC2(800,800),MT,M,WC(800),
     CQSTAR(800)
      DIMENSION X(800),Q(800),A(4),B(4),C(4),XTEMP(800)
C
C     SUBROUTINE CALCULATES QSTAR GIVEN C FROM THE
C     EQUILIBRIUM ISOTHERM
      A(1)=-4.742D0
      B(1)=-1.157D0
      C(1)=-0.07507D0
      A(2)=-1.532D0
      B(2)=-0.589D0
      C(2)=-0.05002D0
      A(3)=-4.212D0
      B(3)=-0.856D0
      C(3)=-0.04703D0
      A(4)=-17.28D0
      B(4)=-3.345D0
      C(4)=-0.1818D0
      DO 10 J=1,NT
      DO 10 K=1,NCOMP
      XTEMP((J-1)*NCOMP+K)=X((J-1)*NCOMP+K)
      IF(X((J-1)*NCOMP+K).GT.0.D0) GOTO 7
      XTEMP((J-1)*NCOMP+K)=1.D-12
      IF(K.EQ.4)XTEMP((J-1)*NCOMP+K)=1.D-8
 7    Q((J-1)*NCOMP+K)=DEXP(A(K)+B(K)*DLOG(XTEMP((J-1)*NCOMP+K))+
     CC(K)*DLOG(XTEMP((J-1)*NCOMP+K))*DLOG(XTEMP((J-1)*NCOMP+K)))
```

```
      IF(K.NE.2)GOTO 10
      Q((J-1)*NCOMP+K)=54759.D0*XTEMP((J-1)*NCOMP+K)/(1.D0
     C+48758.D0*XTEMP((J-1)*NCOMP+K))
   10 CONTINUE
      RETURN
      END
C
      SUBROUTINE DEQUIL (X,DQ)
      IMPLICIT REAL*8 (A-H,O-Z)
      COMMON/LAGR/EL1(800,800),EL2(800,800),NT,N,Y(50000),ROB,
     CRADC,RAD,DC(4),Q0(4),NCOMP,W(800),CREF(4),DP(4),XI(4),
     CEPSS,EPSP,Y0(800),EC1(800,800),EC2(800,800),MT,M,WC(800),
     CQSTAR(800)
      DIMENSION X(800),DQ(800),A(4),B(4),C(4),XTEMP(800)
C     SUBROUTINE CALCULATES DQSTAR/DT GIVEN C FROM THE
C     EQUILIBRIUM ISOTHERM:
      A(1)=-4.742D0
      B(1)=-1.157D0
      C(1)=-0.07507D0
      A(2)=-1.532D0
      B(2)=-0.589D0
      C(2)=-0.05002D0
      A(3)=-4.212D0
      B(3)=-0.856D0
      C(3)=-0.04703D0
      A(4)=-17.28D0
      B(4)=-3.345D0
      C(4)=-0.1818D0
      DO 10 J=1,NT
      DO 10 K=1,NCOMP
      XTEMP((J-1)*NCOMP+K)=X((J-1)*NCOMP+K)
      IF(X((J-1)*NCOMP+K).GT.0.D0) GOTO 7
      XTEMP((J-1)*NCOMP+K)=1.D-12
      IF(K.EQ.4)XTEMP((J-1)*NCOMP+K)=1.D-8
 7    DQ((J-1)*NCOMP+K)=DEXP(A(K)+B(K)*
     CDLOG(XTEMP((J-1)*NCOMP+K))+
     CC(K)*DLOG(XTEMP((J-1)*NCOMP+K))*
     CDLOG(XTEMP((J-1)*NCOMP+K)))*(B(K)/
     CXTEMP((J-1)*NCOMP+K)+2.D0*C(K)*DLOG(XTEMP((J-1)*NCOMP+K))
     C/XTEMP((J-1)*NCOMP+K))
      IF(K.NE.2)GOTO 10
      DQ((J-1)*NCOMP+K)=54759.D0/(1.D0+48758.D0*
     CX((J-1)*NCOMP+K))**2
   10 CONTINUE
      RETURN
      END
C
C
C     ORTHOGONAL COLLOCATION SUBROUNTINES FROM VILLADSEN AND
C     MICHELSON (1978) AND FINLAYSON (1980)
C
C     SUBROUTINE JCOBI
C
C     EVALUATION OF ROOTS AND DERIVATIVES OF JACOBI POLYNOMIALS
```

```
C     P(N) (AL,BE).
C     FIRST EVALUATION OF COEFFICIENTS IN RECURSION FORMULA
C     RECURSION COEFFICIENTS ARE STORED IN DIF1 AND DIF2.
C     SUBROUTINE FROM MICHELSEN AND VILLADSEN, P. 418
C
      SUBROUTINE JCOBI(N,N0,N1,AL,BE,DIF1,DIF2,DIF3,ROOT)
      IMPLICIT REAL*8(A-H,O-Z)
      REAL*8 DIF1,DIF2,DIF3,ROOT
      DIMENSION DIF1(40),DIF2(40),DIF3(40),ROOT(40)
C
      AB=AL+BE
      AD=BE-AL
      AP=BE*AL
      DIF1(1)=(AD/(AB+2.D0)+1.D0)/2.D0
      DIF2(1)=0.0D0
      IF(N.LT.2) GO TO 15
      DO 10 I=2,N
      Z1=I-1.D0
      Z=AB+2.D0*Z1
      DIF1(I)=(AB*AD/Z/(Z+2.D0)+1.D0)/2.D0
      IF (I.NE.2) GO TO 11
      DIF2(I)=(AB+AP+Z1)/Z/Z/(Z+1.D0)
   11 Z=Z*Z
      Y=Z1*(AB+Z1)
      Y=Y*(AP+Y)
      DIF2(I)=Y/Z/(Z-1.D0)
   10 CONTINUE
   15 X=0.D0
      DO 20 I=1,N
   25 XD=0.0D0
      XN=1.0D0
      XD1=0.0D0
      XN1=0.0D0
      DO 30 J=1,N
      XP=(DIF1(J)-X)*XN-DIF2(J)*XD
      XP1=(DIF1(J)-X)*XN1-DIF2(J)*XD1-XN
      XD=XN
      XD1=XN1
      XN=XP
   30 XN1=XP1
      ZC=1.0D0
      Z=XN/XN1
      IF(I.EQ.1) GO TO 21
      DO 22 J=2,I
   22 ZC=ZC-Z/(X-ROOT(J-1))
   21 Z=Z/ZC
      X=X-Z
      IF(DABS(Z).GT.1.0D-12) GO TO 25
      ROOT(I)=X
      X=X+.0001D0
   20 CONTINUE
C
C     ADD INTERPOLATION POINTS AT X=0 AND X=1 IF REQUIRED
C
```

```
      NT=N+N0+N1
      IF(N0.EQ.0) GO TO 35
      DO 31 I=1,N
      J=N+1-I
   31 ROOT(J+1)=ROOT(J)
      ROOT(1)=0.D0
   35 IF(N1.EQ.1) ROOT(NT)=1.0
C
C     EVALUATE DERIVATIVES OF NODAL POLYNOMIAL
C
      DO 40 I=1,NT
      X=ROOT(I)
      DIF1(I)=1.D0
      DIF2(I)=0.D0
      DIF3(I)=0.D0
      DO 40 J=1,NT
      IF(J.EQ.I) GO TO 40
      Y=X-ROOT(J)
      DIF3(I)=Y*DIF3(I)+3.D0*DIF2(I)
      DIF2(I)=Y*DIF2(I)+2.D0*DIF1(I)
      DIF1(I)=Y*DIF1(I)
   40 CONTINUE
      RETURN
      END
C
C
C
C     SUBROUTINE DFOPR
C     FINDS DISCRETIZATION MATRICES AND GAUSSIAN QUADRATURE
C     WEIGHTS FOR GENERAL COLLOCATION APPROXIMATION
C     SUBROUTINE JCOBI MUST BE EXECUTED FIRST TO FIND ZEROS AND
C     DERIVATIVED OF NODAL POLYNOMIAL
C
      SUBROUTINE DFOPR (N,N0,N1,I,ID,DIF1,DIF2,DIF3,ROOT,VECT)
      IMPLICIT REAL*8 (A-H,O-Z)
      DIMENSION DIF1(40),DIF2(40),DIF3(40),ROOT(40),VECT(40)
C
C     GAUSSIAN WEIGHTS NORMALIZED TO SUM 1
C     ID=1 :        DISCRETIZATION MATRIX FOR Y'(X)
C     ID=2 :        DISCRETIZATION MATRIX FOR Y''(X)
C     ID=3 :        GAUSSIAN QUADRATURE WEIGHTS
C     VECT=   COMPUTED DIFFERENTIATION WEIGHTS
C
      NT=N+N0+N1
      IF(ID.EQ.3) GOTO 10
      DO 20 J=1,NT
      IF(J.NE.I) GOTO 21
      IF(ID.NE.1) GOTO 5
      VECT(I)=DIF2(I)/DIF1(I)/2.D0
      GOTO 20
 5    VECT(I)=DIF3(I)/DIF1(I)/3.D0
      GOTO 20
 21   Y=ROOT(I)-ROOT(J)
      VECT(J)=DIF1(I)/DIF1(J)/Y
```

```
      IF(ID.EQ.2) VECT(J)=VECT(J)*(DIF2(I)/DIF1(I)-2.D0/Y)
 20   CONTINUE
      GOTO 50
 10   Y=0.D0
      DO 25 J=1,NT
      X=ROOT(J)
      AX=X*(1.D0-X)
      IF (N0.EQ.0) AX=AX/X/X
      IF (N1.EQ.0) AX=AX/(1.D0-X)/(1.D0-X)
      VECT(J)=AX/DIF1(J)**2
 25   Y=Y+VECT(J)
      DO 60 J=1,NT
 60   VECT(J)=VECT(J)/Y
 50   RETURN
      END
C
C
C
C     SUBROUTINE WEIGHT
C     FINDS GAUSSIAN QUADRATURE WEIGHTS FOR SYMMETRICAL POLY-
C     NOMIALS FOR GENERAL COLLOCATION APPROXIMATION.
C     SUBROUTINE JCOBI MUST BE EXECUTED FIRST TO FIND ZEROS
C     OF THE NODAL POLYNOMIAL.
C     WEIGHTS COMPUTED FROM EQ. 4-207 FINLAYSON 1980
C
      SUBROUTINE WEIGHT (N,N0,N01,AA,X,W)
      IMPLICIT REAL*8 (A-H,O-Z)
      REAL*8 Q,QINV,Z,X,W,Y
      DIMENSION Q(40,40),QINV(40,40),Z(40),X(40),W(40),Y(40)
      N1=N+N0+N01
      DO 30 I=1,N1
      AI=I
      Z(I)=1.D0/(2.D0*AI+AA-2.D0)
 30   CONTINUE
      DO 35 I=1,N1
      Q(I,1)=1.D0
      QINV(I,1)=1.D0
      DO 35 J=2,N1
      Q(I,J)=X(I)**(2.0D0*J-2.0D0)
 35   QINV(I,J)=Q(I,J)
      DETER=SIMUL (N1,QINV,Y,0.1D-19,-1,40)
      DO 50 I=1,N1
      W(I)=0.D0
      DO 50 J=1,N1
      W(I)=W(I)+Z(J)*QINV(J,I)
 50   CONTINUE
      RETURN
      END
C
C
C
      FUNCTION SIMUL(N,A,X,EPS,INDIC,NRC)
C     CALCULATES INVERSE MATRIX IN PLACE
C     FROM APPLIED NUMERICAL METHODS BY CARNAHAN ET AL. PG 290-1
```

```
      IMPLICIT REAL*8(A-H,O-Z)
      DIMENSION IROW(50),JCOL(50),JORD(50),Y(50),A(NRC,NRC),X(N)
      MAX=N
      IF(INDIC.GE.0)MAX=N+1
      IF(N.LE.50)GOTO5
      WRITE (6,200)
      SIMUL=0.D0
      RETURN
5     DETER=1.D0
      DO 18 K=1,N
      KM1=K-1
      PIVOT=0.D0
      DO 11 I=1,N
      DO 11 J=1,N
      IF(K.EQ.1) GO TO 9
      DO 8 ISCAN=1,KM1
      DO 8 JSCAN=1,KM1
      IF(I.EQ.IROW(ISCAN)) GO TO 11
      IF(J.EQ.JCOL(JSCAN)) GO TO 11
8     CONTINUE
9     IF (DABS(A(I,J)).LE.DABS(PIVOT)) GO TO 11
      PIVOT=A(I,J)
      IROW(K)=I
      JCOL(K)=J
11    CONTINUE
      IF(DABS(PIVOT).GT.EPS)GO TO 13
      SIMUL=0.D0
      RETURN
13    IROWK=IROW(K)
      JCOLK=JCOL(K)
      DETER=DETER*PIVOT
      DO 14 J=1,MAX
14    A(IROWK,J)=A(IROWK,J)/PIVOT
      A(IROWK,JCOLK)=1.D0/PIVOT
      DO 18 I=1,N
      AIJCK=A(I,JCOLK)
      IF(I.EQ.IROWK)GO TO 18
      A(I,JCOLK)=-AIJCK/PIVOT
      DO 17 J=1,MAX
17    IF(J.NE.JCOLK)A(I,J)=A(I,J)-AIJCK*A(IROWK,J)
18    CONTINUE
      DO 20 I=1,N
      IROWI=IROW(I)
      JCOLI=JCOL(I)
      JORD(IROWI)=JCOLI
20    IF(INDIC.GE.0) X(JCOLI)=A(IROWI,MAX)
      INTCH=0
      NM1=N-1
      DO 22 I=1,NM1
      IP1=I+1
      DO 22 J=IP1,N
      IF(JORD(J).GE.JORD(I)) GO TO 22
      JTEMP=JORD(J)
      JORD(J)=JORD(I)
```

```
      JORD(I)=JTEMP
      INTCH=INTCH+1
22    CONTINUE
      IF(INTCH/2*2.NE.INTCH)DETER=-DETER
      IF(INDIC.LE.0)GO TO 26
      SIMUL=DETER
      RETURN
26    DO 28 J=1,N
      DO 27 I=1,N
      IROWI=IROW(I)
      JCOLI=JCOL(I)
27    Y(JCOLI)=A(IROWI,J)
      DO 28 I=1,N
28    A(I,J)=Y(I)
      DO 30 I=1,N
      DO 29 J=1,N
      IROWJ=IROW(J)
      JCOLJ=JCOL(J)
29    Y(IROWJ)=A(I,JCOLJ)
      DO 30 J=1,N
30    A(I,J)=Y(J)
      SIMUL=DETER
      RETURN
200   FORMAT(' TOO BIG')
      END
```

```
C*****************************************************************
C                              DCDP.FOR
C*****************************************************************
C     THIS PROGRAM SOLVES FIRST ORDER PDE'S FOR ION EXCHANGE IN
C     ZEOLITES FOR BATCH REACTORS WITH SERIES PORE AND
C     INTRACTRYSTALLINE MASS TRANSFER WHERE CRYSTAL DIFFUSIVITY
C     IS A FUNCTION OF SOLIDS CONCENTRATION AND PORE DIFFUSIVITY
C     IS DUE TO LIQUID & SURFACE MASS TRANSFER IN PARALLEL
C *
C     PDES ARE CONVERTED TO ODES BY ORTHOGONAL COLLOCATION.
C     COLLOCATION POINTS ARE CALCULATED BY SUBROUTINES FROM
C     MICHELSON AND VILLASEN AND FINLAYSON (COLLOC.FOR FILE)
C *
C     ODES ARE IN SUBROUTINE DERIVS (DPDERIVMS.FOR FILE)
C *
C     LSODE SUBROUTINE IS USED TO SOLVE THE RESULTING ODE'S
C *
C     LANGMUIR ISOTHERM (EQDCDPMS.FOR FILE) IS USED FOR
C    SINGLE COMPONENT SYSTEMS.  MODIFIED DUBININ-POLAYNI ISOTHERM
C     (EPDCDPMM.FOR FILE) IS USED FOR MULTICOMPONENT SYSTEMS.
C *
C     INPUT DATA IN IS DCDPMS.DAT; OUTPUT DATA IS IN OUTDCDPMS.DAT
C *
C      TO RUN PROGRAM ON ORNL SCIENCIFIC AND TECHNICAL COMPUTING
C     VAX, USE "FOR", "LINK", AND "RUN" COMMANDS WHERE "LINK" IS:
C      LINK DCDP,DPDERIVMS,COLLOC,EQDCDPMS,SYS$LIBRARY:CORLIB/LIB
C *
C*****************************************************************
C*****************************************************************
C     VOL=VOLUME SOLUTION, ML
C     GRMS=SORBENT ADDED, GR
C     ROB=SORBENT DENSITY, GR/ML
C     RADC=ZEOLITE CRYSTAL RADIUS, CM
C     RAD=PARTICLE RADIUS, CM
C     EPSP=PARTICLE VOID FRACTION
C     DC=CORRECTED ZEOLITE CRYSTAL DIFFUSIVITY, CM^2/S
C     DL=MOLECULAR DIFFUSIVITY/TOROUSITY FACTOR, CM^2/S
C     DS=CORRECTED SURFACE DIFFUSIVITY, CM^2/S
C     CF=FEED CONCENTRATION, MEQ/ML
C     C0=INITIAL CONCENTRATION, MEQ/ML
C     CREF=REFERENCE CONCENTRATION, MEQ/ML
C     TSTEP=RUN TIME, SEC
C     TDISP=OUTPUT TIME INCREMENT, SEC
C     N=NUMBER OF COLLOCATION POINTS ACROSS PARTICLE RADIUS
C     M=NUMBER OF COLLOCATION POINTS ACROSS CRYSTAL RADIUS
C     NCOMP=NUMBER OF COMPONENTS WHERE:
C         1 FOR Sr        2 FOR Cs        3 FOR Ca        4 FOR Mg
C*****************************************************************
      IMPLICIT REAL*8 (A-H,O-Z)
      COMMON/LAGR/EL1(800,800),EL2(800,800),NT,N,Y(50000),ROB,RADC,
     CRAD,DC(4),Q0(4),NCOMP,W(800),CREF(4),DP(800),XI(4),
     CEPSS,EPSP,Y0(800),EC1(800,800),EC2(800,800),MT,M,WC(800),
     CQSTAR(800),QBAR(800),QBARR(800),DL(4),DS(4)
      DIMENSIONDIF1(800),DIF2(800),DIF3(800),ROOT(800),VECT(800),
```

```
      CAKF(4),DIFC1(800),DIFC2(800),DIFC3(800),ROOTC(800),VECTC(800)
      C,SROOTC(800),TEMP(800),TEMP0(800),
      CYOUT(4),QAVG(4),CMAX(4),CMAXN(4),XOUT1(4),XOUT2(4),XOUT3(4)
      C0(4),CF(4),SROOT(800),RWORK(80000),IWORK(2000),XOUT(4)
       EXTERNAL F,JAC
C
C
C      INPUT PARAMETERS
C
       OPEN(UNIT=5,FILE='DCDPMS.DAT', STATUS='OLD')
       REWIND 5
       READ(5,601)CHAR1,CHAR2,CHAR3,CHAR4,CHAR5,CHAR6,CHAR7
 601   FORMAT(X,7A5)
       READ(5,*) NCOMP,AKF(1),AKF(2),AKF(3),AKF(4),DC(1),DC(2)
       READ(5,*) DC(3),DC(4),DS(1),DS(2),DS(3),DS(4),DL(1),DL(2)
       READ(5,*) DL(3),DL(4),GRMS,VOL,ROB
       READ(5,*) RADC,RAD,EPSP
       READ(5,*) CF(1),CF(2),CF(3),CF(4),C0(1),C0(2),C0(3),C0(4)
       READ(5,*) CREF(1),CREF(2),CREF(3),CREF(4)
       READ(5,*) TSTEP
       READ(5,*) N,M
       READ(5,*) TDISP
       OPEN(UNIT=6,FILE='OUTDCDPMS.DAT', STATUS='NEW')
       WRITE(6,602)CHAR1,CHAR2,CHAR3,CHAR4,CHAR5,CHAR6,CHAR7
 602   FORMAT(X,7A5)
C      CALCULATE VOID FRACTION IN BATCH REACTOR
       EPSS=GRMS/VOL/ROB
C      DETERMINE COLLOCATION CONSTANTS FOR SYMMETRICAL SYSTEM
       A=3.0D0
       N0=0
       N1=1
       AL=1.D0
       BE=0.5D0
       NT=N+N0+N1
       MT=M+N0+N1
       NEQ=NCOMP*MT*NT
       CALL JCOBI (N,N0,N1,AL,BE,DIF1,DIF2,DIF3,ROOT)
       WRITE(6,114),MT,NT
 114   FORMAT(2I3,' COLLOCATION POINTS FOR CRYSTAL RADIUS
      C AND PARTICLE RADIUS, RESPECTIVELY')
       DO 200 I=1,NT
       SROOT(I)=DSQRT(ROOT(I))
 200   CONTINUE
       DO 10 J=1,NT
       DO 5 ID=1,2
       CALL DFOPR (N,N0,N1,J,ID,DIF1,DIF2,DIF3,ROOT,VECT)
       DO 5 I=1,NT
       IF(ID.EQ.1) EL1(J,I)=VECT(I)
       IF(ID.EQ.2) EL2(J,I)=VECT(I)
 5     CONTINUE
 10    CONTINUE
       DO 17 J=1,NT
       DO 15 I=1,NT
       EL2(J,I)=4.0D0*ROOT(J)*EL2(J,I)+2.D0*A*EL1(J,I)
```

```
      EL1(J,I)=2.0D0*DSQRT(ROOT(J))*EL1(J,I)
      CALL WEIGHT(N,N0,N1,A,SROOT,VECT)
      W(J)=VECT(J)

 15   CONTINUE
 17   CONTINUE
      CALL JCOBI (M,N0,N1,AL,BE,DIFC1,DIFC2,DIFC3,ROOTC)
      DO 300 I=1,MT
      SROOTC(I)=DSQRT(ROOTC(I))
300   CONTINUE
      DO 310 J=1,MT
      DO 305 ID=1,2
      CALL DFOPR (M,N0,N1,J,ID,DIFC1,DIFC2,DIFC3,ROOTC,VECTC)
      DO 305 I=1,MT
      IF(ID.EQ.1) EC1(J,I)=VECTC(I)
      IF(ID.EQ.2) EC2(J,I)=VECTC(I)
305   CONTINUE
310   CONTINUE
      DO 317 J=1,MT
      DO 315 I=1,MT
      EC2(J,I)=4.0D0*ROOTC(J)*EC2(J,I)+2.D0*A*EC1(J,I)
      EC1(J,I)=2.0D0*DSQRT(ROOTC(J))*EC1(J,I)
      CALL WEIGHT(M,N0,N1,A,SROOTC,VECTC)
      WC(J)=VECTC(J)
 315  CONTINUE
 317  CONTINUE
C     ASSIGN BOUNDARY AND INITIAL CONDITIONS
      DO 21 I=1,NCOMP
      DO 21 J=1,NT
      TEMP(J+(I-1)*NT)=0.
 21   CONTINUE
      NN=0
      DO 22 K=1,NT
      DO 22 I=1,NCOMP
      NN=NN+1
      TEMP(NN)=CREF(I)
 22   CONTINUE
      CALL QEQUIL(TEMP,TEMP0)
      NN=0
      DO 23 K=1,NT
      DO 23 I=1,NCOMP
      NN=NN+1
      Q0(I)=TEMP0(NN)
 23   CONTINUE
      T=0.0D0
      MM=0
      BTOT=0.0
      DO 25 I=1,NCOMP
      DO 20 K=I,NT
      DO 20 J=1,MT
      MM=MM+1
 20   Y(MM)=C0(I)/Q0(I)
      Y(NCOMP*MT*(NT-1)+I*MT)=CF(I)/CREF(I)
      XI(I)=EPSP*CREF(I)/ROB/Q0(I)/(1-EPSP)
```

```
      BTOT=BTOT+CF(I)*VOL
 25   CONTINUE
C     WRITE OUT INITIAL CONDITIONS AND INPUT PARAMETERS
      WRITE(6,26) CF(1),CF(2),CF(3),CF(4),GRMS,VOL,RAD
 26  FORMAT(' CFs=',E12.4,' ',E12.4,' ',E12.4,' ',E12.4,/,' SOLIDS
     C (GMS)=',E12.4,' VOLUME (ML)=',E12.4,' RADIUS (CM)=',E12.4)
      WRITE(6,228) Q0(1),Q0(2),Q0(3),Q0(4)
 228  FORMAT(' Q0s=',E12.4,' ',E12.4,' ',E12.4,' ',E12.4)
      WRITE(6,226)AKF(1),AKF(2),AKF(3),AKF(4),
     CDC(1),DC(2),DC(3),DC(4)
     C,DS(1),DS(2),DS(3),DS(4),DL(1),DL(2),DL(3),DL(4)
 226  FORMAT(' KFs= ',4D10.3,/,' DCs= ',4D10.3,/,' DSs=',4D10.3
     C,/,' DL/Ts=',4D10.3)
      WRITE(6,124)
 124  FORMAT(/,' TIME, MIN              NORMALIZED SOLUTION
     CCONCENTRATIONS')
      WRITE(6,227)TOUT,Y(NCOMP*MT*(NT-1)+MT),Y(NCOMP*MT*
     C(NT-1)+2*MT),Y(NCOMP*MT*(NT-1)+3*MT),Y(NCOMP*MT
     C*(NT-1)+4*MT)
 227  FORMAT(F12.4,' ',E12.4,' ',E12.4,' ',E12.4,' ',E12.4)
      ENDT=TDISP
      IFLAG=0
C     SET PARAMETERS FOR LSODE TO SOLVE ODEs IN DERIVS SUBROUTINE
      MF=22
      RTOL=1.0D-5
      ATOL=1.0D-5
      ITOL=1
      ITASK=1
      ISTATE=1
      IOPT=1
      LRW=80000
      LIW=2000
      DO 31 L=5,10
      RWORK(L)=0.0
      IWORK(L)=0
 31   CONTINUE
      IWORK(6)=500
 30   CONTINUE
      IF(ENDT.LT.TSTEP.OR.IFLAG.EQ.1) GOTO 35
      ENDT=TSTEP
      IFLAG=1
 35   CONTINUE
      CALL LSODE (F,NEQ,Y,T,ENDT,ITOL,RTOL,ATOL,ITASK,ISTATE,IOPT,
     CRWORK,LRW,IWORK,LIW,JAC,MF)
C     PRINT OUT RESULTS
      DO 37 J=1,NCOMP
      XOUT(J)=Y(NCOMP*MT*(NT-1)+J*MT)
      XOUT1(J)=Y(NCOMP*MT*(NT-2)+J*MT)
      XOUT2(J)=Y(NCOMP*MT*(NT-3)+J*MT)
      XOUT3(J)=Y(NCOMP*MT*(NT-4)+J*MT)
 37   CONTINUE
      TOUT=T/60.
      WRITE(6,40)TOUT,XOUT(1),XOUT(2),XOUT(3),XOUT(4)
 40   FORMAT(/,F12.4,' ',E12.4,' ',E12.4,' ',E12.4,' ',E12.4)
```

```
      IF(ISTATE.LT.0) GOTO 80
      GOTO 90
 80   WRITE(6,85) ISTATE
 85   FORMAT(' ERROR IN LSODE.  ISTATE= ',I3)
      GOTO 510
 90   CONTINUE
      IF(IOUTF.EQ.1) WRITE(5,*)T,XOUT1,XOUT2
      ENDT=ENDT+TDISP
      IF(T.GE.TSTEP) GOTO 510
      IF(IFLAG.EQ.1) GOTO 510
      GOTO 30
 510  CONTINUE
      END
C
C     SUBROUTINES TO CALCULATE DERIVATIVES OF ODES
C
      SUBROUTINE  F (NEQ,T,Y,YDOT)
      IMPLICIT REAL*8 (A-H,O-Z)
      DIMENSION Y(80),YDOT(80)
      CALL DERIVS (NEQ,T,Y,YDOT)
      RETURN
      END
C
C     DUMMY SUBROUTINE NEEDED FOR LSODE WHEN MF=22
      SUBROUTINE JAC (NEQ,T,Y,ML,MU,PD,NROWPD)
      IMPLICIT REAL*8 (A-H,O-Z)
      DIMENSION Y(NEQ),PD(NROWPD,NEQ)
      RETURN
      END
C
C
C
C     SUBROUTINE CONTAINING ODES
C
      SUBROUTINE  DERIVS (NEQ,X,V,YP)
      IMPLICIT REAL*8 (A-H,O-Z)
      COMMON/LAGR/EL1(800,800),EL2(800,800),NT,N,Y(50000),
     1ROB,RADC,RAD,DC(4),Q0(4),NCOMP,W(800),CREF(4),DP(800),XI(4),
     2EPSS,EPSP,Y0(800),EC1(800,800),EC2(800,800),MT,M,WC(800)
     3,QSTAR(800),QBAR(800),QBARR(800),dl(4),ds(4)
      DIMENSION V(50000),YP(50000),CSTAR(800),YSUM(800),WW(800),
     CCSUM(50000),COEF(800),XSUM(800),KFLAG(4),TEST(4),ASUM(800),
     CDSTAR(800),Q(800),BSUM(800),YTEMPC(50000),DSUM(50000),
     CZSUM(800),DA(4),DB(4),DCC(4),VSUM(800),YTEMPS(800)
C     SET MAXIMUM ZEOLITE LOADING CAPACITY
      DCC(1)=2.86D0
      DCC(2)=3.35D0
      DCC(3)=2.86D0
      DCC(4)=2.86D0
      NN=0
C     DETERMINE EQUILIBRIUM VALUES AT PARTICLE AND PORE SURFACES
      DO 2 K=1,NT
      DO 2 I=1,NCOMP
      NN=NN+1
```

```
      CSTAR(NN)=V(NN*MT)*CREF(I)
  2   CONTINUE
      CALL QEQUIL (CSTAR,QSTAR)
      NN=0
      DO 3 K=1,NT
      DO 3 I=1,NCOMP
      NN=NN+1
      QSTAR(NN)=QSTAR(NN)/Q0(I)
  3   CONTINUE
C     CALCULATE MICROPORE ODES
      JJ=0
      KK=0
      DO 20 K=1,NT
      DO 20 I=1,NCOMP
      KK=KK+1
      DO 19 J=1,MT
      JJ=JJ+1
      CSUM(JJ)=0.D0
      DSUM(JJ)=0.D0
      DO 15 L=1,M
      ITEMP1=(K-1)*NCOMP*MT+(I-1)*MT
      CSUM(JJ)=CSUM(JJ)+EC2(J,L)*V(ITEMP1+L)
      DSUM(JJ)=DSUM(JJ)+EC1(J,L)*V(ITEMP1+L)
 15   CONTINUE
      CSUM(JJ)=CSUM(JJ)+EC2(J,mt)*QSTAR(KK)
      DSUM(JJ)=DSUM(JJ)+EC1(J,mt)*QSTAR(KK)
      YTEMPC(JJ)=1.D0-V(JJ)*Q0(I)/DCC(I)
      YP(JJ)=DC(I)/RADC/RADC/YTEMPC(JJ)*(CSUM(JJ)+1.D0/YTEMPC(JJ)*
     CDSUM(JJ)*DSUM(JJ))
 19   CONTINUE
      DSTAR(KK)=YP(JJ)
C     YP(JJ) IS TEMPORARILY USED
 20   CONTINUE
C     CALCULATE AVERAGE ZEOLITE CRYSTAL CONCENTRATIONS AND
C     COORSPONDING ODES
      KKK=0
      NNN=0
      DO 22 K=1,NT
      DO 22 I=1,NCOMP
      NNN=NNN+1
      ASUM(NNN)=0.0
      YSUM(NNN)=0.0
      DO 21 J=1,M
      KKK=KKK+1
      ASUM(NNN)=ASUM(NNN)+WC(J)*V(KKK)
      YSUM(NNN)=YSUM(NNN)+WC(J)*YP(KKK)
 21   CONTINUE
      YSUM(NNN)=YSUM(NNN)+WC(mt)*dstar(NNN)
      ASUM(NNN)=ASUM(NNN)+WC(MT)*QSTAR(NNN)
      KKK=KKK+1
      Q(NNN)=3.D0*YSUM(NNN)
      QBAR(NNN)=3.D0*ASUM(NNN)
 22   CONTINUE
      NQ=NT-1
```

```
      II=0
      DO 60 I=1,NCOMP
      DO 30 J=1,NQ
      VSUM(J)=0.D0
      XSUM(J)=0.D0
      ZSUM(J)=0.D0
 30   CONTINUE
      WW(I)=0.0D0
      BSUM(I)=0.D0
      DO 50 J=1,NQ
      II=II+1
      DO 40 K=1,NT
      KK=KK+1
      ZSUM(J)=ZSUM(J)+EL1(J,K)*QSTAR(((K-1)*NCOMP*MT+I*MT)/MT)
      XSUM(J)=XSUM(J)+EL2(J,K)*QSTAR(((K-1)*NCOMP*MT+I*MT)/MT)
      VSUM(J)=VSUM(J)+EL2(J,K)*V((K-1)*NCOMP*MT+I*MT)
 40   CONTINUE
C     CALCULATE MACROPORE ODES
      ITEMP3=(J-1)*NCOMP*MT+I*MT
      YTEMPS(J)=1.D0-QSTAR(ITEMP3/MT)*Q0(I)/DCC(I)
      YP(ITEMP3)=(DL(I)*VSUM(J)+DS(I)/XI(I)*XSUM(J)/YTEMPS(J)
     C+DS(I)*ZSUM(J)**2/XI(I)/YTEMPS(J)**2)/RAD/RAD
     C-Q(ITEMP3/MT)/XI(I)
C     CALCULATE BULK SOLUTION CONCENTRATION FROM BOUNDARY MASS
C     BALANCE
      WW(I)=WW(I)+W(J)*(Q(ITEMP3/MT)/XI(I)+YP((J-1)*
     CNCOMP*MT+I*MT))
      BSUM(I)=BSUM(I)+W(J)*(QBAR(ITEMP3/MT)*(1.0D0-EPSP)+V((J-1)*
     CNCOMP*MT+I*MT)*EPSP*CREF(I)/Q0(I))
 50   CONTINUE
      YP((NT-1)*NCOMP*MT+I*MT)=-3.D0*EPSP*EPSS*(WW(I)+
     CQ(((NT-1)*NCOMP*MT+I*MT)/MT)/XI(I)*W(NT))/
     C(1.D0+3.D0*EPSP*EPSS*W(NT))
      QBARR(I)=3.D0*(BSUM(I)+W(NT)*(QBAR(((NT-1)
     C*NCOMP*MT+I*MT)/MT)*
     C(1.D0-EPSP)+V((NT-1)*NCOMP*MT+I*MT)*EPSP*CREF(I)/Q0(I)))
      II=II+1
 60   CONTINUE
      RETURN
      END
C
C
C
C     SUBROUTINE FOR BINARY EQUILIBRIUM EQUATIONS
C     LANGMUIR MODEL
C
      SUBROUTINE QEQUIL (X,Q)
      IMPLICIT REAL*8 (A-H,O-Z)
      COMMON/LAGR/EL1(800,800),EL2(800,800),NT,N,Y(50000),ROB,
     CRADC,RAD,DC(4),Q0(4),NCOMP,W(800),CREF(4),DP(800),XI(4)
     C,EPSS,EPSP,Y0(800),EC1(800,800),EC2(800,800),MT,M,WC(800),
     CQSTAR(800),QBAR(800),QBARR(800),ds(4),dl(4)
      DIMENSION X(800),Q(800),A(4),B(4),C(4)
C
```

```
C     SUBROUTINE CALCULATES QSTAR GIVEN C FROM THE
C     EQUILIBRIUM ISOTHERM
      A(1)=173702.D0
      B(1)=98176.D0
      A(2)=157009.D0
      B(2)=68574.D0
      A(3)=456942.D0
      B(3)=221015.D0
      A(4)=481696.D0
      B(4)=610790.D0
      DO 10 J=1,NT
      DO 10 K=1,NCOMP
      Q((J-1)*NT+K)=A(K)*X((J-1)*NT+K)/(1.D0+B(K)*X((J-1)*NT+K))
   10 CONTINUE
      RETURN
      END
C
      SUBROUTINE CEQUIL (Q,C)
      IMPLICIT REAL*8 (A-H,O-Z)
      COMMON/LAGR/EL1(800,800),EL2(800,800),NT,N,Y(50000),ROB,
     CRADC,RAD,DC(4),Q0(4),NCOMP,W(800),CREF(4),DP(4),XI(4)
     C,EPSS,EPSP,Y0(800),EC1(800,800),EC2(800,800),MT,M,WC(800),
     CQSTAR(800),QBAR(800),QBARR(800)
      DIMENSION X(800),Q(800),A(4),B(4),C(4)
C
C     SUBROUTINE CALCULATES CSTAR GIVEN Q FROM THE
C     EQUILIBRIUM ISOTHERM
      A(1)=173702.D0
      B(1)=98176.D0
      A(2)=157009.D0
      B(2)=68574.D0
      A(3)=456942.D0
      B(3)=221015.D0
      A(4)=481696.D0
      B(4)=610790.D0
      DO 5 J=1,NT
      DO 5 K=1,NCOMP
      IF(Q((J-1)*NT+K).LE.0.D0)Q((J-1)*NT+K)=1.D-12
    5 CONTINUE
      DO 10 J=1,NT
      DO 10 K=1,NCOMP
      X((J-1)*NT+K)=A(K)/Q((J-1)*NT+K)-B(K)
      C((J-1)*NT+K)=1.D0/X((J-1)*NT+K)
   10 CONTINUE
      RETURN
      END

      SUBROUTINE DEQUIL (X,DQ)
      IMPLICIT REAL*8 (A-H,O-Z)
      COMMON/LAGR/EL1(800,800),EL2(800,800),NT,N,Y(50000),ROB,
     CRADC,RAD,DC(4),Q0(4),NCOMP,W(800),CREF(4),DP(4),XI(4)
     C,EPSS,EPSP,Y0(800),EC1(800,800),EC2(800,800),MT,M,WC(800),
     CQSTAR(800),QBAR(800),QBARR(800)
      DIMENSION X(800),DQ(800),A(4),B(4),C(4)
```

```
C
C     SUBROUTINE CALCULATES DERIVATIVE OF QSTAR/DT FROM THE
C     EQUILIBRIUM ISOTHERM
      A(1)=173702.D0
      B(1)=98176.D0
      A(2)=157009.D0
      B(2)=68574.D0
      A(3)=456942.D0
      B(3)=221015.D0
      A(4)=481696.D0
      B(4)=610790.D0
      DO 10 J=1,NT
      DO 10 K=1,NCOMP
      DQ((J-1)*NT+K)=A(K)/(1.D0+B(K)*X((J-1)*NT+K))**2
   10 CONTINUE
      RETURN
      END
C
C
C
C     SUBROUTINE FOR MULTICOMPONENT EQUILIBRIUM EQUATIONS
C     MODIFIED DUBININ POLYANI MODEL FOR SR, CA, CS
C     LANGMUIR ISOTHERM MODEL FOR CS
C
      SUBROUTINE QEQUIL (X,Q)
      IMPLICIT REAL*8 (A-H,O-Z)
      COMMON/LAGR/EL1(800,800),EL2(800,800),NT,N,Y(50000),ROB,
     CRADC,RAD,DC(4),Q0(4),NCOMP,W(800),CREF(4),DP(4),XI(4),
     CEPSS,EPSP,Y0(800),EC1(800,800),EC2(800,800),MT,M,WC(800),
     CQSTAR(800)
      DIMENSION X(800),Q(800),A(4),B(4),C(4),XTEMP(800)
C
C     SUBROUTINE CALCULATES QSTAR GIVEN C FROM THE
C     EQUILIBRIUM ISOTHERM
      A(1)=-4.742D0
      B(1)=-1.157D0
      C(1)=-0.07507D0
      A(2)=-1.532D0
      B(2)=-0.589D0
      C(2)=-0.05002D0
      A(3)=-4.212D0
      B(3)=-0.856D0
      C(3)=-0.04703D0
      A(4)=-17.28D0
      B(4)=-3.345D0
      C(4)=-0.1818D0
      DO 10 J=1,NT
      DO 10 K=1,NCOMP
      XTEMP((J-1)*NCOMP+K)=X((J-1)*NCOMP+K)
      IF(X((J-1)*NCOMP+K).GT.0.D0) GOTO 7
      XTEMP((J-1)*NCOMP+K)=1.D-12
      IF(K.EQ.4)XTEMP((J-1)*NCOMP+K)=1.D-8
 7    Q((J-1)*NCOMP+K)=DEXP(A(K)+B(K)*DLOG(XTEMP((J-1)*NCOMP+K))+
     CC(K)*DLOG(XTEMP((J-1)*NCOMP+K))*DLOG(XTEMP((J-1)*NCOMP+K)))
```

```
      IF(K.NE.2)GOTO 10
      Q((J-1)*NCOMP+K)=54759.D0*XTEMP((J-1)*NCOMP+K)/(1.D0
     C+48758.D0*XTEMP((J-1)*NCOMP+K))
   10 CONTINUE
      RETURN
      END
C
      SUBROUTINE DEQUIL (X,DQ)
      IMPLICIT REAL*8 (A-H,O-Z)
      COMMON/LAGR/EL1(800,800),EL2(800,800),NT,N,Y(50000),ROB,
     CRADC,RAD,DC(4),Q0(4),NCOMP,W(800),CREF(4),DP(4),XI(4),
     CEPSS,EPSP,Y0(800),EC1(800,800),EC2(800,800),MT,M,WC(800),
     CQSTAR(800)
      DIMENSION X(800),DQ(800),A(4),B(4),C(4),XTEMP(800)
C     SUBROUTINE CALCULATES DQSTAR/DT GIVEN C FROM THE
C     EQUILIBRIUM ISOTHERM:
      A(1)=-4.742D0
      B(1)=-1.157D0
      C(1)=-0.07507D0
      A(2)=-1.532D0
      B(2)=-0.589D0
      C(2)=-0.05002D0
      A(3)=-4.212D0
      B(3)=-0.856D0
      C(3)=-0.04703D0
      A(4)=-17.28D0
      B(4)=-3.345D0
      C(4)=-0.1818D0
      DO 10 J=1,NT
      DO 10 K=1,NCOMP
      XTEMP((J-1)*NCOMP+K)=X((J-1)*NCOMP+K)
      IF(X((J-1)*NCOMP+K).GT.0.D0) GOTO 7
      XTEMP((J-1)*NCOMP+K)=1.D-12
      IF(K.EQ.4)XTEMP((J-1)*NCOMP+K)=1.D-8
 7    DQ((J-1)*NCOMP+K)=DEXP(A(K)+B(K)*
     CDLOG(XTEMP((J-1)*NCOMP+K))+
     CC(K)*DLOG(XTEMP((J-1)*NCOMP+K))*
     CDLOG(XTEMP((J-1)*NCOMP+K)))*(B(K)/
     CXTEMP((J-1)*NCOMP+K)+2.D0*C(K)*DLOG(XTEMP((J-1)*NCOMP+K))
     C/XTEMP((J-1)*NCOMP+K))
      IF(K.NE.2)GOTO 10
      DQ((J-1)*NCOMP+K)=54759.D0/(1.D0+48758.D0*
     CX((J-1)*NCOMP+K))**2
   10 CONTINUE
      RETURN
      END
C
C
C     ORTHOGONAL COLLOCATION SUBROUNTINES FROM VILLADSEN AND
C     MICHELSON (1978) AND FINLAYSON (1980)
C
C     SUBROUTINE JCOBI
C
C     EVALUATION OF ROOTS AND DERIVATIVES OF JACOBI POLYNOMIALS
```

```
C     P(N) (AL,BE).
C     FIRST EVALUATION OF COEFFICIENTS IN RECURSION FORMULA
C     RECURSION COEFFICIENTS ARE STORED IN DIF1 AND DIF2.
C     SUBROUTINE FROM MICHELSEN AND VILLADSEN, P. 418
C
      SUBROUTINE JCOBI(N,N0,N1,AL,BE,DIF1,DIF2,DIF3,ROOT)
      IMPLICIT REAL*8(A-H,O-Z)
      REAL*8 DIF1,DIF2,DIF3,ROOT
      DIMENSION DIF1(40),DIF2(40),DIF3(40),ROOT(40)
C
      AB=AL+BE
      AD=BE-AL
      AP=BE*AL
      DIF1(1)=(AD/(AB+2.D0)+1.D0)/2.D0
      DIF2(1)=0.0D0
      IF(N.LT.2) GO TO 15
      DO 10 I=2,N
      Z1=I-1.D0
      Z=AB+2.D0*Z1
      DIF1(I)=(AB*AD/Z/(Z+2.D0)+1.D0)/2.D0
      IF (I.NE.2) GO TO 11
      DIF2(I)=(AB+AP+Z1)/Z/Z/(Z+1.D0)
   11 Z=Z*Z
      Y=Z1*(AB+Z1)
      Y=Y*(AP+Y)
      DIF2(I)=Y/Z/(Z-1.D0)
   10 CONTINUE
   15 X=0.D0
      DO 20 I=1,N
   25 XD=0.0D0
      XN=1.0D0
      XD1=0.0D0
      XN1=0.0D0
      DO 30 J=1,N
      XP=(DIF1(J)-X)*XN-DIF2(J)*XD
      XP1=(DIF1(J)-X)*XN1-DIF2(J)*XD1-XN
      XD=XN
      XD1=XN1
      XN=XP
   30 XN1=XP1
      ZC=1.0D0
      Z=XN/XN1
      IF(I.EQ.1) GO TO 21
      DO 22 J=2,I
   22 ZC=ZC-Z/(X-ROOT(J-1))
   21 Z=Z/ZC
      X=X-Z
      IF(DABS(Z).GT.1.0D-12) GO TO 25
      ROOT(I)=X
      X=X+.0001D0
   20 CONTINUE
C
C     ADD INTERPOLATION POINTS AT X=0 AND X=1 IF REQUIRED
C
```

```
      NT=N+N0+N1
      IF(N0.EQ.0) GO TO 35
      DO 31 I=1,N
      J=N+1-I
   31 ROOT(J+1)=ROOT(J)
      ROOT(1)=0.D0
   35 IF(N1.EQ.1) ROOT(NT)=1.0
C
C     EVALUATE DERIVATIVES OF NODAL POLYNOMIAL
C
      DO 40 I=1,NT
      X=ROOT(I)
      DIF1(I)=1.D0
      DIF2(I)=0.D0
      DIF3(I)=0.D0
      DO 40 J=1,NT
      IF(J.EQ.I) GO TO 40
      Y=X-ROOT(J)
      DIF3(I)=Y*DIF3(I)+3.D0*DIF2(I)
      DIF2(I)=Y*DIF2(I)+2.D0*DIF1(I)
      DIF1(I)=Y*DIF1(I)
   40 CONTINUE
      RETURN
      END
C
C
C
C     SUBROUTINE DFOPR
C     FINDS DISCRETIZATION MATRICES AND GAUSSIAN QUADRATURE
C     WEIGHTS FOR GENERAL COLLOCATION APPROXIMATION
C     SUBROUTINE JCOBI MUST BE EXECUTED FIRST TO FIND ZEROS AND
C     DERIVATIVED OF NODAL POLYNOMIAL
C
      SUBROUTINE DFOPR (N,N0,N1,I,ID,DIF1,DIF2,DIF3,ROOT,VECT)
      IMPLICIT REAL*8 (A-H,O-Z)
      DIMENSION DIF1(40),DIF2(40),DIF3(40),ROOT(40),VECT(40)
C
C     GAUSSIAN WEIGHTS NORMALIZED TO SUM 1
C     ID=1 :        DISCRETIZATION MATRIX FOR Y'(X)
C     ID=2 :        DISCRETIZATION MATRIX FOR Y''(X)
C     ID=3 :        GAUSSIAN QUADRATURE WEIGHTS
C     VECT=   COMPUTED DIFFERENTIATION WEIGHTS
C
      NT=N+N0+N1
      IF(ID.EQ.3) GOTO 10
      DO 20 J=1,NT
      IF(J.NE.I) GOTO 21
      IF(ID.NE.1) GOTO 5
      VECT(I)=DIF2(I)/DIF1(I)/2.D0
      GOTO 20
 5    VECT(I)=DIF3(I)/DIF1(I)/3.D0
      GOTO 20
 21   Y=ROOT(I)-ROOT(J)
      VECT(J)=DIF1(I)/DIF1(J)/Y
```

```
      IF(ID.EQ.2) VECT(J)=VECT(J)*(DIF2(I)/DIF1(I)-2.D0/Y)
 20   CONTINUE
      GOTO 50
 10   Y=0.D0
      DO 25 J=1,NT
      X=ROOT(J)
      AX=X*(1.D0-X)
      IF (N0.EQ.0) AX=AX/X/X
      IF (N1.EQ.0) AX=AX/(1.D0-X)/(1.D0-X)
      VECT(J)=AX/DIF1(J)**2
 25   Y=Y+VECT(J)
      DO 60 J=1,NT
 60   VECT(J)=VECT(J)/Y
 50   RETURN
      END
C
C
C
C     SUBROUTINE WEIGHT
C     FINDS GAUSSIAN QUADRATURE WEIGHTS FOR SYMMETRICAL POLY-
C     NOMIALS FOR GENERAL COLLOCATION APPROXIMATION.
C     SUBROUTINE JCOBI MUST BE EXECUTED FIRST TO FIND ZEROS
C     OF THE NODAL POLYNOMIAL.
C     WEIGHTS COMPUTED FROM EQ. 4-207 FINLAYSON 1980
C
      SUBROUTINE WEIGHT (N,N0,N01,AA,X,W)
      IMPLICIT REAL*8 (A-H,O-Z)
      REAL*8 Q,QINV,Z,X,W,Y
      DIMENSION Q(40,40),QINV(40,40),Z(40),X(40),W(40),Y(40)
      N1=N+N0+N01
      DO 30 I=1,N1
      AI=I
      Z(I)=1.D0/(2.D0*AI+AA-2.D0)
 30   CONTINUE
      DO 35 I=1,N1
      Q(I,1)=1.D0
      QINV(I,1)=1.D0
      DO 35 J=2,N1
      Q(I,J)=X(I)**(2.0D0*J-2.0D0)
 35   QINV(I,J)=Q(I,J)
      DETER=SIMUL (N1,QINV,Y,0.1D-19,-1,40)
      DO 50 I=1,N1
      W(I)=0.D0
      DO 50 J=1,N1
      W(I)=W(I)+Z(J)*QINV(J,I)
 50   CONTINUE
      RETURN
      END
C
C
C
      FUNCTION SIMUL(N,A,X,EPS,INDIC,NRC)
C     CALCULATES INVERSE MATRIX IN PLACE
C     FROM APPLIED NUMERICAL METHODS BY CARNAHAN ET AL. PG 290-1
```

```
      IMPLICIT REAL*8(A-H,O-Z)
      DIMENSION IROW(50),JCOL(50),JORD(50),Y(50),A(NRC,NRC),X(N)
      MAX=N
      IF(INDIC.GE.0)MAX=N+1
      IF(N.LE.50)GOTO5
      WRITE (6,200)
      SIMUL=0.D0
      RETURN
 5    DETER=1.D0
      DO 18 K=1,N
      KM1=K-1
      PIVOT=0.D0
      DO 11 I=1,N
      DO 11 J=1,N
      IF(K.EQ.1) GO TO 9
      DO 8 ISCAN=1,KM1
      DO 8 JSCAN=1,KM1
      IF(I.EQ.IROW(ISCAN)) GO TO 11
      IF(J.EQ.JCOL(JSCAN)) GO TO 11
 8    CONTINUE
 9    IF (DABS(A(I,J)).LE.DABS(PIVOT)) GO TO 11
      PIVOT=A(I,J)
      IROW(K)=I
      JCOL(K)=J
 11   CONTINUE
      IF(DABS(PIVOT).GT.EPS)GO TO 13
      SIMUL=0.D0
      RETURN
 13   IROWK=IROW(K)
      JCOLK=JCOL(K)
      DETER=DETER*PIVOT
      DO 14 J=1,MAX
 14   A(IROWK,J)=A(IROWK,J)/PIVOT
      A(IROWK,JCOLK)=1.D0/PIVOT
      DO 18 I=1,N
      AIJCK=A(I,JCOLK)
      IF(I.EQ.IROWK)GO TO 18
      A(I,JCOLK)=-AIJCK/PIVOT
      DO 17 J=1,MAX
 17   IF(J.NE.JCOLK)A(I,J)=A(I,J)-AIJCK*A(IROWK,J)
 18   CONTINUE
      DO 20 I=1,N
      IROWI=IROW(I)
      JCOLI=JCOL(I)
      JORD(IROWI)=JCOLI
 20   IF(INDIC.GE.0) X(JCOLI)=A(IROWI,MAX)
      INTCH=0
      NM1=N-1
      DO 22 I=1,NM1
      IP1=I+1
      DO 22 J=IP1,N
      IF(JORD(J).GE.JORD(I)) GO TO 22
      JTEMP=JORD(J)
      JORD(J)=JORD(I)
```

```
      JORD(I)=JTEMP
      INTCH=INTCH+1
22    CONTINUE
      IF(INTCH/2*2.NE.INTCH)DETER=-DETER
      IF(INDIC.LE.0)GO TO 26
      SIMUL=DETER
      RETURN
26    DO 28 J=1,N
      DO 27 I=1,N
      IROWI=IROW(I)
      JCOLI=JCOL(I)
27    Y(JCOLI)=A(IROWI,J)
      DO 28 I=1,N
28    A(I,J)=Y(I)
      DO 30 I=1,N
      DO 29 J=1,N
      IROWJ=IROW(J)
      JCOLJ=JCOL(J)
29    Y(IROWJ)=A(I,JCOLJ)
      DO 30 J=1,N
30    A(I,J)=Y(J)
      SIMUL=DETER
      RETURN
200   FORMAT(' TOO BIG')
      END
```

INTERNAL DISTRIBUTION

1. J. M. Begovich
2. J. T. Bell
3. J. B. Berry
4. W. D. Bond
5-6. D. A. Bostick
7. C. H. Brown, Jr.
8. C. H. Byers
9. R. M. Cannon
10. E. D. Collins
11. A. C. Coroneos
12. R. M. Counce
13. A. G. Croff
14. D. L. Daugherty
15. D. J. Davidson
16. S. M. DePaoli
17. B. Z. Egan
18. R. K. Genung
19. G. A. Guiochon
20. C. M. Kendrick
21. T. M. Kent
22. D. D. Lee
23. R. C. Mason
24. L. E. McNeese
25-29. S. M. Robinson
30. M. K. Savage
31. P. A. Taylor
32. J. S. Watson
33. J. H. Wilson
34. Central Research Library
35. ORNL-Y-12 Tech. Library, Document Reference Section
36. Laboratory Records-RC
37. ORNL Patent Section

EXTERNAL DISTRIBUTION

38. Office of Assistant Manager, Energy Research and Development, DOE-ORO, P.O. Box 2001, Oak Ridge, TN 37831.
39. Office of Scientific and Technical Information, P.O. Box 62, Oak Ridge, TN 37831.